PhD DISSERTATION

Author:
Samuel Morillas Gómez*

Advisors:
Dr. Valentín Gregori Gregori
Dr. Guillermo Peris Fajarnés

Fuzzy metrics and fuzzy logic for colour image filtering

May 24, 2007

* The work developed by the author has been funded by the Spanish Ministry of Education and Science under program "Becas de Formación de Profesorado Universitario FPU".

A mis padres y a mi hermano,
por su incondicional apoyo, confianza, cariño y compresión.

Agradecimientos

En primer lugar, me gustaría agredecer a mi familia: a mis padres, a mi hermano, a mis abuelos y a la tata, a mis tíos y a mis primos; porque siempre he contado con su inquebrantable confianza y su cariño y porque son los que más cerca de mí han estado siempre -ojalá que los que por desgracia ya no están se sientan orgullosos-.

En segundo lugar, me gustaría mencionar a todos los docentes que han influido positivamente en mi educación, que empezaba hace más de veinte años con docentes tan buenos como mis propios padres, y que hoy, gracias en gran parte a la dedicación, las facilidades y la confianza que he recibido de mis directores de Tesis, Dr. Valentín Gregori Gregori y Dr. Guillermo Peris Fajarnés, culmina en esta Tesis Doctoral.

En tercer lugar, me gustaría agradecer a todas las personas que han hecho que mi trabajo dentro de la universidad sea más llevadero y sencillo: Pepe, Rosa, Pedro, Terele, Alman, Ignacio, Joan Gerard, Julio, Bernardino, y, en general, a todos mis compañeros del CITG y del departamento de Matemática Aplicada de la EPS de Gandia. Igualmente me gustaría agradecer al Dr. Etienne E. Kerre y al Dr. Stefan Schulte por su amabilidad durante mi estancia en Gante y por todo lo que aprendí de ellos.

En cuarto lugar, me gustaría mencionar a toda la gente que ha hecho mi vida fuera de la universidad mucho más agradable y divertida: a Alberto y Yeyes; a Oña, Antonio, Manu, Patxy, Rosa, Pepe (que repiten), Aguayo y Cris; a Ramón, Jesús, y Debla y Javi; a Vania; a Bellvis, Toni, Patxi, Borso y Escri; y también de, forma general, a la pandilla russafera.

Por último, y no por ello menos importante, por su tan sincero cariño y apoyo y por más razones que páginas tiene este libro, me gustaría expresar mi más profundo agradecimiento a María, y a Gerardo.

Abstract

Image filtering is an essential image processing task for almost every computer vision system where images are used for automatic analysis or for human inspection. In fact, noise contaminating an image may be a major drawback for most other image processing tasks like, for instance, image analysis, edge detection or pattern and/or object recognition and hence, it should be reduced.

In the last years, the interest in using colour images has grown dramatically in a variety of applications. Therefore, colour image filtering has become an interesting area of research. It has been widely observed that colour images have to be processed taking into account the existing correlation among image channels. Probably, the most well-known approach in this sense is the vector approach. Earliest vector filtering solutions as, for instance, the vector median filter (VMF) or the vector directional filter (VDF), are based on the theory of robust statistics and as a consequence, they are able to perform a robust filtering. Unfortunately, these techniques are non-adaptive to local image statistics which implies that the processed images are usually blurred in edges and image details. To overcome this drawback, a number of adaptive vector processing solutions have been recently proposed.

This PhD dissertation undertakes two main tasks: (i) the study of fuzzy metrics applicability in colour image filtering tasks and (ii) the design of new colour image filtering solutions that take advantage of the observed interesting fuzzy metrics and fuzzy logic properties. Extensive experimental results presented in this dissertation have shown that fuzzy metrics and fuzzy logic are useful to design both non-adaptive and adaptive filtering techniques which are competitive with respect to recent state-of-the-art filters. Moreover, as it is demonstrated in several filter designs introduced in this dissertation, an interesting advantage of fuzzy metrics is that they provide a simple mechanism to simultaneously handle multiple distance criteria.

Resumen

El filtrado de imagen es una tarea fundamental para la mayoría de los sistemas de visión por computador cuando las imágenes se usan para análisis automático o, incluso, para inspección humana. De hecho, la presencia de ruido en una imagen puede ser un grave impedimento para las sucesivas tareas de procesamiento de imagen como, por ejemplo, la detección de bordes o el reconocimiento de patrones u objetos y, por lo tanto, el ruido debe ser reducido.

En los últimos años el interés por utilizar imágenes en color se ha visto incrementado de forma significativa en una gran variedad de aplicaciones. Es por esto que el filtrado de imagen en color se ha convertido en un área de investigación interesante. Se ha observado ampliamente que las imágenes en color deben ser procesadas teniendo en cuenta la correlación existente entre los distintos canales de color de la imagen. En este sentido, la solución probablemente más conocida y estudiada es el enfoque vectorial. Las primeras soluciones de filtrado vectorial, como por ejemplo el filtro de mediana vectorial (VMF) o el filtro direccional vectorial (VDF), se basan en la teoría de la estadística robusta y, en consecuencia, son capaces de realizar un filtrado robusto. Desafortunadamente, estas técnicas no se adaptan a las características locales de la imagen, lo que implica que usualmente los bordes y detalles de las imágenes se emborronan y pierden calidad. A fin de solventar este problema, varios filtros vectoriales adaptativos se han propuesto recientemente.

En la presente Tesis doctoral se han llevado a cabo dos tareas principales: (i) el estudio de la aplicabilidad de métricas difusas en tareas de procesamiento de imagen y (ii) el diseño de nuevos filtros para imagen en color que sacan provecho de las propiedades de las métricas difusas y la lógica difusa. Los resultados experimentales presentados en esta Tesis muestran que las métricas difusas y la lógica difusa son herramientas útiles para diseñar técnicas de filtrado, tanto no adaptativas como adaptativas, que son competitivas respecto a otras técnicas en el estado del arte. Además, como se demuestra en varios de los filtros diseñados en esta Tesis, una ventaja interesante de las métricas difusas es que proporcionan un mecanismo sencillo para manejar simultáneamente múltiples criterios de distancia.

Resum

El filtrat d'imatge és una tasca fonamental per a la majoria dels sistemes de visió per ordinador quan les imatges s'usen per a l'anàlisi automàtica o, fins i tot, per a la inspecció humana. De fet, la presència de soroll en una imatge pot ser un greu impediment per a les successives tasques de processament d'imatge com, per exemple, la detecció de vores o el reconeixement de patrons o objectes i, per tant, el soroll ha de ser reduït.

En els darrers anys l'interés per utilitzar imatges en color s'ha vist incrementat de forma significativa en una gran varietat d'aplicacions. És per açò, que el filtrat d'imatge en color s'ha convertit en una àrea d'investigació interessant. S'ha observat àmpliament que les imatges en color han de ser processades tenint en compte la correlació existent entre els distints canals de color de la imatge. En este sentit, la solució probablement més coneguda i estudiada és l'enfocament vectorial. Les primeres solucions de filtrat vectorial, com per exemple el filtre de mediana vectorial (VMF) o el filtre direccional vectorial (VDF), es basen en la teoria de l'estadística robusta i, en conseqüència, són capaços de realitzar un filtrat robust. Desafortunadament, estes tècniques no s'adapten a les característiques locals de la imatge, la qual cosa implica que usualment les vores i detalls de les imatges s'esborrallen i perden qualitat. A fi de resoldre este problema, uns quants filtres vectorials adaptatius s'han proposat recentment.

En la present Tesi Doctoral s'han dut a terme dos tasques principals: (i) l'estudi de l'aplicabilitat de mètriques difuses en tasques de processament d'imatge i (ii) el disseny de nous filtres per a imatge en color que trauen profit de les propietats de les mètriques difuses i la lògica difusa. Els resultats experimentals presentats en esta Tesi mostren que les mètriques difuses i la lògica difusa són ferramentes útils per a dissenyar tècniques de filtrat, tant no adaptatives com adaptatives, que són competitives respecte d'altres tècniques en l'estat de l'art. A més, com es demostra en alguns dels filtres dissenyats en esta Tesi, un avantatge interessant de les mètriques difuses és que proporcionen un mecanisme senzill per a utilitzar simultàniament múltiples criteris de distància.

Presentation

Image filtering is probably the most common image processing task. Filtering an image or a signal means, in general, to transform that image/signal into a more appropriate one for a particular purpose. Image filtering is commonly applied to eliminate or reduce the noise that may be present in an image and that can alter the structured information contained in it. Indeed, noise filtering is the process of estimating the original image information from noisy data, what makes that the filtering problem can be seen as a problem of information interpretation. In fact, noise contaminating an image may be a grave drawback for most other image processing tasks as, for instance, image analysis, edge detection or pattern and/or object recognition. As a consequence, image filtering becomes an essential step in any computer vision system where images are used for automatic analysis or, even, for human inspection.

First image filtering solutions were developed for gray-scale, one-channel, images. These solutions were usually designed to remove a specific type of noise. Lots of papers can be found in the literature describing image filter designs that use different approaches to process images. One of the most well-known approaches are fuzzy filters. Fuzzy sets and fuzzy logic tools are able to deal with uncertainty and, since images are highly non-stationary in edges and it is difficult to distinguish between noise and edge pixels, these tools were proved to be highly appropriate for image filtering tasks. As a result, a number of fuzzy filtering solutions were published.

In the last years, the interest in using multichannel signals, and in particular colour images, has impressively grown in a variety of applications. Therefore, colour image filtering became an interesting area of research. The earliest solutions to filter colour images were componentwise approaches that used some gray-scale image filter in each colour channel. In this way, each channel was processed independently from the other channels. However, it is known that the existing correlation among the image channels should be taken into account. Otherwise, many colour artefacts and other undesired effects may appear in the processed images. This implied the need of specific colour image filtering solutions.

One of the most studied approaches for colour image processing is the vector approach. According to this approach, each image pixel is treated as

a vector comprised of the colour components and the image is treated as a vector field. Therefore, all image channels are jointly processed and the correlation among the image channels is necessarily taken into account. The first vector filtering solutions as, for instance, the vector median filter (VMF) or the vector directional filter (VDF), are based on the theory of robust statistics. These vector filters are able to perform a robust filtering. That is, they are able to efficiently suppress noise. However, the operation made by these vector filters in each image location is fixed, i.e., they are non-adaptive to local image statistics. It has been widely observed that non-adaptive processing usually results in blurred edges and image details. To overcome this drawback, a number of adaptive vector processing solutions have been recently proposed to adapt the filter to varying image characteristics and noise statistics, and to obtain good performance in real-life applications.

The adaptive processing of colour images have been approached using different techniques and tools. The most recent approaches can be classified according to the technique used to approach adaptiveness. Among these techniques we can find (i) techniques based on weighting coefficients, (ii) techniques that perform a multiple filtering, (iii) switching filtering techniques, (iv) techniques for Gaussian noise smoothing, and (v) fuzzy filtering techniques.

This PhD thesis aims at developing new colour image filtering solutions based on the usage of fuzzy logic and fuzzy metrics. Fuzzy metrics is a mathematical tool that has been extensively studied from the theoretical point of view. However, despite their interesting theoretical properties they have been few times used in real applications. The main objectives pursued by this PhD thesis are two: First, to study the applicability of fuzzy metrics in colour image filtering tasks and to determine in which cases fuzzy metrics may present some advantages over classical metrics; and second, to design new colour image filtering solutions that use fuzzy metrics and fuzzy logic and that take advantage of the observed interesting fuzzy metrics properties.

In order to achieve these objectives the work done within this PhD thesis has been divided into two stages: First, we have implemented some variants of vector filters that use some fuzzy metric instead of the classical metrics or measures they originally used. By analyzing both the proposed vector filters and the observed performance differences in front of their classical versions, we will conclude in which cases and from which viewpoints fuzzy metrics may be more appropriate; second, new colour image filters using fuzzy metrics will be developed. The novel filtering solutions will exploit the interesting properties of fuzzy metrics in order to take full advantage of their usage.

This dissertation is divided into three parts where each part consists of several chapters. Please note that each chapter is followed by the bibliographic references used in it.

Part I includes preliminaries concerning the area of research of this dissertation. Chapter 1 describe the state-of-the-art of colour image filtering.

Chapter 2 introduces some basic concepts about fuzzy sets and fuzzy logic intended to illustrate the reader who is unfamiliar with the fuzzy theory. In addition, Chapter 2 also includes the state-of-the-art of fuzzy topology and fuzzy metrics stressing the importance of the concept of fuzzy metric due to George and Veeramani which is used in this dissertation.

Part II presents the contributions made in this PhD thesis. The novel filtering designs and techniques proposed in this dissertation are presented as a set of articles/contributions that have been published/submitted in/to international journals or conferences. Each contribution, that is included as a chapter of this dissertation in Chapters 4-12, is a self-contained paper that presents the proposed filtering technique, the realized experiments, the achieved results and the drawn conclusions. Notice that due to the self-contained nature of the papers, probably some contents may be repeated along the document. However, in spite of this, we have preferred to include the original content of each published/submitted paper for the best understanding of the reader. Previously to the contributions, Chapter 3 includes a summary of all the contributions presented in Chapters 4-12 where the main content of each contribution is briefly explained.

Finally, Part III presents the conclusions obtained and some possible future research lines.

Table of Contents

Abstract vii

Resumen viii

Resum ix

Presentation xi

Part I Preliminaries

1 State-of-the-art of vector filtering for colour images 3
- 1.1 Nonlinear filtering techniques 4
- 1.2 Order statistics filtering techniques 5
- 1.3 Multivariate data ordering scheme 5
- 1.4 Classical vector filtering techniques 10
- 1.5 Adaptive colour image filters 14
- 1.6 Objective assessment of colour image filters performance 18

References 23

2 Fundamentals of fuzzy sets, fuzzy logic, fuzzy topology and fuzzy metrics 27
- 2.1 Concept of fuzzy set 27
- 2.2 Principles of fuzzy logic 28
- 2.3 Principles of fuzzy topology 30
- 2.4 Probabilistic metric spaces 32
- 2.5 Fuzzy metric spaces of Kaleva and Seikkala 33
- 2.6 Fuzzy metric spaces of Kramosil and Michalek 34
- 2.7 Fuzzy metric space of George and Veeramani 35

References 37

Part II Contributions

3 Summary of contributions ... 41
3.1 Contribution (i): A new vector median filter based on fuzzy metrics ... 42
3.2 Contribution (ii): Fuzzy bilateral filtering for color images ... 44
3.3 Contribution (iii): A fast impulsive noise color image filter using fuzzy metrics ... 46
3.4 Contribution (iv): Fuzzy directional distance vector filter ... 48
3.5 Contribution (v): Local self-adaptive impulsive noise filter for color images using fuzzy metrics ... 50
3.6 Contribution (vi): New adaptive vector filter using fuzzy metrics ... 52
3.7 Contributions (vii)-(viii): Isolating impulsive noise pixels in colour images by peer group techniques ... 54
3.8 Contribution (ix): A new fuzzy impulse noise detection method for colour images ... 56

References ... 59

4 Contribution (i) ... 61
S. Morillas, V. Gregori, G. Peris-Fajarnés, P. Latorre, A new vector median filter based on fuzzy fetrics, *ICIAR05, Lecture Notes in Computer Science* 3656 (2005) 81-90. ... 61
Abstract ... 61
4.1 Introduction ... 61
4.2 An appropriate Fuzzy Metric ... 62
4.3 Image Filtering ... 65
4.4 Experimental results ... 66
Conclusions ... 68

References ... 71

5 Contribution (ii) ... 73
S. Morillas, V. Gregori, A. Sapena, Fuzzy bilateral filtering for colour images, *ICIAR06, Lecture Notes in Computer Science* 4141 (2006) 138-145. ... 73
Abstract ... 73
5.1 Introduction ... 73
5.2 Bilateral Filtering ... 74
5.3 Fuzzy Metric approach ... 75
5.4 Fuzzy Bilateral Filtering ... 76
5.5 Experimental results ... 77
Conclusions ... 78

References ... 83

6 Contribution (iii) 85
S. Morillas, V. Gregori, G. Peris-Fajarnés, P. Latorre, A fast impulsive noise colour image filter using fuzzy metrics, *Real-Time Imaging: Special issue on multichannel image processing* 11 5-6 (2005) 417-428. 85
Abstract 85
6.1 Introduction 85
6.2 Fast Similarity Based Impulsive Noise Reduction Filter (FSVF) 87
6.3 Proposed Fuzzy Metric 89
6.4 Proposed filtering 91
6.5 Experimental results 93
Conclusions 101

References 105

7 Contribution (iv) 107
S. Morillas, V. Gregori, J. Riquelme, B. Defez, G. Peris-Fajarnés, Fuzzy directional distance vector filter, *WILF07, Lecture Notes in Artificial Intelligence*, 4578, 355-361. 107
Abstract 107
7.1 Introduction 107
7.2 A fuzzy metric for vector processing 110
7.3 Experimental results 112
Conclusions 123

References 125

8 Contribution (v) 127
S. Morillas, V. Gregori, G. Peris-Fajarnés, A. Sapena, Local self-adaptive impulsive noise filter for colour images using fuzzy metrics, *accepted for publication in Signal Processing* .. 127
Abstract 127
8.1 Introduction 127
8.2 Central Privileging Approach 129
8.3 Proposed Local Self-Adaptive Filter 131
8.4 Experimental Results and Assessment 134
Conclusions 140

References 141

9 Contribution (vi) 143
S. Morillas, V. Gregori, G. Peris-Fajarnés, A. Sapena, New adaptive vector filter using fuzzy metrics, *accepted for publication in Journal of Electronic Imaging* 143

Abstract 143
9.1 Introduction 143
9.2 A Fuzzy Metric Approach 145
9.3 Proposed filtering 147
9.4 Experimental Study and Performance Comparison 148
Conclusions 153

References 159

10 Contribution (vii) 163
S. Morillas, Fuzzy metrics and peer groups for impulsive noise reduction in colour images, *in Proceedings of 14th European Signal Processing Conference EUSIPCO 2006*, 4-8 September 2006, Florence (Italy) 163
Abstract 163
10.1 Introduction 163
10.2 An appropriate fuzzy metric 164
10.3 Peer Groups in the fuzzy context 165
10.4 Proposed filtering technique 165
10.5 Experimental results 168
Conclusions 169

References 173

11 Contribution (viii) 175
S. Morillas, V. Gregori, G. Peris-Fajarnés, Isolating impulsive noise pixels in colour images by peer group techniques, *accepted for publication in Computer Vision and Image Understanding* 175
Abstract 175
11.1 Introduction 175
11.2 Switching Vector Filters and Peer Groups 176
11.3 Fuzzy metrics peer groups and fuzzy distances 178
11.4 Proposed detection and filtering of corrupted pixels 180
11.5 Experimental results 185
Conclusions 200
Appendix: Computational complexity analysis 200

References 205

12 Contribution (ix) 209
S. Morillas, S. Schulte, E.E. Kerre, G. Peris-Fajarnés, A new fuzzy impulse noise detection method for colour images, *SCIA07, Lecture Notes in Computer Science, 4522 (2007) 492-501* 209
Abstract 209

12.1 Introduction 209
12.2 Fuzzy impulse noise detection 210
12.3 Image denoising method 214
12.4 Parameter setting and experimental results 215
Conclusions 218

References 219

Part III Conclusions and Future Work

Conclusions and future work 223

Part I

Preliminaries

1 State-of-the-art of vector filtering for colour images

In any digital colour image, some pixel colour values may have been altered due to the presence of noise. The general objective of the different noise filtering structures is to eliminate the wrong observations or, at least, to reduce their influence, without affecting those colours that have not been perturbed by noise.

Commonly, two noise types that may corrupt colour images are considered (see Section 1.6). On the one hand, the noise associated to the camera sensor, also called thermal noise, and, on the other hand, the noise that may be introduced during the image transmission through a noisy channel [45]. The camera sensor noise is usually modelled as additive *white* Gaussian noise. Transmission noise is commonly modelled as impulsive noise. Impulsive noise corruption process affects only some image pixels by changing one or more colour components of the affected pixel by values which usually significantly deviates from the originals.

Several filtering techniques have been proposed over years of research. Among the proposed techniques, we can find some linear processing techniques which are mathematically simple and can be designed and implemented easily. These techniques have been used during years due to their simplicity and sufficient performance in several applications. Most of these techniques operate under the assumption that the signal under processing can be represented by means of a stationary model and so, they try to optimize the appropriate parameters for such a model. However, many problems in the area of image processing cannot be efficiently solved by using linear techniques. Unfortunately, linear processing techniques have some lacks for image processing tasks because they cannot deal with the non-linearities of the image formation model and they cannot take into account the non-linear features of human visual system (HVS) [41].

Image signals are composed of flat regions and sharp edges which bear important information for visual perception. Filters which are able to preserve image borders and details are highly appropriate for image filtering and enhancement. Unfortunately, most of linear signal processing techniques tend to blur borders and degrade other image details [45].

1.1 Nonlinear filtering techniques

The need of dealing with complex nonlinear systems, joint with the availability of a higher computational capacity, implied the reevaluation of conventional filtering techniques. New algorithms and techniques that take advantage of the higher computational capacity and that manage more realistic assumptions were needed. To this end, nonlinear signal processing techniques have been introduced. Theoretically, nonlinear techniques are able to suppress non-gaussian noise, to preserve borders and image details and to eliminate image defects that were introduced during image formation or transmission through nonlinear channels. In spite of the recent growth of this kind of techniques and the appearance of new theoretical results, tools and applications, nonlinear filtering techniques still lack a unifying theory. Instead of that, each class of non-linear operators has its own mathematical tools that provide a reasonably good performance analysis. As a result, multiple nonlinear signal processing techniques have appeared in the literature. Nowadays, the following classes of nonlinear processing techniques can be identified [45]:

- Polynomial based techniques
- Homomorphic techniques
- Mathematical morphology based techniques
- Order statistics based techniques

Polynomial filters, specially second order Volterra filters (quadratic filters), have been used for colour image filtering, non-linear channels modelling in telecommunications and for multichannel geophysical signal processing.

Homomorphic filters and their extensions are one of the firsts non-linear filtering classes and have been used in digital image and signal processing. This class of filters has been used in several applications such as dependent multiplicative noise suppression, colour image processing and multichannel satellite image processing. Their basic feature is that they use nonlinearities, mainly logarithms, to transform nonlinearly related signals to additive signals and then they process them with lineal filters. The linear filter output should be transformed according to the inverse nonlinear operation.

Mathematical morphology can be geometrically described in terms of the made actions or the applied operators over binary, monochrome or colour images. The geometric description depends on small synthetic images named structural elements. This form of mathematical morphology, sometimes called structural morphology, is useful for image processing and analysis. Morphology filters can be found in image processing and analysis applications. Specifically, its applications areas include image filtering, image enhancement and edge detection.

In the following section, the family of the order statistics filters is described. This family of filters is probably the most popular family of nonlinear filters and this is the family of filters involved in the work carried out in this dissertation.

1.2 Order statistics filtering techniques

The theoretical basis of order statistics filters is the theory of robust statistics [11]. There exist a number of filters for colour images within this family where the most well-known filter is the vector medial filter (VMF) [3]. The idea behind this approach is that unrepresentative or outlying observations in sets of colour vectors can be seen as contaminating the data and thus they may represent a drawback for further processing tasks. Therefore, order statistics filters provide a tool for interpreting and classifying outliers and methods for managing them by rejecting them or by applying procedures to reduce their influence. Outliers can be defined as scalar (univariate) data samples tough outliers exist in multivariate data such as colour vectors. The basic notion of outlier is an statistically unexpected observation in terms of some basic model that can be extended to multivariate data and, in particular, to colour images. However, the expression of this notion and the determination of the appropriate procedures to identify and adequate outliers are not direct when the operation is made over multivariate data, mainly due to the fact that an outlier in multivariate data does not have a simple representation as a sample that deviates the maximum from the rest of the samples.

In univariate data analysis, there exists a natural data ordering that makes possible extreme values to be identified and the distance from these extreme values to the center can be computed easily. In this way, the problem of identifying and isolating any individual values which are atypical with respect to the rest of the set is simple. Because of this, numerous filtering techniques which are based on univariate data ordering have been introduced in the literature.

The popularity and extensive use of scalar order statistics filters lead to the introduction of similar techniques for the analysis of multivariate data and multichannel signals, as colour vectors and colour images. However, in order to design this sort of filters, the problem of multivariate data ordering should be solved.

In the following, we present some basic techniques to approach the problem of multivariate data ordering and some classical vector filters that use these ordering techniques.

1.3 Multivariate data ordering scheme

A multivariate signal is a signal where each sample has multiple components. This kind of signal is also called vector valued, multichannel or multispectral signal. Colour images are typical examples of multichannel signals. A digital colour image is usually represented by the three primaries in the RGB colour space as a two-dimensional three-variate (three-channel) signal. Let $\mathbf{X}$ denote a p-dimensional random variable and $\mathbf{X} = [X_1, X_2, \ldots, X_p]^\tau$ a p-dimensional vector of random variables and let $\mathbf{x}_1, \mathbf{x}_2, \ldots, \mathbf{x}_n$ denote n ran-

dom samples in $\mathbf{X}$. Each sample $\mathbf{x}_i$ is a vector of p-dimensional observations $\mathbf{x}_i = [x_{i1}, x_{i2}, \ldots, x_{ip}]^\tau$. The objective is to order the n values $(\mathbf{x}_1, \mathbf{x}_2, \ldots, \mathbf{x}_n)$ according to some ordering scheme.

The concept of data ordering that is natural in the univariate case cannot be directly extended to the multidimensional case since there is no unambiguous, universally accepted, way to order n multivariate samples. However, there are some ways to order the data which are called sub-ordering principles in multivariate data [5, 6]. Sub-ordering principles are categorized in four types:

– Marginal ordering or M-ordering
– Conditional ordering or C-ordering
– Partial ordering or P-ordering
– Reduced (aggregated) ordering or R-ordering

1.3.1 M-ordering

According to the marginal ordering or M-ordering scheme, samples are ordered along each of the p-dimensions independently, so obtaining:

$$\mathbf{x}_{1(1)} \leq \mathbf{x}_{1(2)} \leq \ldots \leq \mathbf{x}_{1(n)} \tag{1.1}$$
$$\mathbf{x}_{2(1)} \leq \mathbf{x}_{2(2)} \leq \ldots \leq \mathbf{x}_{2(n)} \tag{1.2}$$
$$\cdots \quad \cdots \tag{1.3}$$
$$\mathbf{x}_{p(1)} \leq \mathbf{x}_{p(2)} \leq \ldots \leq \mathbf{x}_{p(n)} \tag{1.4}$$

where $\mathbf{x}_{i(k)}$ denotes the value of the i-th channel that is ranked in k-th position.

Accordingly, the vector $\mathbf{x}_1 = [x_1(1), x_2(1), \ldots, x_p(1)]^\tau$ consists of the minimal elements in each dimension and the vector $\mathbf{x}_n = [x_1(n), x_2(n), \ldots, x_p(n)]^\tau$ consists of the maximal elements in each dimension, where τ denotes transpose matrix. The marginal median is defined as $\mathbf{x}_{\nu+1} = [x_1(\nu+1), x_2(\nu+1), \ldots, x_p(\nu+1)]^\tau$ for $n = 2\nu + 1$. Notice that this vector may not correspond to any original data. However, in the scalar case, there is a one-to-one correspondence between the original samples $\mathbf{x}_i$ and the order statistics $\mathbf{x}(i)$.

1.3.2 C-ordering

In the conditional ordering case or C-ordering, multivariate data samples are ordered conditionally on one of the sets of marginal observations. Thus, one of the marginal components is ranked and the other components of each vector are listed according to the position of their ranked component. Assuming that the first dimension is ranked, the ordered samples would be represented as follows:

$$\mathbf{x}_{1(1)} \leq \mathbf{x}_{1(2)} \leq \ldots \leq \mathbf{x}_{1(n)} \tag{1.5}$$

$$\mathbf{x}_{2[1]} \leq \mathbf{x}_{2[2]} \leq \ldots \leq \mathbf{x}_{2[n]} \tag{1.6}$$

$$\cdots \quad \cdots \tag{1.7}$$

$$\mathbf{x}_{p[1]} \leq \mathbf{x}_{p[2]} \leq \ldots \leq \mathbf{x}_{p[n]} \tag{1.8}$$

where $\mathbf{x}_1(i), i = 1, 2, \ldots, n$ are the marginal order statistics of the first dimension, and $\mathbf{x}_j[i], j = 1, 2, \ldots, p, i = 1, 2, \ldots, n$ are the quasi-ordered samples in dimensions $j = 2, \ldots, p$ conditionally on the marginal ordering of the first dimension. Indeed, these components are not ordered, but simply listed according to their ordered component in each case. In the two dimensional case, the second non-ordered dimension is called *concomitant* with respect to the first, ordered, dimension.

The main advantage of C-ordering is its simplicity, since only one scalar ordering has to be computed. The disadvantage is that, since only the information in one of the colour channels is used, it is assumed that most of the information is borne by the used channel. If this assumption is not fulfilled then important information will be lost. For instance, we can consider the problem of ordering signals in the YIQ colour space. If a C-ordering is realized on the luminance channel Y then the chromatical information in channels I and Q is ignored for the ordering. Therefore, any advantages of identifying outliers using chromatical information would be lost.

1.3.3 P-ordering

According to the P-ordering scheme, subsets of the data are grouped forming *minimal convex hulls*. The first convex hull is formed such that the perimeter contains a minimum number of points and the resulting hull contains all other points in the given set. The points along this perimeter are denoted as *p-order group 1*. These points form the most extreme group. The perimeter points are then discarded and the process repeats. The new perimeter points are denoted as *p-order group 2* and then removed in order to the process to be continued. P-ordering procedure can be used to isolate outliers but this ordering does not provide any ordering within the groups and thus it is not easily expressed in analytical terms. In addition, the determination of the convex hull is conceptually and computationally difficult, specially when working with high-dimensional data. Therefore, P-ordering is rather infeasible for implementation in colour image processing.

1.3.4 R-orden

In the R-ordering or reduced (aggregated) ordering, each multivariate observation $\mathbf{x}_i$ is associated to a scalar value by means of some combination of the

component sample values. Then univariate ordering can be realized over the resulting scalar values. Thus, the set $\mathbf{x}_1, \mathbf{x}_2, \ldots, \mathbf{x}_n$ can be ordered in terms of the associated scalar values $R_i = R(\mathbf{x}_i), i = 1, 2, \ldots, n$.

In contrast to M-ordering, the aim of R-ordering is to carry out some overall ordering among the original multivariate data. By means of this ordering, the multivariate ordering is reduced to a simple ordering operation in a transformed data set. This ordering cannot be interpreted as the classical ordering between scalar data because there is no sample that can be considered as the minimum or maximum of the data. Since the multivariate ordering is based on the use of a reduction function $R(.)$, points that diverge from the *center* in opposite directions may be in the same order ranks. In addition, by utilizing a reduction function to realize the multivariate ordering, useful information may be lost. Due to the fact that distance functions have a natural mechanism for identification of outliers, the reduction function most frequently used is the generalized (Mahalanobis) distance [6].

$$R(x, \overline{x}, \Gamma) = (x - \overline{x})^{\tau} \Gamma^{-1} (x - \overline{x}) \tag{1.9}$$

where $\overline{x}$ is a location parameter for the data set, or underlying distribution, in consideration and Γ is a dispersion parameter with Γ^{-1} used to apply a differential weighting to the components of the multivariate observation inversely related to the population variability. Parameters of the reduction function may take arbitrary values, such as $\overline{x} = 0$ and $\Gamma = I$ or can be assigned the true mean μ or dispersion S settings. If these values are unknown their standard estimates given by

$$\overline{x} = \frac{1}{n} \sum_{i=1}^{n} x_i \tag{1.10}$$

and

$$S = \frac{1}{n-1} \sum_{i=1}^{n} (x_i - \overline{x})(x_i - \overline{x})^{\tau} \tag{1.11}$$

can be used instead.

Depending on the location parameter used in the ordering procedure the following schemes can be distinguished:

a) Mean R-ordering:
Given a set of n multivariate samples $\mathbf{x}_i, i = 1, 2, \ldots, n$ in a processing window and given $\overline{\mathbf{x}}$ the sample mean, the mean R-ordering is defined as:

$$(\mathbf{x}_{(1)}, \mathbf{x}_{(2)}, \ldots, \mathbf{x}_{(n)} : \overline{\mathbf{x}}) \tag{1.12}$$

where $(\mathbf{x}_{(1)}, \mathbf{x}_{(2)}, \ldots, \mathbf{x}_{(n)})$ is the ordering defined by $d_i^2 = (\mathbf{x}_i - \overline{\mathbf{x}})^{\tau} (\mathbf{x}_i - \overline{\mathbf{x}})$ and $(d_{(1)}^2 \leq d_{(2)}^2 \leq \ldots \leq d_{(n)}^2)$.

b) Marginal median R-ordering:
Given a set of n multivariate samples $\mathbf{x}_i, i = 1, 2, \ldots, n$ in a processing window and given $\mathbf{x}_m$ the marginal mean of the considered data set, the marginal mean R-ordering is defined as:

$$(\mathbf{x}_{(1)}, \mathbf{x}_{(2)}, \ldots, \mathbf{x}_{(n)} : \mathbf{x}_m) \tag{1.13}$$

where $(\mathbf{x}_{(1)}, \mathbf{x}_{(2)}, \ldots, \mathbf{x}_{(n)})$ is the ordering defined by $d_i^2 = (\mathbf{x}_i - \mathbf{x}_m)^\tau (\mathbf{x}_i - \mathbf{x}_m)$ and $(d_{(1)}^2 \leq d_{(2)}^2 \leq \ldots \leq d_{(n)}^2)$.

c) Center sample R-ordering:
Given a set of n multivariate samples $\mathbf{x}_i, i = 1, 2, \ldots, n$ in a processing window and given $\mathbf{x}_c$ the center sample in the window, the center sample R-ordering is defined as:

$$(\mathbf{x}_{(1)}, \mathbf{x}_{(2)}, \ldots, \mathbf{x}_{(n)} : \mathbf{x}_c) \tag{1.14}$$

where $(\mathbf{x}_{(1)}, \mathbf{x}_{(2)}, \ldots, \mathbf{x}_{(n)})$ is the ordering defined by $d_i^2 = (\mathbf{x}_i - \mathbf{x}_c)^\tau (\mathbf{x}_i - \mathbf{x}_c)$ and $(d_{(1)}^2 \leq d_{(2)}^2 \leq \ldots \leq d_{(n)}^2)$.

The R-ordering scheme is specially useful for the detection of outliers in multivariate data samples. Moreover, unlike the M-ordering, data are treated as vectors instead of processing each component separately. Unlike the C-ordering, the R-ordering scheme gives the same importance to each colour channel. Finally, the R-ordering is simpler than the P-ordering and easier to implement. Therefore, the R-ordering is the most used sub-ordering principle in multivariate data analysis and, in particular, in multichannel image processing.

1.3.5 An appropriate vector ordering procedure for colour image processing

The sub-ordering principles above explained can be used to rank any sort of multivariate data. However, to define an ordering scheme which is attractive for colour image processing, this should be focused to the ordering of colour image vectors. Such an ordering should satisfy the following criteria [45]:

1. The proposed scheme should be useful from a robust estimation point of view, allowing the extension of the scalar order statistics filters to the multivariate domain.
2. The scheme should preserve the notion of varying levels of *extremeness* that was present in the scalar ordering case.
3. The proposed ordering should take into account the sort of multivariate data to process. Thus, since the RGB colour space will be commonly used, equal importance should be given to the three channels and all the information contained in each channel has to be considered.

On the basis of these three criteria, the ordering scheme that has been proposed and extensively used in the literature is a variation of the R-ordering that utilizes some appropriate measure of distance or similarity between colour vectors [3, 20, 26, 27, 45, 56]. For each sample in the set $\mathbf{x}_i$, an aggregated measure with respect to all other samples in the set is defined as follows:

$$R_a(\mathbf{x}_i) = \sum_{j=1}^{n} R(\mathbf{x}_i, \mathbf{x}_j) \tag{1.15}$$

This aggregated measure $R_{ai} = R_a(\mathbf{x}_i)$ is used to define the vector ordering, so that:

$$R_{a1} \leq R_{a2} \leq \ldots \leq R_{an} \tag{1.16}$$

$$\mathbf{x}_{(1)} \leq \mathbf{x}_{(2)} \leq \ldots \leq \mathbf{x}_{(n)} \tag{1.17}$$

Using this ordering scheme, ordered samples $\mathbf{x}_{(i)}$ have a one-to-one correspondence with respect to the original samples. This is an important difference with respect to the M-ordering. In addition, all sample components are given equal importance, unlike the C-ordering.

The proposed ordering scheme is focused to take into account the interrelations among the multivariate samples since the distance or similarity between each couple of samples in the data set is used. The output of the ordering procedure depends critically on both the data set and the function $R(\mathbf{x}_i, \mathbf{x}_j)$ used to compute the distance or similarity between each pair of samples.

1.4 Classical vector filtering techniques

Classical vector filtering methods are based on the above ordering scheme to rank the data samples by using different distance or similarity functions. These methods are briefly described in the following.

1.4.1 Vector medial filter VMF [3]

Let I denote a multichannel image and W a processing window of finite length n. Image vector within the window W are denoted as $I_j, j = 1, ..., n$. The *distance* between two vectors I_i, I_j is denoted as $\rho(I_i, I_j)$ where ρ is usually a classical metric. For each vector in the filtering window, an aggregated distance with respect to all other vectors in the window is computed. The scalar value $R_i = \sum_{j=1}^{n} \rho(I_i, I_j)$, is the distance associated to the vector I_i. The ordering of the R_i's:

$$R_{(1)} \leq R_{(2)} \leq ... \leq R_{(n)}, \tag{1.18}$$

where $R_{(k)}$ denotes the value ranked in the k-th position, implies the ordering of the vectors I_i's:

$$I_{(1)} \leq I_{(2)} \leq ... \leq I_{(n)} \tag{1.19}$$

Given this order, the output of the VMF is $I_{VMF} = I_{(1)}$.

In the design of the VMF, the distance between two colour vectors is commonly measured using some distance measure derived from the generalized Minkowski metric or L_γ norm which is defined as:

$$\rho(I_i, I_j) = \left(\sum_{k=1}^{m} |I_i(k) - I_j(k)|^\gamma \right)^{\frac{1}{\gamma}} \tag{1.20}$$

where γ characterizes the used metric. Minkowski metric includes the *city-block* distance ($\gamma = 1$) or L_1 metric, the Euclidean metric ($\gamma = 2$) or $_2$ metric and the *chess-board* distance ($\gamma = \infty$) or L_∞ norm. Other commonly used distance and similarity measures are reviewed in [26, 45].

Since the VMF output is the sample associated to the minimum aggregated distance, VMF minimizes the distance to other vector samples in the filtering window. VMF can be derived either as a maximum likelihood estimate (MLE) when the underlying probability densities of input samples are bi-exponential or by using vector order-statistics techniques. Thus, the VMF is scale, translation and rotation invariant [45]. As well, if the vector dimension is 1 then the VMF reduces to the scalar median. Since the impulse response of the VMF is zero, it excellently suppresses impulsive noise [3, 26]. Other approaches have been introduced with the aim of speeding up the VMF by using a linear approximation of the Euclidean distance [7] and by designing a fast algorithm when using the L_1 norm [8]. On the other hand, the VMF has been extended to fuzzy numbers in [10] by means of *certain fuzzy distances*.

1.4.2 Extended vector median filter EVMF [3, 58]

The combination of the VMF with linear techniques has been used to improve its performance in the suppression of gaussian noise [3, 58]. The filter built as a combination of the VMF and the arithmetic mean filter (AMF) is the so called extended vector median filter (EVMF) [3, 45, 58]. This filter selects between the VMF output I_{VMF} and the AMF output $\overline{I}$ according to the following rule:

$$I_{EVMF} = \left\{ \begin{array}{ll} \overline{I} & if \sum_{j=1}^{n} \rho(\overline{I}, I_j) \leq \sum j = 1^n \rho(I_{VMF}, I_j) \\ I_{VMF} & \text{otherwise} \end{array} \right\} \tag{1.21}$$

where $\overline{I}$ denotes the AMF output is computed as $\overline{I} = \frac{1}{n}\sum_{j=1}^{n} I_j$. As in the VMF case, different distance measures between colour vectors can be considered. The EVMF performs so that near edges or areas with high details it behaves like the VMF. Thus, it avoids the blurring that would be generated by the AMF in these cases. In the smooth parts of the image, it more often chooses the mean vector to be the output value what results in improved noise attenuation, above all, from the Gaussian noise reduction point of view.

1.4.3 Basic vector directional filter BVDF [56]

Directional filtering employs a vector ordering technique that uses the angle between two colour vectors as the distance criterion for the ordering. Since vectors are multichannel samples, they are characterized by their magnitude and direction. These characteristics can be used for designing multichannel image filters.

In the BVDF each vector is associated to an aggregated angular distance measure

$$\alpha_i = \sum_{j=1}^{N} A(\mathbf{I}_i, \mathbf{I}_j) \quad i = 1, 2, \ldots, N, \tag{1.22}$$

where

$$A(\mathbf{I}_i, \mathbf{I}_j) = arccos\left(\frac{\mathbf{I}_i \cdot \mathbf{I}_j}{|\mathbf{I}_i| \cdot |\mathbf{I}_j|}\right) \tag{1.23}$$

represents the angle between the vectors $\mathbf{I}_i$ and $\mathbf{I}_j$.

Using α_i as ordering criterion:

$$\alpha_{(1)} \leq \alpha_{(2)} \leq \ldots \leq \alpha_{(N)}, \tag{1.24}$$

the ordering of the samples in the window is

$$I_{(1)} \leq I_{(2)} \leq \ldots \leq I_{(N)} \tag{1.25}$$

The lowest rank that is associated to the lowest aggregated angular distance represents the BVDF output $I_{BVDF} = I_{(1)}$.

Since BVDF outputs the sample in the set which is the closest one to the other vectors in the set in terms of the angular distance used, and since directionality is associated to chromaticity in the RGB colour space, the BVDF may outperform the VMF in terms of chromaticity preservation.

1.4.4 Generalized directional distance filter GVDF

The set of the r lowest ranked samples in the BVDF ordering constitutes the generalized vector directional filter scheme which is defined as follows:

$$I_{GVDF} = \{I_{(1)}, I_{(2)}, \ldots, I_{(r)}\} \tag{1.26}$$

The GVDF output is a set of r samples whose angle difference α_i, $i = 1, 2, \ldots, N$ is relatively low so that vectors with atypical directions, and thus atypical chromaticities, are removed from the set. In order to choose the final filter output, GVDF should be used in conjunction with some other filter processing vectors according to its magnitude. Usually, GVDF is used as a second level filter so that its output is an input for some other filter that computes the final output.

1.4.5 Directional distance filter DDF [20]

The directional distance filtering (DDF) technique uses simultaneously both distance criteria employed by VMF and BVDF. This implies that this filtering technique is much more computationally demanding than the VMF and BVDF. On the other hand, because of the use of both magnitude and angular distances the DDF outperforms the VMF and BVDF since it is able to reject vectors with atypical magnitude and vectors with atypical direction from the data set and so, it is able to generate a more robust output.

The distance criterion used by the DDF is expressed as a weighted product of the aggregated Minkowski distances and the aggregated angular distances as follows:

$$\Omega_i = \left(\sum_{j=1}^{N} \left(\sum_{k=1}^{m} |I_i(k) - I_j(k)|^{\gamma} \right)^{\frac{1}{\gamma}} \right)^{1-p} \cdot \left(\sum_{j=1}^{n} A(\mathbf{I}_i, \mathbf{I}_j) \right)^{p} \tag{1.27}$$

for $i = 1, 2, \ldots, n$ and $p \in [0, 1]$. DDF output is the sample $I_{(1)}$ associated to the minimum $\Omega_{(1)}$ so that $\Omega_{(1)} \leq \Omega_{(2)} \leq \ldots \Omega_{(N)}$. In the above expression p is a parameters that tunes the importance given to the magnitude criterion in front of the angular criterion. If $p = 0$, DDF behaves as VMF whereas for $p = 1$ DDF nehaves as BVDF.

1.4.6 Hybrid Filters

The introduction of the DDF was based on a set of heuristic filters that tried to simultaneously minimize the distance functions employed by VMF and BVDF. Directional hybrid filters HVFs [45] operate on direction and magnitude of vectors independently and then they apply a combination to generate the output.

The filter HVF_1 makes a non-linear combination of VMF and BVDF according to the following rule:

$$I_{HVF_1} = \left\{ \begin{array}{ll} I_{VMF} & \text{if } I_{VMF} = I_{BVDF} \\ \left(\frac{|I_{VMF}|}{|I_{BVDF}|}\right) I_{BVDF} & \text{otherwise} \end{array} \right\} \tag{1.28}$$

where I_{VMF} denotes the VMF output, I_{BVDF} denotes the BVDF output and $|\cdot|$ denotes the vector magnitude.

Another more complex hybrid filter HVF_2 [45] that also uses the AMF is designed as follows:

$$I_{HVF_2} = \left\{ \begin{array}{ll} I_{VMF} & \text{if } I_{VMF} = I_{BVDF} \\ I_{out1} & \text{if } \sum_{i=1}^{N} |\mathbf{x}_i - I_{out1}| \leq \sum_{i=1}^{N} |\mathbf{x}_i - I_{out2}| \\ I_{out2} & \text{otherwise} \end{array} \right\} \tag{1.29}$$

where

$$I_{out1} = \left(\frac{|I_{VMF}|}{|I_{BVDF}|}\right) I_{BVDF}, \tag{1.30}$$

$$I_{out2} = \left(\frac{|I_{AMF}|}{|I_{BVDF}|}\right) I_{BVDF} \tag{1.31}$$

and I_{AMF} denotes the AMF output.

The HVF_1 and HVF_2 hybrid filters are able to outperform VMF and BVDF since they generate a vector output that is appropriate both from the point of view of vector magnitude and from the point of view of vector direction. However, they are much more computationally expensive since they need to compute the outputs from VMF, BVDF and AMF in the HVF_2 case.

1.5 Adaptive colour image filters

Classical vector filters mentioned in the previous section have the drawback that the operations made in any image location are fixed, i.e. they are non-adaptive to local features. It has been widely observed that non-adaptive processing usually results in blurred edges and image details. To overcome this drawback, a number of vector processing solutions have been proposed to adapt the filter to varying image characteristics and noise statistics, and to obtain good performance in real-life applications such as microarray image processing, television image enhancement, virtual restoration of artworks, and colour video processing. Some recent overviews on vector processing schemes can be found in [26, 27, 28, 45]. In this section we summarize some of the most well-known and/or recent colour image adaptive filters that are more closely related to the content of this PhD thesis.

The adaptive processing of colour images have been approached using different techniques. The most recent approaches can be classified according to the technique used to approach adaptiveness. Among these techniques we can

find (i) techniques based on weighting coefficients, (ii) techniques that perform a multiple filtering, (iii) switching filtering techniques, (iv) techniques for Gaussian noise smoothing, and (v) fuzzy filtering techniques. In the following sections we comment the state-of-the-art works that belong to these classes.

1.5.1 Techniques based on weighting coefficients

Some recent adaptive techniques are based on computing weights that are associated to each pixel in the filtering window. Afterwards, the computed weights are used to compute the output so that the noise is reduced and the original signal structures, such as edges and fine details are preserved. The output is usually calculated either as a weighted average of the vectors in the window or as the output of a weighted vector median procedure.

The main difference between the methods based on weighting coefficients is the technique used to compute the weights. The technique in [24] uses an off-line optimization algorithm to compute appropriate weights. The works in [30, 29, 34, 54] use different statistics to compute the weights. Polynomial functions are used in [4]. The work in [25] computes the weights in order to achieve a better chromaticity preservation and the method in [35] calculates the weights by means of evolutionary computation.

The filtering techniques based on weighting coefficients are appropriate when noise statistics and image characteristics are unknown since these techniques can adapt for removing different types of noise.

1.5.2 Techniques using multiple filtering

Some filtering techniques aim at computing the filter output by using different sub-filters simultaneously or by dividing the filtering procedure in two or more steps. Instead of trying to find a method able to provide an appropriate output in any circumstance, these techniques use different sub-filtering methods or filtering phases and their particular outputs are used to compute the final output.

Within this approach, the methods in [40, 22, 23, 57] propose to simultaneously use several sub-filters in each image location. Then, in [40], the filter output is computed by choosing the most appropriate sub-filter output, and in [22, 23, 57] by fusing the sub-filter outputs. The works [22, 23] use a rational function to perform the fusion and the work in [57] uses a genetic algorithm. The method in [38] analyzes similarities between the neighboring colour vectors in a two-step impulse detection procedure and, a three-step procedure including robust estimation, vector partition and weighted filtering, has been recently introduced in [39].

Since a flexible performance is achieved by using the different sub-filtering techniques or filtering steps, this kind of filters may also be used when the noise and image characteristics are unknown.

1.5.3 Switching filtering techniques

A type of noise that frequently contaminates digital images is the so called impulsive, or fat-tailed, noise (see Section 1.6). Impulsive noise corruption process affects only some pixels in the image while leaving other pixels unchanged.

The switching filtering techniques aim to affect only the noisy pixels while keeping the desired image structures (edges and fine details) unchanged. When the images are contaminated with impulsive noise the switching approaches are widely used due to its sufficient performance and proven computational simplicity. Existing switching vector filters use different approaches to identify impulses. For example, the solution in [1] performs a cluster analysis of the pixel neighbourhood and detects as *noisy* those pixels whose membership degree to the clusters is low. The t-student test vector median filter (tTVMF) [9] assumes that the neighbors of the colour under processing follow some multi-normal distribution. Each colour component is checked to belong to the corresponding distribution with a high confidence level. If at least one of the components does not belong to the distribution then the corresponding colour pixel is considered as noisy. The work in [18] uses a fuzzy inference system which takes as inputs some statistical measures of the pixel under processing and its neighbourhood. The method in [31] checks the difference between the input vector and the mean of several lowest ranked vectors. The method in [32] performs the detection by using the input vector, the vector median, the vector mean and their aggregated distances to other vectors inside the filter window. The work in [33] extends the former work in [32] by utilizing the variance approximation in the multivariate case. The solution presented in [34] uses center weighting coefficients and the methods in [38, 51, 52] use a similarity based vector ordering to increase the importance of the pixel under consideration in the impulse detection process.

The *peer group* concept in [12, 16, 21] has also been used to detect and filter out impulsive noise. The filters introduced in [12, 21] use the difference between the *peer group* of the pixel under consideration and other *peer groups* in its neighbourhood to form the detection rule. The work in [17] proposes to use windows of different size to determine the peer region of each pixel and then check the peer region size and shape. In the approach introduced in [53] for a pixel to be declared as *noise-free* it is required to have a *peer group* of a determined size around it.

As commented above, the switching approaches are very useful to process images contaminated with impulsive noise since they are computationally simple and they can provide successful results. However, this filtering is usually not appropriate for suppressing other types of noise such as, for instance, Gaussian noise.

1.5.4 Techniques for Gaussian noise smoothing

The so called Gaussian noise is other type of noise that usually corrupts digital images. Additive Gaussian noise, which is usually introduced during the acquisition process, is characterized by adding to each image pixel channel a random value from a zero-mean Gaussian distribution. The variance of this distribution determines the intensity of the corrupting noise. The zero-mean property allows to remove such noise by locally averaging pixel channel values (see Section 1.6).

Ideally, removing Gaussian noise would involve to smooth the different areas of an image without degrading neither the sharpness of their edges nor their details. Classical linear filters, such as the Arithmetic Mean Filter (AMF) or the Gaussian Filter, smooth noise but blur edges significantly. Adaptive nonlinear methods have been used to approach this problem. The aim of the methods proposed in the literature is to detect edges by means of local measures and smooth them less than the rest of the image to better preserve their sharpness. A well-known method is the anisotropic diffusion introduced in [43]. In this technique, local image variation is measured at every point and pixels from neighborhoods whose size and shape depend on local variation are averaged. Diffusion methods are inherently iterative since the use of differential equations is involved. A non-iterative interesting method, is the bilateral filter (BF) studied in [55]. The output of the BF at a particular location is a weighted mean of the pixels in its neighborhood where the weight of each pixel depends on the spatial closeness and photometric similarity respect to the pixel in substitution. The BF has been proved to perform effectively in Gaussian noise suppression and it has been the object of further studies [13, 15, 48]. In the works in [13, 15, 48] other techniques are proposed to compute the weights used in the averaging.

The above mentioned techniques are specifically designed for the reduction of Gaussian noise and, therefore, they are not able to reduce other kinds of noise such as, for instance, impulsive-like noise.

1.5.5 Fuzzy filtering techniques

Since the images are highly non-stationary in edges and due to the difficulty in distinguishing between noise and edge pixels, fuzzy sets, that are able to deal with uncertainty, are highly appropriate for image filtering tasks. Indeed, the ability of managing uncertainty which is inherently adaptive implies that fuzzy filtering are useful for the suppression of different kinds of noise.

Over the last years a huge amount of fuzzy-based noise reduction methods for gray-scale images were developed [42], e.g. the histogram adaptive fuzzy filter (HAF) [59, 60], the fuzzy impulse noise detection and reduction method (FIDRM) [46], the iterative fuzzy control based filter (IFCF) [14], the adaptive fuzzy switching filter (AFSF) [61], the fuzzy similarity-based filter (FSB) [19], the fuzzy random impulse noise reduction method (FRINRM)

[47] and so on. These fuzzy filters were developed for images corrupted with fat-tailed noise like impulse noise. They use fuzzy adaptive approaches that outperform rank-order filter schemes (such as the median filter). Although these filters are especially developed for grey-scale images, they can be used to filter colour images by applying them on each colour component separately. However, this approach generally introduces many colour artefacts mainly on edge and texture elements.

To overcome these problems several fuzzy filtering approaches for colour images were successfully introduced. The vector median operations are extended to fuzzy numbers in [10]. In [2] a fuzzy rule based system determines the filter output. In [18] a fuzzy inference system (FISF) for detecting impulses in colour images is combined with a switching scheme to select between an identity filter output and the output from a proposed L-filter design. This L-filter is designed to exploit the ordering techniques of the vector median filters. The final output is calculated by using the optimal magnitude and direction of the vectors. The vector median and some fuzzy measures are used in [**?**, 49, 50] for calculating the fuzzy coefficients to determine the output as a weighted average of the inputs. In [36, 37] fuzzy coefficients determine the filter output by selecting the most representative input vector or as the combination of the vectors inside the filter window. The fuzzy impulse noise detection and reduction method for colour images (FIDRMC), studied in [**?**], is one alternative colour method which does not use vectors at all. The result of the detection method, which is applied on each colour component separately, is used to calculate the noise-free colour component differences of each pixel. These differences are then used by the noise reduction method so that the colour component differences are preserved.

1.6 Objective assessment of colour image filters performance

In addition to visual inspection which is inherently subjective, some objective evaluation of filtering performance is needed in order to assess a particular filtering method. A commonly used procedure to objectively assess the performance achieved by any filtering technique is the following.

First, some appropriate test colour image is selected for the processing. Images presenting some interesting characteristics such as the presence of sharp borders, fine details or textured areas can be considered as appropriate for the tests. Figure 1.2 shows several test images, some of them very well-known, that are used by the scientific community and that are also used in this PhD thesis.

Second, the introduction of some kind of noise in the image is simulated. For this, some noise model is used in the simulation. Mainly, two noise types that may corrupt colour images are considered. On the one hand, the noise associated to the camera sensor, also called thermal noise, and, on the

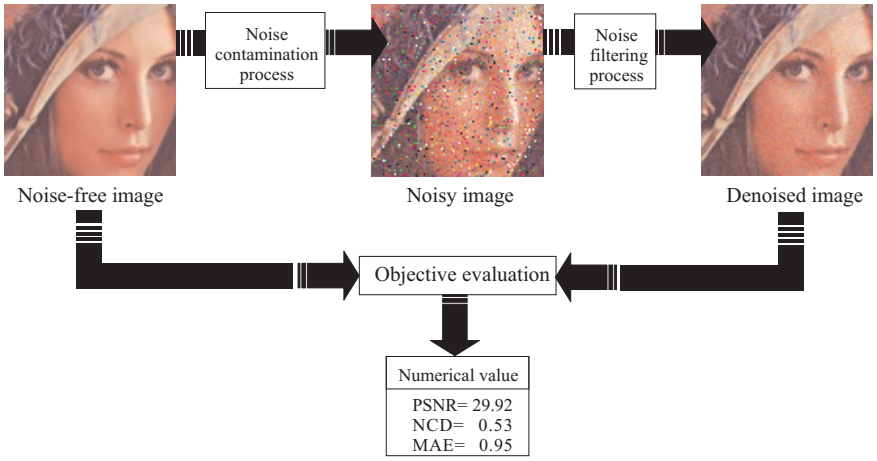

Fig. 1.1. Scheme of a procedure to objectively evaluate a particular filtering method.

other hand, the noise that may be introduced during the image transmission through a noisy channel [45].

The noise associated to the camera sensor or thermal noise is modelled as additive *white* Gaussian noise having the following probability distribution in each colour channel:

$$p(x_n) = \frac{1}{(2\pi\sigma)^{\frac{1}{2}}} e^{\frac{-x^2}{2\sigma^2}} \tag{1.32}$$

where σ denotes the standard deviation of the distribution. This noise is introduced independently in each colour channel however, it can be assumed that all three colour channels have the same average noise magnitude with constant noise variance over the entire image plane.

Transmission noise is commonly modelled as impulsive noise. Impulsive noise corruption process affects only some pixels in the image while leaving other pixels unchanged. Typically, the noise process changes one or more colour components of the affected pixel by replacing its original values with the values which usually significantly deviates from the originals. The most common impulsive noise models consider that the impulse is either an extreme value in the signal range or a random uniformly distributed value within the signal range. For RGB images, these possibilities are represented with the following two well-known models.

In the so-called impulsive noise type I or fixed-value impulsive noise model, the corruption is modeled as follows:

Fig. 1.2. Some classical test images used for filter assessment: (a) Lenna (256×256), (b) Baboon (256 × 256), (c) Peppers (512 × 512), (d) Microscopic (50 × 50), (e) Parrots (256 × 384), (f) Bright Rose(287 × 200), (g) House (256 × 256), (h) Artic Hare (135 × 200), (i) Pills (130 × 200), (j) Boat (576 × 720), and (k) Bird image (900 × 600).

$$\mathbf{F}^* = \begin{cases} \{d_1, F_G, F_B\} & \text{with probability } p \cdot p_1 \,, \\ \{F_R, d_2, F_B\} & \text{with probability } p \cdot p_2 \,, \\ \{F_R, F_G, d_3\} & \text{with probability } p \cdot p_3 \,, \\ \{d_1, d_2, d_3\} & \text{with probability } p \cdot \left(1 - \sum_{i=1}^{3} p_i\right) \,. \end{cases} \tag{1.33}$$

where $\mathbf{F} = \{F_R, F_G, F_B\}$ denotes the original pixel, $\mathbf{F}^*$ denotes the pixel corrupted by the noise process and d_1, d_2, d_3 are independent values equal to 0 or 255 with equal probability. The symbol p is the probability of the noise appearance and $p_i, i = 1, 2, 3$ determine the probability of appearance of the noise in the image channels.

In the so-called impulsive noise type II or random-value impulsive noise model, $\mathbf{F}* = \{d_1, d_2, d_3\}$ is obtained using d_1, d_2, d_3 which are random uniformly distributed independent integer values in the interval $[0, 255]$ with probability p.

Finally, the corrupted image is filtered using the filtering procedure to be assessed and the processed image is compare with the original noise-free image in order to measure the degree in which the output image is similar to the original image. Different functions can be used to measure this similarity. In order to properly assess the quality of the filtering both the noise suppression and the detail preserving abilities have to be evaluated. The *Mean Absolute Error* (MAE) is the most used function to approach the detail-preserving assessment and the *Peak Signal to Noise Ratio* (PSNR) is the function usually used to express the noise suppression ability. In addition, the *Normalized Colour Difference* (NCD) measure is also used since it approaches the human perception [53]. These three objective quality measures have been also used in this dissertation. The mentioned objective quality measures are defined as follows [45]:

$$MAE = \frac{\sum_{i=1}^{N \cdot M} \sum_{q=1}^{Q} \left| F_i^q - \hat{F}_i^q \right|}{N \cdot M \cdot Q} \tag{1.34}$$

$$PSNR = 20 \log \left(\frac{255}{\sqrt{\frac{1}{NMQ} \sum_{i=1}^{N \cdot M} \sum_{q=1}^{Q} \left(F_i^q - \hat{F}_i^q \right)^2}} \right) \tag{1.35}$$

where M, N are the image dimensions, Q is the number of channels of the image ($Q = 3$ for colour images), and F_i^q and $\hat{F}_i^q$ denote the q^{th} component of the original image vector and the filtered image, at pixel position i, respectively, and

$$NCD_{Lab} = \frac{\sum_{i=1}^{N \cdot M} \Delta E_{Lab}}{\sum_{i=1}^{N \cdot M} E^*_{Lab}} \tag{1.36}$$

where $\Delta E_{Lab} = [(\Delta L^*)^2 + (\Delta a^*)^2 + (\Delta b^*)^2]^{\frac{1}{2}}$ denotes the perceptual colour error and $E^*_{Lab} = [(L^*)^2 + (a^*)^2 + (b^*)^2]^{\frac{1}{2}}$ is the *norm* or *magnitude* of the original image colour vector in the $L^*a^*b^*$ colour space.

References

1. H. Allende, J. Galbiati, A non-parametric filter for image restoration using cluster analysis, *Pattern Recognition Letters* 25 8 (2004) 841-847.
2. K. Arakawa, Median filter based on fuzzy rules and its application to image restoration, *Fuzzy Sets and Systems*, 77 1 (1996) 3-13.
3. J. Astola, P. Haavisto, Y. Neuvo, Vector Median Filters, *Proc. IEEE.* 78 4 (1990) 678-689.
4. K.E. Barner, T.C. Aysal, Polynomial weighted median filtering, *IEEE Transactions on Signal Processing*, 54 2 (2006) 636-650.
5. V. Barnett, The ordering of multivariate data. *Journal of royal statistical society A* 139 2 (1976) 331-354.
6. V. Barnett, T. Lewis, *Outliers in multivariate data* , John Wiley and Sons, New York 1994.
7. M. Barni, F. Buti, F. Bartolini, V. Capellini, A Quasi-Euclidean Norm to Speed Up Vector Median Filtering, *IEEE Transactions on Image Processing* 9 10 (2000) 1704-1709.
8. M. Barni, A Fast Algorithm for 1-Norm Vector Median Filtering, *IEEE Transactions on Image Processing* 6 10 (1997) 1452-1455.
9. J. Camacho, S. Morillas, P. Latorre, Efficient impulsive noise suppression based on statistical confidence limits, *Journal of Imaging Science and Technology* 5 6 (2006) 427-436.
10. V. Chatzis, I. Pitas, Fuzzy scalar and vector median filters based on fuzzy distances, *IEEE Transactions on Image Processing* 8 5 (1999) 731-734.
11. H.A. David, *Order Statistics*. John Wiley and Sons, New York 1981.
12. Y. Deng, C. Kenney, MS Moore, BS Manjunath, Peer group filtering and perceptutal color image quantization, *Proceedings of IEEE international symposium on circuits and systems* 4 (1999) 21-4.
13. M. Elad, *On the origin of bilateral filter and ways to improve it*, IEEE Transactions on Image Processing 11 10 (2002) 1141-1151.
14. F. Farbiz and M. B. Menhaj, A fuzzy logic control based approch for image filtering, in *Fuzzy Techniques in Image Processing*, 1st ed., vol. 52, E.E. Kerre and M. Nachtegael, Eds. Heidelberg: Physica Verlag, 2000, pp. 194-221.
15. R. Garnett, T. Huegerich, C. Chui, W. He, *A universal noise removal algorithm with an impulse detector*, IEEE Transactions on Image Processing 14 11 (2005) 1747-1754.
16. G. Hewer, C. Kenney, L. Peterson, A. Van Nevel, Applied partial differential variational techniques, *Proceedings of International Conference on Image Processing ICIP'97*, 3 (1997) 372-375.

17. J. Y. F. Ho, Peer region determination based impulsive noise detection, *Proceedings of International Conference on Acoustics, Speech and Signal Processing ICASSP'03* 3 (2003) 713-716.
18. S. Hore, B. Qiu, and H.R. Wu, Improved vector filtering for color images using fuzzy noise detection, *Optical Engineering* , 42 6 (2003) 1656-1664.
19. I. Kalaykov and G. Tolt, Real-time image noise cancellation based on fuzzy similarity, in *Fuzzy Filters for Image Processing*, 1st ed., vol. 122, M. Nachtegael, D. Van der Weken, D. Van De Ville and E. E. Kerre, Eds. Heidelberg: Physica Verlag, 2003, pp. 54-71.
20. D.G. Karakos, P.E. Trahanias, Generalized multichannel image-filtering structure, *IEEE Transactions on Image Processing* 6 7 (1997) 1038-1045.
21. C. Kenney, Y. Deng, BS Manjunath, G. Hewer, Peer group image enhancement, *IEEE Transactions on Image Processing* 10 2 (2001) 326-334.
22. L. Khriji, M. Gabbouj, Vector median-rational hybrid filters for multichannel image processing, *IEEE Signal Processing Letters*, 6 7 (1999) 186-190.
23. L. Khriji, M. Gabbouj, Adaptive fuzzy order statistics-rational hybrid filters for color image processing, *Fuzzy Sets and Systems*, 128 1 (2002) 35-46.
24. Y. Li, J. Bacca-Rodríguez, G.R. Arce, Weighted median filters for multichannel signals, *in Proc. Int. Conf. Acoustics, Speech and Signal Processing* ICASSP'05 vol. IV, (2005) 157-160.
25. L. Lucchese, S.K. Mitra, A new class of chromatic filters for color image processing: Theory and applications, *IEEE Transactions on Image Processing* , 14 4 (2004) 534-548.
26. R. Lukac, B. Smolka, K. Martin, K.N. Plataniotis, A.N. Venetsanopoulos, Vector Filtering for Color Imaging, *IEEE Signal Processing Magazine, Special Issue on Color Image Processing* 22 1 (2005) 74-86.
27. R. Lukac, K.N. Plataniotis, A taxonomy of color image filtering and enhancement solutions, in *Advances in Imaging and Electron Physics*, (eds.) P.W. Hawkes, Elsevier, 140 (2006) 187-264.
28. R. Lukac and K.N. Plataniotis, *Color Image Processing: Methods and Applications*. Boca Raton, FL., CRC Press / Taylor & Francis, 2006.
29. R. Lukac, K.N. Plataniotis, B. Smolka, A.N. Venetsanopoulos, Generalized Selection Weighted Vector Filters, *EURASIP Journal on applied signal processing: Special Issue on Nonlinear signal and image processing*, 2004 12 (2004) 1870-1885.
30. R. Lukac, B. Smolka, K.N. Plataniotis, A.N. Venetsanopoulos, Selection weighted vector directional filters, *Computer Vision and Image Understanding*, 94 1-3 (2004) 140-167 2004.
31. R. Lukac, Adaptive vector median filtering, *Pattern Recognition Letters* 24 12 (2003) 1889-1899.
32. R. Lukac, K.N. Plataniotis, A.N. Venetsanopoulos, B. Smolka, A Statistically-Switched Adaptive Vector Median Filter, *Journal of Intelligent and Robotic Systems* 42 4 (2005) 361-391.
33. R. Lukac, B. Smolka, K.N. Plataniotis, A.N. Venetsanopoulos, Vector sigma filters for noise detection and removal in color images, *Journal of Visual Communication and Image Representation* 17 1 (2006) 1-26.
34. R. Lukac, Adaptive Color Image Filtering Based on Center Weighted Vector Directional Filters, *Multidimensional Systems and Signal Processing* 15 2 (2004) 169-196.

35. R. Lukac, K.N. Plataniotis, A.N. Venetsanopoulos, Color image image denoising using evolutionary computation, *International Journal of Imaging Systems and Technology* 15 5 (2005) 236-251 .
36. R. Lukac, K.N. Plataniotis, B. Smolka, A.N. Venetsanopoulos, cDNA Microarray Image Processing Using Fuzzy Vector Filtering Framework, *Fuzzy Sets and Systems: Special Issue on Fuzzy Sets and Systems in Bioinformatics*, 152 1 (2005) 17-35.
37. R. Lukac, K.N. Plataniotis, B. Smolka, A.N. Venetsanopoulos, A Multichannel Order-Statistic technique for cDNA Microarray Image Processing, *IEEE Transactions on Nanobioscience* 3 4 (2004) 272-285.
38. Z. Ma, D. Feng, H.R. Wu, A neighborhood evaluated adaptive vector filter for suppression of impulsive noise in color images, *Real-Time Imaging*, 11 5-6 (2005) 403-416.
39. Z. Ma, H.R. Wu, D. Feng, Partition-based vector filtering technique for suppression of noise in digital color images, *IEEE Transactions on Image Processing* , 15 8 (2006) 2324-2342.
40. Z. Ma, H.R. Wu, B. Qiu, A robust structure-adaptive vector filter for color image restoration, *IEEE Transactions on Image Processing* , 14 12 (2005) 1990-2001.
41. D.L. MacAdam, *Visual sensitivities to color differences in daylight*, J. Opt. Soc. Am., 33 (1942) 247-274.
42. M. Nachtegael, D. Van der Weken, D. Van De Ville, E.E. Kerre (eds.): *Fuzzy Filters for Image Processing*, Vol. 122 Springer Physica Verlag, Berlin Heidelberg New York, 2003.
43. P. Perona, J. Malik, Scale-space and edge detection using anisotropic diffusion, *IEEE Transactions on Pattern Analysis and Machine Intelligence* 12 5 (1990) 629-639.
44. I. Pitas, A.N. Venetsanopoulos, *Nonlinear digital filters: Principles and Applications*, Kluwer Academic Publishers, Boston, 1990.
45. K.N. Plataniotis, A.N. Venetsanopoulos, *Color Image processing and applications*, Springer-Verlag, Berlin, 2000.
46. S. Schulte, M. Nachtegael, V. De Witte, D. Van der Weken, E. E. Kerre, A Fuzzy Impulse Noise Detection and Reduction Method, *IEEE Transactions on Image Processing*, 15 5 (2006) 1153-1162.
47. S. Schulte, V. De Witte, M. Nachtegael, D. Van der Weken, E. E. Kerre, Fuzzy random impulse noise reduction method, *Fuzzy Sets and Systems*, 158 3 (2007) 270-283.
48. Y. Shen, K. Barner, *Fuzzy vector median-based surface smoothing*, IEEE Transactions on Visualization and Computer Graphics 10 3 (2004) 252-265.
49. Y. Shen. K.E. Barner, Marginal fuzzy median and fuzzy vector median filtering of color images, *in Proc. 37th Annual Conf. Inf. Sciences & Systems* (2003).
50. Y. Shen, K.E. Barner, Optimization of fuzzy vector median filters, *in Proc. 38th Annual Conf. Inf. Sciences & Systems* (2004).
51. B. Smolka, R. Lukac, A. Chydzinski, K.N. Plataniotis, W. Wojciechowski, Fast adaptive similarity based impulsive noise reduction filter, *Real-Time Imaging, Special Issue on Spectral Imaging* 9 4 (2003) 261-276.
52. B. Smolka, K.N. Plataniotis, A. Chydzinski, M. Szczepanski, A.N. Venetsanopoulos, K. Wojciechowski, Self-adaptive algorithm of impulsive noise reduction in color images, *Pattern Recognition* 35 8 (2002) 1771-1784.

53. B. Smolka, A. Chydzinski, Fast detection and impulsive noise removal in color images, *Real-Time Imaging* 11 5-6 (2005) 389-402.
54. M. Szczepanski, B. Smolka, K.N. Plataniotis, A.N. Venetsanopoulos, On the distance function approach to color image enhancement, *Discrete Applied Mathematics*, 139 1-3 (2004) 283-305.
55. C. Tomasi, R. Manduchi, *Bilateral filter for gray and color images*, Proc. IEEE International Conference Computer Vision, 1998, 839-846.
56. P.E. Trahanias, D. Karakos, A.N. Venetsanopoulos, Directional processing of color images: theory and experimental results, *IEEE Trans. Image Process.* 5 6 (1996) 868-880.
57. H.H. Tsai, P.T. Yu, Genetic-based fuzzy hybrid multichannel filters for color image restoration, *Fuzzy Sets and Systems*, 114 2 (2000) 203-224.
58. T. Viero, K. Oistamo, Y. Neuvo, Three-dimensional median-related filters for color image sequence filtering, *IEEE Transactions on Circuits and Systems for Video Technology* 4 2 (1994) 129-142.
59. J. H. Wang and H. C. Chiu, An adaptive fuzzy filter for restoring highly corrupted images by histogram estimation, *Proceedings of the National Science Council -Part A* 23 (1999) 630-643.
60. J.H. Wang, W.J. Liu, L.D. Lin, Histogram-Based Fuzzy Filter for Image Restoration, *IEEE Transactions on Systems man and cybernetics part B-cybernetics*, 32 2 (2002) 230-238.
61. H. Xu, G. Zhu, H. Peng and D. Wang, Adaptive fuzzy switching filter for images corrupted by impulse noise, Pattern Recognition Letters, 25 (2004) 1657-1663.

2 Fundamentals of fuzzy sets, fuzzy logic, fuzzy topology and fuzzy metrics

2.1 Concept of fuzzy set

A fuzzy set is a *set with a smooth boundary*. Fuzzy set theory generalized classical set theory to allow partial membership. Let us introduce fuzzy sets by analyzing the following limitation of classical sets. A set in classical set theory always has a sharp boundary because membership in a set is a black-and-white concept, i.e., an object either completely belongs to the set or does not belong to the set at all. Even though some sets have sharp boundaries (e.g., the set of married people), many others to not have sharp boundaries (e.g. the set of happily married couples or the set of good graduate schools). Fuzzy set theory addresses this limitation by allowing membership in a set to be a matter of degree. The degree of membership in a set is expressed by a number between 0 and 1; 0 means entirely not in the set, 1 means completely in the set and a number in between means partially in the set. In this way, a smooth and gradual transition from the regions outside the set to those in the set can be described.

A fuzzy set is thus defined by a function that maps object in domain of concern to their membership values in the set. Such a function is called the *membership function*. More specifically, the concept of fuzzy set was introduced by Lofti. A. Zadeh [33] in 1965. A fuzzy set is mathematically defined as an assignment of a value in $[0, 1]$ to each element of a classical set. This value represents the degree of membership of the element to the fuzzy set. Formally, given a non-empty set X, every application $A : X \to [0, 1]$ is called a *fuzzy set* on X. X is named support set of the fuzzy set. The fact that there is a lot of real-life situations where objects do not have a totally defined membership criterion motivates the appearance of this concept and suggests its usefulness. Fuzzy sets have been extensively studied from the theoretical point of view and the developed fuzzy set theory includes concepts regarding relations between classical and fuzzy sets, operations in fuzzy sets, types and design of membership functions, properties of fuzzy sets, and so on (see [19, 31, 32]).

2.2 Principles of fuzzy logic

The term fuzzy logic has been used in two different senses. In a narrow sense, fuzzy logic refers to a logical system that generalizes the two-valued logic for reasoning under uncertainty. In a broad sense, fuzzy logic refers to all of the theories and technologies that employ fuzzy sets. Even though this broad sense, we can explain the basics of fuzzy logic by using the following three basic concepts: (1) the above commented fuzzy sets, (2) linguistic variables and (3) fuzzy if-then rules.

2.2.1 Linguistic variables

Having introduced the fundamental concept of fuzzy set, it is natural to see how it can be used. Like a conventional set, a fuzzy set can be used to describe the value of a variable. For example, the sentence "The amount of trading is heavy" uses a fuzzy set "Heavy" to describe the quantity of the stock market trading in one day. More formally it is expressed as: *TradingQuantity is Heavy*. The variable *TradingQuantity* in this example demonstrates an important concept in fuzzy logic: the linguistic variable. A linguistic variable enables its value to be described both qualitatively by a linguistic term (i.e., a symbol serving as the name of a fuzzy set) and quantitatively by a corresponding membership function (which expresses the meaning of the fuzzy set). The linguistic term is used to express concepts and knowledge in human communication, whereas membership function is useful for processing numeric input data.

A linguistic variable is like a composition of a symbolic variable (a variable whose value is a symbol) and a numeric variable (a variable whose value is a number). In our example about stock market trading activities, there are certainly many other linguistic descriptions about the trading quantity such as "light", "moderate", "heavy", and so on. All these linguistic, descriptions, that are indeed unprecise and vague, can be managed using fuzzy sets. In this way, the numerical value of the variable *TradingQuantity* is expressed in terms of its membership degrees to the fuzzy sets used in the representation. Figure 2.1 shows an example of representation of the linguistic descriptions of the variable *TradingQuantinty* using fuzzy sets.

2.2.2 Fuzzy if-then rules

Among all the techniques developed used fuzzy sets, the fuzzy *if-then* rule (or, in short, fuzzy rule) is by far the most visible one due to its wide range of successful applications. Fuzzy rules have been applied to many disciplines such as control systems, decision making, pattern recognition and system modelling [4, 31, 32]. Fuzzy rules also play a critical role in industrial applications ranging from consumer products, robotics, manufacturing, process control, medical imaging, to financial trading.

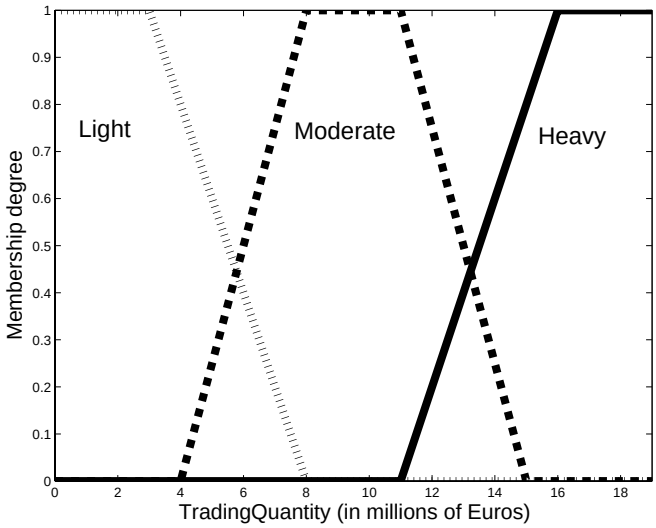

Fig. 2.1. Example of representation of the linguistic descriptions of the variable *TradingQuantinty* using fuzzy sets.

Fuzzy rule-based inference can be understood from several viewpoints. Conceptually, it can be understood using the metaphor of drawing a conclusion using a panel of experts. Mathematically, it can be viewed as an interpolation scheme. Formally, it is a generalization of a logic inference called *modus ponens*.

In classical logic, if we know a rule is true and we also know the antecedent of the rule is true, then it can be inferred, by *modus ponens*, that the consequent of the rule is true. For example, suppose we know that the rule R1 below is true:

Rule 1 *R1:*
`IF` *the annual income of a person is greater than 120000 Euros*
`THEN` *the person is rich*

We also know that the following statement is true: *Maria's annual income is 121000 Euros.*

Based on *modus ponens*, classical logic can deduce that the following statement is also true: *Maria is rich.*

One limitation of *modus ponens* is that it cannot deal with partial matching. To illustrate this, let us consider rule R1 and the case of a person whose income is 119000 Euros. People would say that that person would be somewhat rich however, *modus ponens* would deduce that that person is *not rich*. This problem has two causes: (1) the antecedent of R1 does not represent a smooth transition into the rich category that is often exhibited in human

reasoning, and (2) *modus ponens* cannot deal with a situation where the antecedent of a rule is partially satisfied.

Viewing such a limitation, fuzzy rule-based inference generalizes *modus ponens* to allow its inferred conclusion to be modified by the degree in which the antecedent is satisfied. This is the essence of fuzzy rule-based inference.

Analogously to the classical logic case, the structure of a fuzzy rule has two components: an if-part (also referred to as the antecedent) and a then-part (also referred to as the consequent).

Fuzzy Rule 1 *Structure of a fuzzy rule:*
`IF` <*antecedent*>
`THEN` <*consequent*>

Since it is not the aim of this text to explain in detail how the fuzzy rules and the fuzzy rule-based systems work, in the following, a brief and informal explanation about the basis of their working procedure is given. The interested reader can find extensive information in the existing literature, for instance in [31, 32, 33].

According to above, classical logic, by using a classical rule, is able to determine whether the consequent of the rule is satisfied or not just by looking if the antecedent is satisfied or not. In the case of fuzzy logic, by using a fuzzy rule and when some knowledge about the degree in which the antecedent is satisfied is available, the degree in which the consequent is satisfied can be computed by means of a procedure called *fuzzy rule-based inference*. Any fuzzy rule-based system commonly uses multiple fuzzy rules. The way in which fuzzy-rule based systems work can be explained in a simple way as follows. Let us assume that the fuzzy rule-based system is composed by a set of input variables, a set of fuzzy rules and a set of output variables whose values are to be computed by the system. The system working procedure can be divided in three phases: (1) First, on the basis of the numerical values of the input variables, the degree in which the antecedents of the fuzzy rules are satisfied are computed. This phase is named *fuzzyfication*; (2) Second, the fuzzy rule-based inference procedure is used to compute the degree in which the consequents are satisfied; (3) Finally, output variable values, that may not be fuzzy, are computed by using the degree in which the consequents of the fuzzy rules are satisfied. This phase is named *defuzzyfication*.

2.3 Principles of fuzzy topology

In the following, the concept of fuzzy metric is explained within the context of fuzzy theory.

One of the first research topics that appeared in fuzzy mathematics is fuzzy topology. The first work on fuzzy topology was done by C. L. Chang in 1968 [3]. According to Chang, a topology τ in X is a family of fuzzy sets

on X that is closed for unions and for finite intersections. This family should also contain the constant functions 0 and 1. Notice that this is the most used concept both in the existing literature and the developed theory, however it is not the only one. So, from another point of view, R. Lowen [21, 22] requests, in addition, that τ should contain all constant functions. This topology is the so-called *laminated topology* [29]. Therefore, unlike Chang's topology, a laminated topology does not constitutes a generalization of the topology in the classical sense. On the other hand, Goguen [11] and Hutton [16] generalize the notion given by Chang by replacing the fuzzy range $I = [0, 1]$ by a complemented lattice L, so implying the so-called concept of L-topology.

One of the most interesting and most studied problems in fuzzy topology is to obtain an appropriate notion of fuzzy metric space. Recall that the study of metric spaces is based on the notion of distance between points, however, in many real situations this distance cannot be exactly determined. This problem, that belongs to the fuzzy field, was previously approached from the point of view of the probability theory. Indeed, in 1942 K. Menger [23] introduced the so-called probabilistic metric spaces. In these spaces, if $d(x, y)$ is the distance between two points x and y then the distribution function $F_{xy}(t)$ represents the probability of the distance between x and y to be lower or equal than t. Later, Schweizer and Sklar [27, 28] followed with the study of these spaces and recently many other works have been published on this issue [2], [24], [25], [26], [27], [30].

It is easy to notice that the notion of fuzzy topology has been studied from many different points of view and the same is true in almost all fuzzy concepts that have been studied. Regarding fuzzy metrics, also many authors have approached this concept from many different points of view. Here we make a simple classification of these works into two large groups: On the one hand, a first group would be constituted by those works where a (pseudo-)metric on X is treated as a function $d : \Omega \times \Omega \longrightarrow \mathbb{R}$ where $\Omega \subset I^X$ ($I = [0, 1]$) that satisfies some axioms which are *analogous* to the ones of the classic metrics case. Among these works we point out the works made by Deng Zi-ke [5], Erceg [8], Hu [15], and Artico and Moresco [1]. The most interesting problems within this line are: (i) investigating in which way a fuzzy metric induces a fuzzy (quasi-)uniformity in the sense of [17] and a fuzzy topology [8, 5, 15], (ii) determining the criteria for (pseudo-)metrization [7, 8, 15], (iii) defining the properties of the disjunction in metric spaces [8, 1, 15, 6], (iv) and defining the properties of completion and bounding [1, 6]. On the other hand, a second group would include those works where the distance between objects is fuzzy. The most relevant results published in this line are due to Kaleva and Seikkala [18] and Kramosil and Michalek [20].

In our work, we use the concept of fuzzy metric space given by George and Veeramani. This concept is defined as an appropriate modification of the concept of fuzzy metric from Kramosil and Michalek [20].

Now we make a chronological summary to show the most relevant results concerning the theory of fuzzy metrics.

2.4 Probabilistic metric spaces

Previous to the introduction of the fuzzy theory in the field of metric spaces the study of metrics was associated to probability concepts. In this sense, in 1942 Menger [23] defined the concept of probabilistic metric space as follows.

Definition 2.4.1 *Let X be an arbitrary non-empty set. Let F_{pq} be a family of distribution functions that satisfy the following:*

(M1) $F_{pq}(0) = 0$
(M2) If $p = q$, *then* $F_{pq}(x) = 1\ \forall x > 0$
(M3) If $p \neq q$, *then* $F_{pq}(x) < 1$ *for some* $x > 0$
(M4) $F_{pq} = F_{qp}$
(M5) $F_{pr}(x + y) \geq T(F_{pq}(x), F_{qr}(y))\ \forall p, q, r \in X$ *and* $\forall x, y \in \mathbb{R}$, *where* $T : [0, 1] \times [0, 1] \to [0, 1]$ *is a function that satisfies:*
  (i) $T(a, b) = T(b, a)$
  (ii) $T(a, b) \leq T(c, d)$ *if* $a \leq c\ y\ b \leq d$
  (iii) $T(a, 1) > 0$ *if* $a > 0$, *and* $T(1, 1) = 1$

Let us note that a distribution function $F : \mathbb{R} \to [0, 1]$ is a left-continuous non-decreasing application so that $\inf_{x \in X}\{F(x)\} = 0$ and $\sup_{x \in X}\{F(x)\} = 1$. The statistic metric F_{pq} can be interpreted as the probability of the distance between two points p and q to be lower than x.

Schweizer and Sklar [28] replaced the above condition (M5) by the following:

$$If\ F_{pq}(x) = 1 \text{ and } F_{qr}(y) = 1, \text{ then } F_{pr}(x + y) = 1$$

The resulting space is called weak probabilistic metric space and it generalizes the Menger's probabilistic spaces.

Schweizer and Sklar, also introduced the concept of continuous t-norm which has an important relevance in the development of fuzzy metric space theory.

Definition 2.4.2 *A binary operation* $* : [0, 1] \times [0, 1] \to [0, 1]$ *is a continuous t-norm if it satisfies the following conditions:*

(i) $*$ *is continuous, associative and commutative*
(ii) $a * 1 = a \forall a \in [0, 1]$
(iii) $a * b \leq c * d$ *if* $a \leq c$ *and* $b \leq d$, $a, b, c, d \in [0, 1]$

From this definition, Schweizer and Sklar defined a probabilistic metric space as follows.

Definition 2.4.3 *A probabilistic metric space is a pair (X, F) where X is an arbitrary set and F is an application on $X \times X$ to the set of all possible distribution functions and satisfies:*

(1) $F_{xy}(t) = 1\ \forall t > 0$ *if and only if* $x = y$
(2) $F_{xy}(0) = 0$
(3) $F_{xy} = F_{yx}$
(4) $If\ F_{xy}(t) = 1$ *and* $F_{yz}(s) = 1$, *then* $F_{xz}(t + s) = 1$

A Menger space $(X, F, *)$ is a probabilistic metric space along with a t-norm that satisfies the condition

$$F_{xz}(t + s) \geq F_{xy}(t) * F_{yz}(s)$$

2.5 Fuzzy metric spaces of Kaleva and Seikkala

Since the uncertainty regarding the existing distance between two points is more related to the fuzzy notion than to randomness, Kaleva and Seikkala [18] extended the concept of metric space to the novel fuzzy theory by associating the distance between two points to a fuzzy number.

Definition 2.5.1 *A fuzzy number is an application $x : \mathbb{R} \to [0, 1]$ that associates a degree of membership to each real number.*

A fuzzy number is said to be convex if $x(t) \geq min\{x(s), x(r)\}$ where $s \leq t \leq r$.

For $0 < \alpha \leq 1$ and a fuzzy number x, its α-sets of level $[x]_\alpha$ are defined by

$$[x]_\alpha = \{u : x(u) \geq \alpha\}$$

As a result, x is convex if and only if $[x]_\alpha$ is a convex set in $\mathbb{R}\ \forall \alpha \in]0, 1]$

Additionally, if it exists an element $u \in \mathbb{R}$ so that $x(u) = 1$, then the fuzzy number x is *normal*.

A fuzzy number is said to be non-negative if $x(u) = 0\ \forall u < 0$.

The set of all right semi-continuous non-negative normal convex fuzzy numbers is denoted as $\mathbb{G}$.

Using the above notation Kaleva and Seikkala define the concept of fuzzy metric space as follows.

Definition 2.5.2 *Let X be a non-empty arbitrary set and let $d : X \times X \to \mathbb{G}$ be an application. Let $L, R : [0, 1] \times [0, 1] \to [0, 1]$ be two symmetric applications that are nondecreasing in both arguments and that satisfy $L(0, 0) = 0$ and $R(1, 1) = 1$. We denote by*

$$[d(x, y)]_\alpha = [\lambda_\alpha(x, y), \rho_\alpha(x, y)]\ for\ x, y \in X,\ 0 < \alpha \leq 1$$

The vector (X, d, L, R) is named KS fuzzy metric space and d is a KS fuzzy metric if the following conditions are satisfied:

(a) $d(x, y) = 0$ *if and only if* $x = y$
(b) $d(x, y) = d(y, x)$ *for any* $x, y \in X$
(c) for any $x, y, z \in X$,
(1) $d(x, y)(s + t) \geq L\left(d(x, z)(s), d(z, y)(t)\right)$
if $s \leq \lambda_1(x, z),\ t \leq \lambda_1(z, y)$ *and* $s + t \leq \lambda_1(x, y)$
(2) $d(x, y)(s + t) \leq R\left(d(x, z)(s), d(z, y)(t)\right)$
if $s \geq \lambda_1(x, z),\ t \geq \lambda_1(z, y)$ *y* $s + t \geq \lambda_1(x, y)$

Since non-negative real numbers belong to $\mathbb{G}$, if we assume that

$$L(a, b) = 0 \ \ y \ \ R(a, b) = \begin{cases} 0 & a = b = 0 \\ 1 & \text{otherwise} \end{cases}$$

then the usual metric space may be considered as a KS fuzzy metric space. Additionally, definition 2.5.2 generalizes Menger's spaces as it is proven in the following note.

Note 2.5.3 *Let $(X, F, *)$ a Menger space. We define $d : X \times X \to \mathbb{G}$ as*

$$d(x, y)(t) = \begin{cases} 0 & t < t_{xy} = sup\{t : F_{xy}(t) = 0\} \\ 1 - F_{xy}(t) & t \geq t_{xy} \end{cases}$$

If we take $R(a, b) = 1-((1 - a) * (1 - b))$ and $L(a, b) = 0$, then (X, d, L, R) is a KS fuzzy metric space and so, a Menger space can be considered as KS fuzzy metric space.

In the case that these conditions are fulfilled , then $(X, F, *)$ is a Menger space where $a * b = 1 - R(1 - a, 1 - b)$ for any $a, b \in [0, 1], x, y \in X, s \in \mathbb{R}$,

$$F_{xy}(s) = \begin{cases} 0 & s \leq \lambda_1(x, y) \\ 1 - d(x, y)(s) & s \geq \lambda_1(x, y) \end{cases}$$

Moreover, $(X, F, *)$ is named associated Menger space.

2.6 Fuzzy metric spaces of Kramosil and Michalek

Kramosil and Michalek [20] defined the concept of fuzzy metric space by generalizing the concept of probabilistic metric space to the fuzzy theory in the following way:

Definition 2.6.1 *[12, 20]*

A tern $(X, M, *)$ is said to be a fuzzy metric space of Kramosil and Michalek (KM fuzzy metric space) if X is an arbitrary set, $*$ is a continuous t-norm and M is a fuzzy set on $X \times X \times [0, +\infty[$ that satisfies the following conditions for any $x, y, z \in X$ and $t, s > 0$:

(KM1) $M(x, y, 0) = 0$
(KM2) $M(x, y, t) = 1\ \forall t > 0$ *if and only if* $x = y$
(KM3) $M(x, y, t) = M(y, x, t)$
(KM4) $M(x, y, t) * M(y, z, s) \leq M(x, z, t + s)$
(KM5) $M(x, y, \cdot) : [0, +\infty[\to [0, 1]$ *is continuous*

2.7 Fuzzy metric space of George and Veeramani

The concept of fuzzy metric introduced by George and Veeramani [10, 9] is the concept that we use in this dissertation. The concept is defined as a modification of the concept introduced by Kramosil and Michalek as follows.

The tern $(X, M, *)$ is a fuzzy metric space if X is a non-empty arbitrary set, $*$ is a continuous t-norm and M is a fuzzy set on $X \times X \times]0, +\infty[$ that satisfies the following axioms for any $x, y, z \in X,\ t, s > 0$:

(GV1) $M(x, y, t) > 0$
(GV2) $M(x, y, t) = 1$ if and only if $x = y$
(GV3) $M(x, y, t) = M(y, x, t)$
(GV4) $M(x, y, t) * M(y, z, s) \leq M(x, z, t + s)$
(GV5) $M(x, y, .) :]0, +\infty[\longrightarrow]0, 1]$ is continuous

In the following, by fuzzy metric space we mean the concept due to George and Veeramani. As usual, we will refer a fuzzy metric space X without explicit mention to the fuzzy metric if it is not necessary.

The fuzzy metric M generates a topology τ_M in X. The topology τ_M has as a basis the family of *open balls* $\{B_M(x, r, t) : x \in X,\ 0 < r < 1,\ t > 0\}$ where $B_M(x, r, t) = \{y \in X : M(x, y, t) > 1 - r\}$.

A sequence $\{x_n\}_{n=1}^{\infty}$ in X is called a Cauchy sequence if for each $\varepsilon \in]0, 1[$ y $t > 0$, there exists $n_0 \in \mathbb{N}$ so that $M(x_n, x_m, t) > 1 - \varepsilon$ if $m, n \geq n_0$. X is called complete if every Cauchy sequence is convergent. X is F-bounded if there exists $r \in]0, 1[$ so that $M(x, y, t) > 1 - r$ for any $x, y \in X,\ t > 0$.

If (X, d) is a metric space, then the function $M_d(x, y, t) = \dfrac{t}{t + d(x, y)}$ is a fuzzy metric (called standard) on X, with the product t-norm. The topology τ_{M_d} coincides with the topology induced by d.

A fuzzy metric $(M, *)$ on X is said to be stationary if M does not depend on t, i.e. for each $x, y \in X$ the function $M_{x,y}(t) = M(x, y, t)$ is constant [14].

A subset A of X is said to be F-bounded [10] if there exist $t > 0$ and $s \in]0, 1[$ such that $M(x, y, t) > s$ for all $x, y \in A$.

The above definitions agree with the metric spaces classical theory in the sense that (X, d) is complete (bounded) if and only if $(X, M_d, \cdot)$ is complete (F-bounded).

This definition of fuzzy metric is appropriate and it deserves special attention since, as it was proved by Gregori and Romaguera [13] the class of

metrizable topological spaces coincides with the class of the fuzzy metrizable topological spaces of George and Veeramani.

From now on, we assume as notion of fuzzy metric space the one due to George and Veeramani.

$M(x, y, t)$ may be interpreted as the degree of nearness between x and y with respect to t. In such a case, attending to (GV2), $M(x, y, t) = 0$ should be associated to a classical distance ∞.

The most well-known three continuous t-norms, that we denote by T_i $(i = 1, 2, 3)$, are the following.

$$\begin{aligned} T_1(x, y) &= \min\{x, y\} \\ T_2(x, y) &= xy \\ T_3(x, y) &= \max\{0, x + y - 1\} \end{aligned}$$

Taking into account the above definitions, the following conditions are satisfied:

(i) $T_3(x, y) \leq T_2(x, y) \leq T_1(x, y)$, for any $x, y \in [0, 1]$
(ii) $T(x, y) \leq T_1(x, y)$ for any continuous t-norm T and any $x, y \in [0, 1]$

References

1. G. Artico and R. Moresco, On fuzzy metrizability, *J. Math. Appl.* **107** (1985) 144-147.
2. G. L. Cain Jr. and R. H. Kasriel, Fixed and periodic points of local contraction mappings on probabilistic metric spaces, *Mathematical Systems Theory* **9** (1976) 289-297.
3. C. L. Chang, Fuzzy topological spaces, *J. Math. Anal. Appl.* **24** (1968) 182-190.
4. C.H. Chen, *Fuzzy logic and neural network handbook*, McGraw-Hill, New York 1996.
5. Deng Zi-ke, Fuzzy pseudo metric spaces, *J. Math. Anal. Appl.* **86** (1982) 74-95.
6. Deng Zi-ke, Separation axioms for completeness and total boundedness in fuzzy pseudometric spaces, *J. Math. Anal. Appl.* **112** (1985) 141-150.
7. R. Engelking, General Topology, *PWN-Polish Sci. Publ. Warsawa* (1977) Warsaw, Poland.
8. M. A. Erceg, Metric spaces in fuzzy set theory, *J. Math. Anal. Appl.* **69** (1979) 205-230.
9. A. George and P. Veeramani, On some results of analysis for fuzzy metric spaces, *Fuzzy Sets and Systems* **90** (1997) 365-368.
10. A. George and P. Veeramani, On Some results in fuzzy metric spaces,*Fuzzy Sets and Systems* **64 3** (1994) 395-399.
11. J. Goguen, L-fuzzy sets, *J. Math. Anal. Appl.* **18** (1967) 145-174.
12. M. Grabiec, Fixed points in fuzzy metric spaces, *Fuzzy Sets and Systems* **27** (1988) 385-389.
13. V. Gregori and S. Romaguera, Some properties of fuzzy metric spaces, *Fuzzy Sets and Systems* **115** (2000) 485-489.
14. V. Gregori, S. Romaguera, Characterizing completable fuzzy metric spaces, *Fuzzy Sets and Systems* **144 3** (2004) 411-420.
15. H. Hu, Fuzzy topological spaces, *J. Math. Anal. Appl.* **110** (1985) 141-178.
16. B. Hutton, Products of fuzzy topological spaces, *Topology Appl.* **11** (1980) 59-67.
17. I. Jermolaeva, On a Hausdorffness function of a fuzzy topological space, *Zbornik Radova Filozof. Fakulteta u Nižu. Ser. Mat.* **2** (1988) 73.
18. O. Kaleva and S. Seikkala, On fuzzy metric spaces, *Fuzzy Sets and Systems* **12** (1984) 215-229.
19. E.E. Kerre, *Fuzzy sets and approximate Reasoning* Xian Jiaotong University Press, 1998.
20. I. Kramosil and J. Michalek, Fuzzy metric and statistical metric spaces, *Kybernetica* **11** (1975) 326-334.
21. R. Lowen, Fuzzy topological spaces and fuzzy compactness, *J. Math. Anal. Appl.* **56** (1976) 621-633.

22. R. Lowen, Initial and final fuzzy topologies and the fuzzy Tychonoff theorem, *J. Math. Anal. Appl.* **58** (1977) 11-21.
23. K. Menger, Statistical metrics, *Proc. Nat. Acad. Sci.* **28** (1942) 535-537.
24. E. Pap and O. Hadzic and R. Mesiar, A fixed point theorem in probabilistic metric spaces and an application, *J. Math. Anal. Appl.* **202** 433-449.
25. E. Parau and V. Radu, Some remarks on Tardiff's fixed point theorem on Menger spaces, *Portugal. Math.* **54** (1997) 431-440.
26. V. Rafu, Some fixed point theorems in probabilistic metric spaces, stability problems for stochastic models, *Lecture Notes in Mathematics* **1233** (1987) 125-133.
27. B. Schweizer and A. Sklar, Statistical metric spaces, *Pacific. J. Math.* **10** (1960) 314-334.
28. B. Schweizer and A. Sklar, Probabilistic Metric Spaces, *Elsevier Science Publishing Co.* (1983) New York, USA.
29. A. P. Šostak, Two decades of fuzzy topology: basic ideas, notions and results, *Russian Math. Surveys 4* **4 6** (1989) 125-186.
30. R. M. Tardiff, Contraction maps on probabilistic metric spaces, *J. Math. Anal. Appl.* **165** (1992) 517-523.
31. E. Trillas, *Fundamentos e introducción a la ingeniería fuzzy*, Omron Electronics, Madrid 1994.
32. J. Yen, R. Langari, *Fuzzy logic: intelligence, control and information*, Prentice-Hall, New Jersey 1998.
33. L.A. Zadeh, Fuzzy sets, *Inform. Control* **8** (1965) 338-353.

Part II

Contributions

3 Summary of contributions

As commented in the presentation of this dissertation, the filters proposed in this PhD thesis along with the realized work, the achieved results and the drawn conclusions are presented as a set of articles/contributions that have been published/submitted in/to international journals or conferences. In the following Chapters 4-12, each contribution is included. Notice that since each contribution is a self-contained paper probably some contents of this document may be repeated. In this chapter, we briefly explain the content of each one of the presented contributions.

The main objectives pursued in this dissertation are two: First, to study the applicability of fuzzy metrics in colour image filtering tasks and to determine in which cases fuzzy metrics may present some advantages over classical metrics; and second, to design new colour image filtering solutions that use fuzzy metrics and fuzzy logic and that take advantage of the interesting fuzzy metrics properties.

In order to achieve these objectives, the work that has been carried out has been divided into two parts: First, in Chapters 4-7 we implement some variants of vector filters that use some fuzzy metric instead of the classical metrics or measures originally used. So that, by analyzing the proposed vector filters in front of their classical versions and the observed performance differences, we will observe in which cases and from which viewpoints fuzzy metrics may be more appropriate; second, in Chapters 8-12 we design new colour image filters on the basis of the observed fuzzy metrics performance advantages. These filtering solutions exploit the interesting properties of fuzzy metrics in order to take full advantage of their usage.

In the following we present a summary of each contribution stressing the basic concepts used in each contribution along with the more outstanding novelties, and results obtained. Note that figure and table references in the following summaries are referred to the corresponding chapters.

Also, other publications of the author where some concepts and/or methods in this dissertation has been used are the following:

– J. Camacho, S. Morillas, P. Latorre, Efficient impulse noise suppression based on statistical confidence limits, *Journal of Imaging Science and Technology* 50 5 (2006) 427-436.

- J.G. Camarena, V. Gregori, S. Morillas, G. Peris-Fajarnés, New method for fast detection and removal of impulsive noise using fuzzy metrics, *ICIAR06, Lecture Notes in Computer Science* 4141 (2006) 359-369.
- J. Riquelme, S. Morillas, G. Peris-Fajarnés, D. Castro, Fuzzy metrics application in video spatial deinterlacing *WILF07, Lecture Notes in Computer Science*, to appear.
- J.G. Camarena, V. Gregori, S. Morillas, A. Sapena, Fast detection and removal of impulsive noise using peer groups and fuzzy metrics, *Journal of Visual Communication and Image Representation*, to appear.
- S. Schulte, S. Morillas, V. Gregori, E.E. Kerre, A new fuzzy color correlated impulse noise reduction method, *revised version submitted to IEEE Transactions on Image Processing*.
- V. Gregori, S. Morillas, B. Roig, Rank-ordered differences switching vector filter, *submitted to Signal Processing: Image Communication*.
- J.G. Camarena, V. Gregori, S. Morillas, A. Sapena, Some improvements for image filtering using peer group techniques, *submitted to IEEE Signal Processing Letters*.

3.1 Contribution (i): A new vector median filter based on fuzzy metrics

In this paper we propose a variant of the vector median filter (VMF) [1] that uses a fuzzy metric as distance criterion instead of the classical metrics used in VMF. According to [1] and as it is explained in Section 4.3.1, the output of the VMF is defined as follows:

Denote by $\mathbf{F}$ a colour image and by $\mathbf{F}_i$ the RGB colour vector located at position i in the image $\mathbf{F}$ and consider the use of a filter window W of size $n \times n$. Then VMF output is the vector $\mathbf{F}_{k^*} \in W$ that minimizes the aggregated distance to the other samples in W. That is, the output is that $\mathbf{F}_{k^*}$ for which $k^* = arg\ min_k \sum_{j=1, j\neq k}^{n^2} \rho(\mathbf{F}_k, \mathbf{F}_j),\ k = 1, \ldots, n^2$, and where ρ is the L_1 (city-block) or L_2 (Euclidean) metric.

In this contribution we propose to use a fuzzy metric instead of the ρ function above. The proposed fuzzy metric M_K is given by

$$M_K(\mathbf{F}_i, \mathbf{F}_j) = \prod_{l=1}^{3} \frac{min\{F_i(l), F_j(l)\} + K}{max\{F_i(l), F_j(l)\} + K} \tag{3.1}$$

where Z is the real interval $[0, 255]$, $X = Z^3$, $K > 0$. $(F_i(1), F_i(2), F_i(3))$ denotes the element $\mathbf{F}_i \in X$. As it is proved in Proposition 1 of Chapter 4, M_K is a stationary fuzzy metric on X in the sense of [2] since the axioms given in Section 2.7 are fulfilled.

Then, according to axiom (GV2) in Section 2.7 and as it is described in Section 4.3.2, the proposed filter output should be the vector $\mathbf{F}_{k^*} \in W$ that

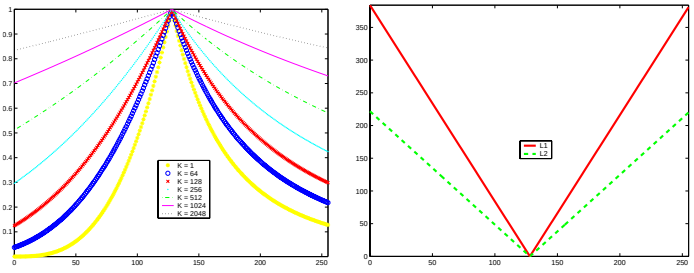

(a) (b)

Fig. 3.1. Values given by (a) M_K for different values of K and (b) L_1 and L_2 metrics, when comparing a colour vector $[128, 128, 128]$ with the colour vectors $[V, V, V]$ where $V = 0, 1, \ldots, 255$.

maximizes the aggregated fuzzy distance to the other samples in W, that is, $\mathbf{F}_{k^*}$ for which $k^* = arg\ max_k \sum_{j=1, j\neq k}^{n^2} M_K(\mathbf{F}_k, \mathbf{F}_j),\ k = 1, \ldots, n^2$.

Note that, as described in Section 4.4.1, the fuzzy metric M_K presents a particular behaviour since the value given for two distinct pairs of consecutive (or equally distanced) vectors may not be the same. This effect can be smoothed by increasing the value of the K parameter in Eq. (3.1). So, the value of K should be set high enough to reduce this effect. However, if $K \to \infty$ then $M_K(\mathbf{F}_i, \mathbf{F}_j) \to 1$, so very high values of K should also be avoided. Several experiences have shown that for a range of values in $[0, C]$ appropriate values of K are in the range $[2C, 2^3C]$. This is shown in the below figure and Figures 4.1-4.2 for the case of RGB values where $K = 1024$ is an appropriate value. Indeed, the below figure show that the behaviour of M_K for the suggested values of K is very similar, except range and scaling, to the behaviour of classical L_1 and L_2 (Euclidean) metrics.

In order to compare the performance of the VMF using the metrics L_1, L_2 and the proposed fuzzy metric M_K we use the procedure explained in Section 1.7[1]. The images Lenna, Peppers and Baboon have been contaminated with different densities or impulsive, Gaussian and mixed impulsive-Gaussian noise. From the obtained results in terms of MAE, PSNR and NCD that are shown in Tables 4.2, 4.3 and 4.4 and Figures 4.3 and 4.4 it can be seen that the VMF using the proposed fuzzy metric outperforms the classical metrics for images where impulsive noise density is more important than Gaussian noise density. So, it can be concluded that M_K is suitable for multichannel image filtering. Moreover, computational analysis of M_K in front of the classical metrics L_1 and L_2 shows that, by means of the usage a look-up table, M_K is less computationally demanding than L_1 and L_2 (see Table 4.1).

[1] The same procedure is used to assess all the filters proposed in this dissertation.

3.2 Contribution (ii): Fuzzy bilateral filtering for color images

In this contribution we propose a variant of the well-known bilateral filter (BF) [10]. The bilateral filter is designed to remove Gaussian noise both in gray-scale and colour images. Removing Gaussian noise should involve to smooth the different areas of an image without degrading neither the sharpness of their edges nor their details. The output of the BF at a particular location is a weighted average of the pixels in its neighborhood where the weight of each pixel depends on the spatial closeness and photometric similarity with respect to the pixel under processing. In the variant we propose, the spatial closeness and the similarity between colour vectors are measured by means of a fuzzy metric which is built by combining other two fuzzy metrics.

According to [10] and as it is explained is Section 5.2, the BF is defined as follows. Let $\mathbf{F}$ represent a multichannel image and let W be a sliding window of finite size $n \times n$. Consider the pixels in W represented in Cartesian Coordinates and so, denote by $\mathbf{i} = (i_1, i_2) \in Y^2$ the position of a pixel $\mathbf{F_i}$ in W where $Y = \{0, 1, \ldots, n-1\}$ is endowed with the usual order. The BF replaces the central pixel of each filtering window by a weighted average of its neighbor colour pixels. The weighting function is designed to smooth in regions of similar colours while keeping edges intact by heavily weighting those pixels that are both spatially close and photometrically similar to the central pixel.

Denote by $||\cdot||_2$ the Euclidean norm and by $\mathbf{F_i}$ the central pixel under consideration. Then, the weight $\mathcal{W}(\mathbf{F_i}, \mathbf{F_j})$ corresponding to the vector $\mathbf{F_j}$ with respect to $\mathbf{F_i}$ is the product of two components, one spatial and one photometrical

$$\mathcal{W}(\mathbf{F_i}, \mathbf{F_j}) = \mathcal{W}_s(\mathbf{F_i}, \mathbf{F_j})\mathcal{W}_p(\mathbf{F_i}, \mathbf{F_j}) \tag{3.2}$$

where the spatial component $\mathcal{W}_s(\mathbf{F_i}, \mathbf{F_j})$ is given by

$$\mathcal{W}_s(\mathbf{F_i}, \mathbf{F_j}) = e^{-\frac{||\mathbf{i}-\mathbf{j}||_2^2}{2\sigma_s^2}} \tag{3.3}$$

and the photometrical component $\mathcal{W}_p(\mathbf{F_i}, \mathbf{F_j})$ is given by

$$\mathcal{W}_p(\mathbf{F_i}, \mathbf{F_j}) = e^{-\frac{\Delta E_{Lab}(\mathbf{F_i}, \mathbf{F_j})^2}{2\sigma_p^2}} \tag{3.4}$$

where $\Delta E_{Lab} = [(\Delta L^*)^2 + (\Delta a^*)^2 + (\Delta b^*)^2]^{\frac{1}{2}}$ denotes the perceptual colour error in the $L^*a^*b^*$ colour space, and $\sigma_s, \sigma_p > 0$ are two filter smoothing parameters.

The colour vector output $\widetilde{\mathbf{F_i}}$ is computed using the normalized weights and so it is given by

$$\widetilde{\mathbf{F_i}} = \frac{\sum_{\mathbf{F_j} \in W} \mathcal{W}(\mathbf{F_i}, \mathbf{F_j}) \mathbf{F_j}}{\sum_{\mathbf{F_j} \in W} \mathcal{W}(\mathbf{F_i}, \mathbf{F_j})} \tag{3.5}$$

The $\mathcal{W}_s$ weighting function decreases as the spatial distance in the image between $\mathbf{i}$ and $\mathbf{j}$ increases, and the $\mathcal{W}_p$ weighting function decreases as the perceptual colour difference between the colour vectors increases. The spatial component decreases the influence of the furthest pixels reducing blurring while the photometric component reduces the influence of those pixels which are perceptually different respect to the one under processing. In this way, only perceptually similar areas of pixels are averaged together and the sharpness of edges is preserved.

In the proposed fuzzy bilateral filter (FBF) we propose to compute the weight of each colour vector by using a fuzzy metric that takes into account both the photometric similarity and the spatial distance. To build the desired fuzzy metric we join the fuzzy metric proposed in Proposition 1 of Chapter 4 that is used to measure the similarity between colour vectors (o photometrical similarity), and the so-called standard fuzzy metric deduced from the Euclidean norm from [2] Example 2.9 that is used to measure the spatial distance between the pixels in comparison. The resulting fuzzy metric is given by

$$CFM(\mathbf{F_i}, \mathbf{F_j}, t) = \prod_{s=1}^{3} \frac{min\{F_{\mathbf{i}}^s, F_{\mathbf{j}}^s\} + K}{max\{F_{\mathbf{i}}^s, F_{\mathbf{j}}^s\} + K} \cdot \frac{t}{t + ||\mathbf{i} - \mathbf{j}||_2} \tag{3.6}$$

If we identify each pixel $\mathbf{F_i}$ with $(F_{\mathbf{i}}^1, F_{\mathbf{i}}^2, F_{\mathbf{i}}^3, i_1, i_2)$, according to Section 5.4 and [4], then CFM can be proved to be a fuzzy metric on $X^3 \times Y^2$. Notice that the first term of CFM represents the similarity between the colour vectors whereas the second term models the spatial closeness criterion where t is the filter smoothing parameter. In this way, the use of the above fuzzy metric is enough to simultaneously model the spatial closeness and photometric similarity criteria. FBF is built by replacing $\mathcal{W}(\mathbf{F_i}, \mathbf{F_j})$ by $CFM(\mathbf{F_i}, \mathbf{F_j}, t)$ in Eq. 3.5.

The main design difference between BF and FBF is that BF has two filter parameters while FBF has only one. This is achieved because the FBF uses a stationary fuzzy metric (see Section 2.7) to represent the similarity between the colour vectors. This makes the FBF easier to adjust but a little less flexible.

Experimental results in Table 5.1 and Figures 5.1-5.3 using the images Lenna, Peppers and Baboon contaminated with different densities of Gaussian noise show that the FBF presents a better detail preserving ability than its classical version. So, FBF may receive better results than BF for low densities of Gaussian noise and for highly textured images. Therefore, it can be concluded that the proposed representation using fuzzy metrics is, at least, as suitable as it is the classical modelling made in BF.

3.3 Contribution (iii): A fast impulsive noise color image filter using fuzzy metrics

In this paper we study a vector filtering technique for impulsive noise removal which is based on measuring the similarity between colour vectors in a sliding window (FSVF) [5]-[8]. FSVF is based on *privileging* the central pixel in each filtering window in order to replace it only when it is really noisy and preserve the original undistorted image structures. The method proposed in this paper is based on replacing the colour vector similarity measures used in FSVF [5]-[8] by a fuzzy metric.

According to [5]-[8] and as it is described in Section 6.2, FSVF is defined as follows. Let assume a filtering window W containing $n+1$ image pixels $\{\mathbf{F}_0, \mathbf{F}_1, \ldots, \mathbf{F}_n\}$, where n is the number of neighbors of the central pixel $\mathbf{F}_0$. It is considered a similarity function $\mu : [0; \infty) \to I\!R$ which is non-ascending and convex in $[0; \infty)$ and satisfies $\mu(0) = 1$, and $\lim_{x \to \infty} \mu(x) = 0$. The similarity between two pixels of the same colour should be 1, and the similarity between pixels with very different colours should be very close to 0. The function defined as $\mu(||\mathbf{F}_i - \mathbf{F}_j||)$ where $||\cdot||$ denotes the specific vector norm (typically the L_1 or L_2 vector norms), can easily satisfy the above conditions when it is a decreasing function and $\mu(0) = 1$. The cumulated sum M_k of similarities between a given pixel $\mathbf{F}_k$ $(k = 0, \ldots, n)$ and all other pixels belonging to the window W is defined as

$$M_0 = \sum_{j=1}^{n} \mu(\mathbf{F}_0, \mathbf{F}_j), \quad M_k = \sum_{\substack{j=1 \\ j \neq k}}^{n} \mu(\mathbf{F}_k, \mathbf{F}_j)\,, \tag{3.7}$$

which means that for those $\mathbf{F}_k$ which are neighbors of $\mathbf{F}_0$, the similarity between $\mathbf{F}_k$ and $\mathbf{F}_0$ is not taken into account, what *privileges* the central pixel. Hence, the reference pixel $\mathbf{F}_0$ is replaced by one of its neighbors if $M_0 < M_k,\ k = 1, \ldots, n$, only when it is noisy, preserving the original undistorted image structures. If this is the case then, $\mathbf{F}_0$ is replaced by that $\mathbf{F}_{k^*}$ for which $k^* = \arg\max_k M_k$.

In the filter introduced in this contribution, we propose to replace the μ function above by the stationary F-bounded fuzzy metric defined in Proposition 2 of Chapter 6 which is designed as a modification of the stationary fuzzy metric from Proposition 1 of Chapter 4. The fuzzy metric is given by

$$M^{\alpha}(\mathbf{x}, \mathbf{y}) = \prod_{i=1}^{3} \left(\frac{min\{x_i, y_i\} + K}{max\{x_i, y_i\} + K} \right)^{\alpha} \tag{3.8}$$

where X is a real interval $[a, b]$, $K > |a| > 0$, $\alpha > 0$, $\mathbf{x} = (x_1, \ldots, x_3), \mathbf{y} = (y_1, \ldots, y_3)$. According to the proof in appendix of Chapter 6, M^{α} is an F-bounded fuzzy metric [2] since there exists $s \in]0, 1[$ such that $M^{\alpha}(x, y) > s$

for all $x, y \in X^p$. Notice that M^α fulfills the above conditions regarding the μ function.

As explained in Sections 6.4.1-6.4.2, K and α are two filter parameters. In section 6.4.1 it is explained that an appropriate value of K for RGB image processing is $K = 1024$. On the other hand, experimental results in Figures 6.2, 6.9 and 6.10 show that the value of the α parameter influences the intensity of the filtration process. Since the α parameter determines the lower bound of the fuzzy metric, and since the lower bound of the fuzzy metric is also the minimum advantage given to the central pixel, then the advantage conferred to the central pixel that determines the probability of replacing the pixel is influenced by the value of α. Figures 6.9 and 6.10 show that the value of α should be set proportionally to the needed smoothing, that is, proportionally to the percentage of contaminating noise.

Experimental comparison, in terms of MAE, PSNR and NCD, of the proposed filter performance against the original FSVF and other vector filters have been carried out using the Microscopic, Lenna, Baboon, Artic Hare and Bright Rose images that have been contaminated with different percentages of fixed-value impulsive noise. From the results shown in Tables 6.3-6.7 and Figures 6.4-6.8 it can be seen that the proposed method outperforms its original version for images of low frequency and reduced colour set. In general, it can be considered that the performances are competitive. In addition, the proposed filter outperforms the other filters in the comparison (see Table 6.2). Moreover, computational analysis performed in Sections 6.3.1, 6.4 and Table 6.1 shows that the proposed method is computationally cheaper than the original FSVF. Note that in order to achieve a similarity measure between colour vectors the classical FSVF uses a distance measure followed by a convex function. Unlike this, the proposed fuzzy metric provides directly a similarity measure and it does not need to use any convex function. These results claim for the appropriateness of the proposed fuzzy metric M^α for the considered filter design.

3.4 Contribution (iv): Fuzzy directional distance vector filter

As commented above, the most well-known vector filter is the vector median filter (VMF). According to Sections 3.1, 4.3.1 and [1], this filter outputs the vector in the filtering window that minimizes the accumulated distance to other samples. The distance measure usually used is the Euclidean metric that measures magnitude distance between the vector samples. However, any particular case of the generalized Minkowski metric can be used instead. The generalized Minkowski metric (L_p metric) is expressed as

$$L_\beta(\mathbf{F}_k, \mathbf{F}_j) = \left(\sum_{i=1}^{N} | \left(F_k(i) - F_j(i)\right) |^\beta \right)^{\frac{1}{\beta}}, \tag{3.9}$$

where the Euclidean metric corresponds to $\beta = 2$.

On the other hand, other well-known vector filter is the basic vector directional filter (BVDF) [11] that follows the same procedure that the VMF but using the angular distance between vectors that is given by

$$A(\mathbf{F}_k, \mathbf{F}_j) = cos^{-1}\left(\frac{\mathbf{F}_k \cdot \mathbf{F}_j}{||\mathbf{F}_k||_2 \cdot ||\mathbf{F}_j||_2} \right). \tag{3.10}$$

where $|| \cdot ||_2$ denotes the Euclidean norm. It is known that directional filtering may outperform VMF in terms of chromaticity preservation because RGB vector directions are associated to chromaticity.

From a more general point of view, the directional distance filter (DDF), [3], minimizes a combination of the aggregated distance measures used in the VMF and the BVDF. In the DDF, the accumulated distance R_k associated to each vector $\mathbf{F}_k, k = 0, \ldots, n$ in the filtering window is now calculated as follows

$$R_k = \left[\sum_{j=0}^{n} L_\beta(\mathbf{F}_k, \mathbf{F}_j) \right]^{1-q} \cdot \left[\sum_{j=0}^{n} A(\mathbf{F}_k, \mathbf{F}_j) \right]^{q}, \tag{3.11}$$

where L_β denotes the specific metric used, A is the angular distance function above and $q \in [0, 1]$ is a parameter which allows to tune the importance of the angle criterion versus the distance criterion.

In this contribution first we use the fuzzy metric defined in Proposition 1 of Chapter 4 to measure directional differences between colour vectors and then we propose a variant of the BVDF using this fuzzy metric. Note that this fuzzy metric was originally used in Contribution (i) to measure magnitude differences between colour vectors. Next, we define a novel fuzzy metric between colour vectors that takes simultaneously into account the magnitude and the directional differences. Using this hybrid fuzzy metric we propose a variant of the DDF.

Let us recall that the M_K fuzzy metric defined in Contribution (i) is given by

$$M_K(\mathbf{F}_i, \mathbf{F}_j) = \prod_{l=1}^{3} \frac{min\{F_i(l), F_j(l)\} + K}{max\{F_i(l), F_j(l)\} + K} \tag{3.12}$$

where K is a parameter that is set to $K = 1024$ when using RGB colour vectors. Now we denote by $\hat{\mathbf{F}}_k$ the unitary vector associated to the colour image vector $\mathbf{F}_k$ (see Eq. (7.5) in Section 7.2.1). Then, as it is explained in Section 7.2.1, we can measure directional distance between colour vectors if we use the M_K fuzzy metric between two unitary vectors as $M_{K'}(\hat{\mathbf{F}}_k, \hat{\mathbf{F}}_j)$, where the value of K' should be appropriate for unitary vectors and so, as explained in Section 7.2.1, it is set to $K' = 4$. The vector filter that parallelizes the BVDF operation but using $M_{K'}$ as distance criterion is named fuzzy metric vector directional filter (FMVDF).

Next in this paper, in order to approach a simultaneous fuzzy magnitude-directional distance, from a fuzzy point of view it should be appropriate to join both $M_K(\mathbf{F}_i, \mathbf{F}_j)$ and $M_{K'}(\hat{\mathbf{F}}_i, \hat{\mathbf{F}}_j)$ with an appropriate t-norm. The product t-norm will be used since it is involved in M_K, then, according to Section 7.2.2, the function

$$M_{KK'} = M_K(\mathbf{F}_i, \mathbf{F}_j) \cdot M_{K'}(\hat{\mathbf{F}}_i, \hat{\mathbf{F}}_j) \tag{3.13}$$

represents the fuzzy distance between the colour vectors $\mathbf{F}_i$ and $\mathbf{F}_j$ taking simultaneously into account both magnitude and directional criteria. Moreover, according to Section 7.2.2 and [4], it is easy to verify that $M_{KK'}$ is a fuzzy metric, as well. In this case, the vector filter that parallelizes the BVDF operation but using $M_{KK'}$ as distance criterion is named fuzzy metric directional distance filter (FMDDF).

In order to assess the performances of the proposed vector filters we compare their performance in terms of objective quality measures against their classical versions. For this, we have contaminated the Lenna, Baboon and Bright rose images with different densities of Gaussian noise, fixed-value impulsive noise and mixed Gaussian-fixed-value-impulsive noise. The results in Table 7.1 and Figures 7.3-7.11 show that the FMDDF performs better than the DDF for impulsive noise removal and similar for Gaussian noise suppression. When considering mixed Gaussian-impulsive noise, FMDDF outperforms DDF when the component of impulsive noise is higher than the one of Gaussian noise and similar in other cases. Also, it can be seen that the performances of BVDF and FMVDF are alike in most of the cases for all considered types of noise.

It has also been observed that the FMDDF is sensibly faster than the classical DDF. This is due to the fact that the DDF needs to compute two accumulated distances, one in magnitude and one in direction, which are combined afterwards, whereas the FMDDF computes only one accumulation of the hybrid $M_{KK'}$ fuzzy metric.

3.5 Contribution (v): Local self-adaptive impulsive noise filter for color images using fuzzy metrics

In this contribution we present an advanced variant of the impulsive noise filtering technique studied in Contribution (iii) and [5]-[8]. Recall that the filtering technique in Contribution (iii) is based on performing a kind of reduced vector ordering where the (central) vector under processing is privileged to be the lowest ranked vector that will finally be the filter output. The fuzzy metric used in Contribution (iii) to perform the ordering is the following

$$M^{\alpha}(\mathbf{x},\mathbf{y}) = \prod_{i=1}^{3} \left(\frac{min\{x_i, y_i\} + K}{max\{x_i, y_i\} + K} \right)^{\alpha} \tag{3.14}$$

where, according to Contribution (iii), $K = 1024$, $\alpha > 0$. The α parameter is used to adjust the filter performance. As it was determined in Section 6.4.2, in order to the filter adapts to the image under processing the α parameter should be set proportionally to the needed smoothing, that is, proportionally to the percentage of corrupting impulsive noise. Notice that the necessity of having to tune the α parameter may limit the filter performance. Indeed, according to Section 8.1, many adaptive filtering techniques have the disadvantage of having to tune an adaptive parameter to achieve an appropriate performance. This fact motivates us to study in this contribution the possibility of designing a self-adaptive variant of the filter introduced in Contribution (iii). Additionally, in this paper we also use extension of the above fuzzy metric to the directional and magnitude-directional domain analogously to the approach presented in Contribution (iv).

To approach the design of a self-adaptive filter we will design a procedure to automatically determine the value of α. Moreover, we will determine this value for each pixel under processing so that the adaptation is made locally and the filter may perform different in each image location.

According to Section 6.4.2, the value of α determines the minimum advantage given to the central pixel for being the filter output. In order to avoid noisy colour vectors being the output of the filtering, the given advantage should be lower (higher value of α) for noisy vectors. Therefore, according to Section 8.3, we propose to estimate the noisiness of a given colour vector according to its multivariate dispersion with respect to its neighbors. The multivariate dispersion is estimated either as the difference between the colour vector and the vector mean of the neighbors or as the difference between the colour vector and the vector median of the neighbors as follows (see Section 8.3.1).

Denote by $\bar{\mathbf{F}}$ the vector mean of the vectors in the filter window, that is $\bar{\mathbf{F}} = \frac{1}{n+1} \sum_{i=0}^{n} \mathbf{F}_i$, and denote by $\hat{\mathbf{F}}$ the vector median [1] of the vectors in the sliding window. The multivariate dispersion of a pixel $\mathbf{F}_i$ with respect to the vector mean $\bar{\mathbf{F}}$ is given by

$$\sigma_{\bar{\mathbf{F}}}(\mathbf{F}_i) = ||\mathbf{F}_i - \bar{\mathbf{F}}||_2 \tag{3.15}$$

and the multivariate dispersion of any pixel $\mathbf{F}_i$ with respect to the vector median $\hat{\mathbf{F}}$ is given by

$$\sigma_{\hat{\mathbf{F}}}(\mathbf{F}_i) = ||\mathbf{F}_i - \hat{\mathbf{F}}||_2 \tag{3.16}$$

where $||\cdot||_2$ denotes the Euclidean norm.

Finally, the estimated multivariate dispersion of the central pixel is used to locally determine the value of α. Some experiments show that the values of $\sigma_{\bar{\mathbf{F}}}(\mathbf{F}_0)$ or $\sigma_{\hat{\mathbf{F}}}(\mathbf{F}_0)$ can not be directly used as the α parameter since these values are too large and the advantage given to the central pixel would not be appropriate. Therefore, it is necessary to use an scaling parameter c in order to adequate these values. So, the value of α is given by

$$\alpha = c \cdot \sigma_{\bar{\mathbf{F}}}(\mathbf{F}_0) \tag{3.17}$$

or

$$\alpha = c \cdot \sigma_{\hat{\mathbf{F}}}(\mathbf{F}_0) \tag{3.18}$$

Some simulations show that an appropriate value of the scaling factor c is $c = 0.05$. Values around this one are also suitable. Then, as it is explained in Section 8.3.2, we obtain a local self-adaptive filter structure by replacing α in Eq. (3.14) by the expressions in Eqs. (3.17)-(3.18).

To assess the proposed filter the Baboon, Lenna and Microscopic images have been contaminated with different densities of fixed-value and random-value impulsive noise and filtered with the proposed self-adaptive technique and the filtering techniques in Table 8.1. The results in Tables 8.2-8.4 and Figures 8.1 and 8.3 show that the proposed technique outperforms all the techniques in comparison. Moreover, in order to better illustrate the advantages of the local self-adaptive approach, the Lenna image has been contaminated with different densities of fixed-value impulsive noise in its upper half and lower half and the obtained results are shown in Figure 8.2 and Table 8.5. It can be seen that the proposed approach receives better results than the rest of the filtering technique in the comparison.

3.6 Contribution (vi): New adaptive vector filter using fuzzy metrics

In this contribution we present a new adaptive vector filter for impulsive noise reduction that uses fuzzy metrics. The main idea behind the proposed method is that the output vector for a given filter window will be the one which best fulfills two criteria: to be similar in signal value and to be spatially close to all the other pixels in the filter window. Unlike the classical vector median filter (VMF) [1] that determines as output the vector that is the most similar in signal value to the rest of the vectors in the window, in the proposed vector filter we include the spatial closeness criterion to perform the selection. The use of fuzzy metrics allows to simultaneously handle both criteria.

In order to measure the similarity in signal value between colour vectors, we propose to use the fuzzy metric R given by

$$R(\mathbf{F_i}, \mathbf{F_j}) = \frac{C}{C + ||\mathbf{F_i} - \mathbf{F_j}||_2} \tag{3.19}$$

where $||\cdot||_2$ denotes the L_2 norm, C is a positive real parameter used to control the spread of the function that, according to Section 9.2, can be set to $C = 150$ and $\mathbf{F_k} = (F^1_\mathbf{k}, F^2_\mathbf{k}, F^3_\mathbf{k})$ represents the colour vector of the image pixel at position $\mathbf{k}$ comprising its R, G and B components. From [2] Example 2.9, R is a stationary fuzzy metric on X^3 where X is the set $\{0, 1, \ldots, 255\}$. Notice that various fuzzy metrics, such as those listed in [2], could be used instead of R in the same conditions.

For the case of spatial closeness between pixels, we consider the pixels in a $n \times n$ filter window W represented in Cartesian coordinates and so, we denote by $\mathbf{i} = (i_1, i_2) \in Y^2$ the position of a pixel $\mathbf{F_i}$ in W where $Y = \{0, 1, \ldots, n-1\}$. We consider the standard fuzzy metric S deduced from the L_∞ metric ([2] Remark 2.10) given by

$$S(\mathbf{i}, \mathbf{j}, t) = \frac{t}{t + ||\mathbf{i} - \mathbf{j}||_\infty} \tag{3.20}$$

where $\mathbf{i}, \mathbf{j} \in Y^2$, $t > 0$ and $||\mathbf{i} - \mathbf{j}||_\infty$ is the L_∞ metric on Y^2 given by $||\mathbf{i} - \mathbf{j}||_\infty = max\{|i_1 - j_1|, |i_2 - j_2|\}$. We aim that all neighbors in a 3×3 neighborhood (and analogously for further neighborhoods) should receive the same closeness degree with respect to the central pixel. To achieve this we have used the L_∞ metric between the pixel positions $\mathbf{i}, \mathbf{j}$. Hence, some experiments have shown that this approach provides better results than the usage of the Euclidean metric and any other metric. Then, according to Section 2.7, $S(\mathbf{i}, \mathbf{j}, t)$ measures the spatial closeness between the colour pixels $\mathbf{F_i}$ and $\mathbf{F_j}$ with respect to t. The parameter t is used to adjust the importance given to the spatial closeness criterion.

To handle both criteria of similarity in signal value and spatial closeness simultaneously we join the R and S fuzzy metrics to build the following CFM fuzzy metric given by

$$CFM(\mathbf{F_i}, \mathbf{F_j}, t) = R(\mathbf{F_i}, \mathbf{F_j}) \cdot S(\mathbf{i}, \mathbf{j}, t) = \frac{C}{C + ||\mathbf{F_i} - \mathbf{F_j}||} \cdot \frac{t}{t + ||\mathbf{i} - \mathbf{j}||} \quad (3.21)$$

If we identify each pixel $\mathbf{F_i}$ with $(F_{\mathbf{i}}^1, F_{\mathbf{i}}^2, F_{\mathbf{i}}^3, i_1, i_2)$ then, according to Section 9.2 and [4] Proposition 3.5 it can be proved that CFM is a fuzzy metric on $X^3 \times Y^2$.

According to Section 9.3, the proposed vector filtering technique is achieved by performing a reduced vector ordering using the CFM fuzzy metric as distance criterion. Then, it can be easily noticed that the order of computational complexity of the proposed method and the VMF is the same. As explained in Sections 9.3 and it is illustrated in Figure 9.2, the t parameter allows to adjust the importance of the spatial criterion. When $t \to \infty$ the spatial criterion is not taken into account and the proposed filter will behave as a classical VMF. On the other hand, in the extreme case that $t \to 0$ the filter approaches the identity operation. Therefore, the value of t should be determined to find an appropriate balance between the VMF operation and the identity operation so, it seems intuitive to determine the value of t according to the density of contaminating noise. In Section 9.4 and Figures 9.4-9.5 it is illustrated how the value of the t parameter influences the filter performance. A correlation based study using optimal experimental values of t and percentages of contaminating impulsive noise is performed in Section 9.4. As a result, an adjusting function is computed so that the value of the t parameter can be determined as a function of the percentage of contaminating noise. Also in Section 9.4 it is explained how the percentage of impulsive noise can be estimated.

Finally in Section 9.4, the proposed filter is assessed in comparison to some classical and well-known vector filters, some recent vector filters with good detail-preserving ability and also with some impulsive noise filters for gray-scale images applied in a componentwise way. For this, the Lenna, Peppers and Baboon images have been contaminated with different percentages of fixed-value and random-value impulsive noise. Experimental results for comparison are presented in Tables 9.1-9.3 and Figures 9.6-9.8. From these results it can be seen that the proposed approach is able to suppress different densities of the two types of impulsive noise and can outperform the competition in terms of performance. By visually inspecting the results in Figures 9.6-9.8, it can be observed that VMF and the proposed filters show similar noise suppression ability, except for small impulses. On the other hand, the sharpness of edges and the fine details are better preserved by the proposed method.

3.7 Contributions (vii)-(viii): Isolating impulsive noise pixels in colour images by peer group techniques

First it should be noted that Contribution (vii), that was presented in the EUSIPCO 2006 conference, contains only preliminary results of Contribution (viii). So, we present Contribution (viii) because this paper includes the results in Contribution (vii). We have preferred to include Contribution (vii) in addition to Contribution (viii) because it is an already published paper whereas Contribution (viii) is a paper submitted to an international journal.

As commented in Section 1.5.3, switching filtering is a well known approach for impulsive noise reduction. Switching filtering techniques aim to affect only the noisy pixels while keeping the desired image structures (edges and fine details) unchanged. In this paper a new switching vector filter is proposed. The proposed method uses fuzzy metrics to represent magnitude, direction and hybrid magnitude-directional differences between colour vectors in an analogous manner as it is done in Contribution (iv).

The main motivation of this paper is the filter proposed in [9] which is based on the peer group concept defined as follows. Let $||\cdot||$ be a norm on a non-empty set X and let $h > 0$. If $x \in X$, we denote by $\mathcal{P}(x,h)$ the set $\{y \in X : ||x-y|| \leq h\}$. Now, let W be a subset of X containing x and let m be a nonnegative integer. A subset of $\mathcal{P}(x,h) \cap W$ containing $m+1$ elements is called a *peer group* of cardinality m contained in W, and it is denoted by $\mathcal{P}(x,W,h,m)$ or $\mathcal{P}(x,h,m)$ if confusion is not possible.

Following the prior findings presented in [9], a pixel x is considered as *noise-free* only if there exists a *peer group* $\mathcal{P}(x,h,m)$ for some positive value of m. Otherwise, the pixel should be considered as *noisy*. The particular setting of the m parameter determines the filter performance. On the one hand, lower values of m provide a better signal-preserving ability to the filtering but sometimes also a lack of robustness. On the other hand, higher values of m provide a robust performance though a more smoothed output image is obtained. As a result, the work in [9] proposed to use intermediate values of m in order to reach an appropriate trade-off between signal-preserving and noise smoothing.

On the basis of this work, the method proposed in Contribution (viii) aims at achieving a filtering procedure which is robust in removing impulsive noise and preserving fine details. This performance is achieved by using two different values of the m parameter in the noise detection process. First, a set of *noise-free* pixels of high reliability is determined by applying a demanding condition on the *peer group* cardinality. Afterwards, an iterative detection process is used to refine the initial findings by detecting additional *noise-free* pixels. The remaining, undetected pixels represent impulses.

As it is explained in Section 11.3 and analogously to Contribution (iv), the proposed method uses fuzzy metrics between colour vectors to determine the peer groups and also to perform the filtering of noisy pixels. The proposed

filtering method is defined in Section 11.4 and illustrated in Figures 11.3 and 11.4. The proposed procedure performs first the noise detection as follows.

(i) For each image pixel $\mathbf{F}_i$, if there can be found a peer group $\mathcal{P}_M(\mathbf{F}_i, W, d, m)$ then the pixel $\mathbf{F}_i$ is declared as *noise-free*. In other case, the pixel $\mathbf{F}_i$ is declared as *non-assigned*.
(ii) For each *non-assigned* pixel $\mathbf{F}_i$, let W' be the set of *noise-free* pixels in W. If there can be found a peer group $\mathcal{P}_M(\mathbf{F}_i, W', d, 1)$, then the pixel $\mathbf{F}_i$ is declared as *noise-free*. Note that this condition is fulfilled if there exists some pixel $\mathbf{F}_j \in W'$ such that $M(\mathbf{F}_i, \mathbf{F}_j) \geq d$.
(iii) If new *noise-free* pixels were determined in the previous step, repeat (ii).
(iv) Each *non-assigned* pixel is finally declared as *noisy* .

Above, W size is $n \times n$, $m = n + 1$ and $\mathcal{P}_M$ denotes the peer group determined by using the fuzzy metric M as distance criterion. The fuzzy metrics used in this contribution are described in Section 11.3.

In step (i), the proposed method detects a set of pixels which can be declared as *noise-free* with a high reliability since they are *similar* to a considerable number m of their neighbors. In steps (ii) and (iii), initial findings are refined. The underlying idea is that if a pixel, which was initially marked as *non-assigned*, is *similar* to some *noise-free* neighbor then it should be considered as *noise-free*, as well. After the iterative procedure is completed, the remaining (undetected) pixels represent the noise. The *noisy* pixels are corrected using the filter proposed in Contribution (i).

Computational analysis of the proposed method, that is detailed in Appendix of Chapter 11, demonstrates that the computational complexity of the proposed method is lower than the one of the VMF and quite similar to the one of the method in [9].

The filter parameters have been set experimentally as it is described in Section 11.5.1. The Parrots, House, Peppers, Baboon and Pills images have been used to compare the filter performance in front of other state of the art filters. These images have been corrupted with different densities of fixed-value and random-value impulsive noise and mixed Gaussian-impulsive noise. The results in Tables 11.2-11.7 and Figures 11.8-11.10 show that the proposed method is able to outperform all the methods in the comparison in terms of objective quality measures and that it generates visually pleasing images. Experiments over images corrupted with mixed Gaussian-impulsive noise (see Table 11.6 and Figure 11.11) have shown that the method is able to reduce impulsive noise even in the presence of Gaussian noise. However, the performance of the proposed method in the mixed noise case is sometimes even inferior to the VMF because the switching structure is not appropriate to remove mixed noise and it is only able to reduce the impulses. In addition, the proposed method has been tested using real noisy images (see Figures 11.12-11.13) and its performance has been compared with the method in [9]. It can be seen that the proposed method is able to perform a more accurate *noisy*-pixel selection and that the generated output images are less smoothed.

3.8 Contribution (ix): A new fuzzy impulse noise detection method for colour images

In this contribution we develop a new fuzzy impulse noise detection method. The proposed method processes colour images taking into account the correlation between the colour channels but in a different way that the vector approach. Vector-based methods have these two major drawbacks: (i) the higher the noise level is the lower the noise reduction capability is in comparison to the component-wise approaches and (ii) they tend to cluster the noise into a larger array which makes it even more difficult to reduce. The reason for these disadvantages is that the vector-based approaches consider each pixel as a whole unit, while the noise can appear in only one of the three components.

As explained in Section 12.2, in comparison to the vector-based approaches the proposed method is performed in each colour component separately. This implies that a fuzzy membership degree (within $[0, 1]$) in the fuzzy set *noise-free* will be assigned to each colour component of each pixel. When processing a colour, the proposed detection method examines two different relations between the central colour and its neighbouring colours to perform the detection: it is checked both (i) whether each colour component value is similar to the neighbours in the same colour band and (ii) whether the value differences in each colour band corresponds to the value differences in the other bands.

According to Section 12.2, expressions (12.1)-(12.3) are used to compute the degree in which each central colour component is similar to the neighbors in the same colour band. So that, we denote by μ^R, μ^G and μ^B the degree of similarity of the central colour with respect to its neighbors in the Red, Green and Blue colour bands, respectively. In addition, expressions (12.4) and (12.5) are used to compute the degree in which the observed differences in a colour band are similar to the observations in the other colour bands. Indeed, we denote by μ^{RG}, μ^{RB} and μ^{GB} the mentioned degree between the Red-Green, Red-Blue and Green-Blue colour bands, respectively. Notice that some fuzzy similarity measures are used in the above computations.

Finally, the membership degrees of the central colour components in the fuzzy set *noise-free*, that are denoted by $NF_{F_0^R}$, $NF_{F_0^G}$ and $NF_{F_0^B}$, respectively, are computed using the following fuzzy rule. The calculation is illustrated for the R component only but is performed in an analogous way for the G and B component.

Fuzzy Rule 2 *Defining the membership degree $NF_{F_0^R}$ for the red component F_0^R in the fuzzy set* noise-free*:*

`IF` μ^R *is* large *AND* μ^{RG} *is* large *AND* μ^G *is* large `OR`
μ^R *is* large *AND* μ^{RB} *is* large *AND* μ^B *is* large
`THEN` *the noise-free degree of* F_0^R *is* large

A colour component is considered as noise-free if (i) it is similar to its neighbour values (μ^R) and (ii) the observed differences with respect to its neighbours are similar to the observed differences in the other colour components (μ^{RG} and μ^{GB}). In addition, the degrees of similarity of the other component values with respect to their neighbour values, i.e. μ^G and μ^B, are included so that a probably noisy component (with a low μ^G or μ^B value) can not be taken as a reference for the similarity between the observed differences. The example of the proposed noise detection performance which is shown in Figure 12.2 demonstrates the accuracy of the method.

Section 12.3 explains an image denoising method that uses the above fuzzy detection. The image is denoised so that (i) each colour component is smoothed according to its noisy degree and (ii) the colour information is used to estimate the output values. We propose to compute a weight for each colour component in order to calculate a weighted averaging to obtain the output. Now we illustrate the case of the R component but it is done in an analogous way for the G and B components. The denoised R component is obtained as follows

$$\hat{F}_0^R = \frac{\sum_{k=0}^{n^2-1} W_{F_k^R} F_k^R}{\sum_{k=0}^{n^2-1} W_{F_k^R}} \tag{3.22}$$

where $\hat{F}_0^R$ denotes the estimated value for the R component, $F_k^R, k = 0, ..., n^2 - 1$ denote the R component values in the filter window and $W_{F_k^R}$ are their respective weights. The weight of the component being processed $W_{F_0^R}$ is set proportionally to its noise-free degree $NF_{F_0^R}$ so that it will be less weighted, and therefore more smoothed, if its noise-free degree is lower. The weight of the neighbour components is set inversely proportional to the noise-free degree of the component being denoised $NF_{F_0^R}$. Therefore, the neighbours are more weighted as $NF_{F_0^R}$ is lower. In addition, in order to take into account the colour information, we will weigh more those components F_k^R for which it can be observed that F_k^G is similar to F_0^G or that F_k^B is similar to F_0^B. The underlying reasoning is that if two colours have similar G or B components then it is observed that the R component is also similar.

Section 12.4 explains that the filter parameters have been set experimentally. Also in this section, the proposed method is assessed both visually and in terms of the PSNR quality measure. The Baboon, Boats and Parrots images have been corrupted with different densities of random-value impulsive noise and the filter performance has been compared with other state-of-the-art filters including gray-scale filters applied in a componentwise way, some vector filters and some fuzzy colour image filters. Experimental results are shown in Tables 12.1 and 12.2 and Figure 12.3. Numerical results show that

the proposed method achieves the best results in almost all cases. By visually analyzing Figure 12.3 it can be seen that the best visual results were obtained by the proposed method. We observe that the proposed method reduces the noise very well while preserving the colour information and the important image features like edges and textures. In addition, it is also observed that the proposed method does not introduce blurring nor colour artifacts.

References

1. J. Astola, P. Haavisto, Y. Neuvo, *Vector Median Filters*, Proc. IEEE. 78 4 (1990) 678-689.
2. A. George, P. Veeramani, On Some results in fuzzy metric spaces, *Fuzzy Sets and Systems* 64 3 (1994) 395-399.
3. D.G. Karakos, P.E. Trahanias, Generalized multichannel image-filtering structure, *IEEE Transactions on Image Processing* 6 7 (1997) 1038-1045.
4. A. Sapena, A contribution to the study of fuzzy metric spaces, *Appl. Gen. Topology* 2 1(2001) 63-76.
5. B. Smolka,K.N. Plataniotis, R. Lukac, A.N. Venetsanopoulos, Similarity based impulsive noise removal in colour images, *International Conference on Image Processing ICIP 2003* .
6. B. Smolka, R. Lukac, A. Chydzinski, K.N. Plataniotis, W. Wojciechowski, Fast adaptive similarity based impulsive noise reduction filter, *Real-Time Imaging* 9 4 (2003) 261-276.
7. B. Smolka, A. Chydzinski, K.N. Plataniotis, A.N. Venetsanopoulos, New filtering technique for the impulsive noise removal in color images, *Mathematical Problems in Engineering* 1 (2004) 79-91.
8. B. Smolka, K.N. Plataniotis, A. Chydzinski, M. Szczepanski, A.N. Venetsanopoulos, K. Wojciechowski, Self-adaptive algorithm of impulsive noise reduction in color images, *Pattern Recognition* 35 8 (2002) 1771-1784.
9. B. Smolka, A. Chydzinski, Fast detection and impulsive noise removal in color images, *Real-Time Imaging* 11 5-6 (2005) 389-402.
10. C. Tomasi, R. Manduchi, *Bilateral filter for gray and color images*, Proc. IEEE International Conference Computer Vision, 1998, 839-846.
11. P.E. Trahanias, D. Karakos, A.N. Venetsanopoulos, Directional processing of color images: theory and experimental results, *IEEE Trans. Image Process.* 5 6 (1996) 868-880.

4 Contribution (i)

S. Morillas, V. Gregori, G. Peris-Fajarnés, P. Latorre, A new vector median filter based on fuzzy metrics, *ICIAR05, Lecture Notes in Computer Science* 3656 (2005) 81-90.

Abstract

Vector median filtering is a well known technique for reducing noise in colour images. These filters are defined on the basis of a suitable distance or similarity measure, being the most common used the Euclidean and City-Block distances. In this paper, a Fuzzy Metric, in the sense of George and Veeramani (1994), is defined and applied to colour image filtering by means of a new Vector Median Filter. It is shown that the standard Vector Median Filter is outperformed when using this Fuzzy Metric instead of the Euclidean and City-Block distances.

4.1 Introduction

Images are acquired by photoelectronic or photochemical methods. The sensing devices and the transmission process tend to degrade the quality of the digital images by introducing noise, geometric deformation and/or blur due to motion or camera misfocus [8, 27].

Noise introduced into images may corrupt any of the following image processing steps mostly related to image analysis (edge detection, image segmentation, and pattern recognition) and computer vision applications. Therefore, filtering is an essential part of any image processing system whether the final product is used for human inspection or for an automatic analysis [28].

Several nonlinear multichannel filters which utilize correlation among multivariate vectors, using various *distance measures*, have been proposed in the literature. Nonlinear filters applied to images are required to remove different types of noise without degrading the quality of the image, preserving edges, corners and other image details. One of the most important families

of nonlinear filters is based on the ordering of vectors in a predefined sliding window [27, 28]. The output of this filter is defined as the lowest ranked vector according to a specific ordering criterion based on vectors magnitude and/or vectors direction.

Probably the most well-known filter is the *vector median filter* (VMF) [3] which uses the L_1 (City-Block) or L_2 (Euclidean) norm to order vectors according to their relative magnitude differences. VMF can be derived as a maximum likelihood estimate (MLE) when the underlying probability densities of input samples are double exponential.

The direction of the image vectors can also be used as an ordering criterion to remove vectors with atypical direction, which means atypical chromaticity. The *basic vector directional filter* (BVDF) parallelizes the VMF operation employing the angle between colour vectors as a distance criterion. The BVDF uses only information about directions, so, it is not able to remove achromatic noisy pixels from the image. The *Directional Distance Filter* (DDF) overcomes the difficulties of the BVDF by using both magnitude and direction in the distance criterion [33].

On this basis, the order statistics filters have been improved including high level techniques such as the use of fuzzy rules [2], cluster analysis [1], weighting coefficients [19], adaptive mechanisms [20], rational functions [17] and digital paths [32].

In the colour image processing field both magnitude and chromatic relations play a major role [6]. This relationships are usually represented using a distance or similarity measure. Many different distance and similarity measures have been introduced in the literature [28, 6, 7, 35, 36, 29]. Some of them are based on fuzzy theory [6, 7, 35, 36, 29] and have been recently applied with many different purposes in image processing, such as, image retrieval [9], image comparison [34], object recognition [11], or region extraction [10].

In this paper, a fuzzy metric in the terms of George and Veeramani [12] is defined and applied to colour image filtering by adapting the well-known VMF. The paper is organized as follows. The fuzzy metric is defined in Section 4.2. In Section 4.3, the proposed filtering is explained. In Section 4.4, some experimental results are shown. Finally, conclusions are presented in Section 5.5.

4.2 An appropriate Fuzzy Metric

One of the most important problems in Fuzzy Topology is to obtain an appropriate concept of fuzzy metric. This problem has been investigated by many authors from different points of view. In particular, George and Veeramani [12] have introduced and studied the following notion of fuzzy metric which constitutes a slight modification of the one due to Kramosil and Michalek [18].

According to [12] a fuzzy metric space is an ordered triple $(X, M, *)$ such that X is a (nonempty) set, $*$ is a continuous t-norm and M is a fuzzy set of $X \times X \times]0, +\infty[$ satisfying the following conditions for all $x, y, z \in X,\ s, t > 0$:

(FM1) $M(x, y, t) > 0$

(FM2) $M(x, y, t) = 1$ if and only if $x = y$

(FM3) $M(x, y, t) = M(y, x, t)$

(FM4) $M(x, z, t + s) \geq M(x, y, t) * M(y, z, s)$

(FM5) $M(x, y, \cdot) :]0, +\infty[\longrightarrow [0, 1]$ is continuous.

$M(x, y, t)$ represents the degree of nearness of x and y with respect to t. If $M(x, y, *)$ is a fuzzy metric space we will say that $(M, *)$ is a fuzzy metric on X. In the following, by a fuzzy metric we mean a fuzzy metric in the George and Veeramani's sense.

The authors proved in [12] that every fuzzy metric $(M, *)$ on X generates a Hausdorff topology on X. Actually, this topology is metrizable as it was proved in [13, 14], and so the above definition can be considered an appropriate concept of fuzzy metric space.

A fuzzy metric $(M, *)$ on X is said to be stationary if M does not depend on t, i.e. for each $x, y \in X$ the function $M_{x,y}(t) = M(x, y, t)$ is constant [15].

A subset A of X is said to be F-bounded [12] if there exist $t > 0$ and $s \in]0, 1[$ such that $M(x, y, t) > s$ for all $x, y \in A$.

Example 4.4 of [30] suggests the next proposition.

Proposition 1. *Let X be the closed real interval $[a, b]$ and let $K > |a| > 0$. Consider for each $n = 1, 2, \cdots$ the function $M_n : X^n \times X^n \times]0, +\infty[\longrightarrow]0, 1]$ given by*

$$M_n(x, y, t) = \prod_{i=1}^{n} \frac{min\{x_i, y_i\} + K}{max\{x_i, y_i\} + K} \tag{4.1}$$

where $x = (x_1, \cdots, x_n), y = (y_1, \cdots, y_n)$, and $t > 0$. Then, $(M_n, \cdot)$ is a stationary F-bounded fuzzy metric on X^n, where the t-norm $\cdot$ is the usual product in $[0, 1]$.

Proof. Axioms (FM1)-(FM3) and (FM5) are obviously fulfilled. We show, by induction, the triangular inequality (FM4).

An easy computation shows that M_1 verifies (FM4). Now, suppose it is true for M_{n-1}. Then, for each $x = (x_1, \cdots, x_n), y = (y_1, \cdots, y_n), z = (z_1, \cdots, z_n)$ and for each $t, s > 0$ we have

$$\begin{gathered} M_n(x, z, t + s) = \prod_{i=1}^{n} \frac{min\{x_i, z_i\} + K}{max\{x_i, z_i\} + K} = \\ = \prod_{i=1}^{n-1} \frac{min\{x_i, z_i\} + K}{max\{x_i, z_i\} + K} \cdot \frac{min\{x_n, z_n\} + K}{max\{x_n, z_n\} + K} \geq \\ \geq \prod_{i=1}^{n-1} \frac{min\{x_i, y_i\} + K}{max\{x_i, y_i\} + K} \cdot \prod_{i=1}^{n-1} \frac{min\{y_i, z_i\} + K}{max\{y_i, z_i\} + K} \cdot \frac{min\{x_n, y_n\} + K}{max\{x_n, y_n\} + K} \cdot \frac{min\{y_n, z_n\} + K}{max\{y_n, z_n\} + K} = \\ = \prod_{i=1}^{n} \frac{min\{x_i, y_i\} + K}{max\{x_i, y_i\} + K} \cdot \prod_{i=1}^{n} \frac{min\{y_i, z_i\} + K}{max\{y_i, z_i\} + K} = M_n(x, y, t) \cdot M_n(y, z, s), \end{gathered} \tag{4.2}$$

so M_n is a fuzzy metric on X^n, for $n = 1, 2, \cdots$ and clearly it is stationary.

Finally, X^n is F-bounded, for $n = 1, 2, \cdots$ Indeed, if we write $\mathbf{a} = (\overbrace{a, \ldots, a}^{n})$ and $\mathbf{b} = (\overbrace{b, \ldots, b}^{n})$, then for each $x, y \in X^n$ and $t > 0$ we have

$$M_n(x, y, t) \geq M_n(\mathbf{a}, \mathbf{b}, t) = \left(\frac{a + K}{b + K}\right)^n > 0, \text{ for } n = 1, 2, \cdots \tag{4.3}$$

□

In next sections we will use the above fuzzy metric and it will be denoted $M_n(x, y)$, since it does not depend on t.

4.2.1 Computational Analysis

Computationally efficient distances are of interest in the field of order statistics filters [4, 5]. For this reason, the use of the L_1 Norm is preferred to the L_2 Norm in many cases [28].

The particular case of the proposed fuzzy metric M_n suitable for 3-channel image processing tasks will be M_3, where $M_3(I_i, I_j)$ will denote the fuzzy distance between the pixels I_i and I_j in the I image. For each calculation of M_3: 3 comparisons, 6 additions, 3 divisions and 2 products have to be computed. In the case of L_1 Norm are necessary 3 comparisons (absolute value), 3 subtractions and 2 additions whereas for the L_2 Norm 3 subtractions, 3 powers, 2 additions and 1 square-root have to be done. As can be seen in Table 6.1, the computational complexity of M_3 is even higher that the L_2 Norm. However, an optimization in the calculus of M_3 (Fast M_3) may be applied.

Given a fixed parameter K in (4.1), numerator and denominator of each division in (4.1) are in a bounded set $[K, 255 + K]$ when processing RGB images. All the possible divisions can be precalculated in a square matrix C where

$$C(i, j) = \frac{min\{i, j\} + K}{max\{i, j\} + K} \quad i, j \in [0, 255] \tag{4.4}$$

Using the pre-calculus matrix, the calculation of Fast M_3 for two pixels $I_i = (I_i(1), I_i(2), I_i(3)), I_j = (I_j(1), I_j(2), I_j(3))$ is reduced to

$$M_3(I_i, I_j) = \prod_{l=1}^{3} C(I_i(l), I_j(l)) \tag{4.5}$$

Table 4.1. Computational comparison between the classical metrics L_1 and L_2 and the proposed fuzzy metric M_3 measured in a Pentium IV 2.4GHz

Metric	1 calculus (μs)	Calculus per second
L_1 Norm	28.37	$3.524\ 10^4$
L_2 Norm	30.10	$3.322\ 10^4$
M_3	34.68	$2.883\ 10^4$
Fast M_3	26.98	$3.706\ 10^4$

By means of this optimization, 3 accesses to matrix and 2 products are enough to make the calculus.

The time measured for the construction of the matrix C is about 0.8 seconds in a Pentium IV 2.4GHz. Although it supposes an initial cost, the gain is approx. $8\mu s$ (see Table 4.1) in each calculus, so, the initial cost is compensated when 10^5 calculus have to be computed (which is roughly the calculus involved in the filtering of a $50 \cdot 50$ pixels image[1]).

The results presented in Table 4.1 show that the M_3 Fuzzy Metric is computationally cheaper than the classical L_1 and L_2 Norms when the optimization of the pre-calculus matrix is applied.

4.3 Image Filtering

4.3.1 Classical Vector Median Filter [3, 28]

Let I represents a multichannel image and let W be a window of finite size n (filter length). The noisy image vectors in the filtering window W are denoted as $I_j, j = 0, 1, ..., n-1$. The *distance* between two vectors I_i, I_j is denoted as $\rho(I_i, I_j)$. For each vector in the filtering window, a global, accumulated distance to all other vectors in the window has to be calculated. The scalar quantity $R_i = \sum_{j=0}^{n-1} \rho(I_i, I_j)$, is the distance associated to the vector I_i. The ordering of the $R_{(i)}$'s: $R_{(0)} \leq R_{(1)} \leq ... \leq R_{(n-1)}$, implies the same ordering of the vectors I_i's: $I_{(0)} \leq I_{(1)} \leq ... \leq I_{(n-1)}$. Given this order, the output of the filter is $I_{(0)}$.

4.3.2 Proposed Vector Median Filter

The proposed filter will parallelize the operation of the classical VMF with just one modification. The ordering criterion usually used as defined above has to be inverted due to the axiom (FM2) of the fuzzy metric (4.1), and then the vector median must now be defined as the vector in the sliding window that maximizes the *accumulated* fuzzy distance, as follows.

Being the fuzzy distance between two pixels I_i, I_j of the image I in the n length sliding window W denoted as $M_3(I_i, I_j)$, the scalar quantity $M^i = \sum_{j=0, j\neq i}^{n-1} M_3(I_i, I_j)$, is the accumulated fuzzy distance associated to the vector I_i. According to VMF, the ordering of the $M^{(i)}$'s is now defined as: $M^{(0)} \geq M^{(1)} \geq ... \geq M^{(n-1)}$, therefore, the ordering of the vectors $I_{(i)}$ is: $I_{(0)} \geq I_{(1)} \geq ... \geq I_{(n-1)}$. Given this order, the output of the filter I_{out} is defined as $I_{(0)}$.

This is, in general, the straightforward adaptation of the VMF when using a similarity measure instead of a distance measure [28].

[1] For all the filters studied in this article has been used a 8-neighborhood 3×3 size window W.

4.4 Experimental results

In this section, the classical gaussian model for the thermal noise and the impulsive noise model for the transmission noise, as defined in [28, 32], has been used to add noise to the well-known images Lenna ($256 \cdot 256$), Peppers ($512 \cdot 512$) and Baboon ($512 \cdot 512$). The performance of the filter has been evaluated by using the common measures MSE, SNR and NCD as defined in [32].

Three different types of noise, according to the models in [28, 32], have been considered in this section:
- Type A = low contaminated impulsive noise $p = 7\%, p_1 = p_2 = p_3 = 0.3$
- Type B = high contaminated impulsive noise $p = 30\%, p_1 = p_2 = p_3 = 0.3$
- Type C = mixed gaussian impulsive noise $\sigma = 10, p = 15\%, p_1 = p_2 = p_3 = 0.3$

4.4.1 Adjusting the K parameter

The K parameter included in the definition of the Fuzzy Metric M_3 (4.1) has an important influence on the filter performance. The metric is non-uniform in the sense that the measure given by M_3 for two different pairs of consecutive numbers (or vectors) may not be the same. However, this feature may be very interesting since it is known that the human perception of colour is also non-uniform [26]. Clearly, increasing the value of K reduces this non-uniformity. This effect is shown in Figure 4.1 where the content of the matrix C (4.4) for different values of K is presented.

After performing several tests, the results seem to show that a suitable value for the K parameter for a variety of noise types is $K = 2^{10}$. The dependence of the performance on the value of K is shown in Fig. 4.2. The use of a proper value for K may lead to an improvement of the filter performance up to 60%. In Fig. 4.2 the performance (MSE) of the filter dependent on K is shown for the filtering of the Lenna image contaminated with type B noise. For other performance measures as SNR and NCD the behavior is similar to MSE. The performance is low for lower values of K. Increasing K leads to a maximum performance and then it decreases slightly for higher values of K. Finding the optimum K is a problem we are trying to solve since it depends on the particular image and noise. In spite of it, it has been found that in the most of the tested cases the optimum is in the range $[2^9, 2^{15}]$, as the case shown in Fig. 4.2

4.4.2 Comparing performances

In order to compare the performance of the VMF using the metrics L_1, L_2 and M_3, different images contaminated with different types of noise have been used.

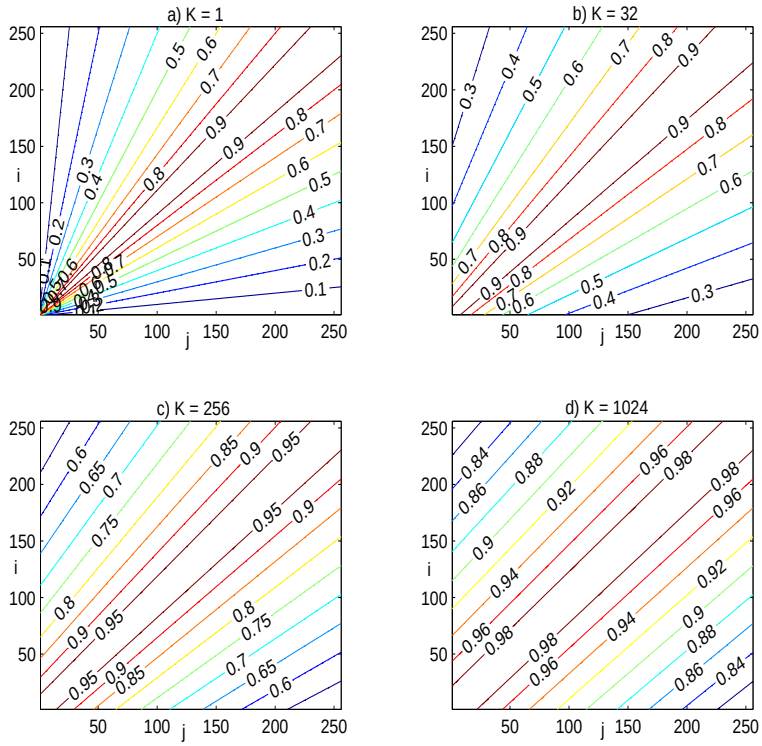

Fig. 4.1. Content of the pre-calculus matrix $C(i, j)$ for several values of K.

Table 4.2. Comparison of the performance measured in terms of MSE, SNR and NCD using the Lenna image contaminated with different types of noise

Filter	A Noise			B Noise			C Noise		
	MSE	SNR	NCD_{Lab}	MSE	SNR	NCD_{Lab}	MSE	SNR	NCD_{Lab}
None	552.9	15.17	4.92 10^{-2}	2318.51	9.35	20.80 10^{-2}	1246.86	12.04	17.90 10^{-2}
VMF L_1	42.18	26.75	1.81 10^{-2}	59.63	25.25	2.19 10^{-2}	91.59	23.38	6.40 10^{-2}
VMF L_2	45.56	26.41	1.79 10^{-2}	76.05	24.19	2.46 10^{-2}	97.01	23.13	6.35 10^{-2}
VMF M_3	41.81	26.78	1.80 10^{-2}	59.18	25.28	2.17 10^{-2}	90.49	23.43	6.36 10^{-2}

The results of the performance measured in tems of MSE, SNR and NCD are shown in Tables 4.2,4.3 and 4.4. Fig. 4.4 presents the peppers image contaminated with type B noise (30% impulsive) and the output of the compared filters, standing out a detail of each image.

The results show that the VMF using the proposed fuzzy metric may give better performance than using the classical metrics.

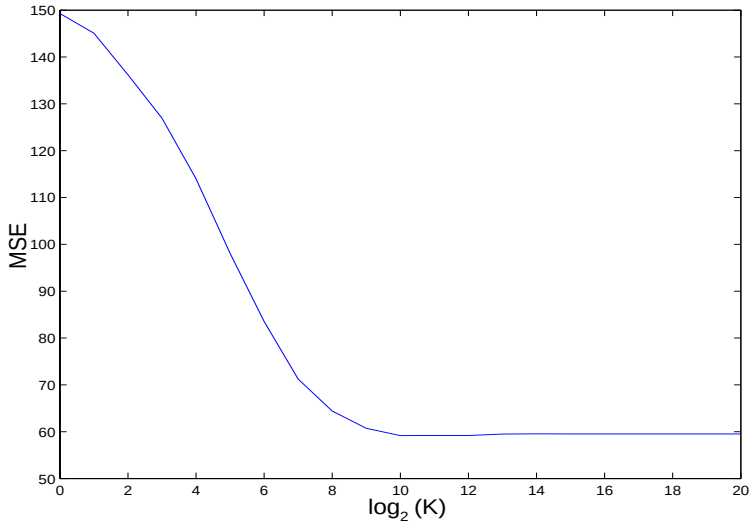

Fig. 4.2. Performance of the VMF using M_3 in terms of MSE depending on K using the Lenna image contaminated with type B noise.

Table 4.3. Comparison of the performance measured in terms of MSE, SNR and NCD using the Peppers image contaminated with different types of noise

Filter	A Noise			B Noise			C Noise		
	MSE	SNR	NCD_{Lab}	MSE	SNR	NCD_{Lab}	MSE	SNR	NCD_{Lab}
None	566.94	14.42	4.84 10^{-2}	2493.27	7.99	21.09 10^{-2}	1324.56	10.73	19.66 10^{-2}
VMF L_1	18.87	29.19	4.84 10^{-2}	35.49	26.45	2.34 10^{-2}	63.10	23.95	7.53 10^{-2}
VMF L_2	19.30	29.10	1.88 10^{-2}	40.37	25.89	2.46 10^{-2}	64.98	23.82	7.51 10^{-2}
VMF M_3	18.71	29.23	1.86 10^{-2}	33.35	26.72	2.29 10^{-2}	62.10	24.02	7.48 10^{-2}

Table 4.4. Comparison of the performance measured in terms of MSE, SNR and NCD using the Baboon image contaminated with different types of noise

Filter	A Noise			B Noise			C Noise		
	MSE	SNR	NCD_{Lab}	MSE	SNR	NCD_{Lab}	MSE	SNR	NCD_{Lab}
None	535.33	15.52	4.83 10^{-2}	2301.44	9.18	20.76 10^{-2}	1238.64	11.88	17.37 10^{-2}
VMF L_1	287.66	18.22	4.07 10^{-2}	326.93	17.66	4.48 10^{-2}	350.65	17.36	7.93 10^{-2}
VMF L_2	295.07	18.11	4.02 10^{-2}	351.71	17.34	4.61 10^{-2}	359.89	17.24	7.72 10^{-2}
VMF M_3	287.98	18.21	4.05 10^{-2}	326.73	17.67	4.46 10^{-2}	350.27	17.36	7.88 10^{-2}

Conclusions

The metric (4.1) proposed in section 4.2, which has been proved to be a Fuzzy Metric in the sense of George and Veeramani [12], is a suitable fuzzy metric to be used in multichannel image filtering. The adaptation of the Vector Median Filter (Section 4.3) for the use of the proposed fuzzy metric

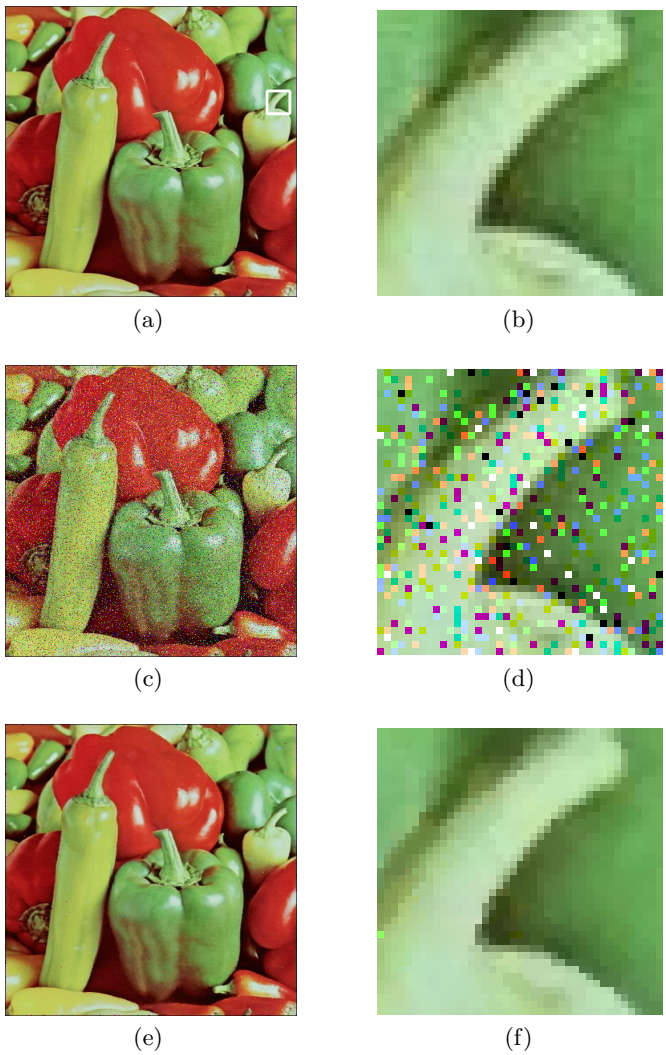

(a) (b) (c) (d) (e) (f)

Fig. 4.3. (a) Original image peppers pointing out the detailed area,(b) detailed area,(c) peppers corrupted with noise type B and (d) detail, (e) result of the VMF using L_1 and (f) detail...(continued)

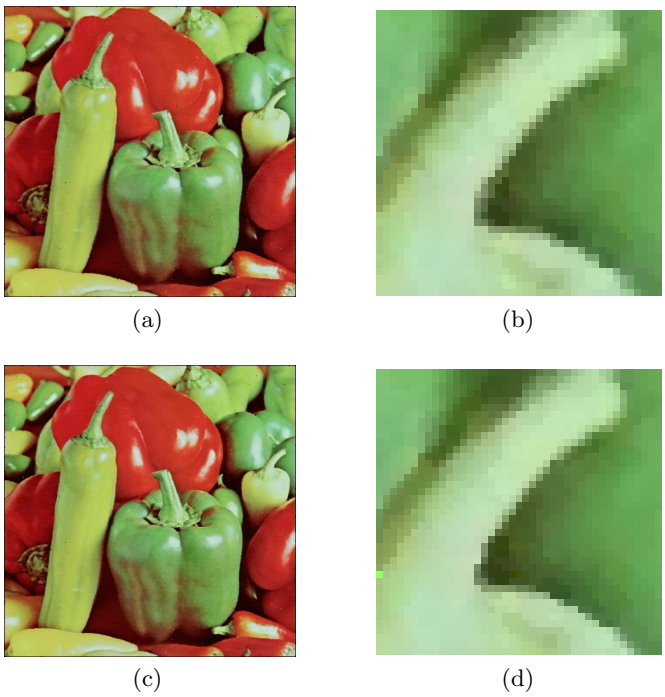

Fig. 4.4. (continue)... (a) result of the VMF using L_2 and (b) detail, (c) result of the proposed filter using M_3 and (d) detail

outperforms the usual VMF's using the classical metrics L_1 and L_2, specially when the impulsive noise present in the image is high, as has been shown in Section 4.4. Moreover, the proposed metric presents a nice computational cost (see Section 4.2.1).

Fuzzy Metrics are a powerful tool which may be successfully applied in image processing tasks since they are able to represent more complex relations than the classical metrics.

References

1. H. Allende, J. Galbiati, *A non-parametric filter for image restoration using cluster analysis*, Pattern Recognition Letters 25 8 (2004) 841-847.
2. K. Arakawa, *Median filter based on fuzzy rules and its application to image restoration*, Fuzzy Sets and Systems 77 1 (1996) 3-13.
3. J. Astola, P. Haavisto, Y. Neuvo, *Vector Median Filters*, Proc. IEEE. 78 4 (1990) 678-689.
4. M. Barni, F. Buti, F. Bartolini, V. Capellini, *A Quasi-Euclidean Norm to Speed Up Vector Median Filtering*, IEEE Transactions on Image Processing 9 10 (2000) 1704-1709.
5. M. Barni, *A Fast Algorithm for 1-Norm Vector Median Filtering*, IEEE Transactions on Image Processing, 6 10 (1997) 1452-1455.
6. I. Bloch, *Fuzzy spatial relationships for image processing and interpretation: a review*, Image and Vision Computing 23 2 (2005) 89-110.
7. I. Bloch, *On fuzzy spatial distances*, Advances in imaging and electron physics 128 (2003).
8. C. Boncelet,*Image noise models*, in: A. Bovik (Ed.), Handbook of Image and Video Processing. Academic Press, 2000.
9. T. Chaira, A.K. Ray, *Fuzzy Measures for color image retrieval*, Fuzzy Sets and Systems 150 3 (2005) 545-560.
10. T. Chaira, A.K. Ray, *Fuzzy approach for color region extraction*, Pattern Recognition Letters 24 12 (2003) 1943-1950.
11. O. Coillot, A.V. Tuzikov, R.M. Cesar, I.Bloch, *Approximate reflectional simmetries of fuzzy objects with an application in model based object recognition*, Fuzzy Sets and Systems 147 1 (2004) 141-163.
12. A. George, P. Veeramani,*On Some results in fuzzy metric spaces*, Fuzzy Sets and Systems 64 3 (1994) 395-399.
13. A. George, P. Veeramani, *Some theorems in fuzzy metric spaces* , J. Fuzzy Math. 3 (1995) 933-940.
14. V. Gregori, S. Romaguera, *Some properties of fuzzy metric spaces*, Fuzzy Sets and Systems 115 3 (2000) 477-483.
15. V. Gregori, S. Romaguera, *Characterizing completable fuzzy metric spaces*, Fuzzy Sets and Systems 144 3 (2004) 411-420.
16. D.G. Karakos, P.E. Trahanias, *Generalized multichannel image-filtering structures* , IEEE Transactions on Image Processing 6 7 (1997) 1038-1045.
17. L. Khriji, M. Gabbouj, *Adaptive fuzzy order statistics-rational hybrid filters for color image processing*, Fuzzy Sets and Systems 128 1 (2002) 35-46.
18. I. Kramosil, J. Michalek, *Fuzzy metric and statistical metric spaces*, Kybernetica 11 (1975) 326-334

19. R. Lukac, B. Smolka, K.N. Plataniotis, A.N. Venetsanopoulos, *Selection weighted vector directional filters*, Computer Vision and Image Understanding 94 (2004) 140-167.
20. R. Lukac, *Adaptive vector median filtering*, Pattern Recognition Letters, 24 12 (2003) 1889-1899.
21. R. Lukac, B. Smolka, K. Martin, K.N. Plataniotis, A.N. Venetsanopoulos, *Vector Filtering for Color Imaging*, IEEE Signal Processing Magazine, Special Issue on Color Image Processing, 22 1 (2005) 74-86.
22. R. Lukac, K.N. Plataniotis, B. Smolka, A.N. Venetsanopoulos, *Generalized Selection Weighted Vector Filters*, EURASIP Journal on applied signal processing, Special Issue on Nonlinear signal and image processing 12 (2004) 1870-1885.
23. R. Lukac, K.N. Plataniotis, B. Smolka, A.N. Venetsanopoulos, *A Multichannel Order-Statistic Technique for cDNA Microarray Image Processing* IEEE Transactions on Nanobioscience 3 4 (2004) 272-285.
24. R. Lukac, K.N. Plataniotis, B. Smolka, A.N. Venetsanopoulos, *cDNA Microarray Image Processing Using Fuzzy Vector Filtering Framework* Fuzzy Sets and Systems, Special Issue on Fuzzy Sets and Systems on Bioinformatics 152 1 (2005) 17-35.
25. R. Lukac, *Adaptive Color Image Filtering Based on Center Weighted Vector Directional Filters* Multidimensional Systems and Signal Processing 15 (2004) 169-196.
26. D.L. MacAdam, *Visual sensitivities to color differences in daylight*, J. Opt. Soc. Am., 33 (1942) 247-274
27. I. Pitas, *Digital image processing algorithms and applications*, John Wiley & Sons, 2000.
28. K.N. Plataniotis, A.N. Venetsanopoulos, *Color Image processing and applications*, Springer-Verlag, Berlin, 2000.
29. S. Santini, R. Jain, *Similarity Measures*, IEEE Transactions on pattern recognition and machine intelligence 21 9 (1999) 871-883.
30. A. Sapena, *A contribution to the study of fuzzy metric spaces* Appl. Gen. Topology 2 1(2001) 63-76.
31. B. Smolka, R. Lukac, A. Chydzinski, K.N. Plataniotis, W. Wojciechowski *Fast adaptive similarity based impulsive noise reduction filter* Real-Time Imaging 9 4 (2003) 261-276.
32. M. Szczepanski, B. Smolka, K.N. Plataniotis, A.N. Venetsanopoulos, *On the distance function approach to color image enhancement*, Discrete Applied Mathematics 139 (2004) 283-305.
33. P.E. Trahanias, D. Karakos, A.N. Venetsanopoulos, *Vector Directional Filters: a new class of multichannel image processing filters*, IEEE Trans. Image Process. 2 4 (1993) 528-534.
34. D. Van der Weken, M. Nachtegael, E.E. Kerre, *Using similarity measures and homogeneity for the comparison of images*, Image and Vision Computing 22 9 (2004) 695-702.
35. W.J. Wang, *New similarity measures on fuzzy sets and on elements*, Fuzzy sets and systems 85 3 (1997) 305-309.
36. D. Yong, S. Wenkang, D. Feng, L. Qi, *A new similarity measure of generalized fuzzy numbers and its application to pattern recognition*, Pattern Recognition Letters 25 8 (2004) 875-883.

5 Contribution (ii)

S. Morillas, V. Gregori, A. Sapena, Fuzzy bilateral filtering for colour images, *ICIAR06, Lecture Notes in Computer Science* 4141 (2006) 138-145.

Abstract

Bilateral filtering is a well-known technique for smoothing gray-scale and colour images while preserving edges and image details by means of an appropriate nonlinear combination of the colour vectors in a neighborhood. The pixel colours are combined based on their spatial closeness and photometric similarity. In this paper, a particular class of fuzzy metrics is used to represent the spatial and photometric relations between the colour pixels adapting the classical bilateral filtering. It is shown that the use of these fuzzy metrics is more appropriate than the classical measures used.

5.1 Introduction

Any image is systematically affected by the introduction of noise during its acquisition and transmission process. A fundamental problem in image processing is to effectively suppress noise while keeping intact the features of the image. Fortunately, two noise models can adequately represent most noise corrupting images: additive Gaussian noise and impulsive noise [12].

Additive Gaussian noise, which is usually introduced during the acquisition process, is characterized by adding to each image pixel channel a random value from a zero-mean Gaussian distribution. The variance of this distribution determines the intensity of the corrupting noise. The zero-mean property allows to remove such noise by locally averaging pixel channel values.

Ideally, removing Gaussian noise would involve to smooth the different areas of an image without degrading neither the sharpness of their edges nor their details. Classical linear filters, such as the Arithmetic Mean Filter (AMF) or the Gaussian Filter, smooth noise but blur edges significantly. Nonlinear methods have been used to approach this problem. The aim of the methods proposed in the literature is to detect edges by means of local

measures and smooth them less than the rest of the image to better preserve their sharpness. A well-known method is the anisotropic diffusion introduced in [11]. In this technique, local image variation is measured at every point and pixels from neighborhoods whose size and shape depend on local variation are averaged. Diffusion methods are inherently iterative since the use of differential equations is involved. On the other hand, a non-iterative interesting method, which is the motivation of this work, is the bilateral filter (BF) studied in [15]. The output of the BF at a particular location is a weighted mean of the pixels in its neighborhood where the weight of each pixel depends on the spatial closeness and photometric similarity respect to the pixel in substitution. The BF has been proved to perform effectively in Gaussian noise suppression and it has been the object of further studies [2, 3, 14].

In this paper, a certain class of fuzzy metrics is used to model the relations of spatial closeness and photometric similarity between image pixels used in the BF. Then, the BF structure is adapted an the, from now on called, *Fuzzy Bilateral Filter* (FBF) is proposed. The use of fuzzy metrics instead of the measures used in [15] makes the filter easier to use since the number of adjusting parameters is lower. Moreover, the performance of the proposed filter is improved respect to the other filters in the comparison in the sense that will be shown.

The paper is arranged as follows. The classical BF is described in Section 5.2. The use of fuzzy metrics to model the spatial and photometric relations is detailed in Section 5.3. Section 5.4 defines the *Fuzzy Bilateral Filter*. Experimental results and discussions are presented in Section 5.5 and conclusions are given in Section 5.6.

5.2 Bilateral Filtering

Let $\mathbf{F}$ represent a multichannel image and let W be a sliding window of finite size $n \times n$. Consider the pixels in W represented in Cartesian Coordinates and so, denote by $\mathbf{i} = (i_1, i_2) \in Y^2$ the position of a pixel $\mathbf{F_i}$ in W where $Y = \{0, 1, \ldots, n-1\}$ is endowed with the usual order. According to [15], the BF replaces the central pixel of each filtering window by a weighted average of its neighbor colour pixels. The weighting function is designed to smooth in regions of similar colours while keeping edges intact by heavily weighting those pixels that are both spatially close and photometrically similar to the central pixel.

Denote by $||\cdot||_2$ the Euclidean norm and by $\mathbf{F_i}$ the central pixel under consideration. Then the weight $\mathcal{W}(\mathbf{F_i}, \mathbf{F_j})$ corresponding to any pixel $\mathbf{F_j}$ respect to $\mathbf{F_i}$ is the product of two components, one spatial and one photometrical

$$\mathcal{W}(\mathbf{F_i}, \mathbf{F_j}) = \mathcal{W}_s(\mathbf{F_i}, \mathbf{F_j})\mathcal{W}_p(\mathbf{F_i}, \mathbf{F_j}) \tag{5.1}$$

where the spatial component $\mathcal{W}_s(\mathbf{F_i}, \mathbf{F_j})$ is given by

$$\mathcal{W}_s(\mathbf{F_i}, \mathbf{F_j}) = e^{-\frac{||\mathbf{i}-\mathbf{j}||_2^2}{2\sigma_s^2}} \tag{5.2}$$

and the photometrical component $\mathcal{W}_p(\mathbf{F_i}, \mathbf{F_j})$ is given by

$$\mathcal{W}_p(\mathbf{F_i}, \mathbf{F_j}) = e^{-\frac{\Delta E_{Lab}(\mathbf{F_i}, \mathbf{F_j})^2}{2\sigma_p^2}} \tag{5.3}$$

where $\Delta E_{Lab} = [(\Delta L^*)^2 + (\Delta a^*)^2 + (\Delta b^*)^2]^{\frac{1}{2}}$ denotes the perceptual colour error in the $L^*a^*b^*$ colour space, and $\sigma_s, \sigma_p > 0$

The colour vector output $\widetilde{\mathbf{F_i}}$ of the filter is computed using the normalized weights and so it is given by

$$\widetilde{\mathbf{F_i}} = \frac{\sum_{\mathbf{F_j} \in W} \mathcal{W}(\mathbf{F_i}, \mathbf{F_j})\mathbf{F_j}}{\sum_{\mathbf{F_j} \in W} \mathcal{W}(\mathbf{F_i}, \mathbf{F_j})} \tag{5.4}$$

The $\mathcal{W}_s$ weighting function decreases as the spatial distance in the image between $\mathbf{i}$ and $\mathbf{j}$ increases, and the $\mathcal{W}_p$ weighting function decreases as the perceptual colour difference between the colour vectors increases. The spatial component decreases the influence of the furthest pixels reducing blurring while the photometric component reduces the influence of those pixels which are perceptually different respect to the one under processing. In this way, only perceptually similar areas of pixels are averaged together and the sharpness of edges is preserved.

The parameters σ_s and σ_p are used to adjust the influence of the spatial and the photometric components, respectively. They can be considered as rough thresholds for identifying pixels sufficiently close or similar to the central one. Note that when $\sigma_p \to \infty$ the BF approaches a Gaussian filter and when $\sigma_s \to \infty$ the filter approaches a range filter with no spatial notion. In the case when both $\sigma_p \to \infty$ and $\sigma_s \to \infty$ the BF behaves as the AMF.

5.3 Fuzzy Metric approach

According to [4], a fuzzy metric space is an ordered triple $(X, M, *)$ such that X is a (nonempty) set, $*$ is a continuous t-norm and M is a fuzzy set of $X \times X \times]0, +\infty[$ satisfying the following conditions for all $x, y, z \in X,\ s, t > 0$:

(FM1) $M(x, y, t) > 0$
(FM2) $M(x, y, t) = 1$ if and only if $x = y$
(FM3) $M(x, y, t) = M(y, x, t)$
(FM4) $M(x, z, t + s) \geq M(x, y, t) * M(y, z, s)$
(FM5) $M(x, y, \cdot) :]0, +\infty[\longrightarrow [0, 1]$ is continuous.

$M(x, y, t)$ represents the degree of nearness of x and y with respect to t. If $(X, M, *)$ is a fuzzy metric space we will say that $(M, *)$ is a fuzzy metric on X. According to [5, 6], the above definition can be considered an appropriate

concept of fuzzy metric space. In the following, by a fuzzy metric we mean a fuzzy metric in the George and Veeramani's sense (from now on we will omit the mention to the continuous t-norm $*$ since in all the cases it will be the usual product in $[0,1]$).

A fuzzy metric M on X is said to be stationary if M does not depend on t, i.e. for each $x, y \in X$ the function $M_{x,y}(t) = M(x,y,t)$ is constant [7]. In such case we write $M(x,y)$ instead of $M(x,y,t)$.

In this paper two fuzzy metrics, in a first step, will be used. The first one to measure the photometric fuzzy distance between colour vectors and the second one to measure the spatial fuzzy distance between the pixels under comparison. In order to appropriately measure the photometric fuzzy distance between colour vectors we will use the following fuzzy metric M:

Take $X = \{0, 1, 2, \ldots, 255\}$ and let $K > 0$ fixed. Denote by $(F_{\mathbf{i}}^1, F_{\mathbf{i}}^2, F_{\mathbf{i}}^3) \in X^3$ the colour vector of a pixel $\mathbf{F_i}$. The function $M : X^3 \times X^3 \to]0,1]$ defined by

$$M(\mathbf{F_i}, \mathbf{F_j}) = \prod_{s=1}^{3} \frac{min\{F_{\mathbf{i}}^s, F_{\mathbf{j}}^s\} + K}{max\{F_{\mathbf{i}}^s, F_{\mathbf{j}}^s\} + K} \tag{5.5}$$

is, according to [9], a stationary fuzzy metric on X^3. Previous works [9, 10] have shown that a suitable value of the K parameter for standard RGB images is $K = 1024$, so, this value will be assumed from now on throughout the paper. Then, $M(\mathbf{F_i}, \mathbf{F_j})$ will denote the photometric fuzzy distance between the colour pixels $\mathbf{F_i}$ and $\mathbf{F_j}$.

Now for the case of spatial fuzzy distance between pixels and using the terminology in Section 5.2, denote by $\mathbf{i} = (i_1, i_2) \in Y^2$ the position of the pixel $\mathbf{F_i}$ in the window W. The function $M_{||\cdot||_2} : Y^2 \times]0, +\infty \longrightarrow]0,1]$ given by

$$M_{||\cdot||_2}(\mathbf{i}, \mathbf{j}, t) = \frac{t}{t + ||\mathbf{i} - \mathbf{j}||_2} \tag{5.6}$$

is a fuzzy metric on Y^2 called the standard fuzzy metric deduced from the Euclidean norm $||\cdot||_2$ ([4] Example 2.9). Then, $M_{||\cdot||_2}(\mathbf{i}, \mathbf{j}, t)$ will denote the spatial fuzzy distance between the colour pixels $\mathbf{F_i}$ and $\mathbf{F_j}$ with respect to t. Notice that $M_{||\cdot||_2}$ does not depend on the length of Y but on the relative position in the image of the pixels $\mathbf{F_i}$ and $\mathbf{F_j}$ under comparison. The t parameter may be interpreted as a parameter to adjust the importance given to the spatial closeness criterion.

5.4 Fuzzy Bilateral Filtering

In order to define the *Fuzzy Bilateral Filter* (FBF) it is just necessary to determine how the weight of each pixel in the filtering window is computed by using the fuzzy metrics in Section 5.3.

Since each pixel $\mathbf{F_i}$ is characterized by its RGB colour vector $(F_\mathbf{i}^1, F_\mathbf{i}^2, F_\mathbf{i}^3)$ and by its location (i_1, i_2) in the window, for our purpose, in a second step, it will be considered a fuzzy metric combining M (5.5) with $M_{||\cdot||_2}$ (5.6). So, to compute the weight of each pixel $\mathbf{F_j}, \mathbf{j} \in W$ it will be considered the following function

$$\begin{aligned} CFM(\mathbf{F_i}, \mathbf{F_j}, t) &= M(\mathbf{F_i}, \mathbf{F_j}) \cdot M_{||\cdot||_2}(\mathbf{i}, \mathbf{j}, t) = \\ &= \prod_{s=1}^{3} \frac{min\{F_\mathbf{i}^s, F_\mathbf{j}^s\} + K}{max\{F_\mathbf{i}^s, F_\mathbf{j}^s\} + K} \cdot \frac{t}{t + ||\mathbf{i} - \mathbf{j}||_2} \end{aligned} \tag{5.7}$$

If we identify each pixel $\mathbf{F_i}$ with $(F_\mathbf{i}^1, F_\mathbf{i}^2, F_\mathbf{i}^3, i_1, i_2)$ then (from [13] Proposition 3.5) the above function CFM is a fuzzy metric on $X^3 \times Y^2$. In this way, the use of the above fuzzy metric is enough to simultaneously model the spatial closeness and photometric similarity criteria commented in Sections 11.1-5.2. The FBF output will be calculated as follows

$$\widetilde{\mathbf{F_i}} = \frac{\sum_{\mathbf{F_j} \in W} CFM(\mathbf{F_i}, \mathbf{F_j}, t)\mathbf{F_j}}{\sum_{\mathbf{F_j} \in W} CFM(\mathbf{F_i}, \mathbf{F_j}, t)} \tag{5.8}$$

where the only t parameter is used to tune the importance of the spatial closeness criterion respect to the photometric criterion. Notice that, in a similar way to the BF, when $t \to \infty$ the FBF approaches a range filter without spatial notion. The reduction of the number of parameters respect to the BF makes the FBF easier to tune, however it can not behave as the Gaussian filter nor the AMF as in the case of the BF. The study of the t parameter is done in the following section.

5.5 Experimental results

In order to study the performance of the proposed filter, some details of the well-known images Lenna, Peppers and Baboon have been contaminated with Gaussian noise following its classical model [12]. Performance comparison has been done using the *Normalized Colour Difference* (NCD) objective quality measure since it approaches human perception and which is defined as

$$NCD_{Lab} = \frac{\sum_{i=1}^{N} \sum_{j=1}^{M} \Delta E_{Lab}}{\sum_{i=1}^{N} \sum_{j=1}^{M} E^*_{Lab}} \tag{5.9}$$

where M, N are the image dimensions and $\Delta E_{Lab} = [(\Delta L^*)^2 + (\Delta a^*)^2 + (\Delta b^*)^2]^{\frac{1}{2}}$ denotes the perceptual colour error and $E^*_{Lab} = [(L^*)^2 + (a^*)^2 + (b^*)^2]^{\frac{1}{2}}$ is the *norm* or *magnitude* of the original image colour vector in the $L^*a^*b^*$ colour space.

Table 5.1. Comparison of the performance in terms of NCD (10^{-2}) using details of the Baboon, Peppers and Lenna images contaminated with different intensities of additive gaussian noise.

Filter	Detail of Baboon			Detail of Peppers			Detail of Lenna		
	$\sigma = 10$	$\sigma = 20$	$\sigma = 30$	$\sigma = 5$	$\sigma = 15$	$\sigma = 30$	$\sigma = 10$	$\sigma = 20$	$\sigma = 30$
None	10.08	20.14	29.90	3.86	11.57	22.85	9.11	17.49	25.75
AMF	7.42	9.58	11.81	3.74	5.43	8.38	5.08	7.28	9.73
VMMF	8.49	11.56	14.89	3.74	6.19	10.06	5.67	8.73	11.75
VMF	9.93	14.37	18.99	4.36	7.90	13.31	6.97	11.36	15.24
EVMF	8.55	11.25	13.96	3.90	6.20	9.50	5.68	8.50	11.29
BVDF	10.34	13.91	17.98	4.14	7.53	12.37	6.56	10.48	14.14
DDF	9.01	12.81	17.22	3.98	7.10	12.07	6.34	10.30	13.94
BF	6.91	9.38	11.70	3.39	5.25	8.37	4.79	7.21	9.70
FBF	6.42	9.24	11.61	3.43	5.29	8.33	4.74	7.12	9.64

The proposed filter is assessed in front of the classical BF and other well-known vector filters: the Arithmetic Mean Filter (AMF), the Vector Marginal Median Filter (VMMF) [12], the Vector Median Filter (VMF) [1], the Extended Vector Median Filter (EVMF), the Basic Vector Directional Filter (BVDF) [16] and the Distance-Directional Filter (DDF) [8]. In all the cases it has been considered a 3×3 window size.

For both the classical BF and the proposed FBF extensive experiments have been carried out trying to find the optimal parameters that reach the best filter performance. The proposed filter has been much easier to adjust since only one parameter (t) is involved in the adjusting process in contrast to the BF where the presence of two parameters (σ_s and σ_p) makes this process more complex. Appropriate values of the t parameter are in the range $[1, 10]$ for Gaussian noise densities (σ) in $[0, 30]$. For higher values of t the smoothing performed is higher, as well, and the value of the t parameter in $[1, 10]$ can be easy set by simple proportionality respect to the noise density $\sigma \in [0, 30]$.

From the results shown in Table 5.1 and Figures 5.1-5.3 it can be stated that the performance presented by the proposed filter is competitive respect to the BF and outperforms the rest of the techniques in comparison. The results seem to indicate that the FBF behaves better than the BF when dealing with highly textured images, as the Baboon image, and slightly worse in images with many homogeneous areas, as the Peppers image.

Conclusions

In this paper a certain class of fuzzy metrics has been used to simultaneously model a double relation between colour pixels: spatial closeness and photometric similarity, using an only fuzzy metric. Notice that, as far as the authors know, this could not be done using a classical metric.

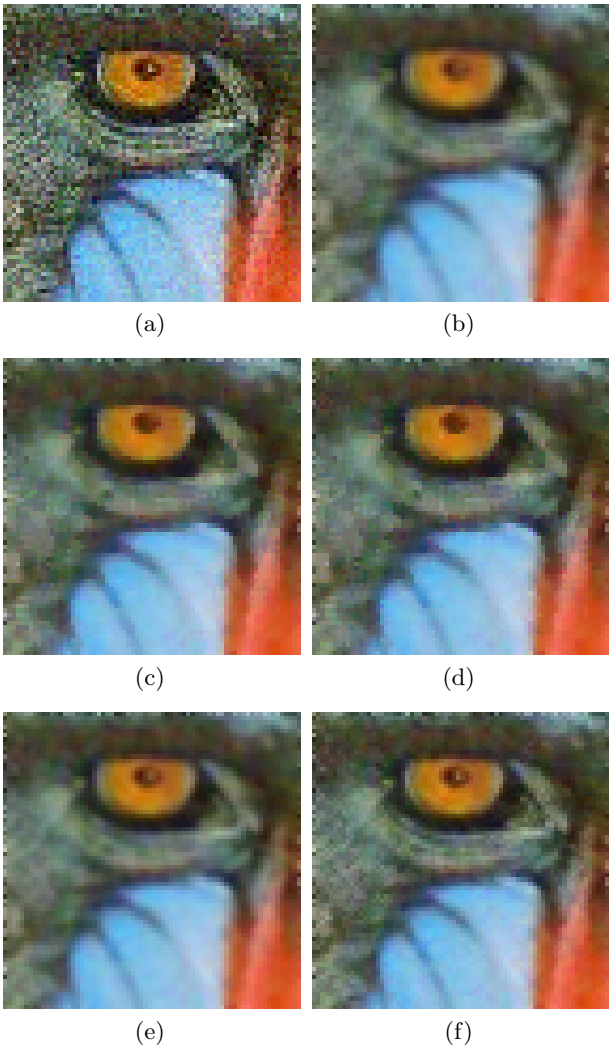

Fig. 5.1. Performance comparison: (a) Detail of Baboon image contaminated with Gaussian noise $\sigma = 10$, (b) AMF output, (c) VMMF output, (d) EVMF output, (e) BF output, (f) FBF output.

The proposed fuzzy metric has been used to adapt the classical BF, then the FBF has been proposed. The proposed filter is easier to use than its classical version since the filter adjusting process becomes simpler. The performance presented by the proposed filter is competitive respect to the BF outperforming it in many cases. These results indicate that this fuzzy metric

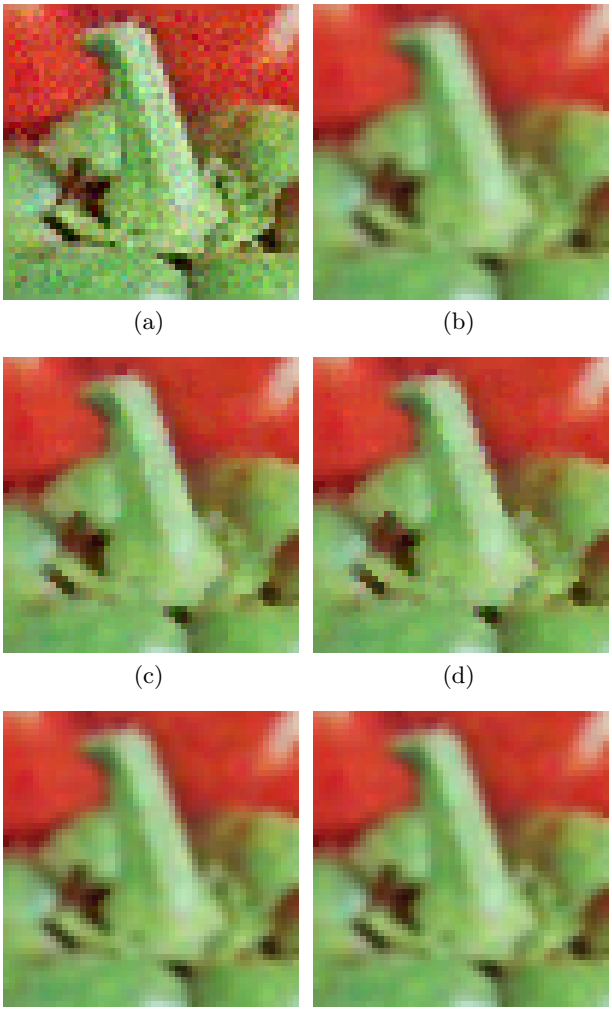

Fig. 5.2. Performance comparison: (a) Detail of Peppers image contaminated with Gaussian noise $\sigma = 15$, (b) AMF output, (c) VMMF output, (d) EVMF output, (e) BF output, (f) FBF output.

may be considered more appropriate than the measures used in the classical BF.

The experiences of this paper constitute another proof of the appropriateness of the fuzzy metrics to model complex relations which motivates its further study.

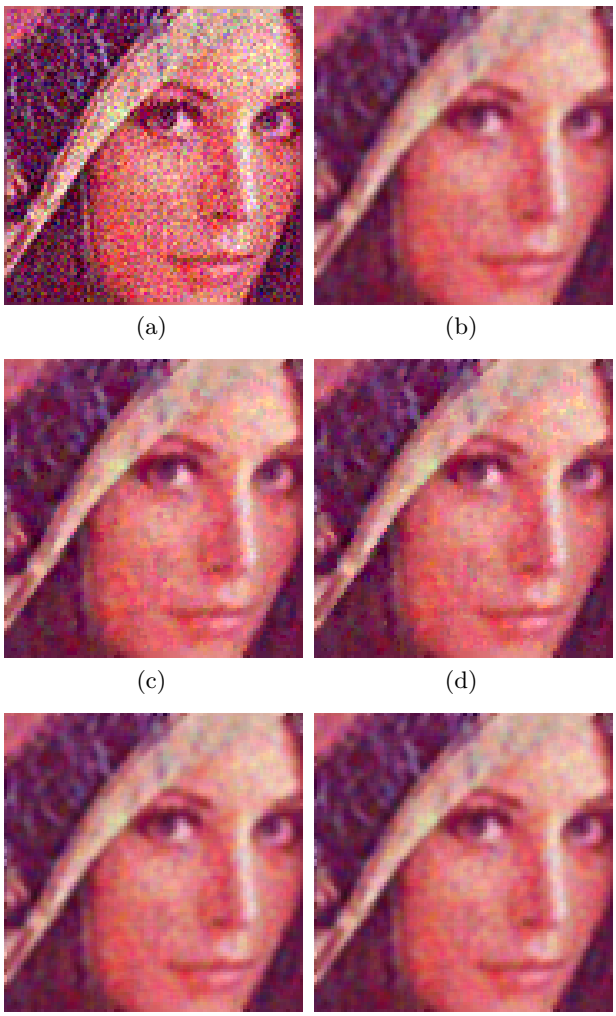

Fig. 5.3. Performance comparison: (a) Detail of Lenna image contaminated with Gaussian noise $\sigma = 30$, (b) AMF output, (c) VMMF output, (d) EVMF output, (e) BF output, (f) FBF output.

References

1. J. Astola, P. Haavisto, Y. Neuvo, *Vector Median Filters*, Proc. IEEE. 78 4 (1990) 678-689.
2. M. Elad, *On the origin of bilateral filter and ways to improve it*, IEEE Transactions on Image Processing 11 10 (2002) 1141-1151.
3. R. Garnett, T. Huegerich, C. Chui, W. He, *A universal noise removal algorithm with an impulse detector*, IEEE Transactions on Image Processing 14 11 (2005) 1747-1754.
4. A. George, P. Veeramani, *On Some results in fuzzy metric spaces*, Fuzzy Sets and Systems 64 3 (1994) 395-399.
5. A. George, P. Veeramani, *Some theorems in fuzzy metric spaces* , J. Fuzzy Math. 3 (1995) 933-940.
6. V. Gregori, S. Romaguera, *Some properties of fuzzy metric spaces*, Fuzzy Sets and Systems 115 3 (2000) 477-483.
7. V. Gregori, S. Romaguera, *Characterizing completable fuzzy metric spaces*, Fuzzy Sets and Systems 144 3 (2004) 411-420.
8. D.G. Karakos, P.E. Trahanias, *Generalized multichannel image-filtering structures* , IEEE Transactions on Image Processing 6 7 (1997) 1038-1045.
9. S. Morillas, V. Gregori, G. Peris-Fajarnés, P. Latorre, *A new vector median filter based on fuzzy metrics*, ICIAR'05, Lecture Notes in Computer Science 3656 (2005) 81-90.
10. S. Morillas, V. Gregori, G. Peris-Fajarnés, P. Latorre, *A fast impulsive noise color image filter using fuzzy metrics*, Real-Time Imaging 11 5-6 (2005) 417-428.
11. P. Perona, J. Malik, *Scale-space and edge detection using anisotropic diffusion*, IEEE Transactions on Pattern Analysis and Machine Intelligence 12 5 (1990) 629-639.
12. K.N. Plataniotis, A.N. Venetsanopoulos, *Color Image processing and applications*, Springer-Verlag, Berlin, 2000.
13. A. Sapena, *A contribution to the study of fuzzy metric spaces* Appl. Gen. Topology 2 1(2001) 63-76.
14. Y. Shen, K. Barner, *Fuzzy vector median-based surface smoothing*, IEEE Transactions on Visualization and Computer Graphics 10 3 (2004) 252-265.
15. C. Tomasi, R. Manduchi, *Bilateral filter for gray and color images*, Proc. IEEE International Conference Computer Vision, 1998, 839-846.
16. P.E. Trahanias, D. Karakos, A.N. Venetsanopoulos, *Vector Directional Filters: a new class of multichannel image processing filters*, IEEE Trans. Image Process. 2 4 (1993) 528-534.

6 Contribution (iii)

S. Morillas, V. Gregori, G. Peris-Fajarnés, P. Latorre, A fast impulsive noise colour image filter using fuzzy metrics, *Real-Time Imaging: Special issue on multichannel image processing* 11 5-6 (2005) 417-428.

Abstract

In this paper, the problem of impulsive noise reduction in multichannel images is addressed. A new filter is proposed on the basis of a recently introduced family of computationally attractive filters with a good detail preserving ability (FSVF). FSVF is based on *privileging* the central pixel in each filtering window in order to replace it only when it is really noisy and preserve the original undistorted image structures. The new filter is based on a novel fuzzy metric and it is created by combining the mentioned scheme and the fuzzy metric. The use of the fuzzy metric makes the filter computationally simpler and it allows to adjust the *privilege* of the central pixel giving the filter an adaptive nature. Moreover, it is shown that the new filter outperforms the classical order statistics filtering techniques and its performance is similar to FSVF outperforming it in some cases.

6.1 Introduction

Images are acquired by photoelectronic or photochemical methods. The sensing devices and the transmission process tend to degrade the quality of the digital images by introducing noise, geometric deformation and/or blur due to motion or camera misfocus [6, 25]. The presence of noise in an image may be a drawback in any subsequent processing to be done over the noisy image such as edge detection, image segmentation or pattern recognition. As a consequence, filtering the image to reduce the noise without degrading its quality, preserving edges, corners and other details, is a major step in any computer vision application [26].

One of the most important families of nonlinear filters which takes advantage of the theory of robust statistics [8, 13] is based on the ordering of

vectors in a predefined sliding window [26, 25]. Generally, when the vectors are ranked using the reduced ordering principle by means of a suitable *distance or similarity measure*, the lowest ranked vectors are those which are *close* to all the other vectors in the window according to the *distance or similarity measure* used. On the other hand, atypical vectors, susceptible to be considered as noisy or outliers, occupy the highest ranks. Since the vectors are ranked without using any a priori information about the signals distribution, order-statistics filters such as the VMF, BVDF or DDF described below, can be considered robust estimators. The output of these filter is defined as the lowest ranked vector as follows.

Let $\mathbf{F}$ represent a multichannel image and let W be a window of finite size $n+1$ (filter length). The image vectors in the filtering window W are denoted as $\mathbf{F}_j, j = 0, 1, ..., n$. The *distance* between two vectors $\mathbf{F}_k, \mathbf{F}_j$ is denoted as $\rho(\mathbf{F}_k, \mathbf{F}_j)$. For each vector in the filtering window, a global or accumulated distance to all the other vectors in the window has to be calculated. The scalar quantity $R_k = \sum_{j=0, j\neq k}^{n} \rho(\mathbf{F}_k, \mathbf{F}_j)$, is the accumulated distance associated to the vector $\mathbf{F}_k$. The ordering of the R_k's: $R_{(0)} \leq R_{(1)} \leq ... \leq R_{(n)}$, implies the same ordering of the vectors $\mathbf{F}_k$'s: $\mathbf{F}_{(0)} \leq \mathbf{F}_{(1)} \leq ... \leq \mathbf{F}_{(n)}$. Given this order, the output of the filter is $\mathbf{F}_{(0)}$.

In this way, the *vector median filter* (VMF) [3], which is probably the most well-known vector filter, uses the L_1 (City-Block) or L_2 (Euclidean) norm to define the above ρ distance function. VMF can be derived either as a maximum likelihood estimate (MLE) when the underlying probability densities of input samples are bi-exponential or by using vector order-statistics techniques. Thus, the VMF is scale, translation and rotation invariant [26]. As well if the vector dimension is 1 then the VMF reduces to the scalar median. Since the impulse response of the VMF is zero, it excellently suppresses impulsive noise [3, 19]. The combination of the VMF with linear techniques has been used to improve its performance in the suppression of gaussian noise [3, 35]. Other approaches have been introduced with the aim of speeding up the VMF by using a linear approximation of the Euclidean distance [4] and by designing a fast algorithm when using the L_1 norm [5]. On the other hand, the VMF has been extended to fuzzy numbers in [7] by means of *certain fuzzy distances*.

The direction of the image vectors can also be used as an ordering criterion to remove vectors with atypical direction. The *basic vector directional filter* (BVDF) [33] parallelizes the VMF operation employing the angle between colour vectors as a distance criterion, so the output of the BVDF is the vector whose direction is the MLE of the directions of the input vectors [19]. Since the vectors directions are associated to their chromaticity, the angular minimization may give better result than VMF-based techniques in terms of colour preservation. On the other hand, since the BVDF uses only information about directions it is not able to remove achromatic noisy pixels from the image. The *directional distance filter* (DDF) [14] overcomes the difficulties of

the BVDF by using both magnitude and direction in the distance criterion. A different chromatic filter can be found in [16].

However, those traditional vector filters are designed to perform a fixed amount of smoothing and they are not able to adapt to local image statistics [19]. Within this aim, many different filters have been recently introduced in the literature. In [2, 17, 20, 21, 22, 23, 32] different techniques are presented to calculate fuzzy coefficients used to determine the filter output as a combination of the vectors in the filtering window. [1, 18] propose to determine first if the vector in consideration is likely to be noisy using cluster analysis [1] or an adaptive rule based system [18] and then apply the filtering operation only when it is necessary. In a similar way, in [34] a genetic algorithm is used to decide in each image position performing the VMF operation, BVDF operation or the identity operation. The simultaneous use of different vector filters in each image position and the combination of their particular outputs by means of a rational function to determine the final output is proposed in [15].

Fuzzy metrics listed in [9] have recently been applied to colour image filtering by adapting the classical VMF presenting good computational and performance results [24]. In this paper, a fuzzy metric as listed in [9] is introduced and a new filter for impulsive noise reduction in colour images is proposed by combining the fuzzy metric and the *fast similarity based impulsive noise removal vector filter FSVF* scheme introduced in [28, 29, 30, 31]. The proposed filter is computationally faster than the VMF and FSVF presenting better performance than VMF and similar performance to FSVF outperforming it in some cases.

This paper is organized as follows. In section 6.2 the FSVF as introduced in [28, 29, 30, 31] is summarized. The proposed fuzzy metric is described in section 6.3. In Section 6.4 the proposed filtering is explained. Experimental results are shown in section 6.5. Finally, conclusions are presented in section 6.6.

6.2 Fast Similarity Based Impulsive Noise Reduction Filter (FSVF)

According to the family of filters introduced by Smolka et al. in [28, 29, 30, 31], the FSVF is defined as follows. Let assume a filtering window W containing $n+1$ image pixels $\{\mathbf{F}_0, \mathbf{F}_1, \ldots, \mathbf{F}_n\}$, where n is the number of neighbors of the central pixel $\mathbf{F}_0$. It is considered a similarity function $\mu : [0; \infty) \rightarrow I\!R$ which is non-ascending and convex in $[0; \infty)$ and satisfies $\mu(0) = 1$, and $\lim_{x \rightarrow \infty} \mu(x) = 0$. The similarity between two pixels of the same colour should be 1, and the similarity between pixels with very different colours should be very close to 0. The function defined as $\mu(||\mathbf{F}_i - \mathbf{F}_j||)$ where $||\cdot||$ denotes the specific vector norm (typically the L_1 or L_2 vector norms), can easily satisfy

the above conditions when it is a decreasing function and $\mu(0) = 1$. The cumulated sum M_k of similarities between a given pixel $\mathbf{F}_k$ $(k = 0, \ldots, n)$ and all other pixels belonging to the window W is defined as

$$M_0 = \sum_{j=1}^{n} \mu(\mathbf{F}_0, \mathbf{F}_j), \quad M_k = \sum_{\substack{j=1 \\ j \neq k}}^{n} \mu(\mathbf{F}_k, \mathbf{F}_j)\,, \tag{6.1}$$

which means that for those $\mathbf{F}_k$ which are neighbors of $\mathbf{F}_0$, the similarity between $\mathbf{F}_k$ and $\mathbf{F}_0$ is not taken into account, what *privileges* the central pixel. Hence, the reference pixel $\mathbf{F}_0$ is replaced by one of its neighbors if $M_0 < M_k,\ k = 1, \ldots, n$, only when it is really noisy, preserving the original undistorted image structures. If this is the case then, $\mathbf{F}_0$ is replaced by that $\mathbf{F}_{k^*}$ for which $k^* = \arg\max_k M_k$.

Several convex functions fulfilling the above conditions have been proposed in [28, 29, 30, 31]. The best results were achieved [29] for the simplest similarity function

$$\mu_7(x) = \begin{cases} 1 - x/h & \text{if } x \leq h \\ 0 & \text{if } x > h \end{cases} \tag{6.2}$$

where $h \in (0, \infty)$. This function allows to construct a fast noise reduction algorithm [28, 29, 30, 31]. The detailed implementation of the FSVF is described as a modification of the VMF as follows [29].

Instead of the original function R_k in section 11.1 the following modified cumulative distance function R_k^* is proposed

$$R_k^* = \begin{cases} -h + \sum\limits_{j=1}^{n} \rho(\mathbf{F}_k, \mathbf{F}_j)\,, & \text{for} \quad k = 0\ , \\ \sum\limits_{j=1}^{n} \rho(\mathbf{F}_k, \mathbf{F}_j)\,, & \text{for} \quad k = 1, \ldots, n\,, \end{cases} \tag{6.3}$$

where ρ denotes the particular distance function, typically the L_1 or L_2 distances.

In the same way as in VMF, the original vector $\mathbf{F}_0$ in the filtering window W is being replaced by $\mathbf{F}_{k^*}$ such that $k^* = \arg\min_k R_k^*$. As it can be easily seen, the parameter h in (6.3) influences the intensity of the filtration process since the number of pixels replaced by the filter is a decreasing function of h. For $h \to 0$ this number is close to that caused by VMF. On the other hand, for $h \to \infty$ this number approaches zero (there is no filtering at all). Moreover, h can be controlled for the best effectiveness of the filter depending on image structure and noise statistics. In this way, the FSVF tries to overcome the drawback of the VMF of replacing too many uncorrupted image pixels, as commented in section 6.1.

It is easy to observe that the FSVF is faster than VMF. It can be shown using a simple matrix representation, (for the sake of simplicity in the 4-neighborhood system case). In order to find R_k and R_k^* using the VMF and FSVMF method respectively, we have to add the elements in rows or columns of the following matrices

$$\mathbf{T}_{VMF} = \begin{bmatrix} 0 & \rho_{01} & \rho_{02} & \rho_{03} & \rho_{04} \\ \rho_{10} & 0 & \rho_{12} & \rho_{13} & \rho_{14} \\ \rho_{20} & \rho_{21} & 0 & \rho_{23} & \rho_{24} \\ \rho_{30} & \rho_{31} & \rho_{32} & 0 & \rho_{34} \\ \rho_{40} & \rho_{41} & \rho_{42} & \rho_{43} & 0 \end{bmatrix}, \quad \mathbf{T}_{FSVF\mu_7} = \begin{bmatrix} -h & \rho_{01} & \rho_{02} & \rho_{03} & \rho_{04} \\ 0 & 0 & \rho_{12} & \rho_{13} & \rho_{14} \\ 0 & \rho_{21} & 0 & \rho_{23} & \rho_{24} \\ 0 & \rho_{31} & \rho_{32} & 0 & \rho_{34} \\ 0 & \rho_{41} & \rho_{42} & \rho_{43} & 0 \end{bmatrix}, \tag{6.4}$$

where $\rho_{ij} = \rho(\mathbf{F}_i, \mathbf{F}_j)$. Obviously, the symmetry of the matrix $\mathbf{T}_{VMF}$ causes that effectively 10 distances (36 in the 8-neighborhood case) and then 15 additions (63 in the 8-neighborhood case) are to be calculated. In the case of FSVF, the number of distances needed is still 10 but there are only 12 additions (56 in the 8-neighborhood case), so FSVF is faster than VMF and it also outperforms VMF in terms of commonly used objective measures [28, 29, 30, 31].

6.3 Proposed Fuzzy Metric

One of the most important problems in fuzzy topology is to obtain an appropriate concept of fuzzy metric. According to [9] a fuzzy metric space is an ordered triple $(X, M, *)$ such that X is a (nonempty) set, $*$ is a continuous t-norm and M is a fuzzy set of $X \times X \times]0, +\infty[$ satisfying the following conditions for all $x, y, z \in X,\ s, t > 0$:

(FM1) $M(x, y, t) > 0$
(FM2) $M(x, y, t) = 1$ if and only if $x = y$
(FM3) $M(x, y, t) = M(y, x, t)$
(FM4) $M(x, z, t + s) \geq M(x, y, t) * M(y, z, s)$
(FM5) $M(x, y, \cdot) :]0, +\infty[\longrightarrow [0, 1]$ is continuous.

$M(x, y, t)$ represents the degree of nearness of x and y with respect to t. If $M(x, y, *)$ is a fuzzy metric space we will say that $(M, *)$ is a fuzzy metric on X. In the following, by a fuzzy metric we mean a fuzzy metric in the George and Veeramani's sense.

The authors proved in [9] that every fuzzy metric $(M, *)$ on X generates a Hausdorff topology on X. Actually, this topology is metrizable as it was proved in [10, 11], and so the above definition can be considered an appropriate concept of fuzzy metric space. A fuzzy metric $(M, *)$ on X is said to be stationary if M does not depend on t, i.e. for each $x, y \in X$ the function $M_{x,y}(t) = M(x, y, t)$ is constant [12]. A subset A of X is said to be F-bounded

[9] if there exist $t > 0$ and $s \in]0,1[$ such that $M(x,y,t) > s$ for all $x, y \in A$. Example 4.4 of [27] suggests the following proposition.

Proposition 2. *Let X be the closed real interval $[a,b]$, let $K > |a| > 0$ and let $\alpha > 0$. Consider for each $p = 1, 2, \ldots$ the function $M_p^\alpha : X^p \times X^p \times]0, +\infty[\longrightarrow]0,1]$ given by*

$$M_p^\alpha(\mathbf{x}, \mathbf{y}, t) = \prod_{i=1}^{p} \left(\frac{min\{x_i, y_i\} + K}{max\{x_i, y_i\} + K} \right)^\alpha \tag{6.5}$$

where $\mathbf{x} = (x_1, \ldots, x_p), \mathbf{y} = (y_1, \ldots, y_p)$, and $t > 0$. Then, $(M_p^\alpha, \cdot)$ is a stationary F-bounded fuzzy metric on X^p, where the t-norm $\cdot$ is the usual product in $[0,1]$. (The proof is included in the appendix)

In next sections the above fuzzy metric will be denoted $M_p^\alpha(\mathbf{x}, \mathbf{y})$, since it does not depend on t.

6.3.1 Computational Analysis

Computationally efficient distances are of interest in the field of order statistics filters [4, 5]. For this reason, the use of the L_1 norm is preferred to the L_2 norm in some cases [26].

The particular case of the proposed fuzzy metric M_p^α suitable for 3-channel image processing tasks will be M_3^α, and then $M_3^\alpha(\mathbf{F}_i, \mathbf{F}_j)$ will denote the *fuzzy distance* between the pixels $\mathbf{F}_i$ and $\mathbf{F}_j$ in the $\mathbf{F}$ image. For each calculation of M_3^α, 3 comparisons, 6 additions, 3 divisions, 2 products and 1 power have to be computed. In the case of L_1 norm, 3 comparisons (absolute value), 3 subtractions and 2 additions are necessary, whereas for the L_2 norm, 3 subtractions, 3 powers, 2 additions and 1 square-root have to be done. As can be seen in Table 6.1, the computational complexity of M_3^α is even higher than the one of L_2 norm. However, an optimization strategy in the computation of M_3^α (Fast M_3^α) may be applied.

Given the fixed parameters K and α in (6.5), numerator and denominator of each fraction in (6.5) are in a bounded set $[K, 255 + K]$ when processing RGB images. All the possible powered fractions can be pre-calculated in a square matrix C^α where

Table 6.1. Computational comparison between the classical metrics L_1 and L_2 and the proposed fuzzy metric M_3 measured in a Pentium IV 2.4GHz

Metric	1 computation (μs)	Computations per second
L_1 norm	28.83	$3.469\ 10^4$
L_2 norm	30.58	$3.270\ 10^4$
M_3^α	43.09	$2.037\ 10^4$
Fast M_3^α	27.51	$3.635\ 10^4$

$$C^{\alpha}(i,j) = \left(\frac{min\{i,j\}+K}{max\{i,j\}+K}\right)^{\alpha} \qquad i,j \in [0,255] \tag{6.6}$$

Using the pre-computation matrix, the calculation of Fast M_3^{α} between two pixels $\mathbf{F}_i = (F_i(1), F_i(2), F_i(3)), \mathbf{F}_j = (F_j(1), F_j(2), F_j(3))$ is reduced to

$$M_3^{\alpha}(\mathbf{F}_i, \mathbf{F}_j) = \prod_{l=1}^{3} C^{\alpha}(F_i(l), F_j(l)) \tag{6.7}$$

By means of this optimization, 3 accesses to matrix and 2 products are enough to make the computation.

The time measured for the construction of the matrix C^{α} is about 0.9 seconds in a Pentium IV 2.4GHz. Although it supposes an initial cost, the gain reached is approx. $15.5\mu s$ (see Table 6.1) in each computation, so, the initial cost is compensated when $6 \cdot 10^4$ computations have to be computed (which is roughly the computation involved in the filtering of a $40 \cdot 40$ pixels image[1]). Moreover, the pre-computation matrix may be used for successive filterings, for instance, when filtering a sequence of images.

The results presented in Table 6.1 show that the M_3^{α} fuzzy metric is computationally cheaper than the classical L_1 and L_2 norms when the optimization of the pre-computation matrix is applied.

6.4 Proposed filtering

The filtering method described in section 6.2 can be adapted to use the fuzzy metric proposed in section 6.3. Both, the vector norm L_i $(i = 1, 2)$ and the convex function μ operating over it are replaced by the fuzzy metric M_3^{α}. This makes the filtering computationally simpler by the omission of the μ function and the use of a fuzzy metric computationally more efficient than the vector norms L_1 and L_2 (see Table 6.1).

In the proposed filtering, the cumulated sum M_k of similarities between a given pixel F_k $(k = 0, \ldots, n)$ and all other pixels belonging to the window W is defined as

$$M_0 = \sum_{j=1}^{n} M_3^{\alpha}(\mathbf{F}_0, \mathbf{F}_j), \quad M_k = \sum_{\substack{j=1 \\ j \neq k}}^{n} M_3^{\alpha}(\mathbf{F}_k, \mathbf{F}_j)\,, \tag{6.8}$$

As explained in section 6.2, for those $\mathbf{F}_k$ which are neighbors of $\mathbf{F}_0$, the similarity between $\mathbf{F}_k$ and $\mathbf{F}_0$ is not taken into account. This *privileges* the central pixel.

In the construction of the proposed filter, the reference pixel $\mathbf{F}_0$ in the window W is replaced by one of its neighbors if $M_0 < M_k,\ k = 1, \ldots, n$. If this

[1] For all the filters studied in this article has been used a 8-neighborhood 3×3 size window W, which means 36 comparisons per pixel (see section 6.2)

is the case, then $\mathbf{F}_0$ is replaced by that $\mathbf{F}_{k^*}$ for which $k^* = \arg\max_k M_k,\ k = 1, \ldots, n$.

Using a matrix representation as done in the section 6.2, the appropriate matrix in the 4-neighborhood case for the new filter has the form

$$\mathbf{T}_{M_3^\alpha} = \begin{bmatrix} 0 & M_3^\alpha(0,1) & M_3^\alpha(0,2) & M_3^\alpha(0,3) & M_3^\alpha(0,4) \\ 0 & 0 & M_3^\alpha(1,2) & M_3^\alpha(1,3) & M_3^\alpha(1,4) \\ 0 & M_3^\alpha(2,1) & 0 & M_3^\alpha(2,3) & M_3^\alpha(2,4) \\ 0 & M_3^\alpha(3,1) & M_3^\alpha(3,2) & 0 & M_3^\alpha(3,4) \\ 0 & M_3^\alpha(4,1) & M_3^\alpha(4,2) & M_3^\alpha(4,3) & 0 \end{bmatrix} \tag{6.9}$$

The number of values to be calculated is 10 but there are only 11 additions (12 in the FSVF and 15 in the VMF (see section 6.2)). In the 8-neighborhood case, the number of additions is 55 instead of 56 of the FSVF, and 63 in the VMF (see section 6.2) [28, 29, 30, 31]. Clearly, this filter is faster than the filters proposed in [28, 29, 30, 31] presenting a similar performance, even better in some cases, as it will be shown in section 8.4.

6.4.1 Adjusting the K parameter

The K parameter included in the definition of the fuzzy metric M_3^α (11.1) has an important influence on the filter performance, according to [24]. The metric is non-uniform in the sense that the measure given by M_3^α for two different pairs of consecutive numbers (or vectors) may not be the same. Increasing the value of K reduces this non-uniformity. This effect is shown in Fig. 6.1 where the content of the matrix C^1 (6.6) for different values of K is presented. However, as it was explained in [24], the optimum value of the K parameter depends on the particular image structures and noise. A suitable value for the K parameter for a variety of noise types is $K = 2^{10}$.

6.4.2 Adjusting the α parameter

Using a value of $K = 2^{10}$ makes the lower bound (6.15) of the fuzzy metric be relatively close to 1 (see Fig. 6.1). This lower bound is also the minimum advantage given to the central pixel (see (9)). Increasing the value of α , the lower bound (6.15) of the fuzzy metric decreases, and the advantage given to the central pixel is lower. Therefore, the value of α influences the intensity of the filtration process. The number of pixels replaced by the filter is an increasing function of α. The effect of increasing the value of α is shown in Fig. 6.2 where the content of the matrix C^α (6.6) for different values of α is presented.

Using an appropriate value of α has a great importance for the filter performance. This will be shown in section 6.5. The α parameter can be set experimentally or can be determined adaptively using the technique described in [29, 31].

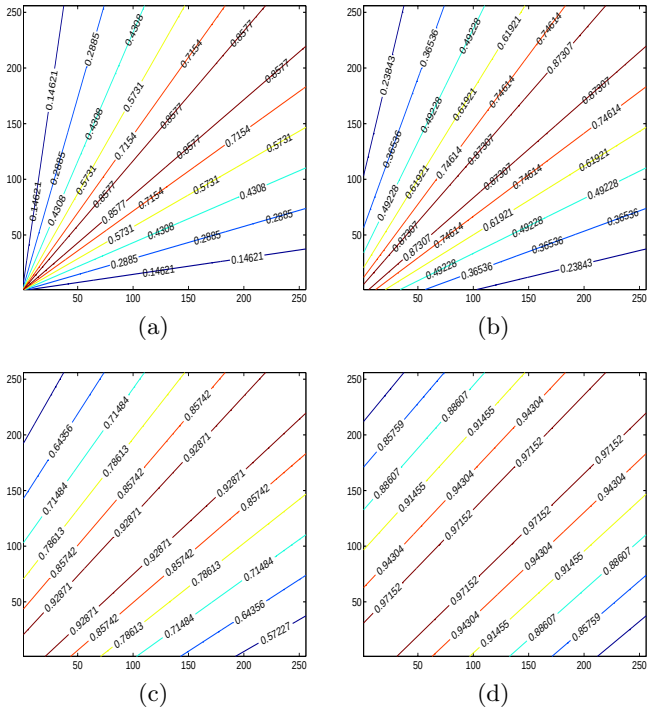

Fig. 6.1. Content of the pre-computation matrix $C^1(i,j)$ for several values of K: (a) K = 1, (b) K = 32, (c) K = 256, (d) K = 1024.

6.5 Experimental results

For the evaluation of the filter proposed in section 6.4, two types of impulsive noise have been used to simulate different distortions which may corrupt colour images [29, 32].

– I. Impulsive noise.
Let $\mathbf{F} = \{F_R, F_G, F_B\}$ denote the original pixel and let $\mathbf{F}'$ denote the pixel corrupted by the noise process. Then the image pixels are distorted according to the following scheme

$$\mathbf{F}' = \begin{cases} \{d_1, F_G, F_B\} & \text{with probability } p \cdot p_1\,, \\ \{F_R, d_2, F_B\} & \text{with probability } p \cdot p_2\,, \\ \{F_R, F_G, d_3\} & \text{with probability } p \cdot p_3\,, \\ \{d_1, d_2, d_3\} & \text{with probability } p \cdot \left(1 - \sum_{i=1}^{3} p_i\right)\,. \end{cases} \tag{6.10}$$

where d_1, d_2, d_3 are independent and equal to 0 or 255 with equal probability.

– II. Uniform noise.

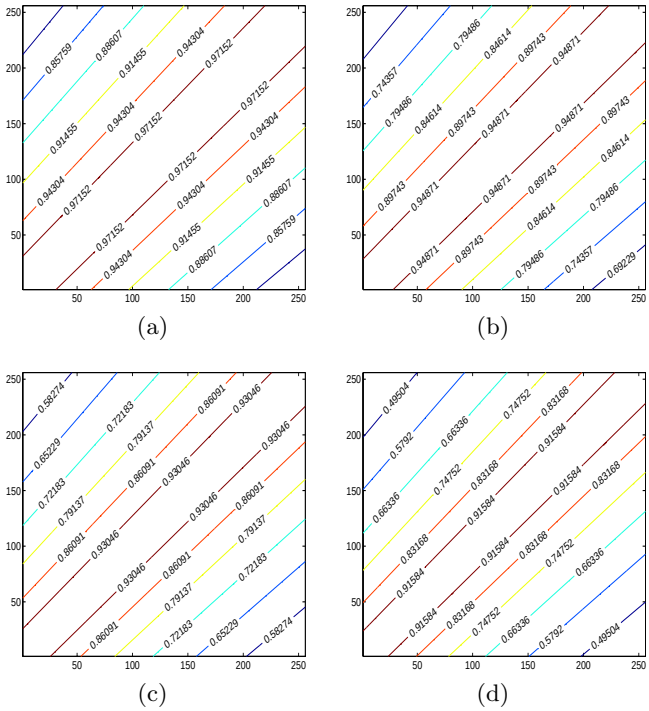

Fig. 6.2. Content of the pre-computation matrix $C^{\alpha}(i,j)$ with $K = 1024$ for several values of α: (a) $\alpha = 1$, (b) $\alpha = 2$, (c) $\alpha = 3$, (d) $\alpha = 4$.

$\mathbf{F}' = \{d_1, d_2, d_3\}$ with probability p, where d_1, d_2, d_3 are random uniformly distributed independent integer values in the interval $[0, 255]$.

The *Mean Absolute Error* (MAE), *Peak Signal to Noise Ratio* (PSNR) and *Normalized Colour Difference* (NCD) [26, 32] have been used to assess the performance of the proposed filter. These quality measures are defined as follows

$$MAE = \frac{\sum_{i=1}^{N}\sum_{j=1}^{M}\sum_{q=1}^{Q}\left|F^q(i,j) - \hat{F}^q(i,j)\right|}{N \cdot M \cdot Q}, \tag{6.11}$$

$$PSNR = 20\log\left(\frac{255}{\sqrt{\frac{1}{NMQ}\sum_{i=1}^{N}\sum_{j=1}^{M}\sum_{q=1}^{Q}\left(F^q(i,j) - \hat{F}^q(i,j)\right)^2}}\right), \tag{6.12}$$

where M, N are the image dimensions, Q is the number of channels of the image ($Q = 3$ for colour image), and $F^q(i,j)$ and $\hat{F}^q(i,j)$ denote the q^{th} component of the original image vector and the filtered image, at pixel position (i,j), respectively, and

$$NCD_{Lab} = \frac{\sum_{i=1}^{N}\sum_{j=1}^{M} \Delta E_{Lab}}{\sum_{i=1}^{N}\sum_{j=1}^{M} E^*_{Lab}} \tag{6.13}$$

where $\Delta E_{Lab} = [(\Delta L^*)^2 + (\Delta a^*)^2 + (\Delta b^*)^2]^{\frac{1}{2}}$ denotes the perceptual colour error and $E^*_{Lab} = [(L^*)^2 + (a^*)^2 + (b^*)^2]^{\frac{1}{2}}$ is the *norm* or *magnitude* of the original image colour vector in the $L^*a^*b^*$ colour space.

Several images and some details of them (see Fig. 6.3) contaminated with different types and densities of noise have been used to compare the performance of the proposed filter with the FSVF [28, 29, 30, 31] and with the classical filters (see table 6.2). The performance comparison is presented in tables 6.3-6.7. Some filtering results of the techniques under comparison are shown in Figs. 6.4-6.8.

Table 6.2. Filters taken for comparison and notation.

Notation	**Filter**
VMF	Vector Median Filter [3]
BVDF	Basic Vector Directional Filter [33]
DDF	Directional Distance Filter [14]
$\mu_7(L_1)$	FSVF using μ_7 over L_1 norm [29]
$\mu_7(L_2)$	FSVF using μ_7 over L_2 norm [29]
M_3^{α}	Proposed filter

Table 6.3. Comparison of the performance in terms of MAE, PSNR and NCD using the detail of the Brandy Rose image (see Fig. 6.3) contaminated with 5% Noise Type I.

Filter	MAE	PSNR	NCD (10^{-2})
Noisy	2.46	21.49	2.71
VMF	3.59	30.91	2.40
BVDF	3.90	29.94	2.40
DDF	3.54	30.87	2.33
$\mu_7(L_1)$	0.83	33.89	0.54
$\mu_7(L_2)$	0.39	37.68	0.33
$M_3^{3.5}$	0.37	37.95	0.36

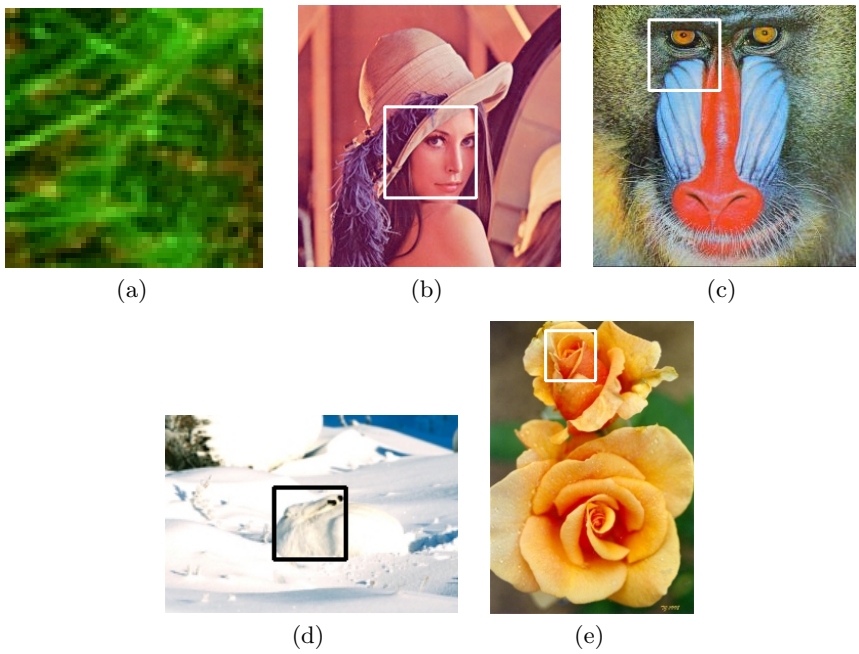

Fig. 6.3. Test Images: (a) Microscopic image, (b) Detail of Lenna image, (c) Detail of Mandrill image, (d) Detail of Artic Hare image (Copyright photo courtesy of Robert E. Barber), (e) Detail of Brandy Rose image (Copyright photo courtesy of Toni Lankerd)

Table 6.4. Comparison of the performance in terms of MAE, PSNR and NCD using the Microscopic image (see Fig. 6.3) contaminated with 10% Noise Type I.

Filter	MAE	PSNR	NCD (10^{-2})
Noisy	4.80	18.40	6.41
VMF	4.85	29.15	4.23
BVDF	6.20	27.01	5.17
DDF	4.91	29.08	4.24
$\mu_7(L_1)$	32.61	33.89	1.15
$\mu_7(L_2)$	34.79	37.68	0.86
$M_3^{3.8}$	34.24	37.95	0.92

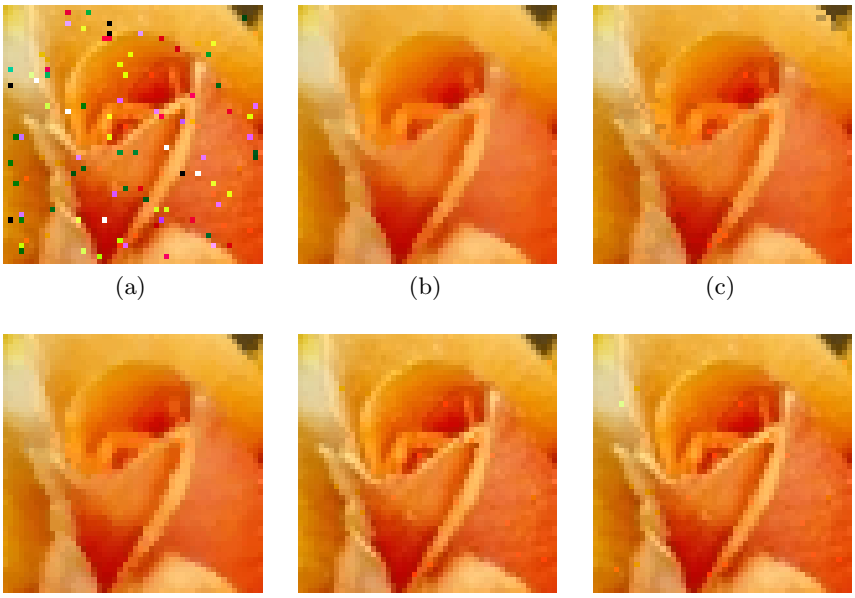

Fig. 6.4. Test Images: (a) Detail of Brandy Rose image contaminated with 5% noise type I, (b) VMF output, (c) BVDF output, (d) DDF output, (e) $\mu_7(L_2)$ output, (f) Proposed filter output.

Table 6.5. Comparison of the performance in terms of MAE, PSNR and NCD using the detail of the Artic Hare image (see Fig. 6.3) contaminated with 15% Noise Type II.

Filter	MAE	PSNR	NCD (10^{-2})
Noisy	14.19	14.90	7.51
VMF	4.57	27.70	1.20
BVDF	5.29	26.29	1.27
DDF	4.47	27.51	1.11
$\mu_7(L_1)$	2.21	26.93	0.65
$\mu_7(L_2)$	1.59	28.92	0.40
$M_3^{3,4}$	1.30	30.43	0.38

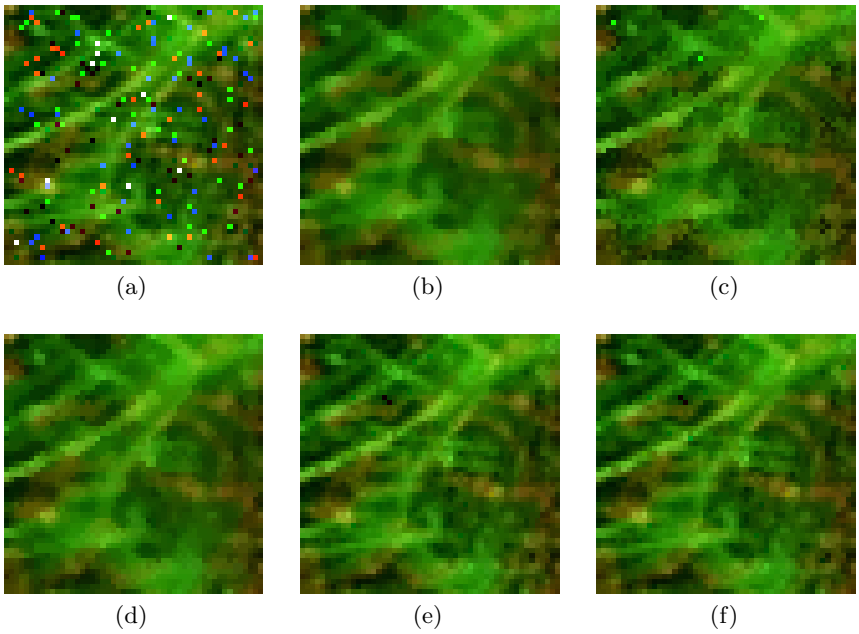

Fig. 6.5. Test Images: (a) Microscopic image contaminated with 10% noise type I, (b) VMF output, (c) BVDF output, (d) DDF output, (e) $\mu_7(L_2)$ output, (f) Proposed filter output.

Table 6.6. Comparison of the performance in terms of MAE, PSNR and NCD using the detail of the Mandrill image (see Fig. 6.3) contaminated with 25% Noise Type I.

Filter	MAE	PSNR	NCD (10^{-2})
Noisy	12.25	15.33	18.30
VMF	11.48	22.81	6.54
BVDF	13.91	20.68	7.09
DDF	11.31	22.75	6.22
$\mu_7(L_1)$	7.62	23.17	4.61
$\mu_7(L_2)$	5.83	24.21	3.99
M_3^5	6.92	23.47	4.40

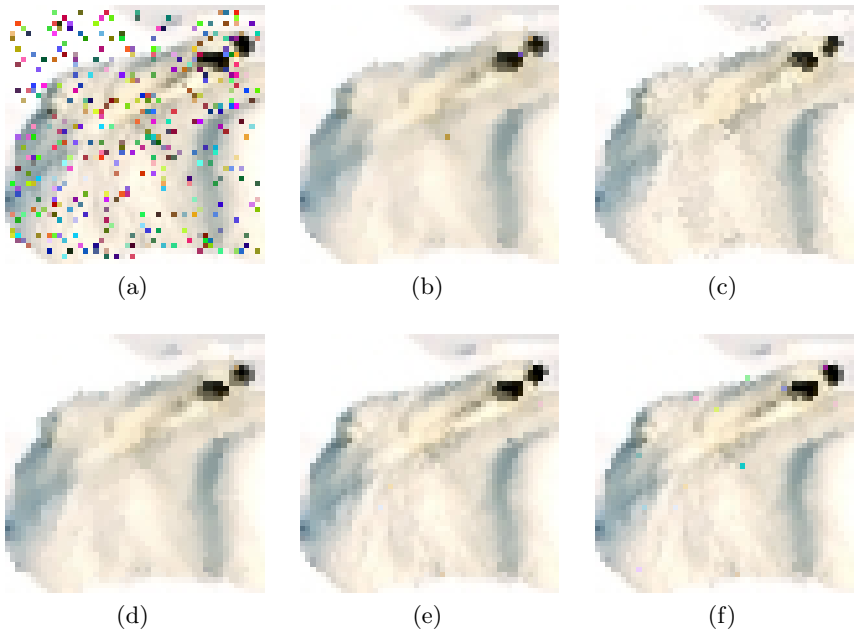

Fig. 6.6. Test Images: (a) Detail of Artic Hare image contaminated with 5% noise type I, (b) VMF output, (c) BVDF output, (d) DDF output, (e) $\mu_7(L_2)$ output, (f) Proposed filter output.

Table 6.7. Comparison of the performance in terms of MAE, PSNR and NCD using the detail of the Lenna image (see Fig. 6.3) contaminated with 30% Noise Type II.

Filter	MAE	PSNR	NCD (10^{-2})
Noisy	22.48	13.90	20.24
VMF	6.93	25.46	4.47
BVDF	7.81	23.81	4.69
DDF	6.67	25.70	4.21
$\mu_7(L_1)$	3.71	27.08	2.34
$\mu_7(L_2)$	3.32	27.59	2.16
$M_3^{5.5}$	3.19	27.87	2.11

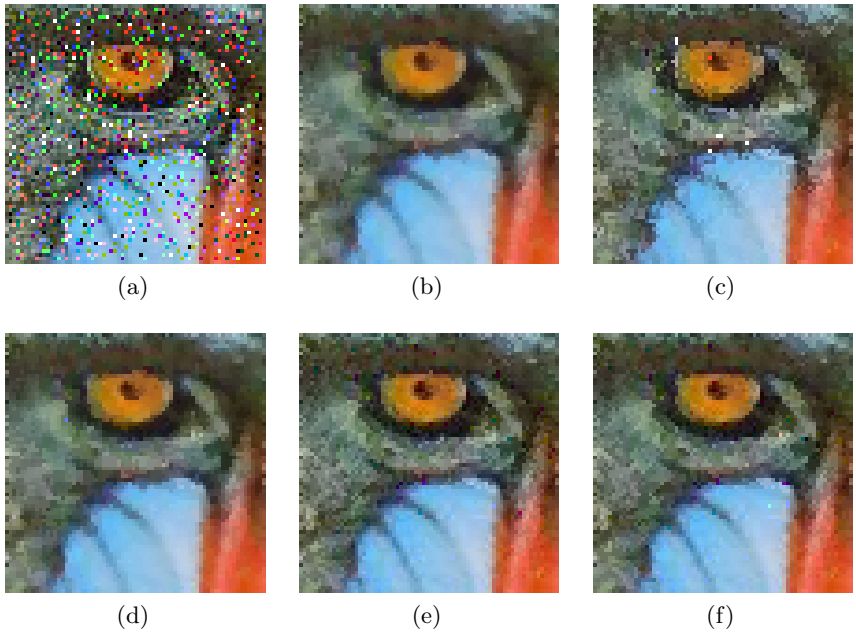

Fig. 6.7. Test Images: (a) Detail of Mandrill image contaminated with 25% noise type I, (b) VMF output, (c) BVDF output, (d) DDF output, (e) $\mu_7(L_2)$ output, (f) Proposed filter output.

The results in tables 6.3-6.7 and Figs. 6.4-6.8 show that the proposed filter outperforms, in terms of objective quality measures, the classical filtering techniques and its performance is similar to the FSVF [28, 29, 30, 31] and even better in some cases. For a particular type of images of low frequency and reduced colour set (as the details of the Brandy Rose and Artic Hare images shown in Fig. 6.3 (d,e)) the results seem to show that the proposed filter works better than the FSVF (see tables 6.3,6.6 and Fig. 6.4,6.6). As well, the proposed filter presents better performance when suppressing noise type II than noise type I.

As it was commented in section 6.4.2, the value of the α parameter has an important influence on the filtering process. In Fig. 6.9 it is shown the dependence of the percentage of replaced pixels on α. The number of replaced pixels is an increasing function of α. The maximum performance is reached when the percentage of replaced pixels is very close to the percentage of noisy pixels. This can be seen in Figs. 6.9,6.10. Therefore, depending on the percentage of noisy pixels in the image, the optimum value of α is different . The higher the percentage of contaminated pixels is, the higher the value of α.

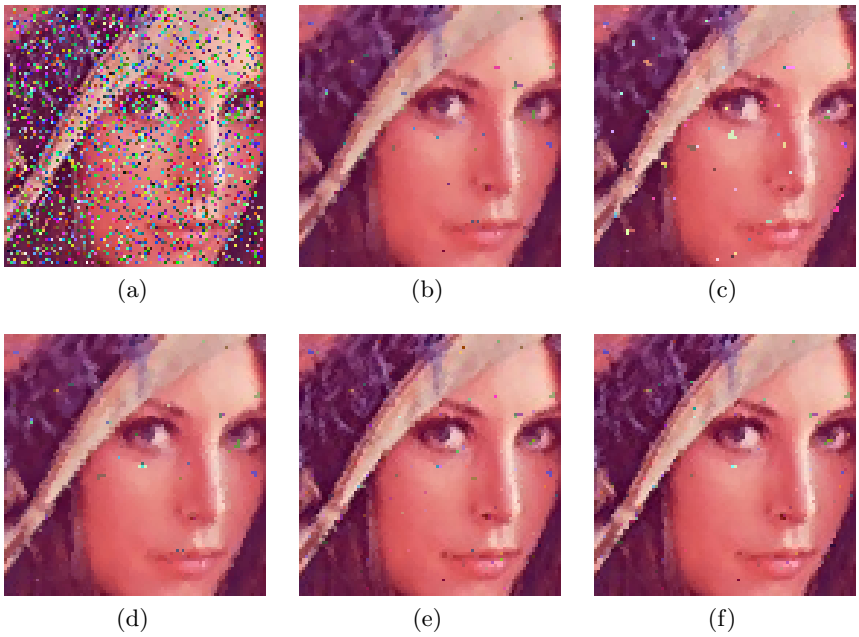

Fig. 6.8. Test Images: (a) Detail of Lenna image contaminated with 30% noise type II, (b) VMF output, (c) BVDF output, (d) DDF output, (e) $\mu_7(L_2)$ output, (f) Proposed filter output.

Conclusions

Firstly, in this paper we introduce a fuzzy metric in the sense of George and Veeramani [9] which is computationally simpler than the classical L-norms.

Secondly, the proposed fuzzy metric has been combined with the FSVF technique [28, 29, 30, 31] to define a computationally efficient filter. This filter is faster than FSVF since the filtering process is simpler and the fuzzy metric used is faster than the classical metrics used in FSVF [28, 29, 30, 31]. Moreover, the proposed filter outperforms the classical vector median filtering techniques and it presents similar performance to the FSVF, outperforming it in some cases.

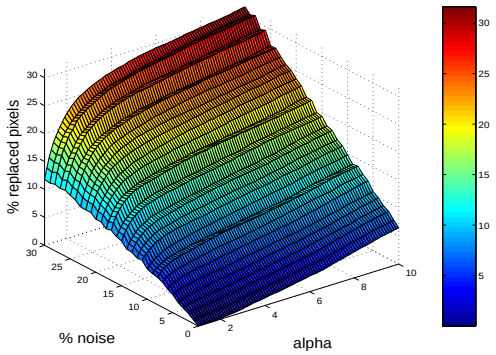

(a)

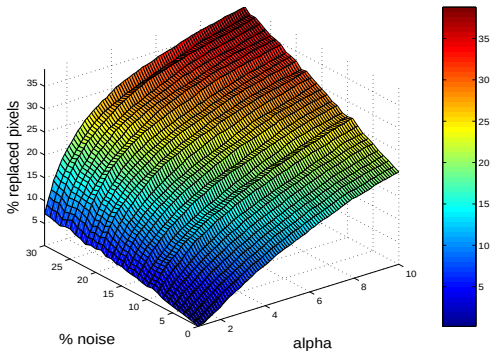

(b)

Fig. 6.9. Percentage of pixels replaced by the proposed filter when filtering the details of the Lenna (a) and baboon (b) images contaminated with noise type II and I respectively as a function of α and the percentage of noise.

Proof of proposition 1

Proof. Proof Axioms (FM1)-(FM3) and (FM5) are obviously fulfilled. We show, by induction, the triangular inequality (FM4).

An easy computation shows that M_1^α verifies (FM4). Now, suppose it is true for M_{p-1}^α. Then, for each $\mathbf{x} = (x_1, \cdots, x_p), \mathbf{y} = (y_1, \cdots, y_p), \mathbf{z} = (z_1, \cdots, z_p)$ and for each $t, s > 0$ we have

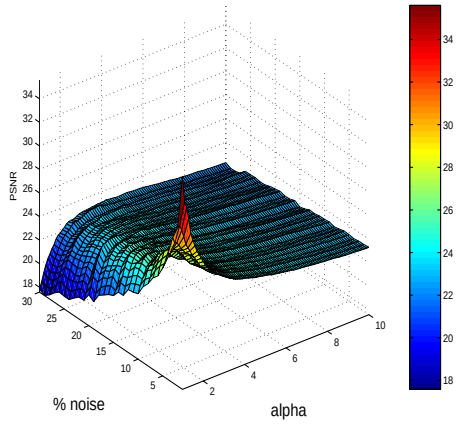

(a)

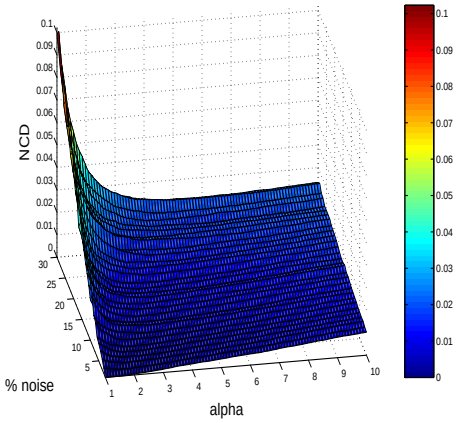

(b)

Fig. 6.10. (a) Performance in terms of PSNR of the proposed filter for the Mandrill image contaminated with noise type I as a function of α and the percentage of noise, (b) Performance in terms of NCD of the proposed filter for the Lenna image contaminated with noise type II as a function of α and the percentage of noise.

$$
\begin{aligned}
M_p^{\alpha}(\mathbf{x},\mathbf{z},t+s) = \prod_{i=1}^{p}\left(\frac{min\{x_i,z_i\}+K}{max\{x_i,z_i\}+K}\right)^{\alpha} = \\
= \prod_{i=1}^{p-1}\left(\frac{min\{x_i,z_i\}+K}{max\{x_i,z_i\}+K}\right)^{\alpha}\cdot\left(\frac{min\{x_p,z_p\}+K}{max\{x_p,z_p\}+K}\right)^{\alpha} \geq \\
\geq \prod_{i=1}^{p-1}\left(\frac{min\{x_i,y_i\}+K}{max\{x_i,y_i\}+K}\right)^{\alpha}\cdot\prod_{i=1}^{p-1}\left(\frac{min\{y_i,z_i\}+K}{max\{y_i,z_i\}+K}\right)^{\alpha}\cdot \\
\cdot\left(\frac{min\{x_p,y_p\}+K}{max\{x_p,y_p\}+K}\right)^{\alpha}\cdot\left(\frac{min\{y_p,z_p\}+K}{max\{y_p,z_p\}+K}\right)^{\alpha} = \\
= \prod_{i=1}^{p}\left(\frac{min\{x_i,y_i\}+K}{max\{x_i,y_i\}+K}\right)^{\alpha}\cdot\prod_{i=1}^{p}\left(\frac{min\{y_i,z_i\}+K}{max\{y_i,z_i\}+K}\right)^{\alpha} = M_p^{\alpha}(\mathbf{x},\mathbf{y},t)\cdot M_p^{\alpha}(\mathbf{y},\mathbf{z},s),
\end{aligned}
\tag{6.14}
$$

so M_p^α is a fuzzy metric on X^p, for $p = 1, 2, \ldots$ and clearly it is stationary.

Finally, X^p is F-bounded, for $p = 1, 2, \ldots$. Indeed, if we write $\mathbf{a} = (\overbrace{a, \ldots, a}^{p})$ and $\mathbf{b} = (\overbrace{b, \ldots, b}^{p})$, then for each $\mathbf{x}, \mathbf{y} \in X^p$ and $t > 0$ we have

$$M_p^\alpha(\mathbf{x}, \mathbf{y}, t) \geq M_p^\alpha(\mathbf{a}, \mathbf{b}, t) = \left(\frac{a + K}{b + K}\right)^{p\alpha} > 0, \text{ for } p = 1, 2, \ldots \square \qquad (6.15)$$

References

1. H. Allende, J. Galbiati, A non-parametric filter for image restoration using cluster analysis, *Pattern Recognition Letters* 25 8 (2004) 841-847.
2. K. Arakawa, Median filter based on fuzzy rules and its application to image restoration, *Fuzzy Sets and Systems* 77 1 (1996) 3-13.
3. J. Astola, P. Haavisto, Y. Neuvo, Vector Median Filters, *Proc. IEEE.* 78 4 (1990) 678-689.
4. M. Barni, F. Buti, F. Bartolini, V. Capellini, A Quasi-Euclidean Norm to Speed Up Vector Median Filtering, *IEEE Transactions on Image Processing* 9 10 (2000) 1704-1709.
5. M. Barni, A Fast Algorithm for 1-Norm Vector Median Filtering, *IEEE Transactions on Image Processing* 6 10 (1997) 1452-1455.
6. C. Boncelet, *Image noise models, in: A. Bovik (Ed.), Handbook of Image and Video Processing* (Academic Press, San Diego, 2000).
7. V. Chatzis, I. Pitas, Fuzzy scalar and vector median filters based on fuzzy distances, *IEEE Transactions on Image Processing* 8 5 (1999) 731-734.
8. H.A. David, *Order Statistics* (John Wiley and Sons, New York, 1981)
9. A. George, P. Veeramani, On Some results in fuzzy metric spaces, *Fuzzy Sets and Systems* 64 3 (1994) 395-399.
10. A. George, P. Veeramani, Some theorems in fuzzy metric spaces, *J. Fuzzy Math.* 3 (1995) 933-940.
11. V. Gregori, S. Romaguera, Some properties of fuzzy metric spaces, *Fuzzy Sets and Systems* 115 3 (2000) 477-483.
12. V. Gregori, S. Romaguera, Characterizing completable fuzzy metric spaces, *Fuzzy Sets and Systems* 144 3 (2004) 411-420.
13. P.S. Huber, *Robust Statistics* (John Wiley and Sons, New York, 1981)
14. D.G. Karakos, P.E. Trahanias, Generalized multichannel image-filtering structure, *IEEE Transactions on Image Processing* 6 7 (1997) 1038-1045.
15. L. Khriji, M. Gabbouj, Adaptive fuzzy order statistics-rational hybrid filters for color image processing, *Fuzzy Sets and Systems* 128 1 (2002) 35-46.
16. L. Lucchese, S.K. Mitra, A new class of chromatic filters for color image processing: theory and applications, *IEEE Transactions on Image Processing* 15 2 (2004) 534-548.
17. R. Lukac, B. Smolka, K.N. Plataniotis, A.N. Venetsanopoulos, Selection weighted vector directional filters, *Computer Vision and Image Understanding* 94 (2004) 140-167.
18. R. Lukac, Adaptive vector median filtering, *Pattern Recognition Letters* 24 12 (2003) 1889-1899.

19. R. Lukac, B. Smolka, K. Martin, K.N. Plataniotis, A.N. Venetsanopoulos, Vector Filtering for Color Imaging, *IEEE Signal Processing Magazine, Special Issue on Color Image Processing* 22 1 (2005) 74-86.
20. R. Lukac, K.N. Plataniotis, B. Smolka, A.N. Venetsanopoulos, cDNA Microarray Image Processing Using Fuzzy Vector Filtering Framework, *Fuzzy Sets and Systems: Special Issue on Fuzzy Sets and Systems in Bioinformatics* 152 1 (2005) 17-35.
21. R. Lukac, K.N. Plataniotis, B. Smolka, A.N. Venetsanopoulos, A Multichannel Order-Statistic technique for cDNA Microarray Image Processing, *IEEE Transactions on Nanobioscience* 3 4 (2004) 272-285.
22. R. Lukac, K.N. Plataniotis, B. Smolka, A.N. Venetsanopoulos, Generalized Selection Weighted Vector Filters, *EURASIP Journal on applied signal processing: Special Issue on Nonlinear signal and image processing* 12 (2004) 1870-1885.
23. R. Lukac, Adaptive Color Image Filtering Based on Center Weighted Vector Directional Filters, *Multidimensional Systems and Signal Processing* 15 (2004) 169-196.
24. S. Morillas, V. Gregori, G. Peris-Fajarnés, P. Latorre, *A new vector median filter based on fuzzy metrics*, ICIAR'05, Lecture Notes in Computer Science 3656 (2005) 81-90.
25. I. Pitas, *Digital image processing algorithms and applications* (John Wiley & Sons, 2000).
26. K.N. Plataniotis, A.N. Venetsanopoulos, *Color Image processing and applications* (Springer-Verlag, Berlin, 2000).
27. A. Sapena, A contribution to the study of fuzzy metric spaces, *Appl. Gen. Topology* 2 1 (2001) 63-76.
28. B. Smolka,K.N. Plataniotis, R. Lukac, A.N. Venetsanopoulos, Similarity based impulsive noise removal in color images, *International Conference on Image Processing ICIP 2003* .
29. B. Smolka, R. Lukac, A. Chydzinski, K.N. Plataniotis, W. Wojciechowski, Fast adaptive similarity based impulsive noise reduction filter, *Real-Time Imaging* 9 4 (2003) 261-276.
30. B. Smolka, A. Chydzinski, K.N. Plataniotis, A.N. Venetsanopoulos, New filtering technique for the impulsive noise removal in color images, *Mathematical Problems in Engineering* 1 (2004) 79-91.
31. B. Smolka, K.N. Plataniotis, A. Chydzinski, M. Szczepanski, A.N. Venetsanopoulos, K. Wojciechowski, Self-adaptive algorithm of impulsive noise reduction in color images, *Pattern Recognition* 35 8 (2002) 1771-1784.
32. M. Szczepanski, B. Smolka, K.N. Plataniotis, A.N. Venetsanopoulos, On the distance function approach to color image enhancement, *Discrete Applied Mathematics* 139 (2004) 283-305.
33. P.E. Trahanias, D. Karakos, A.N. Venetsanopoulos, Vector Directional Filters: a new class of multichannel image processing filters, *IEEE Trans. Image Process.* 2 4 (1993) 528-534.
34. H.H. Tsai, P.T. Yu, Genetic-based fuzzy hybrid multichannel filters for color image restoration, *Fuzzy Sets and Systems* 114 2 (2000) 203-224.
35. T. Viero, K. Oistamo, Y. Neuvo, Three-dimensional median-related filters for color image sequence filtering, *IEEE Transactions on Circuits and Systems for Video Technology* 4 2 (1994) 129-142.

7 Contribution (iv)

S. Morillas, V. Gregori, J. Riquelme, B. Defez, G. Peris-Fajarnés, Fuzzy directional distance vector filter, *WILF07, Lecture Notes in Artificial Intelligence*, 4578, 355-361.

Abstract

A well-known family of nonlinear multichannel image filters based on the theory of robust statistics uses the reduced ordering of vectors in a predefined sliding window by means of an appropriate *distance or similarity measure* between vectors. Distances which take into account magnitude, directional and magnitude-directional criteria have been studied in the literature. In this paper a novel *fuzzy metric* already used to measure *fuzzy magnitude distances* between image vectors is extended to the directional domain. Then, a hybrid approach which takes into account both magnitude and directional criteria is proposed by realizing the fuzzy fusion of the *fuzzy magnitude distances* and the *fuzzy directional distances*. The proposed *fuzzy distance* measures are used to propose two new vector filters. Experimental results are presented to state the appropriateness of the proposed vector filters.

7.1 Introduction

Nonlinear vector filters based on the theory of robust statistics [6, 12], commonly use the reduced ordering principle amongst vectors in a predefined sliding window [15, 20]. This ordering of vectors identifies outliers of the population in the highest ranks while the lower ranks are occupied by the vectors which are *similar* (in some sense) to all the other vectors of the population. The output of the reduced ordering based vector filters is defined as the lowest ranked vector as follows [20].

Let $\mathbf{F}$ represent a multichannel image and let W be a window of finite size $n+1$ (filter length). The image vectors in the filtering window W are denoted as $\mathbf{F}_j = (F_j(1), F_j(3), F_j(3)), j = 0, 1, ..., n$. The *distance* between two vectors $\mathbf{F}_k, \mathbf{F}_j$ is denoted as $\rho(\mathbf{F}_k, \mathbf{F}_j)$. For each vector in the filtering

window, a global or accumulated distance to all the other vectors in the window has to be calculated. The scalar quantity $R_k = \sum_{j=0,j\neq k}^{n} \rho(\mathbf{F}_k, \mathbf{F}_j)$, is the accumulated distance associated to the vector $\mathbf{F}_k$. The ordering of the R_k's: $R_{(0)} \leq R_{(1)} \leq ... \leq R_{(n)}$, implies the same ordering of the vectors $\mathbf{F}_k$'s: $\mathbf{F}_{(0)} \leq \mathbf{F}_{(1)} \leq ... \leq \mathbf{F}_{(n)}$. Given this order, the output of the filter is $\mathbf{F}_{(0)}$.

Following the above scheme, the *vector median filter* (VMF) uses the generalized Minkowski metric (L_p norm) expressed as

$$L_\beta(\mathbf{F}_k, \mathbf{F}_j) = \left(\sum_{i=1}^{N} |\left(F_k(i) - F_j(i)\right)|^\beta \right)^{\frac{1}{\beta}}, \tag{7.1}$$

and usually its particular cases the $L_1(\mathbf{F}_k, \mathbf{F}_j) = \sum_{i=1}^{N} |F_k(i) - F_j(i)|$ and $L_2(\mathbf{F}_k, \mathbf{F}_j) = \left(\sum_{i=1}^{N} \left(F_k(i) - F_j(i)\right)^2 \right)^{\frac{1}{2}}$ metrics as the ρ distance function between vectors. VMF can be derived as a maximum likelihood estimate (MLE) when the underlying probability densities of input samples are bi-exponential and the output vector is restricted to be one of the vectors in the population [2, 20]. Thus it is scale, translation and rotation invariant and since the impulse response of VMF is zero it excellently suppresses impulsive noise [2, 15]. VMF has been combined with linear techniques to improve its performance in the suppression of gaussian noise [2, 25]. Other approaches have been introduced with the aim of speeding up the VMF by using a linear approximation of the Euclidean distance [3], and by designing a fast algorithm when using the L_1 norm [4].

On the other hand the *basic vector direcional filter* BVDF [23], uses the difference in direction among the image vectors as the distance criterion for the ordering. The function usually used to measure angular differences between vectors is defined [23], as

$$A(\mathbf{F}_k, \mathbf{F}_j) = cos^{-1} \left(\frac{\mathbf{F}_k \cdot \mathbf{F}_j}{||\mathbf{F}_k|| \cdot ||\mathbf{F}_j||} \right). \tag{7.2}$$

The BVDF uses the A function as the ρ distance function above for defining the vector ordering. The output of the BVDF is the vector whose direction is the MLE of the directions of the input vectors [15]. This approach exploits the fact that in RGB images the vectors directions are associated to their chromaticity and therefore, the angular minimization may give better results than techniques based on VMF in terms of colour preservation. However, the BVDF is not able to remove achromatic noise from the image because it only uses information about vector directions.

From a more general point of view, the *directional distance filter* (DDF), [13], tries to minimize a combination of the distance measures used in the VMF and the BVDF. The accumulated distance R_k associated to each vector $\mathbf{F}_k, k = 0, \ldots, n$ in the filtering window is now calculated as follows

$$R_k = \left[\sum_{j=0}^{n} L_\beta(\mathbf{F}_k, \mathbf{F}_j)\right]^{1-q} \cdot \left[\sum_{j=0}^{n} A(\mathbf{F}_k, \mathbf{F}_j)\right]^{q}, \tag{7.3}$$

where L_β denotes the specific metric used, A is the angular distance function above and $q \in [0, 1]$ is a parameter which allows to tune the importance of the angle criterion versus the distance criterion. If $q = 0$, the DDF operates as the VMF, whereas for $q = 1$ DDF is equivalent to the BVDF. For $q = 0.5$ the weight is equivalent for both criteria. In this way, the DDF constitutes a generalization of the VMF and BVDF. It is useful in multichannel image processing since it inherits the properties of its ancestors [13]. The disadvantage of DDF is a relatively high computational complexity because two different aggregated measures are to be calculated.

The traditional vector filters described above have the disadvantage of being designed to perform a fixed amount of smoothing and they are not able to adapt to local image statistics. Many different approaches have been recently introduced in the literature with the aim of being able to properly adapt the smoothing performed in each particular case, for extensive information the reader is referred to the recent overview made in [15].

The use of fuzzy techniques for image filtering has been studied in the literature. The VMF has been extended to fuzzy numbers in [5] by means of certain fuzzy distances. A fuzzy rule based system to decide the filtering is proposed in [1]. The simultaneous use of different vector filters and its combination within a fuzzy approach is proposed in [14, 24]. Some fuzzy coefficients are introduced in [16] to perform weighted vector median operation. A fuzzy smoothing operation based on fuzzy membership functions and the so-called fuzzy transformation are studied in [7, 19, 22].

In this paper the use of the novel fuzzy metric introduced in [17, 18] to measure *fuzzy magnitude distances* between colour vectors is extended to the directional domain. Then a fuzzy hybrid approach combining both magnitude and directional criteria is proposed and a unique fuzzy expression which models the *nearness* of two colour vectors in both direction and magnitude is obtained. A set of vector filters following the reduced ordering procedure is proposed according to these approaches. It will be shown that the proposed approaches present some advantages respect to the classical vector filters. Notice that the fuzzy metric can be used in combination with most of the advanced techniques listed above and some improvements should be expected. Since it is not the aim of the authors to enlarge nor diversify the content of this paper, this study is not included.

The paper is organized as follows. In Section 7.2 the novel fuzzy metric and its use in magnitude and directional vector processing is described. Experimental results including performance comparison are shown in Section 7.3. Finally, conclusions are presented in Section 7.4.

7.2 A fuzzy metric for vector processing

Let X be a non-empty set and $*$ a continuous t-norm. A (stationary) fuzzy metric [8, 11] on X is a function $M(x, y)$ defined on $X \times X$ with values in $]0, 1]$, symmetric respect to x and y, which satisfies for all $x, y, z \in X$

(FM1) $M(x, y) = 1$ if and only if $x = y$

(FM2) $M(x, z) \geq M(x, y) * M(y, z)$

$M(x, y)$ represents the degree of nearness of x and y and according to (FM1) $M(x, y)$ is close to 0 when x is far from y. From now on $*$ will be the usual product in $]0, 1]$.

According to [17, 18] a stationary fuzzy metric fulfilling the above conditions suitable for RGB colour vectors is the following.

Proposition 3. *Let Z be the real interval $[0, 255]$, put $X = Z^3$ and take $K > 0$. Denote by $(F_i(1), F_i(2), F_i(3))$ the element $\mathbf{F}_i \in X$. The function M_K given by*

$$M_K(\mathbf{F}_i, \mathbf{F}_j) = \prod_{l=1}^{3} \frac{min\{F_i(l), F_j(l)\} + K}{max\{F_i(l), F_j(l)\} + K} \tag{7.4}$$

for all $\mathbf{F}_i, \mathbf{F}_j \in X$, is a fuzzy metric on X.

Notice the fuzzy metric presents a particular behaviour since the value given for two distinct pairs of consecutive (or equally distanced) vectors may not be the same. This effect can be smoothed by increasing the value of the K parameter in Eq. (7.4). Therefore, the value of K should be set high enough to reduce this effect (see Figure 7.4). Several experiences have shown that for RGB colour vectors appropriate values for K are in the range $[512, 2048]$ [17, 18].

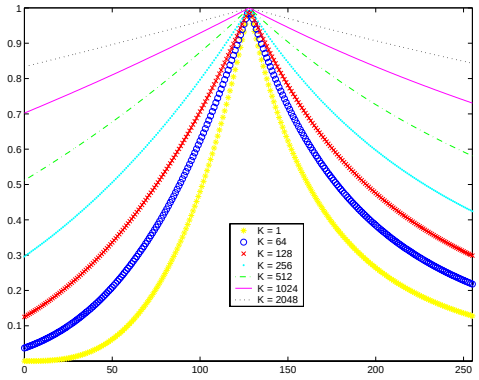

Fig. 7.1. Values given by M_K when comparing a colour vector $[128, 128, 128]$ with the colour vectors $[L, L, L]$ where $L = 0, 1, \ldots, 255$, for different values of K.

7.2.1 Using M_K to measure fuzzy directional distance between colour vectors

Following the above notation, to approach directional processing of RGB colour vectors instead of considering the colour vector itself and according to [23] we can consider the unitary vector associated to each colour vector which characterizes its direction in the vector space. Let $\hat{\mathbf{F}}_k$ denote the unitary vector associated to the colour image vector $\mathbf{F}_k$ which is obtained as

$$\hat{\mathbf{F}}_k = \frac{\mathbf{F}_k}{||\mathbf{F}_k||} = \left(\frac{F_k(1)}{||\mathbf{F}_k||}, \frac{F_k(2)}{||\mathbf{F}_k||}, \frac{F_k(3)}{||\mathbf{F}_k||} \right) \tag{7.5}$$

where $||\cdot||$ denotes the vector norm. Notice the above expression has no sense for the RGB black colour vector $(0,0,0)$ since $||(0,0,0)|| = 0$. To overcome this it is proposed to take into account that the gray scale in RGB corresponds to the vectors with the form $V_a = (a,a,a)$, where $a \in [0,255]$ and that these colour vectors should be assigned with the same chromaticity. Now, for any $a > 0$, $||V_a|| = a\sqrt{3}$ and $\hat{V}_a = (\frac{1}{\sqrt{3}}, \frac{1}{\sqrt{3}}, \frac{1}{\sqrt{3}})$, then for $Z = (0,0,0)$ we will assign $\hat{Z} = (\frac{1}{\sqrt{3}}, \frac{1}{\sqrt{3}}, \frac{1}{\sqrt{3}})$, extending so the definition of the above function.

So, the fuzzy metric $M_{K'}$ over the unitary vectors defined as above can be used to measure directional distance between colour vectors. In this way

$$M_{K'}(\hat{\mathbf{F}}_k, \hat{\mathbf{F}}_j) = \prod_{l=1}^{3} \frac{min\{\hat{F}_k(l), \hat{F}_j(l)\} + K'}{max\{\hat{F}_k(l), \hat{F}_j(l)\} + K'} \tag{7.6}$$

will be the fuzzy directional distance between $\mathbf{F}_k$ and $\mathbf{F}_j$. In this case, the value of K' must be appropriate for unitary vectors. Several experiences have shown that appropriate values for K' are in $[2,8]$, which agrees, by simple proportionality, with the explanation above.

7.2.2 A fuzzy magnitude-directional distance measure

In order to approach a simultaneous magnitude-directional distance, from a fuzzy point of view it should be appropriate to join both *fuzzy magnitude distances* $M_K(\mathbf{F}_i, \mathbf{F}_j)$ and *fuzzy directional distances* $M_{K'}(\hat{\mathbf{F}}_i, \hat{\mathbf{F}}_j)$ with an appropriate t-norm. The product t-norm will be used since it is involved in (7.4), then, the function

$$M_{KK'} = M_K(\mathbf{F}_i, \mathbf{F}_j) \cdot M_{K'}(\hat{\mathbf{F}}_i, \hat{\mathbf{F}}_j) \tag{7.7}$$

models the *nearness* of the colour vectors $\mathbf{F}_i$ and $\mathbf{F}_j$ taking simultaneously into account both magnitude and directional criteria (compare with [13]). Moreover, according to [21] it is easy to verify that $M_{KK'}$ is a fuzzy metric, as well.

7.2.3 Proposed vector filters

Following the reduced ordering based vector filter procedure explained in Section 7.1 three different vector filters can be defined by using the expressions (7.4), (7.6) and (7.7) as the distance criterion between colour vectors. These filters will be called *Fuzzy Metric Vector Median Filter* FMVMF (already defined in [17]), *Fuzzy Metric Vector Directional Filter* FMVDF and *Fuzzy Metric Distance Directional Filter* FMDDF, respectively. Unlike the classical VMF, BVDF and DDF, in these vector filters the vector output is defined as the highest ranked vector since according to (FM1) the accumulated distance has to be maximized.

Notice the filters proposed in this paper parallelize the operation of the VMF, BVDF and DDF decribed in Section 7.1. In the next section, the FMVMF, the FMVDF and the FMDDF will be assessed by comparing their performance in front of those vector filters.

7.3 Experimental results

The classical gaussian model for the thermal noise and the impulsive noise model for the transmission noise, as defined in [20], have been used to assess the performance of the proposed filters by adding noise to the details of the images in Figure 7.2.

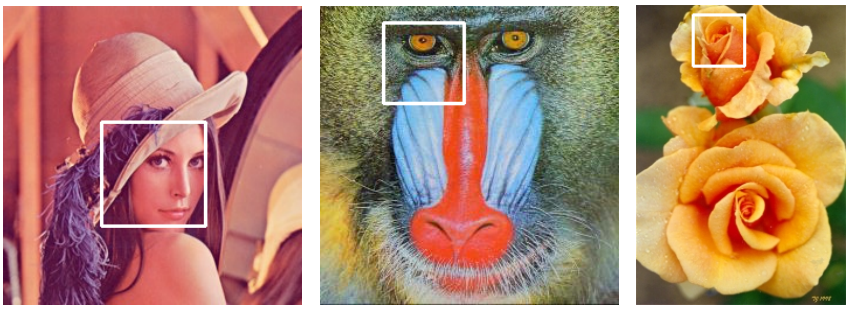

(a) (b) (c)

Fig. 7.2. Test Images: (a) Detail of Lenna image, (b) Detail of Mandrill image, (c) Detail of Brandy Rose image (Copyright photo courtesy of Toni Lankerd)

The *Peak Signal to Noise Ratio* (PSNR), *Normalized Colour Difference* (NCD) and the recently introduced *Structural Similarity Index* (SSI) [26][1] have been used to assess the performance of the proposed filters. The SSI has

[1] The used MATLAB implementation is available online at http://www.cns.nyu.edu/∼lcv/ssim/.

been used since it was proved to be more appropriate in image quality assessment than previous quality measures [26]. It has been applied to each colour channel and the mean value has been used for the assessment. According to [20], the PSNR and NCD measures are defined as

$$PSNR = 20 \log \left(\frac{255}{\sqrt{\frac{1}{NMQ} \sum_{i=1}^{N} \sum_{j=1}^{M} \sum_{q=1}^{Q} \left(F^q(i,j) - \widetilde{F}^q(i,j) \right)^2}} \right), \tag{7.8}$$

where M, N are the image dimensions, Q is the number of channels of the image ($Q = 3$ for RGB images), and $F^q(i,j)$ and $\widetilde{F}^q(i,j)$ denote the q^{th} component of the original image vector and the filtered image, at pixel position (i,j), respectively, and

$$NCD_{Lab} = \frac{\sum_{i=1}^{N} \sum_{j=1}^{M} \Delta E_{Lab}}{\sum_{i=1}^{N} \sum_{j=1}^{M} E^*_{Lab}} \tag{7.9}$$

where $\Delta E_{Lab} = [(\Delta L^*)^2 + (\Delta a^*)^2 + (\Delta b^*)^2]^{\frac{1}{2}}$ denotes the perceptual colour error and $E^*_{Lab} = [(L^*)^2 + (a^*)^2 + (b^*)^2]^{\frac{1}{2}}$ is the *norm* or *magnitude* of the original image colour vector in the $L^*a^*b^*$ colour space.

Table 7.1. Performance comparison in terms of PSNR, NCD and SSI using the test images contaminated different densities of noise.

Filter	Lenna 5% impulsive and $\sigma = 5$ Gaussian			Brandy Rose 15% impulsive and $\sigma = 10$ Gaussian			Baboon 25% impulsive		
	PSNR	NCD (10^{-2})	SSI	PSNR	NCD (10^{-2})	SSI	PSNR	NCD (10^{-2})	SSI
Noisy	22.127	7.777	0.677	16.821	13.790	0.397	15.329	18.305	0.423
VMF	28.702	4.671	0.868	28.237	5.840	0.781	22.806	6.535	0.674
FMVMF	28.837	4.790	0.870	28.498	5.808	0.791	23.116	6.508	0.691
BVDF	27.000	4.669	0.812	26.584	5.663	0.713	20.681	7.094	0.582
FMVDF	26.942	4.730	0.813	26.927	5.573	0.728	20.350	7.326	0.576
DDF	28.506	4.507	0.863	28.001	5.620	0.774	22.746	6.219	0.673
FMDDF	28.746	4.544	0.869	28.410	5.610	0.785	23.035	6.114	0.690

In the experiences we have set $q = 0.5$ for the DDF giving both magnitude and direction criteria the same weight, and $K = 1024, K' = 4$ for the proposed filters.

The experimental results in Figures 7.3-7.11 and Table 7.1 show that the proposed FMVMF and FMDDF filters present a better performance than their classical versions when filtering impulsive noise and a similar performance when dealing with gaussian noise. In general, when considering mixed gaussian and impulsive noise, the results show that the proposed

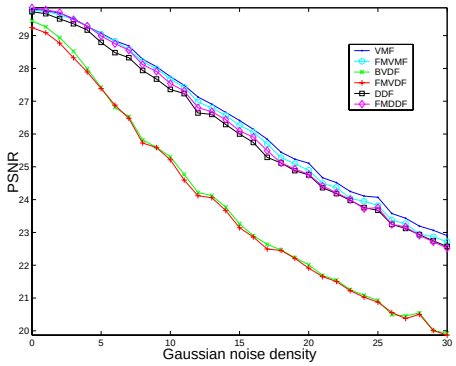

(a)

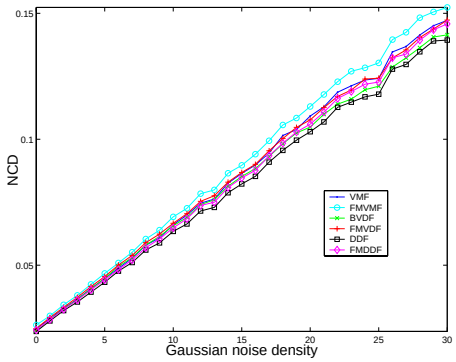

(b)

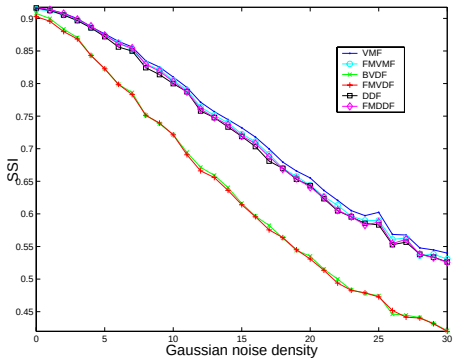

(c)

Fig. 7.3. Performance comparison of filters in terms of (a) PSNR, (b) NCD and (c) SSI for the detail of the Lenna image contaminated with different densities of gaussian noise.

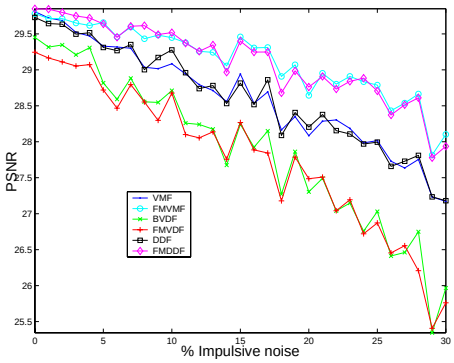

(a)

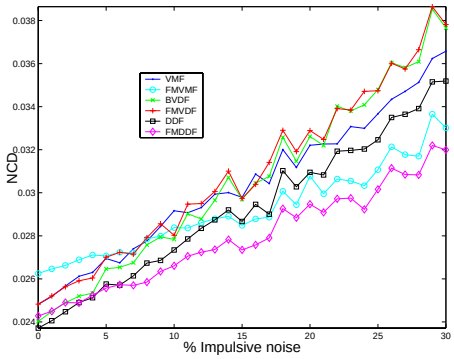

(b)

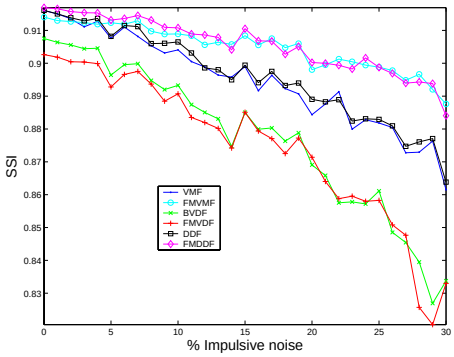

(c)

Fig. 7.4. Performance comparison of filters in terms of (a) PSNR, (b) NCD and (c) SSI for the detail of the Lenna image contaminated with different percentage of impulsive noise.

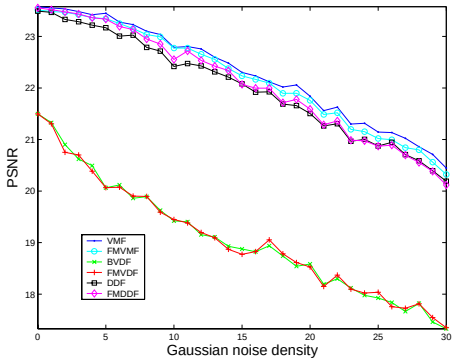

(a)

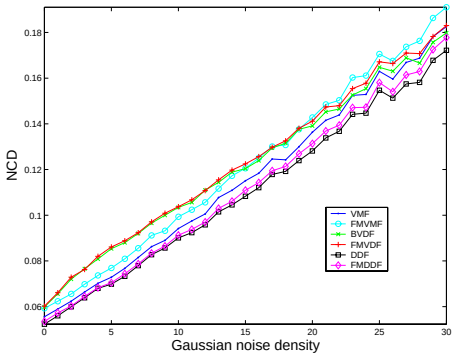

(b)

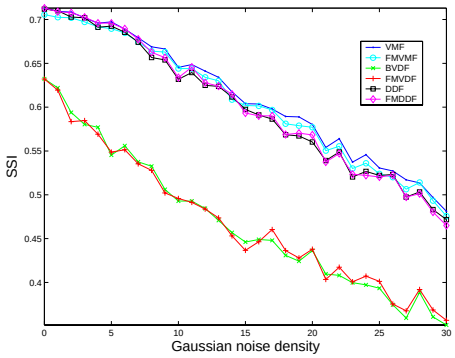

(c)

Fig. 7.5. Performance comparison of filters in terms of (a) PSNR, (b) NCD and (c) SSI for the detail of the Baboon image contaminated with different densities of gaussian noise.

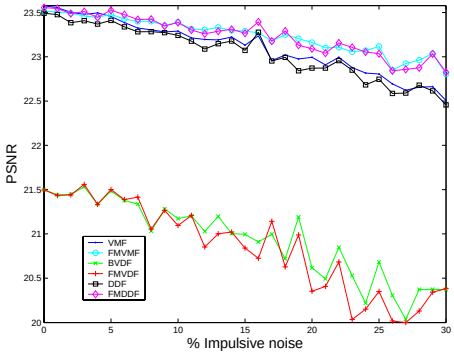

(a)

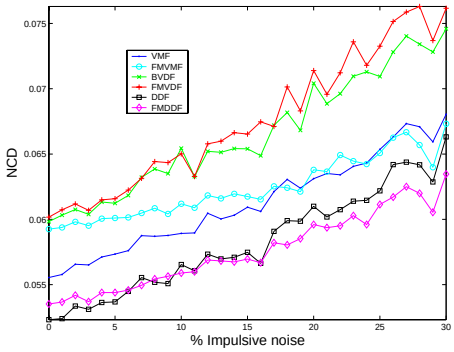

(b)

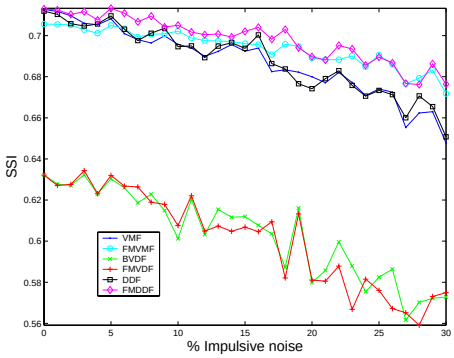

(c)

Fig. 7.6. Performance comparison of filters in terms of (a) PSNR, (b) NCD and (c) SSI for the detail of the Baboon image contaminated with different percentage of impulsive noise.

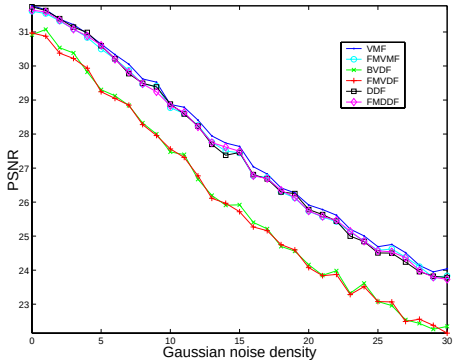

(a)

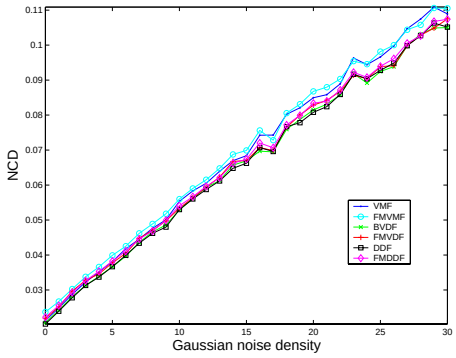

(b)

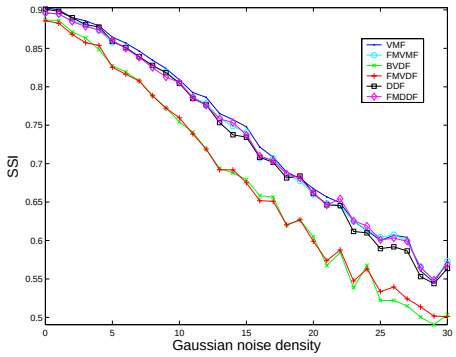

(c)

Fig. 7.7. Performance comparison of filters in terms of (a) PSNR, (b) NCD and (c) SSI for the detail of the Brandy Rose image contaminated with different densities of gaussian noise.

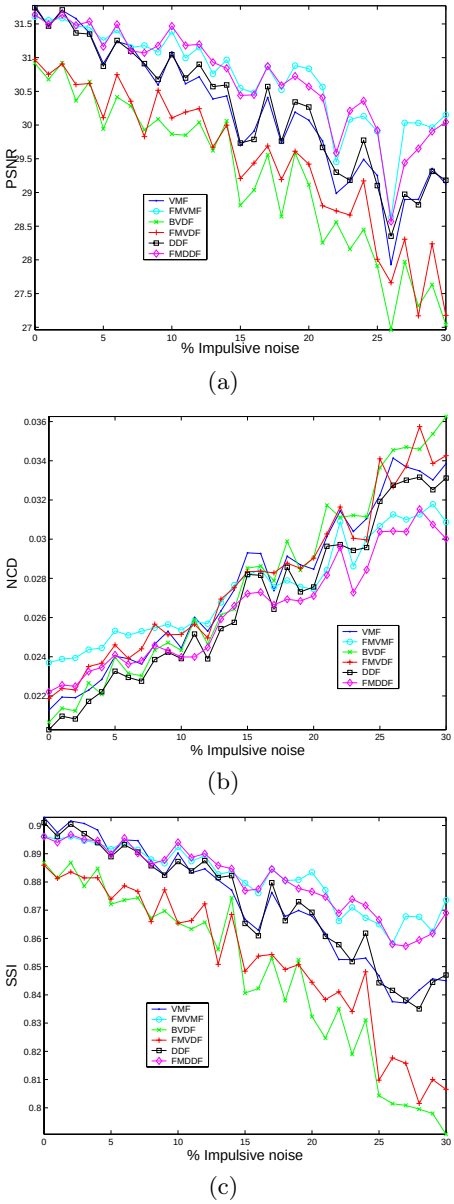

Fig. 7.8. Performance comparison of filters in terms of (a) PSNR, (b) NCD and (c) SSI for the detail of the Brandy Rose image contaminated with different percentage of impulsive noise.

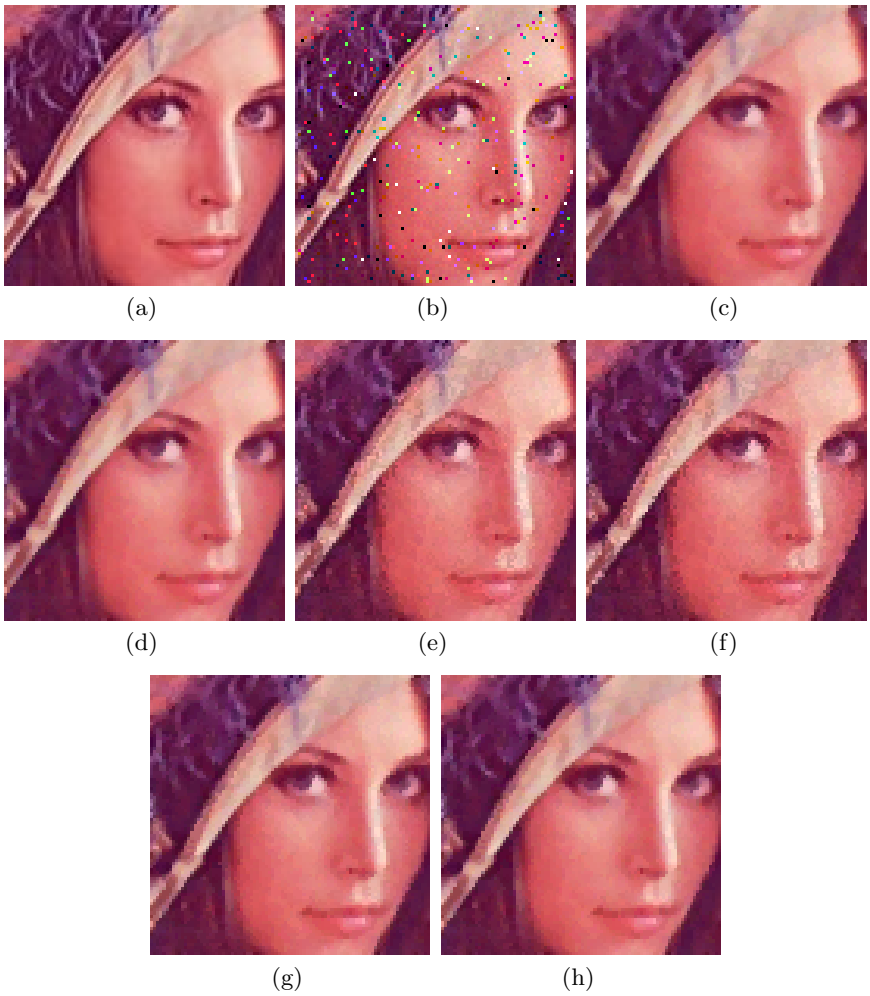

Fig. 7.9. Test Images: (a) Detail of the Lenna image, (b) Detail of the Lenna image contaminated with 5% Impulsive noise and $\sigma = 5$ Gaussian noise, (c) VMF output, (d) FMVMF output, (e) BVDF output, (f) FMVDF output, (g) DDF output, (h) FMDDF output.

filters outperform their classical versions when the component of impulsive noise present domains over the gaussian component and it is similar in other cases. The performances of the BVDF and the FMVDF are alike in most of the cases for both types of noise.

It should be pointed out that the improvement reached is lower than the one that may be reached using the advanced filtering techniques listed in Section 1 that propose changes in the filtering methodology. Here we propose

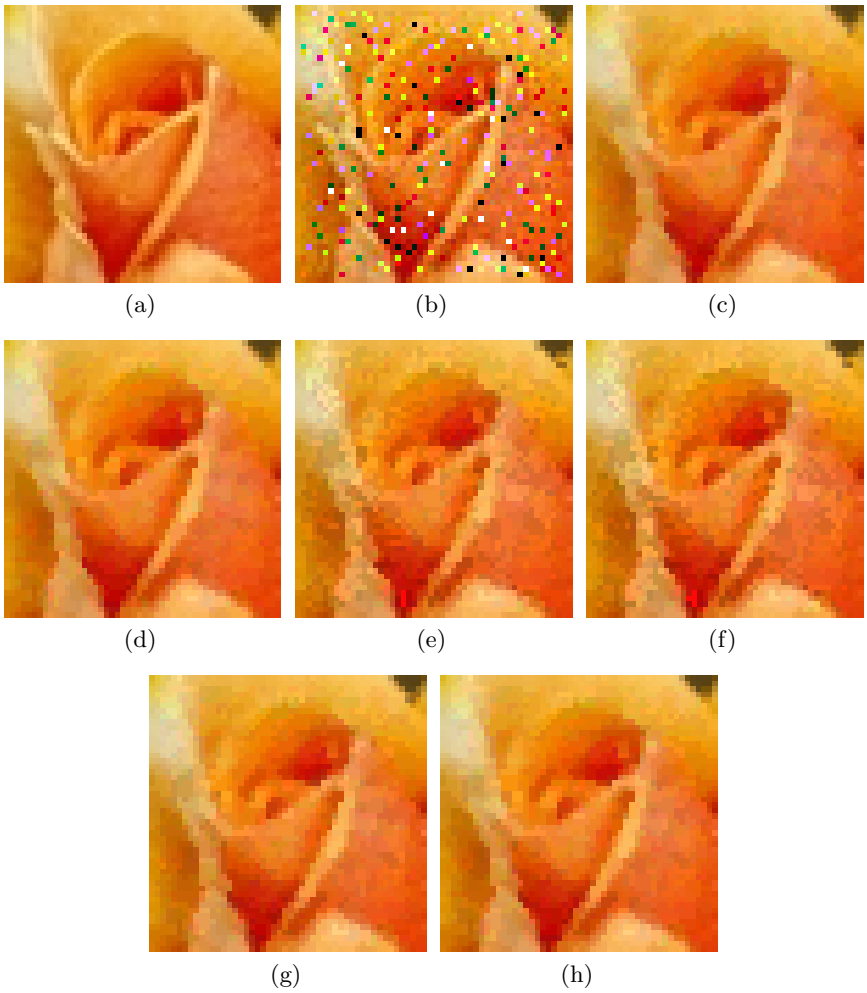

Fig. 7.10. Test Images: (a) Detail of the Brandy Rose image, (b) Detail of the Brandy Rose image contaminated with 15% Impulsive noise and $\sigma = 10$ Gaussian noise, (c) VMF output, (d) FMVMF output, (e) BVDF output, (f) FMVDF output, (g) DDF output, (h) FMDDF output.

a different way to reach some improvement over classical filtering by changing the measures used. Notice this is compatible, in most of the cases, with the changes in the methodology.

It has also been observed that the FMDDF is sensibly faster than the classical DDF. This is due to the fact that the DDF needs to compute two accumulated distances, one in magnitude and one in direction, which are

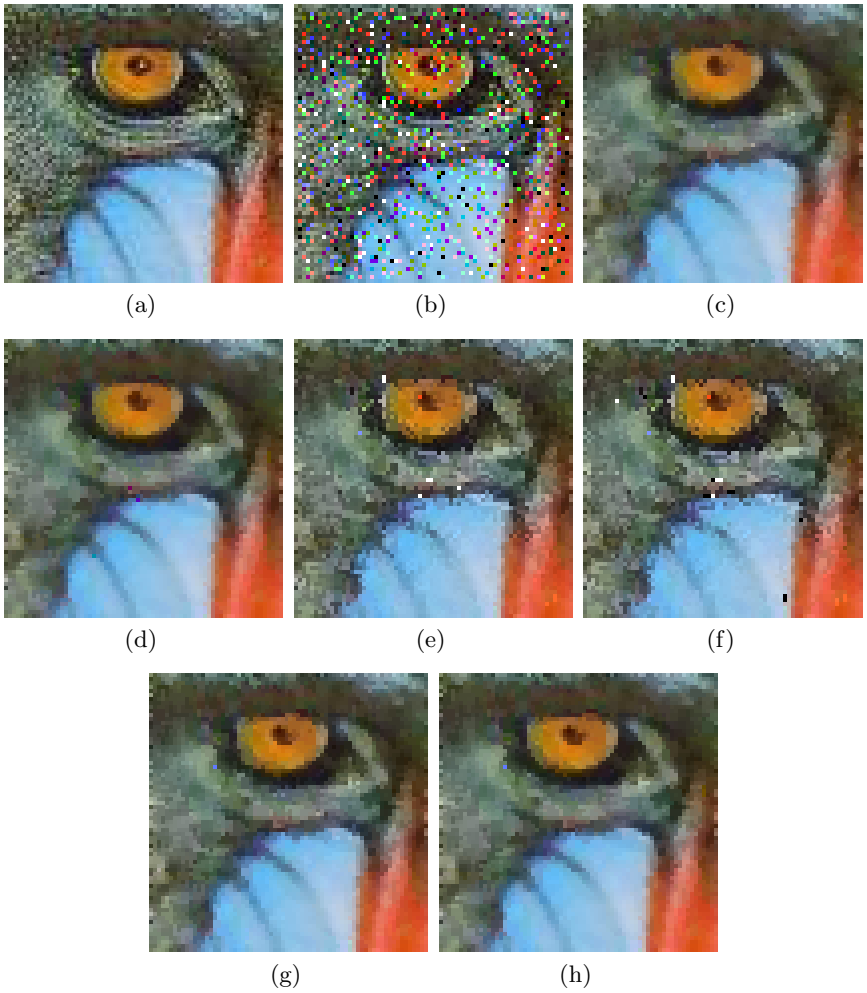

Fig. 7.11. Test Images: (a) Detail of the Baboon image, (b) Detail of the Baboon image contaminated with 25% Impulsive noise, (c) VMF output, (d) FMVMF output, (e) BVDF output, (f) FMVDF output, (g) DDF output, (h) FMDDF output.

combined afterwards, while the FMDDF computes only one accumulation of the hybrid fuzzy magnitude-directional distance measure (7.7).

Furthermore, after extensive experiments it has been observed that the proposed filters present better results when filtering reduced colour set images, for instance the detail of the Brandy Rose image in Figure 7.2 (c).

Conclusions

The usefulness of a novel fuzzy metric, previously introduced by the authors [17], in colour image filtering using vector reduced ordering techniques has been further studied in this paper. The fuzzy metric (7.4) which had been previously used to measure fuzzy magnitude distances has been extended to measure fuzzy directional distances. Using a fuzzy approach, a hybrid fuzzy metric between two colour vectors which takes simultaneously into account magnitude and direction criteria has been obtained.

A family of vector filters (FMVMF, FMVDF, FMDDF) using the classical approaches of the VMF, BVDF and DDF filters has been introduced by using the proposed fuzzy distance measures. The proposed filters outperform their classical versions when the impulsive noise component of the noisy images is higher than the gaussian component. Furthermore, the use of the hybrid fuzzy distance measure in the FMDDF has reduced the computational cost of the classical DDF.

Fuzzy metrics are a powerful tool which may be successfully applied in image processing tasks since they are able to represent more complex relations than the classical metrics in a simple way. The fuzzy measures presented in this paper can be used in many other image processing tasks which motivates its further study.

References

1. K. Arakawa, Median filter based on fuzzy rules and its application to image restoration, *Fuzzy Sets and Systems* 77 1 (1996) 3-13.
2. J. Astola, P. Haavisto, Y. Neuvo, Vector Median Filters, *Proc. IEEE.* 78 4 (1990) 678-689.
3. M. Barni, F. Buti, F. Bartolini, V. Capellini, A Quasi-Euclidean Norm to Speed Up Vector Median Filtering, *IEEE Transactions on Image Processing* 9 10 (2000) 1704-1709.
4. M. Barni, A Fast Algorithm for 1-Norm Vector Median Filtering, *IEEE Transactions on Image Processing* 6 10 (1997) 1452-1455.
5. V. Chatzis, I. Pitas, Fuzzy scalar and vector median filters based on fuzzy distances, *IEEE Transactions on Image Processing* 8 5 (1999) 731-734.
6. H.A. David, *Order Statistics*, New York: John Wiley and Sons 1981.
7. A. Flaig, K.E. Barner, G.R. Arce, Fuzzy Ranking: theory and applications, *Signal Processing* 80 6 (2000) 1017-1036.
8. A. George, P. Veeramani, On Some results in fuzzy metric spaces, *Fuzzy Sets and Systems* 64 3 (1994) 395-399.
9. A. George, P. Veeramani, Some theorems in fuzzy metric spaces, *J. Fuzzy Math.* 3 (1995) 933-940.
10. V. Gregori, S. Romaguera, Some properties of fuzzy metric spaces, *Fuzzy Sets and Systems* 115 3 (2000) 477-483.
11. V. Gregori, S. Romaguera, Characterizing completable fuzzy metric spaces, *Fuzzy Sets and Systems* 144 3 (2004) 411-420.
12. P.S. Huber, *Robust Statistics*, New York: John Wiley and Sons 1981.
13. D.G. Karakos, P.E. Trahanias, Generalized multichannel image-filtering structure, *IEEE Transactions on Image Processing* 6 7 (1997) 1038-1045.
14. L. Khriji, M. Gabbouj, Adaptive fuzzy order statistics-rational hybrid filters for color image processing, *Fuzzy Sets and Systems* 128 1 (2002) 35-46.
15. R. Lukac, B. Smolka, K. Martin, K.N. Plataniotis, A.N. Venetsanopoulos, Vector Filtering for Color Imaging, *IEEE Signal Processing Magazine, Special Issue on Color Image Processing* 22 1 (2005) 74-86.
16. R. Lukac, K.N. Plataniotis, B. Smolka, A.N. Venetsanopoulos, cDNA Microarray Image Processing Using Fuzzy Vector Filtering Framework, *Fuzzy Sets and Systems: Special Issue on Fuzzy Sets and Systems in Bioinformatics* 152 1 (2005) 17-35.
17. S. Morillas, V. Gregori, G. Peris-Fajarnés, P. Latorre, *A new vector median filter based on fuzzy metrics*, ICIAR'05, Lecture Notes in Computer Science 3656 (2005) 81-90.

18. S. Morillas, V. Gregori, G. Peris-Fajarnés, P. Latorre, *A fast impulsive noise color image filter using fuzzy metrics*, Real-Time Imaging 11 5-6 (2005) 417-428.
19. Y. Nie, K.E. Barner, The fuzzy transformation and its applications in image processing, *IEEE Transactions on Image Processing* 15 4 (2006) 910-927.
20. K.N. Plataniotis, A.N. Venetsanopoulos, *Color Image processing and applications* Berlin: Springer-Verlag 2000.
21. A. Sapena, A contribution to the study of fuzzy metric spaces, *Appl. Gen. Topology* 2 1 (2001) 63-76.
22. Y. Shen, K. Barner, Fuzzy vector median-based surface smoothing, *IEEE Transactions on Visualization and Computer Graphics* 10 3 (2004) 252-265.
23. P.E. Trahanias, D. Karakos, A.N. Venetsanopoulos, Directional processing of color images: theory and experimental results, *IEEE Trans. Image Process.* 5 6 (1996) 868-880.
24. H.H. Tsai, P.T. Yu, Genetic-based fuzzy hybrid multichannel filters for color image restoration, *Fuzzy Sets and Systems* 114 2 (2000) 203-224.
25. T. Viero, K. Oistamo, Y. Neuvo, Three-dimensional median-related filters for color image sequence filtering, *IEEE Transactions on Circuits and Systems for Video Technology* 4 2 (1994) 129-142.
26. Z. Wang, A.C. Bovik, H.R. Sheikh, E.P. Simoncelli, Image quality assessment: from error visibility to structural similarity, *IEEE Transactions on Image Processing* 13 4 (2004) 600-612.

8 Contribution (v)

S. Morillas, V. Gregori, G. Peris-Fajarnés, A. Sapena, Local self-adaptive impulsive noise filter for colour images using fuzzy metrics, *accepted for publication in Signal Processing*

Abstract

In this work, a new filter for impulsive noise reduction in colour images is proposed. The filter is designed on the basis of a recently introduced family of vector filters with good detail-preserving ability. In these approaches, the central pixel in each filtering window is *privileged* to replace it only when it is likely to be noisy. In this way, the uncorrupted image structures are preserved. The use of a recently introduced fuzzy metric allows to create a local self-adaptive filter. The *privilege* given to each central pixel will depend on its estimated *multivariate dispersion* with respect to its neighbors. As well, the fuzzy metric allows to generalize in a straightforward way the proposed filter structure to the use of fuzzy magnitude distances, fuzzy directional distances and combined fuzzy magnitude-directional distances. The proposed filtering technique is robust and presents a good balance between noise attenuation and detail-preservation. Experimental results are given to show the filter performance is competitive with respect to classical and recently introduced techniques for impulsive noise removal in colour images.

8.1 Introduction

During the image acquisition and transmission process the quality of the digital images is affected by the introduction of noise. In particular, it is mostly in the transmission process when the so-called impulsive noise appears. In order to avoid noise perturbing subsequent image processing tasks, the filtering process becomes an essential task.

Several vector filters for colour images taking advantage of the existing correlation amongst the colour image channels have been proposed to date.

A well-known family of nonlinear vector filters is based on the theory of robust statistics [4, 9]. When the vectors in a predefined sliding window are ranked using the reduced ordering principle the lowest ranked vectors are those which are *close* to all the other vectors in the window according to the *distance or similarity measure* used [15, 23]. On the other hand, atypical vectors, susceptible to be considered as noisy or outliers, occupy the highest ranks. Hence, in these filter structures the filter output is commonly defined as the lowest ranked vector. The *vector median filter* (VMF), [2], the *basic vector directional filter* (BVDF), [33], and the *directional-distance filter* (DDF), [10], are well-known vector filters of this family which present good noise suppression and other interesting properties[1].

The traditional vector filters described above have the disadvantage of being designed to perform the same in any image location and they are not able to adapt to local image statistics [15]. Many different approaches have been recently introduced in the literature with the aim of address this drawback, for instance: Weighted vector median filtering [13, 16, 17, 31], fuzzy weighted averaging techniques [1, 32, 5, 25], switching filtering [3, 14, 19, 22, 30], hybrid filtering techniques [11, 12, 34] or center privileging approaches [18, 21, 26, 27, 28, 29].

Many of the techniques listed above have the disadvantage of having to tune an adaptive parameter to reach an appropriate filter performance. This fact motivates us to introduce a local self-adaptive impulsive noise vector filter structure for colour images. In this paper, the approach of *privileging* the input central pixel studied in [21, 26, 27, 28, 29] is used. Some approaches [3, 29] try to automatically determine the value of the adaptive parameter to filter a hole image such that the filter may perform different for distinct images. Unlike this, in this paper it is proposed to compute the value of the adaptive parameter for each image location. So, the filter may perform different in each image location. Hence, the *privilege* given to each particular pixel in consideration will depend on its estimated *multivariate dispersion* with respect to its neighbors. The filter will perform more smoothing by decreasing the *privilege* given to the input central pixel when it is estimated to be far from its neighbors. In this way, the filter may perform well, for instance, in images where the noise is concentrated in a part of the image thanks to its local adaptive nature.

The paper is organized as follows. In Section 8.2 the filter structure based on privileging the central pixel is described. Section 8.3 details the approach used to estimate the dispersion of the central pixel. Then, the local self-adaptive filter structure using a fuzzy metric and the estimated dispersion is proposed. Experimental study and some comparisons in front of recent and well-known vector filters are shown in Section 8.4. Finally, Section 8.5 presents the conclusions.

[1] For a detailed description of these vector filters and their properties the reader is refered to [15, 23]

8.2 Central Privileging Approach

According to the Fast Impulsive Vector Filter technique introduced in [21, 26, 27, 28, 29] (from now on FIVF), an appropriate filter structure for impulsive noise reduction in RGB images is defined as follows.

Let $X = [0, 255]$ and assume a filtering window W containing a set of $n+1$ image pixels $\{\mathbf{F}_0, \mathbf{F}_1, \ldots, \mathbf{F}_n\} \subset X^3$, where each $\mathbf{F}_k = (F_k(1), F_k(2), F_k(3))$ is comprised by its R, G and B components and n is the number of neighbors of the central pixel $\mathbf{F}_0$. It is considered a function $\mu : X^3 \times X^3 \rightarrow [0, 1]$ which satisfies that $\mu(\mathbf{F}_i, \mathbf{F}_i) = 1$ and $\mu(\mathbf{F}_i, \mathbf{F}_j) \rightarrow 0$ when $\mathbf{F}_i$ and $\mathbf{F}_j$ are pixels with very different colour. Any function defined by means of a non-ascending convex function over some norm of the vector difference $||\mathbf{F}_i - \mathbf{F}_j||$ can easily satisfy the above conditions. As well, any fuzzy metric, in the sense of [6], between colour vectors can be used as the μ function, as in [21]. The cumulated sum R_k of similarities between a given pixel $\mathbf{F}_k$ $(k = 0, \ldots, n)$ and all the other pixels in W is defined as

$$R_0 = \sum_{j=1}^{n} \mu(\mathbf{F}_0, \mathbf{F}_j), \quad R_k = \sum_{j=1, j\neq k}^{n} \mu(\mathbf{F}_k, \mathbf{F}_j)\,, \tag{8.1}$$

which means that for those $\mathbf{F}_k, (k = 1, \ldots, n)$ which are neighbors of $\mathbf{F}_0$, the value $\mu(\mathbf{F}_k, \mathbf{F}_0)$ is not taken into account when computing R_k, which *privileges* the central pixel. Indeed, the reference pixel $\mathbf{F}_0$ is replaced by its neighbor $\mathbf{F}_{k^*}$ for which $k^* = \arg\max_k R_k$ if and only if $R_0 < R_{k^*}$. So, it is substituted only when it is really noisy and the original undistorted image structures are preserved.

Several functions fulfilling the above conditions have been proposed in [21, 26, 27, 28, 29] to be used as the μ function above. These functions include an adaptive parameter able to tune the privilege given to the central pixel. This privilege influences the intensity of the filtering process. The best performance and computational results were achieved, in our experiences [21], when using the function M_K^α given by

$$M_K^\alpha(\mathbf{F}_i, \mathbf{F}_j) = \prod_{l=1}^{3} \left(\frac{min\{F_i(l), F_j(l)\} + K}{max\{F_i(l), F_j(l)\} + K} \right)^\alpha \tag{8.2}$$

where $\mathbf{F}_i, \mathbf{F}_j \in X^3$. M_K^α is, according to [6, 7, 8], a stationary fuzzy metric on X^3, with respect to the usual product in $[0, 1]$. This fuzzy metric presents an special behaviour in the sense that the value given by M_K^α between two pairs of equally distanced (or consecutive) vectors may not be the same. This *non-uniformity* is negligible from a practical point of view if a large enough value of the K parameter is set. Previous works [20, 21] have shown that a suitable values of the K parameter when processing RGB colour vectors are around $K_1 = 1024$. On the other hand, the α parameter is able to tune

the *privilege* given to the central pixel. In fact, the values given by the fuzzy metric are in a bounded interval, such that

$$1 \geq M_{1024}^{\alpha}(\mathbf{F}_i, \mathbf{F}_j) \geq M_{1024}^{\alpha}((0,0,0),(255,255,255)) = \left(\frac{255}{1279}\right)^{3\alpha} > 0 \quad (8.3)$$

where the value of the lower bound is the minimum *privilege* given to the central pixel. Obviously, the lower bound of the fuzzy metric decreases as the value of α increases. So, increasing the value of α reduces the advantage given to the central pixel. Therefore, the likelihood to replace it is higher and the intensity of the filtering process is higher, as well. The computation of the α parameter is addressed in Section 8.3. For a more detailed information about this fuzzy metric, its properties and parameters, the interested reader is refered to [20, 21, 24].

8.2.1 Using M_K^{α} to measure fuzzy magnitude distance between colour vectors

Notice M_K^{α} was directly used in [21] between the colour vector component values so it measures the *fuzzy magnitude distances* between the colour vectors. However, some works have shown that taking into account directional distances is also interesting in RGB image processing [10, 15, 33]. In these works it is stated that it exists a close relation between colour vector direction and chromaticity. In this subsection we extend the use of M_K^{α} to the directional domain. This will allow us to define some vectors filters, which use this fuzzy metric, taking into account magnitude, directional and hybrid distance criteria.

Following the above notation, to each colour image vector, for instance $\mathbf{F}_i$, we can associate its unitary vector $\mathbf{F}_i^{'}$ that characterizes its direction in the vector space and which is given by

$$\mathbf{F}_i^{'} = \frac{\mathbf{F}_i}{||\mathbf{F}_i||_2} \quad (8.4)$$

where $||\cdot||_2$ denotes the Euclidean norm. The above expression has no sense for the RGB black colour vector $\mathbf{Z} = (0,0,0)$ since $||\mathbf{Z}||_2 = ||(0,0,0)||_2 = 0$. Now, taking into account that the gray-scale vectors (that should be assigned with the same chromaticity) in RGB correspond to the vectors with the form $\mathbf{V}_a = (a,a,a)$ where $a \in [0,255]$ and that for any $a > 0$, $||\mathbf{V}_a||_2 = a\sqrt{3}$ and $\mathbf{V'}_a = (\frac{1}{\sqrt{3}}, \frac{1}{\sqrt{3}}, \frac{1}{\sqrt{3}})$, then we will extend the above function by defining the unitary vector $\mathbf{Z'} = (\frac{1}{\sqrt{3}}, \frac{1}{\sqrt{3}}, \frac{1}{\sqrt{3}})$.

So, the fuzzy metric M_K^{α} over the unitary vectors defined as above can be used to measure directional distances between colour vectors. In this way $M_{K_2}^{\alpha}(\mathbf{F}_i^{'}, \mathbf{F}_j^{'})$ will be the fuzzy directional distance between $\mathbf{F}_i$ and $\mathbf{F}_j$. In this case, the value of the parameter K_2 must be appropriate for a vector

components value range in $[0, 1]$. Notice an appropriate value of the K parameter for the RGB range ($[0, 255]$) is $K_1 = 1024$. Then, it has been checked that a value of $K_2 = 4$ is appropriate for vector component values in $[0, 1]$, as it could be expected by simple proportionality. As commented above, the α parameter is able to adjust the privilege given to the central pixel and so, the intensity of the filtering process. Its computation is addressed in Section 8.3.

8.3 Proposed Local Self-Adaptive Filter

Following the FIVF approach described in Section 8.2 our aim is to design a local self-adaptive filter where the privilege given to each pixel will depend on its estimated *multivariate dispersion*. Since the value of the α parameter in Eq. (8.2) tunes the *privilege* given to the central pixel, in order to create a local self-adaptive filter it is necessary to locally determine the value of α. In the following sections it will be proposed how to approach the *multivariate dispersion* of the central pixel and then a method to determine the value of the α parameter using this dispersion.

8.3.1 Approaching the *Multivariate Dispersion* of the Central Pixel

According to the notation used in Section 8.2, denote by $\bar{\mathbf{F}}$ the vector mean of the vectors in the sliding window, that is $\bar{\mathbf{F}} = \frac{1}{n+1} \sum_{i=0}^{n} \mathbf{F}_i$, and denote by $\hat{\mathbf{F}}$ the vector median [2] of the vectors in the sliding window. In the existing literature, the vector mean and the vector median are statistical concepts that have been used to define switching vector filters [3, 19]. Now, it seems natural to define the *multivariate dispersion* of any pixel $\mathbf{F}_i$ with respect to the vector mean $\bar{\mathbf{F}}$ as

$$\sigma_{\bar{\mathbf{F}}}(\mathbf{F}_i) = ||\mathbf{F}_i - \bar{\mathbf{F}}||_2 \tag{8.5}$$

and the *multivariate dispersion* of any pixel $\mathbf{F}_i$ with respect to the vector median $\hat{\mathbf{F}}$ as

$$\sigma_{\hat{\mathbf{F}}}(\mathbf{F}_i) = ||\mathbf{F}_i - \hat{\mathbf{F}}||_2 \tag{8.6}$$

where $||\cdot||_2$ denotes the L_2 (Euclidean) norm. So, two *multivariate dispersion* of the central pixel, $\sigma_{\bar{\mathbf{F}}}(\mathbf{F}_0)$ and $\sigma_{\hat{\mathbf{F}}}(\mathbf{F}_0)$, may be considered. The use of the vector median may provide certain robustness against noise, however, it can be easily observed that its use is much more computationally demanding than the use of the vector mean.

8.3.2 Local Self-Adaptive Filters

In this section, the estimated *multivariate dispersion* of the central pixel is used to locally determine the value of α in (8.2). Our experiments show that the values of $\sigma_{\bar{\mathbf{F}}}(\mathbf{F}_0)$ or $\sigma_{\hat{\mathbf{F}}}(\mathbf{F}_0)$ can not be directly used as the α parameter since these values are too high and the advantage given to the central pixel would not be appropriate. Therefore, it is necessary to use an scaling parameter c in order to adequate the range of these values. So, we will compute the value of α at each image location as

$$\alpha = c \cdot \sigma_{\bar{\mathbf{F}}}(\mathbf{F}_0) \tag{8.7}$$

or

$$\alpha = c \cdot \sigma_{\hat{\mathbf{F}}}(\mathbf{F}_0) \tag{8.8}$$

We have experimentally determined that appropriate values for c are in the range $[0.040, 0.070]$ (which means that we take the 4%-7% of the value of the dispersion), and in the following it will be assumed the use of $c = 0.055$.

Now, we define several local self-adaptive vector filters using the filter structure explained in Section 8.2 and the fuzzy distance measures in magnitude, direction and a combined magnitude-directional approach. For this, we make use of the fuzzy metric in Eq. (8.2) and the estimation of the *multivariate dispersion* for each pixel to compute the value of α (see Sections 8.2 and 8.3.1).

Taking the cumulated measure R_k in Eq. (8.1) of the FIVF in Section 8.2, we can define two Local Self-Adaptive Magnitude Impulsive Vector Filters denoted by $SMF_{\sigma_{\bar{\mathbf{F}}}}$ and $SMF_{\sigma_{\hat{\mathbf{F}}}}$ using $\sigma_{\bar{\mathbf{F}}}$ and $\sigma_{\hat{\mathbf{F}}}$, respectively, as a modification of the FIVF, where the value of α is computed using Eqs. (8.7) and (8.8) and so the R_k values will be calculated as follows.

$$R_0 = \sum_{j=1}^{n} M_{K_1}^{c\sigma_{\bar{\mathbf{F}}}(\mathbf{F}_0)}(\mathbf{F}_0, \mathbf{F}_j), \quad R_k = \sum_{j=1, j\neq k}^{n} M_{K_1}^{c\sigma_{\bar{\mathbf{F}}}(\mathbf{F}_0)}(\mathbf{F}_k, \mathbf{F}_j) \tag{8.9}$$

in the case of the $SMF_{\sigma_{\bar{\mathbf{F}}}}$, and,

$$R_0 = \sum_{j=1}^{n} M_{K_1}^{c\sigma_{\hat{\mathbf{F}}}(\mathbf{F}_0)}(\mathbf{F}_0, \mathbf{F}_j), \quad R_k = \sum_{j=1, j\neq k}^{n} M_{K_1}^{c\sigma_{\hat{\mathbf{F}}}(\mathbf{F}_0)}(\mathbf{F}_k, \mathbf{F}_j) \tag{8.10}$$

for the $SMF_{\sigma_{\hat{\mathbf{F}}}}$.

In a similar way we can define two Local Self-Adaptive Directional Impulsive Vector Filters denoted by $SDF_{\sigma_{\bar{\mathbf{F}}}}$ and $SDF_{\sigma_{\hat{\mathbf{F}}}}$ using $\sigma_{\bar{\mathbf{F}}}$ and $\sigma_{\hat{\mathbf{F}}}$, respectively, as a modification of the FIVF, where

$$R_0 = \sum_{j=1}^{n} M_{K_2}^{c\sigma_{\bar{\mathbf{F}}}(\mathbf{F}_0)}(\mathbf{F}_0^{'}, \mathbf{F}_j^{'}), \quad R_k = \sum_{j=1, j\neq k}^{n} M_{K_2}^{c\sigma_{\bar{\mathbf{F}}}(\mathbf{F}_0)}(\mathbf{F}_k^{'}, \mathbf{F}_j^{'}) \quad (8.11)$$

in the case of the $SDF_{\sigma_{\bar{\mathbf{F}}}}$, and,

$$R_0 = \sum_{j=1}^{n} M_{K_2}^{c\sigma_{\hat{\mathbf{F}}}(\mathbf{F}_0)}(\mathbf{F}_0^{'}, \mathbf{F}_j^{'}), \quad R_k = \sum_{j=1, j\neq k}^{n} M_{K_2}^{c\sigma_{\hat{\mathbf{F}}}(\mathbf{F}_0)}(\mathbf{F}_k^{'}, \mathbf{F}_j^{'}) \quad (8.12)$$

for the $SDF_{\sigma_{\hat{\mathbf{F}}}}$.

In order to define an analogous filter using a fuzzy distance combining the magnitude and the directional criteria, an intuitive approach may consist of joining the fuzzy magnitude distance and the fuzzy directional distance by using an appropriate mean. Since M_K^{α} is a fuzzy metric with respect to the usual product in $[0, 1]$, the geometric mean between the fuzzy magnitude distance and the fuzzy directional distance seems to be appropriate. Notice that in this way it is obtained a unique fuzzy expression to simultaneously model the magnitude and directional criteria for each comparison between colour vectors (compare with [10]).

Therefore, we define two Local Self-Adaptive Directional-Distance Impulsive Vector Filters denoted by $SDDF_{\sigma_{\bar{\mathbf{F}}}}$ and $SDDF_{\sigma_{\hat{\mathbf{F}}}}$ using $\sigma_{\bar{\mathbf{F}}}$ and $\sigma_{\hat{\mathbf{F}}}$, respectively, as a modification of the FIVF, where

$$R_0 = \sum_{j=1}^{n} \sqrt{M_{K_1}^{c\sigma_{\bar{\mathbf{F}}}(\mathbf{F}_0)}(\mathbf{F}_0, \mathbf{F}_j) \cdot M_{K_2}^{c\sigma_{\bar{\mathbf{F}}}(\mathbf{F}_0)}(\mathbf{F}_0', \mathbf{F}_j')}, \quad (8.13)$$

$$R_k = \sum_{j=1\, j\neq k}^{n} \sqrt{M_{K_1}^{c\sigma_{\bar{\mathbf{F}}}(\mathbf{F}_0)}(\mathbf{F}_k, \mathbf{F}_j) \cdot M_{K_2}^{c\sigma_{\bar{\mathbf{F}}}(\mathbf{F}_0)}(\mathbf{F}_k', \mathbf{F}_j')} \quad (8.14)$$

in the case of the $SDDF_{\sigma_{\bar{\mathbf{F}}}}$, and,

$$R_0 = \sum_{j=1}^{n} \sqrt{M_{K_1}^{c\sigma_{\hat{\mathbf{F}}}(\mathbf{F}_0)}(\mathbf{F}_0, \mathbf{F}_j) \cdot M_{K_2}^{c\sigma_{\hat{\mathbf{F}}}(\mathbf{F}_0)}(\mathbf{F}_0', \mathbf{F}_j')}, \quad (8.15)$$

$$R_k = \sum_{j=1\, j\neq k}^{n} \sqrt{M_{K_1}^{c\sigma_{\hat{\mathbf{F}}}(\mathbf{F}_0)}(\mathbf{F}_k, \mathbf{F}_j) \cdot M_{K_2}^{c\sigma_{\hat{\mathbf{F}}}(\mathbf{F}_0)}(\mathbf{F}_k', \mathbf{F}_j')} \quad (8.16)$$

in the case of the $SDDF_{\sigma_{\hat{\mathbf{F}}}}$.

The proposed filters suitability will be assessed in the following section by presenting some experimental results for comparison in front of some classical vector filters and some recently introduced vector filters.

8.4 Experimental Results and Assessment

For the evaluation of the filters proposed in Section 8.3, two types of impulsive noise have been used to simulate different distortions which may corrupt colour images [27, 31]. Let $\mathbf{F} = \{F_R, F_G, F_B\}$ be the original pixel, let $\mathbf{F}^*$ denote the pixel corrupted by the noise process and suppose that p is the probability of the noise appearance. Then, the two types of impulsive noise considered are defined as follows.

Table 8.1. Filters taken for performance comparison and notation.

Notation	**Filter**
VMF	Vector Median Filter [2]
BVDF	Basic Vector Directional Filter [**?**]
DDF	Directional Distance Filter [10]
FIVF	Fast Impulsive Noise Vector Filter [21]
SAMF	Switching Arithmetic Mean Filter [30]
AVMF	Adaptive Vector Median Filter [19]
MAVMF	Modified Adaptive Vector Median Filter[19]
$SMF_{\sigma_{\bar{\mathbf{F}}}}$	Local Self-Adaptive Magnitude Impulsive Vector Filter using $\sigma_{\bar{\mathbf{F}}}$
$SMF_{\sigma_{\hat{\mathbf{F}}}}$	Local Self-Adaptive Magnitude Impulsive Vector Filter using $\sigma_{\hat{\mathbf{F}}}$
$SDF_{\sigma_{\bar{\mathbf{F}}}}$	Local Self-Adaptive Directional Impulsive Vector Filter using $\sigma_{\bar{\mathbf{F}}}$
$SDF_{\sigma_{\hat{\mathbf{F}}}}$	Local Self-Adaptive Directional Impulsive Vector Filter using $\sigma_{\hat{\mathbf{F}}}$
$SDDF_{\sigma_{\bar{\mathbf{F}}}}$	Local Self-Adaptive Distance Directional Impulsive Vector Filter using $\sigma_{\bar{\mathbf{F}}}$
$SDDF_{\sigma_{\hat{\mathbf{F}}}}$	Local Self-Adaptive Distance Directional Impulsive Vector Filter using $\sigma_{\hat{\mathbf{F}}}$

– I. Impulsive noise.
The image pixels are distorted according to the following scheme

$$\mathbf{F}^* = \begin{cases} \{d_1, F_G, F_B\} & \text{with probability } p \cdot p_1\,, \\ \{F_R, d_2, F_B\} & \text{with probability } p \cdot p_2\,, \\ \{F_R, F_G, d_3\} & \text{with probability } p \cdot p_3\,, \\ \{d_1, d_2, d_3\} & \text{with probability } p \cdot \left(1 - \sum_{i=1}^{3} p_i\right)\,. \end{cases} \tag{8.17}$$

where d_1, d_2, d_3 are independent and equal to 0 or 255 with equal probability, and $p_i, i = 1, 2, 3$ determine the probability of appearance of the noise in the image channels.
– II. Uniform noise.
$\mathbf{F}^* = \{d_1, d_2, d_3\}$ with probability p, where d_1, d_2, d_3 are random uniformly distributed independent integer values in the interval $[0, 255]$.

Now, in order to assess the performance of the proposed filter, the *Mean Absolute Error* (MAE), *Peak Signal to Noise Ratio* (PSNR) and *Normalized*

Table 8.2. Comparison of the performance measured in terms of MAE, PSNR and NCD using the Baboon image contaminated with different percentages of impulsive noise type I.

Filter	10% impulsive type I			25% impulsive type I		
	MAE	PSNR	NCD (10^{-2})	MAE	PSNR	NCD (10^{-2})
None	5.10	19.13	7.73	11.72	15.47	18.12
VMF	10.55	23.32	6.10	10.92	23.09	6.42
BVDF	12.58	21.20	6.33	14.02	20.22	7.13
DDF	10.48	23.17	5.61	11.26	22.68	6.15
FIVF	2.96	24.94	3.80	6.96	23.41	4.34
SAMF	3.77	25.68	2.19	5.76	24.36	3.78
AVMF	4.27	25.60	2.56	5.35	24.13	4.81
MAVMF	4.31	25.53	2.66	5.51	23.84	5.17
$SMF_{\sigma_{\bar{\mathbf{F}}}}$	4.46	24.67	2.73	6.07	23.75	4.56
$SMF_{\sigma_{\hat{\mathbf{F}}}}$	4.57	24.53	2.77	6.20	23.61	4.59
$SDF_{\sigma_{\bar{\mathbf{F}}}}$	2.56	26.38	1.56	5.80	22.08	3.40
$SDF_{\sigma_{\hat{\mathbf{F}}}}$	2.92	25.48	1.67	5.90	22.09	3.49
$SDDF_{\sigma_{\bar{\mathbf{F}}}}$	3.24	26.14	1.82	5.02	24.84	3.13
$SDDF_{\sigma_{\hat{\mathbf{F}}}}$	3.41	25.78	1.86	5.14	24.46	3.17

Table 8.3. Comparison of the performance measured in terms of MAE, PSNR and NCD using the Lenna image contaminated with different percentages of impulsive noise type II.

Filter	10% impulsive type II			20% impulsive type II		
	MAE	PSNR	NCD (10^{-2})	MAE	PSNR	NCD (10^{-2})
None	6.40	19.38	5.78	15.23	15.59	14.19
VMF	4.61	28.85	3.04	5.60	27.36	3.74
BVDF	4.71	28.33	2.84	6.33	25.79	3.81
DDF	4.44	28.88	2.77	5.47	27.35	3.53
FIVF	0.93	33.31	0.62	2.01	30.02	1.47
SAMF	0.88	34.92	0.50	1.98	30.97	1.25
AVMF	1.19	33.11	0.77	2.67	27.13	2.13
MAVMF	1.27	32.60	0.85	2.99	26.30	2.45
$SMF_{\sigma_{\bar{\mathbf{F}}}}$	0.96	33.22	0.61	2.12	29.66	1.54
$SMF_{\sigma_{\hat{\mathbf{F}}}}$	0.97	33.24	0.60	2.05	30.08	1.43
$SDF_{\sigma_{\bar{\mathbf{F}}}}$	0.79	34.26	0.48	2.17	28.89	1.39
$SDF_{\sigma_{\hat{\mathbf{F}}}}$	0.78	34.25	0.48	2.09	29.22	1.31
$SDDF_{\sigma_{\bar{\mathbf{F}}}}$	0.80	34.54	0.50	1.92	30.55	1.34
$SDDF_{\sigma_{\hat{\mathbf{F}}}}$	0.83	34.28	0.52	1.87	30.76	1.26

Colour Difference (NCD) [23, 31] have been used. These objective quality measures are defined as follows

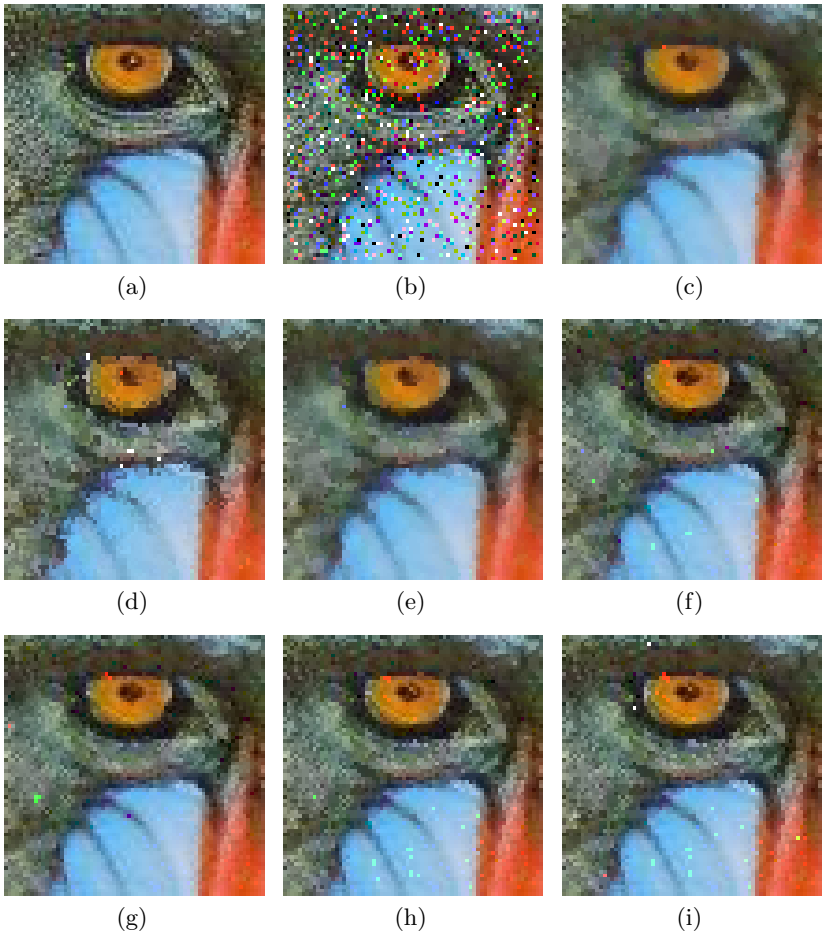

Fig. 8.1. Performance comparison: (a) Detail of Baboon image, (b) Detail of Baboon image with 25% impulsive noise type I, (c) VMF output, (d) BVDF output, (e) DDF output, (f) FIVF output, (g) SAMF output, (h) $SDDF_{\sigma_{\hat{\mathbf{F}}}}$ output, (i) $SDDF_{\sigma_{\hat{\mathbf{F}}}}$ output.

$$MAE = \frac{\sum_{i=1}^{N}\sum_{j=1}^{M}\sum_{q=1}^{Q}\left|F^q(i,j) - \hat{F}^q(i,j)\right|}{N \cdot M \cdot Q}, \tag{8.18}$$

$$PSNR = 20\log\left(\frac{255}{\sqrt{\frac{1}{NMQ}\sum_{i=1}^{N}\sum_{j=1}^{M}\sum_{q=1}^{Q}\left(F^q(i,j) - \hat{F}^q(i,j)\right)^2}}\right), \tag{8.19}$$

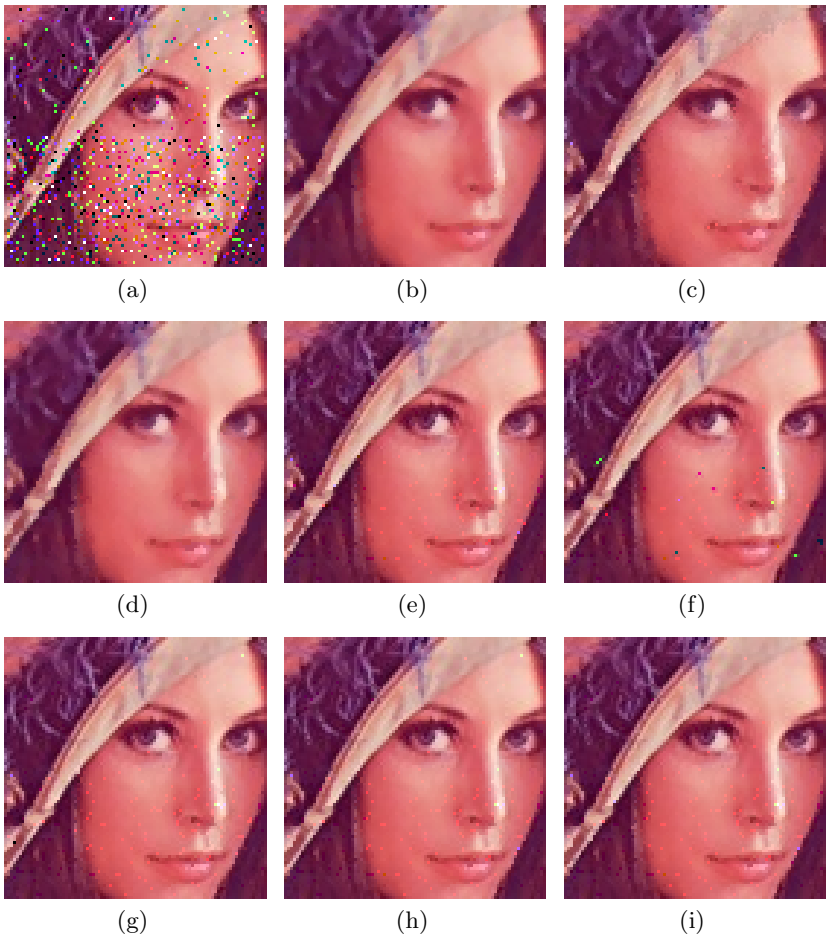

Fig. 8.2. Performance comparison: (a) Detail of Lenna image with 5% impulsive noise type I in the upper half and 25% impulsive noise type I in the lower half, (b) VMF output, (c) BVDF output, (d) DDF output, (e) FIVF output, (f) SAMF output, (g) $SDF_{\sigma_{\hat{\mathbf{F}}}}$ output, (h) $SDDF_{\sigma_{\hat{\mathbf{F}}}}$ output, (i) $SDDF_{\sigma_{\hat{\mathbf{F}}}}$ output.

where M, N are the image dimensions, Q is the number of channels of the image ($Q = 3$ for colour image), and $F^q(i,j)$ and $\hat{F}^q(i,j)$ denote the q^{th} component of the original image vector and the filtered image, at pixel position (i,j), respectively, and

$$NCD_{Lab} = \frac{\sum_{i=1}^{N}\sum_{j=1}^{M} \Delta E_{Lab}}{\sum_{i=1}^{N}\sum_{j=1}^{M} E^*_{Lab}} \tag{8.20}$$

Table 8.4. Comparison of the performance measured in terms of MAE, PSNR and NCD using the Microscopic image contaminated with different percentages of impulsive noise type I.

Filter	10% impulsive type I			20% impulsive type I		
	MAE	PSNR	NCD (10^{-2})	MAE	PSNR	NCD (10^{-2})
None	3.28	20.29	4.40	8.94	15.89	11.91
VMF	4.76	29.32	4.30	5.10	28.86	4.63
BVDF	6.03	26.70	5.01	6.64	26.15	5.46
DDF	4.77	29.30	4.07	5.12	28.71	4.41
FIVF	0.68	34.79	0.95	1.81	31.31	1.75
SAMF	0.58	36.46	0.76	1.47	32.57	1.66
AVMF	1.18	33.78	1.08	1.93	30.67	2.12
MAVMF	1.27	33.32	1.17	1.97	30.29	2.33
$SMF_{\sigma_{\bar{\mathbf{F}}}}$	0.66	35.13	0.84	1.60	31.44	1.87
$SMF_{\sigma_{\hat{\mathbf{F}}}}$	0.71	34.69	0.87	1.58	31.69	1.86
$SDF_{\sigma_{\bar{\mathbf{F}}}}$	0.60	34.03	0.63	1.93	27.43	1.91
$SDF_{\sigma_{\hat{\mathbf{F}}}}$	0.55	35.55	0.59	1.98	27.37	1.99
$SDDF_{\sigma_{\bar{\mathbf{F}}}}$	0.51	37.70	0.56	1.46	32.28	1.56
$SDDF_{\sigma_{\hat{\mathbf{F}}}}$	0.57	36.80	0.58	1.47	32.38	1.57

Table 8.5. Comparison of the performance measured in terms of MAE, PSNR and NCD using the Lenna image contaminated with 5% of impulsive noise type I in the upper half and 25% of impulsive noise type I in the lower half.

Filter	MAE	PSNR	NCD (10^{-2})
None	7.22	17.53	10.22
VMF	4.43	29.16	2.95
BVDF	5.03	27.98	3.03
DDF	4.69	28.66	2.93
FIVF	1.59	31.04	1.32
SAMF	1.45	30.84	1.30
AVMF	1.71	29.99	1.66
MAVMF	1.85	29.04	1.90
$SMF_{\sigma_{\bar{\mathbf{F}}}}$	1.42	31.25	1.35
$SMF_{\sigma_{\hat{\mathbf{F}}}}$	1.39	31.45	1.30
$SDF_{\sigma_{\bar{\mathbf{F}}}}$	1.18	32.72	1.00
$SDF_{\sigma_{\hat{\mathbf{F}}}}$	1.16	32.94	1.03
$SDDF_{\sigma_{\bar{\mathbf{F}}}}$	1.18	32.74	1.07
$SDDF_{\sigma_{\hat{\mathbf{F}}}}$	1.28	32.02	1.15

where $\Delta E_{Lab} = [(\Delta L^*)^2 + (\Delta a^*)^2 + (\Delta b^*)^2]^{\frac{1}{2}}$ denotes the perceptual colour error and $E^*_{Lab} = [(L^*)^2 + (a^*)^2 + (b^*)^2]^{\frac{1}{2}}$ is the *norm* or *magnitude* of the original image colour vector in the $L^*a^*b^*$ colour space.

The proposed filters are assessed in front of the classical vector filters and recently introduced adaptive vector filters for impulsive noise removal with

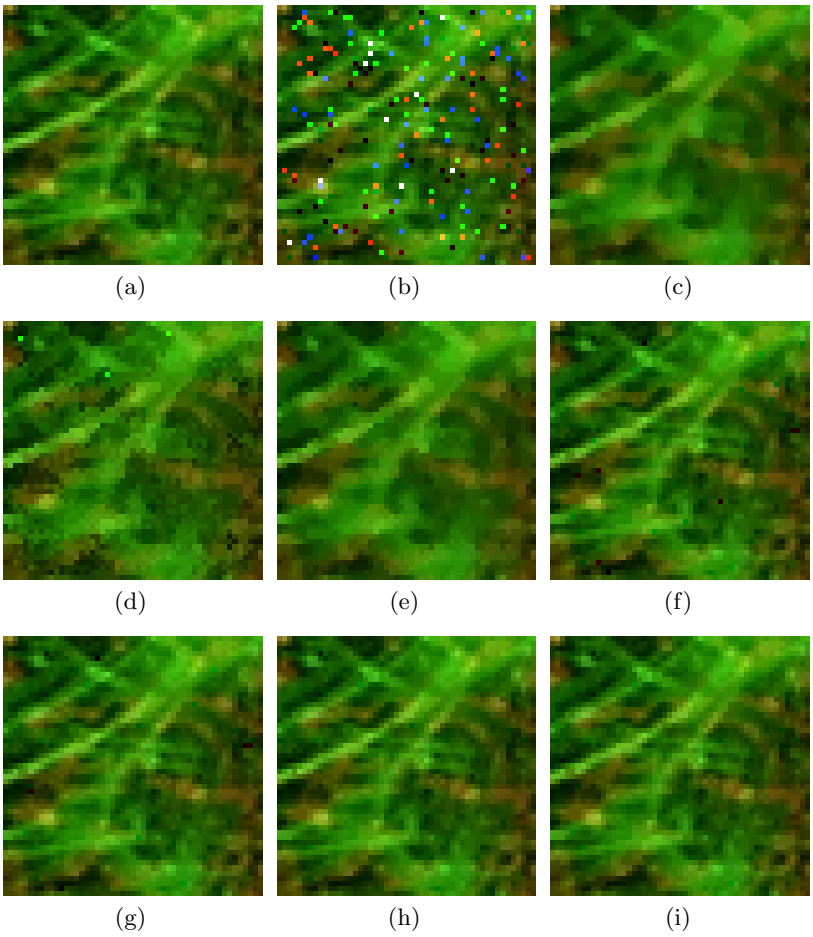

Fig. 8.3. Performance comparison: (a) Detail of Microscopic image, (b) Detail of Microscopic image with 10% impulsive noise type I, (c) VMF output, (d) BVDF output, (e) DDF output, (f) FIVF output, (g) SAMF output, (h) $SDDF_{\sigma_{\hat{\mathbf{F}}}}$ output, (i) $SDDF_{\sigma_{\hat{\mathbf{F}}}}$ output.

good detail preserving ability in Table 8.1. Several test images contaminated with different densities of impulsive noise types I and II, have been used.

Some performance results for comparison are shown in Tables 8.2-8.5 and Figures 8.1-8.3. The results show that the presented technique outperforms classical vector filters and recently introduced vector filters presenting the advantage of being self-adaptive. The self-adaptive mechanism can be considered suitable since the images were contaminated with both low and high densities of impulsive noise and the performance is good in all the cases.

In general, the proposed filters best results correspond to the $SDDF_{\sigma_{\bar{\mathbf{F}}}}$ and $SDDF_{\sigma_{\hat{\mathbf{F}}}}$. The *multivariate dispersion* estimation based on the vector median $\hat{\mathbf{F}}$ is more useful than the one using the vector mean $\bar{\mathbf{F}}$ when dealing with impulsive noise type II. However, in general, the performance using the vector mean $\bar{\mathbf{F}}$ or the vector median $\hat{\mathbf{F}}$ to estimate the *multivariate dispersion* are similar, so it is rather preferred to use the vector mean $\bar{\mathbf{F}}$ since in this case the computational cost of the filtering process is lower.

The proposed filters are specially useful for two wide classes of images thank to their local adaptive nature. The first class corresponds to highly non-homogeneous images, with many textures and edges, since the use of distinct values of the adjusting parameter is necessary in different parts of the image (as can be seen for the Baboon image in Table 8.2 and Figure 8.1). The second class corresponds to images where the contaminating impulsive noise is not uniformly distributed along the image. In fact, this situation may occur, for instance, when the noise appears with more intensity in an interval of the transmission process. The filter performances in these cases are depicted in Table 8.5 and Figure 8.2 where the detail of the Lenna image has been contaminated with different densities of noise in its upper half and its lower half. In such cases, obviously, local adaptive methods may present better performance than those methods which use the same value of the adjusting parameter to filter the hole image.

Conclusions

In this paper, a local self-adaptive filter structure using a fuzzy metric has been introduced. The proposed filter is based on a recently introduced technique for impulsive noise removal with good detail-preserving ability and nice computational cost.

Fuzzy metrics are specially useful within this technique since the use of a fuzzy metric has allowed to create a local self-adaptive filter structure and to extend it to the use of fuzzy magnitude distances, fuzzy directional distances and combined fuzzy magnitude-directional distances in a straightforward way.

The proposed filters are able to remove impulsive noise of different types and densities from colour images presenting a good balance between noise suppression and detail-preserving and they are easy to use due to their self-adaptive nature. Since the proposed filters perform well for low and high densities of impulsive noise, the self-adaptive mechanism may be considered suitable. Furthermore, the local adaptiveness allows to perform well in highly non-homogeneous images and in images where the density of contaminating noise is distinct in different parts of the image. This local adaptiveness is approached by using an estimated *multivariate dispersion* of the pixels with respect to the vector mean or to the vector median of its neighborhood. So, when the estimated dispersion is higher, the conditions to keep the original pixel are less demanding and the likelihood to substitute the pixel increases.

References

1. K. Arakawa, Median filter based on fuzzy rules and its application to image restoration, *Fuzzy Sets and Systems* 77 1 (1996) 3-13.
2. J. Astola, P. Haavisto, Y. Neuvo, Vector Median Filters, *Proc. IEEE.* 78 4 (1990) 678-689.
3. J. Camacho, S. Morillas, P. Latorre, Efficient impulsive noise suppression based on statistical confidence limits, *Journal of Imaging Science and Technology*, to appear.
4. H.A. David, *Order Statistics* (John Wiley and Sons, New York, 1981)
5. R. Garnett, T. Huegerich, C. Chui, W. He, A universal noise removal algorithm with an impulse detector, *IEEE Transactions on Image Processing* 14 11 (2005) 1747-1754.
6. A. George, P. Veeramani, On Some results in fuzzy metric spaces, *Fuzzy Sets and Systems* 64 3 (1994) 395-399.
7. V. Gregori, S. Romaguera, Some properties of fuzzy metric spaces, *Fuzzy Sets and Systems* 115 3 (2000) 477-483.
8. V. Gregori, S. Romaguera, Characterizing completable fuzzy metric spaces, *Fuzzy Sets and Systems* 144 3 (2004) 411-420.
9. P.S. Huber, *Robust Statistics* (John Wiley and Sons, New York, 1981)
10. D.G. Karakos, P.E. Trahanias, Generalized multichannel image-filtering structure, *IEEE Transactions on Image Processing* 6 7 (1997) 1038-1045.
11. L. Khriji, M. Gabbouj, Adaptive fuzzy order statistics-rational hybrid filters for color image processing, *Fuzzy Sets and Systems* 128 1 (2002) 35-46.
12. L. Khriji, M. Gabbouj, Adaptive fuzzy order statistics-rational hybrid filters for color image processing, *Fuzzy Sets and Systems*, 128 1 (2002) 35-46.
13. R. Lukac, B. Smolka, K.N. Plataniotis, A.N. Venetsanopoulos, Selection weighted vector directional filters, *Computer Vision and Image Understanding* 94 (2004) 140-167.
14. R. Lukac, Adaptive vector median filtering, *Pattern Recognition Letters* 24 12 (2003) 1889-1899.
15. R. Lukac, B. Smolka, K. Martin, K.N. Plataniotis, A.N. Venetsanopoulos, Vector Filtering for Color Imaging, *IEEE Signal Processing Magazine, Special Issue on Color Image Processing* 22 1 (2005) 74-86.
16. R. Lukac, K.N. Plataniotis, B. Smolka, A.N. Venetsanopoulos, cDNA Microarray Image Processing Using Fuzzy Vector Filtering Framework, *Fuzzy Sets and Systems: Special Issue on Fuzzy Sets and Systems in Bioinformatics* 152 1 (2005) 17-35.

17. R. Lukac, K.N. Plataniotis, B. Smolka, A.N. Venetsanopoulos, Generalized Selection Weighted Vector Filters, *EURASIP Journal on applied signal processing: Special Issue on Nonlinear signal and image processing* 12 (2004) 1870-1885.
18. R. Lukac, Adaptive Color Image Filtering Based on Center Weighted Vector Directional Filters, *Multidimensional Systems and Signal Processing* 15 (2004) 169-196.
19. R. Lukac, K.N. Plataniotis, A.N. Venetsanopoulos, B. Smolka, A Statistically-Switched Adaptive Vector Median Filter, *Journal of Intelligent and Robotic Systems* 42 (2005) 361-391.
20. S. Morillas, V. Gregori, G. Peris-Fajarnés, P. Latorre, A new vector median filter based on fuzzy metrics, *ICIAR 2005, Lecture Notes in Computer Science* 3656 (2005) 81-90.
21. S. Morillas, V. Gregori, G. Peris-Fajarnés, P. Latorre, A fast impulsive noise color image filter using fuzzy metrics, *Real-Time Imaging* 11 5-6 (2005) 417-428.
22. S. Morillas, Fuzzy metrics and peer groups for impulsive noise removal in color image, *in Proc. of European Signal Processing Conference EUSIPCO 2006* Florence, Italy 2006.
23. K.N. Plataniotis, A.N. Venetsanopoulos, *Color Image processing and applications* (Springer-Verlag, Berlin, 2000).
24. A. Sapena, A contribution to the study of fuzzy metric spaces, *Appl. Gen. Topology* 2 1 (2001) 63-76.
25. Y. Shen, K.E. Barner, "Fuzzy Vector Median Based Surface Smoothing", *IEEE Transactions on Visualization and Computer Graphics*, 10 3 (2004) 252-265.
26. B. Smolka,K.N. Plataniotis, R. Lukac, A.N. Venetsanopoulos, Similarity based impulsive noise removal in color images, *International Conference on Image Processing ICIP 2003* .
27. B. Smolka, R. Lukac, A. Chydzinski, K.N. Plataniotis, W. Wojciechowski, Fast adaptive similarity based impulsive noise reduction filter, *Real-Time Imaging* 9 4 (2003) 261-276.
28. B. Smolka, A. Chydzinski, K.N. Plataniotis, A.N. Venetsanopoulos, New filtering technique for the impulsive noise removal in color images, *Mathematical Problems in Engineering* 1 (2004) 79-91.
29. B. Smolka, K.N. Plataniotis, A. Chydzinski, M. Szczepanski, A.N. Venetsanopoulos, K. Wojciechowski, Self-adaptive algorithm of impulsive noise reduction in color images, *Pattern Recognition* 35 8 (2002) 1771-1784.
30. B. Smolka, A. Chydzinski, Fast detection and impulsive noise removal in color images, *Real-Time Imaging* 11 (2005) 389-402.
31. M. Szczepanski, B. Smolka, K.N. Plataniotis, A.N. Venetsanopoulos, On the distance function approach to color image enhancement, *Discrete Applied Mathematics* 139 (2004) 283-305.
32. C. Tomasi, R. Manduchi, Bilateral filtering for gray and color images, *in Proc. IEEE Int. Conf. Computer Vision* (1998) 839-846.
33. P.E. Trahanias, D. Karakos, A.N. Venetsanopoulos, Directional processing of color images: theory and experimental results, *IEEE Trans. Image Process.* 5 6 (1996) 868-880.
34. H.H. Tsai, P.T. Yu, Genetic-based fuzzy hybrid multichannel filters for color image restoration, *Fuzzy Sets and Systems* 114 2 (2000) 203-224.

9 Contribution (vi)

S. Morillas, V. Gregori, G. Peris-Fajarnés, A. Sapena, New adaptive vector filter using fuzzy metrics, *accepted for publication in Journal of Electronic Imaging*

Abstract

Classical nonlinear vector median-based filters are well-known methods for impulsive noise suppression in colour images but mostly they lack good detail-preserving ability. In this paper a class of fuzzy metrics is used to introduce a vector filter aimed at improving the detail-preserving ability of classical vector filters while effectively removing impulsive noise. The main idea behind the proposed method is that the output pixel for a given filter window will be the one which best fulfills two criteria: to be *similar in signal value* and to be *spatially close* to all the other pixels in the filter window. The use of fuzzy metrics allows to simultaneously handle both criteria. The filter is designed so that the importance of the spatial criterion can be adjusted. It is shown that the filter can adapt to the density of the contaminating noise by adjusting the spatial criterion importance. Classical and recent filters are used to assess the proposed filtering. The experimental results show that the proposed technique exhibits a competitive performance.

9.1 Introduction

Nonlinear vector filters based on the theory of robust statistics [9] commonly use the reduced ordering principle amongst vectors in a predefined sliding window [20, 34] because this ordering takes into account the existing correlation amongst the image channels. The reduced ordering commonly identifies outliers of the population in the highest ranks and therefore, the filter output is defined as the lowest ranked vector. Building on the concept of robust order statistics, numerous filters, with a detailed overview to be found in [20, 34, 21], have been proposed. Within this context, the *vector median filter* (VMF) [4] uses the L_1 (city-block) or L_2 (Euclidean) metrics as the distance function between colour vectors. The VMF concept has been extended to the directional domain by using the angular distance in the *basic vector directional*

filter BVDF [44]. The work in [46] defines a different vector median operation using a conditional ordering in the Hue-Saturation-Value (HSV) colour space.

The traditional vector filters described above have the disadvantage of being designed to perform a fixed amount of smoothing which sometimes leads to insufficient signal preservation [20]. To avoid this drawback, the filters introduced in [22]-[25] make use of different weighting coefficients to preserve the original signal structures, such as edges and fine details. The approaches in [2]-[6] propose switching methods where only pixels identified by the impulse detection procedure are filtered. In order to detect the noisy pixels [2] checks the cluster membership of each pixel after a cluster analysis of its neighborhood. The work in [26] performs a deviation test with respect to the set of a few lowest ranked vectors. The methods in [27, 28] use approximation of the multivariate dispersion, and the technique in [6] is based on computing the confidence limits extracted from the neighborhood assuming a multi-normal distribution of the colour vectors. In [39]-[33] a special vector ordering procedure that increases the probability of the filter window central pixel to be the filter output is used. This fact reduces the number of unnecessary substitutions and improves the detail-preserving ability of the filtering. The method in [30] analyzes similarities between the neighboring colour vectors in a two-step impulse detection procedure. A three-step procedure including robust estimation, vector partition and weighted filtering has been recently introduced in [31]. The methods in [32]-[45] propose to simultaneously use several sub-filters in each image location and the filter output is computed by choosing the most appropriate sub-filter output [32] or by fusing the sub-filter outputs using a rational function [16, 17] or a genetic algorithm [45]. Recently, a class of chromatic filters has been proposed to achieve better chromatic smoothness [19]. Additionally, other good detail-preserving methods for impulsive noise have been recently introduced in [41]-[7]. On the other hand, also different fuzzy approaches have been proposed in the literature [8]-[29]. The scalar and vector median operations are extended to fuzzy numbers in [8]. In [3] and [14] a fuzzy rule based system determines the filter output. The vector median and some fuzzy measures are used in [36, 37, 38] for calculating the fuzzy coefficients to determine the output as a weighted average of the inputs. The work in [43] computes the fuzzy coefficients taking into account spatial and value nearness relations between pixels, and the inclusion of an impulse detector in this procedure is addressed in [10]. In [29] fuzzy coefficients determine the filter output by selecting the most representative input vector or as the combination of the vectors inside the filter window.

In this paper we propose to use a fuzzy metric as the distance criterion to perform the reduced ordering of the vectors in the filter window. This fuzzy metric for comparing two pixels will simultaneously handle two criteria: the *value similarity* between the colour vectors and the *spatial closeness* of the

pixels in the image. The inclusion of the spatial closeness criterion in the distance measure is the main novelty presented in the paper. Unlike the approaches in [43, 10] which perform fuzzy weighted averaging, the method proposed in this paper uses fuzzy metrics to order the input vectors. Hence, the output of the filtering process is the vector which is simultaneously the most *similar in value* and *spatially close* to all the other vector pixels in the filter window. Moreover, by adjusting the spatial criterion importance, the proposed filter adapts to the density of impulsive noise in the image.

The paper is organized as follows. In Section 9.2 the fuzzy metric approach is introduced. Section 9.3 describes the proposed filter. Experimental study and performance comparison are shown in Section 9.4. Finally, Section 9.5 presents the conclusions.

9.2 A Fuzzy Metric Approach

Let X be a non-empty set. A function $M(x, y, t)$ defined on $X \times X \times]0, +\infty[$ with values in $]0, 1]$ is called a fuzzy metric [11, 12] if it is symmetric with respect to x and y, continuous on t and it satisfies the following conditions for all $x, y, z \in X$ and $t, s > 0$:

$(FM1)$ $M(x, y, t) = 1$ if and only if $x = y$

$(FM2)$ $M(x, z, t + s) \geq M(x, y, t) \cdot M(y, z, s)$

$M(x, y, t)$ represents the degree of nearness, or similarity, of x and y with respect to t. Fuzzy metrics behave *similarly* to classical metrics [12] since, as classical metrics take values in the interval $[0, \infty[$, M takes values in $]0, 1]$. M is called stationary, [13], if it does not depend on t and in such a case we write $M(x, y)$ instead of $M(x, y, t)$.

In the following we aim at measuring the *fuzzy value similarity* between colour vectors. Consider the function R given by

$$R(\mathbf{F_i}, \mathbf{F_j}) = \frac{C}{C + ||\mathbf{F_i} - \mathbf{F_j}||} \tag{9.1}$$

where $|| \cdot ||$ denotes the vector norm, C is a positive real parameter used to control the spread of the function, X is the set $\{0, 1, \ldots, 255\}$ and $\mathbf{F_k} = (F^1_{\mathbf{k}}, F^2_{\mathbf{k}}, F^3_{\mathbf{k}})$ represents the colour vector of the image pixel at position $\mathbf{k}$ comprising its R, G and B components. From [11] Example 2.9, R is a stationary fuzzy metric on X^3. Notice that various fuzzy metrics, such as those listed in [11], could be used instead of R in the same conditions.

The influence of the value of C is illustrated in FIG. 9.1. Using a low value of C reduces the value of R to 0 too quickly as the Euclidean distance increases. On the other hand, if a high value is used the value of R decreases too slowly. So intermediate values of C are more adequate. Hence, in the case of the L_2 metric any value of C in $[50, 250]$ can be used without significantly affecting the filter performance while values out of the interval are less appropriate.

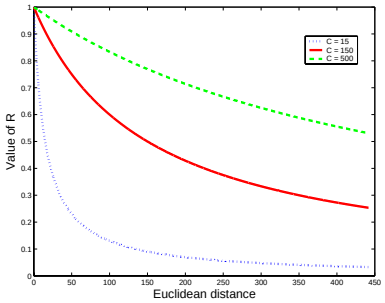

Fig. 9.1. Behavior of R for different values of C as a function of the Euclidean distance between the colour vectors.

For the case of *fuzzy spatial closeness* between pixels, let us consider the pixels in a $n \times n$ filter window W represented in Cartesian coordinates and so, denote by $\mathbf{i} = (i_1, i_2) \in Y^2$ the position of a pixel $\mathbf{F_i}$ in W where $Y = \{0, 1, \ldots, n-1\}$. We consider the *standard fuzzy metric* S deduced from the L_∞ metric ([11] Remark 2.10) given by $S(\mathbf{i}, \mathbf{j}, t) = \frac{t}{t+||\mathbf{i}-\mathbf{j}||_\infty}$ where $\mathbf{i}, \mathbf{j} \in Y^2$, $t > 0$ and $||\ ||_\infty$ is the L_∞ metric given by $||\mathbf{i}-\mathbf{j}||_\infty = max\{|i_1 - j_1|, |i_2 - j_2|\}$. We propose that all neighbors in a 3×3 neighborhood (and analogously for further neighborhoods) should receive the same closeness degree with respect to the central pixel. To achieve this we have used the L_∞ metric between the pixel positions $\mathbf{i}, \mathbf{j}$. Hence, some experiments have shown that this approach provides better results than the usage of the Euclidean metric which is proposed in [43, 10]. Then, $S(\mathbf{i}, \mathbf{j}, t)$ measures the *fuzzy spatial closeness* between the colour pixels $\mathbf{F_i}$ and $\mathbf{F_j}$ with respect to t. The parameter t is used to adjust the importance given to the *spatial closeness* criterion.

Now, since each pixel is represented as a three-component RGB colour vector occupying some location in the filter window, for our purpose we will consider a fuzzy metric combining R with S. So, the following function is proposed:

$$CFM(\mathbf{F_i}, \mathbf{F_j}, t) = R(\mathbf{F_i}, \mathbf{F_j}) \cdot S(\mathbf{i}, \mathbf{j}, t) = \frac{C}{C + ||\mathbf{F_i} - \mathbf{F_j}||} \cdot \frac{t}{t + ||\mathbf{i} - \mathbf{j}||} \quad (9.2)$$

If we identify each pixel $\mathbf{F_i}$ with $(F_\mathbf{i}^1, F_\mathbf{i}^2, F_\mathbf{i}^3, i_1, i_2)$ then from [35] Proposition 3.5 it can be proved that CFM is a fuzzy metric on $X^3 \times Y^2$. This fuzzy metric is used to simultaneously model the *value similarity* and *spatial closeness* criteria commented in Section 9.1. Notice the main novelty presented in this paper is that the measure used to perform the vector ordering includes a *spatial closeness* criterion. It is possible to find expressions different from the fuzzy metrics used in this paper to simultaneously model these criteria. In this paper we have preferred the use of fuzzy metrics for three main reasons: First they present a strong axiomatic system which is very close to the one of the

classical metrics; second, two fuzzy metrics can be joined in a straightforward way since both take values in the same interval $]0,1]$; third, the value given by any fuzzy metric $M(x,y,t)$ can be considered as the *certainty degree* of a fuzzy logic proposition and then the product of two fuzzy metrics corresponds to the *certainty degree* of the fuzzy connector *AND* (when the product t-norm is chosen instead of the minimum t-norm), which might be useful in many applications.

9.3 Proposed filtering

The scheme of a vector ordering procedure based on the reduced ordering principle [34] can be described as follows.

For simplicity, we denote by $\mathbf{F}_q, q = 0, 1, \ldots, n^2-1$ the n^2 colour vectors in W. The *distance* and *similarity* between two vectors $\mathbf{F}_i, \mathbf{F}_j$ is denoted as $\rho(\mathbf{F}_i, \mathbf{F}_j)$ (The interested reader may find the most common distance and similarity measures used in the field in the overview made in [20].). For each vector $\mathbf{F}_k$ in the filter window, an accumulated measure $R_k = \sum_{j=0, j\neq k}^{n^2-1} \rho(\mathbf{F}_k, \mathbf{F}_j)$ to all the other vectors in the window has to be calculated to perform the reduced ordering [20, 34]. The R_k values are ordered in an ascending sequence (in which the value located in the *r-th* position is written as $R_{(r)}$) as follows: $R_{(0)} \leq R_{(1)} \leq ... \leq R_{(n^2-1)}$. This order implies the same ordering of the $\mathbf{F}_k$'s vectors: $\mathbf{F}_{(0)} \leq \mathbf{F}_{(1)} \leq ... \leq \mathbf{F}_{(n^2-1)}$.

The proposed method uses the fuzzy metric CFM as the ρ function. Since according to (FM1) the associated measure must be maximized, the filter output will be the vector $\mathbf{F}_{(n^2-1)}$ occupying the highest rank in the ordered sequence. Note that the t parameter allows to adjust the importance of the spatial criterion. When $t \to \infty$ the spatial criterion is not taken into account and the proposed filter will behave as a classical VMF. For lower values of t, increasing the size of the filter window does not increase too much the smoothing performed. The pixels far from the central pixel help deciding the filter output but, actually, they are not likely to be the filter output as they are not *spatially close* to all the other pixels in the window. Hence, mostly one of the pixels *spatially close* to the central pixel will be the filter output independently of the filter window size. Example in FIG. 9.2 illustrates this behavior. Furthermore, in the extreme case when $t \to 0$ the filter will approach the identity operation. The value of t should be determined to find an appropriate balance between the VMF operation and the identity operation so, it seems intuitive to determine the value of t according to the density of contaminating noise.

It can be easily noticed that the order of computational complexity of proposed method and the VMF is the same. Both methods use the same ordering procedure and the number of needed distance calculations is the

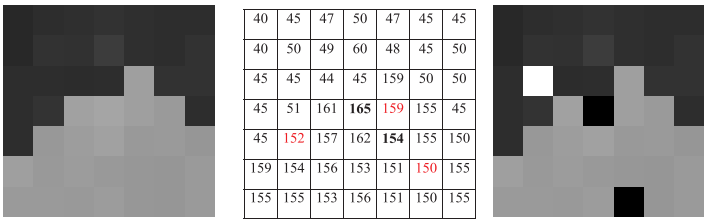

(a)

40	45	47	50	47	45	45
40	50	49	60	48	45	50
45	45	44	45	159	50	50
45	51	161	**165**	159	155	45
45	152	157	162	**154**	155	150
159	154	156	153	151	150	155
155	155	153	156	151	150	155

(b)

(c)

40	45	47	50	47	45	45
40	50	49	60	48	45	50
45	255	44	45	159	50	50
45	51	161	0	159	155	45
45	152	157	**162**	**154**	155	150
159	154	156	153	151	150	155
155	155	153	156	0	150	155

(d)

Outputs	**Median**	**CFM**
(a-b) 3x3	159	**165**
(a-b) 5x5	152	**165**
(a-b) 7x7	150	**154**
(c-d) 3x3	157	**162**
(c-d) 5x5	152	**162**
(c-d) 7x7	60	**154**

(e)

Fig. 9.2. Example of the proposed procedure. (a),(b) Sample of an edge in a gray-scale image (used for simplicity) and (c), (d) the result after adding some impulses. We have computed the outputs of processing the central pixel (165) using the median filter (in red colour) and the CFM filter (with $C = 150, t = 1.5$, in bold font) using filter windows of size 3×3, 5×5 and 7×7. The outputs are summarized in the table (e). Similar results are obtained for similar t values.

same. However, the CFM function is a little more computationally demanding than the L_1 or L_2 metrics commonly used by the VMF. This drawback could be alleviated by using some *look-up tables* for the calculation of S. This makes the CFM filter perform a little bit slower than the VMF but within the same complexity order.

9.4 Experimental Study and Performance Comparison

First in this section, we study the influence of the t parameter in the filter performance. For this, the test images in FIG. 9.3 were corrupted with impulsive noise. We consider the following two impulsive noise models for RGB images [34].

Let $\mathbf{F} = \{F_R, F_G, F_B\}$ be the original pixel, let $\mathbf{F}^*$ denote the pixel corrupted by the noise process and suppose that p is the probability of noise appearance. Then, the two types of impulsive noise considered are defined as follows.

– I. Fixed-value impulsive noise.
The image pixels are distorted according to the following scheme

$$\mathbf{F}^* = \begin{cases} \{d_1, F_G, F_B\} \text{ with probability } p \cdot p_1 \,, \\ \{F_R, d_2, F_B\} \text{ with probability } p \cdot p_2 \,, \\ \{F_R, F_G, d_3\} \text{ with probability } p \cdot p_3 \,, \\ \{d_1, d_2, d_3\} \quad \text{with probability } p \cdot \left(1 - \sum_{i=1}^{3} p_i\right) \,. \end{cases} \tag{9.3}$$

where d_1, d_2, d_3 are independent and equal to 0 or 255 with equal probability, and p_i for $i = 1, 2, 3$ determine the probability of appearance of the noise in the image channels.

– II. Random-value impulsive noise.
$\mathbf{F}^* = \{d_1, d_2, d_3\}$ with probability p, where d_1, d_2, d_3 are random integer values uniformly distributed in $[0, 255]$.

The *Mean Absolute Error* (MAE), *Peak Signal to Noise Ratio* (PSNR) and *Normalized Colour Difference* (NCD) objective quality measures as defined in [34] have been used to evaluate the filtering.

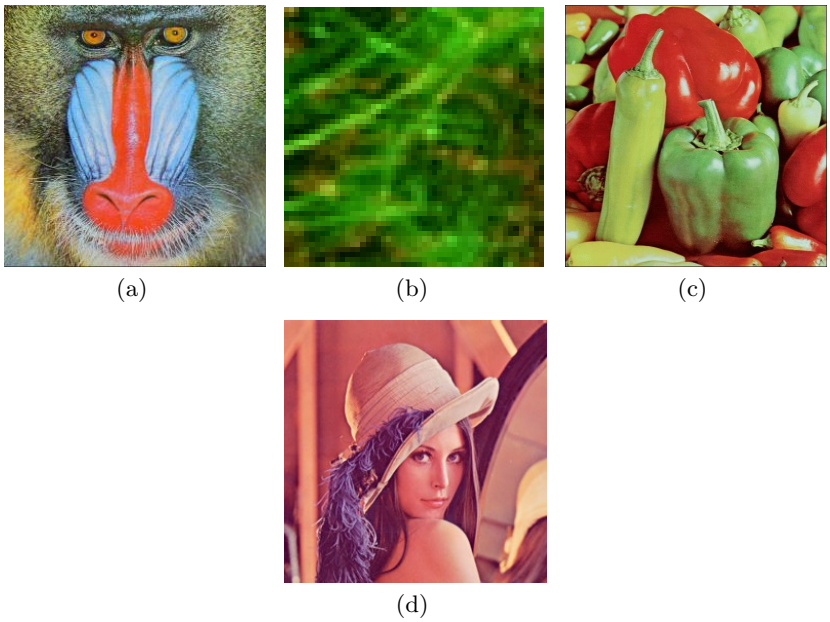

(a) (b) (c)

(d)

Fig. 9.3. Test images: (a) Mandrill image (256 × 256), (b) Detail of a microscopic image, (c) Peppers image (256 × 256), (d) Lenna image (256 × 256).

First we study the importance of the filter window size. We have experimentally found that the 3 × 3 size is the most appropriate one when the image is corrupted with a low impulsive noise percentage (< 40% approx.). For medium noise percentages (between 40% and 60%) a 5 × 5 size is more appropriate. And, for high noise densities (> 60%) a 7 × 7 filtering window

is rather preferred. FIG. 9.4 (a) shows these results. Notice that the larger window size the more important the spatial criterion is.

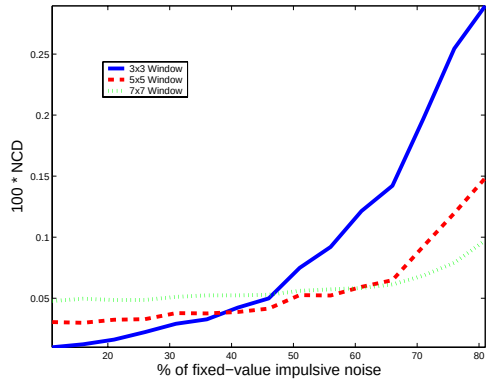

(a)

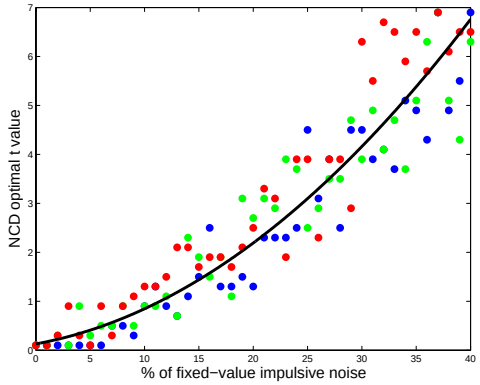

(b)

Fig. 9.4. (a) Performance of the proposed filter in terms of NCD for different window sizes and optimal t values: 3×3 (blue solid line), 5×5 (red dashed line), 7×7 (green dotted line), on the Peppers image contaminated with different densities of fixed-value impulsive noise. (b) NCD optimal t values in the CFM filter for different percentages of noise where blue points correspond to Baboon, green points to Micro, red points to Peppers and black line to the adjusting function

Second, the filter performance has been assessed as a function of the t parameter in the CFM fuzzy metric in Eq. (9.2). As it is shown in FIG. 9.5 the intensity of the smoothing process and the performance presented by the filters depend on the value of the t parameter. For higher values of t the importance of the positional criterion in Eq. (9.2) is lower and the number of performed substitutions increases (FIG. 9.5 (a)). By analyzing the optimum

performance presented for each density of noise it is shown that the higher the density of the contaminating noise is, the higher the needed value of t (FIG. 9.5 (b),(c),(d)).

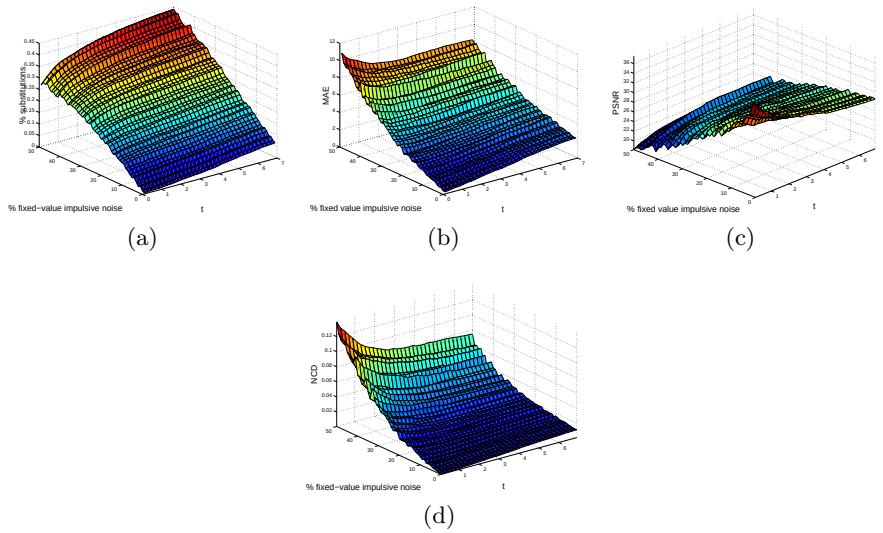

Fig. 9.5. (a) Percentage of substitutions, and performance in terms of (b) MAE, (c) PSNR and (d) NCD for the CFM filter, as a function of t and the percentage of impulsive noise contaminating the Peppers image.

In order to set the value of the t parameter we propose two different approaches. On the one hand, we have experimentally found that a value of $t = 4$ receives a good performance for many different images and noise densities. This value can be used when the density of the contaminating noise is unknown. On the other hand, as commented above, the value of t should be higher when the density of the contaminating noise is higher. So, we also propose to determine the value of t according to the density of contaminating noise. For this, the relation between the t parameter and the filter performance is investigated by means of the following regression study. The optimal value of t in terms of NCD is computed for each one of the test images Baboon, Micro and Peppers against varying the noise density from 0% to 40%. The optimal values are shown as the set of points in FIG. 9.4 (b). The correlation study is done over this set of points. Since the t parameter has the constraint of being a real positive value (see Section 9.2) we must use a function f such that $t = f(p) > 0, \forall p$. To address this we have considered the parabolic function $f(p) = (a + bp)^2$ that fulfills the mentioned condition and gives a good adjustment to the set of points. The adjusting function we have computed using the least squares method is $t = f(p) = (0.36{+}0.056p)^2$, which

is shown in FIG. 9.4 (b). The correlation coefficient is $r = 0.955$ and the 95% confidence intervals of the adjusting function parameters are $[0.32, 0.40]$ and $[0.052, 0.060]$ for a and b, respectively. The data may be considered properly adjusted since the correlation factor is high ($r > 0.95$). As a result, we define the CFM' function by replacing t in Eq. (9.2) by the computed adjusting function, i.e. $CFM'(\mathbf{F_i}, \mathbf{F_j}, t) = CFM(\mathbf{F_i}, \mathbf{F_j}, f(p))$. It can be proved that the function CFM' is also a fuzzy metric on $X^3 \times Y^2$. This proposed t parameter adjustment approach will be validated in the following using an image different from those used for the regression. In this way, it is possible to determine a suitable value of the t parameter from an estimated noise percentage of the input image.

Actually, the noise percentage may be quite accurately estimated using the technique described in [39, 40]. This method consists of detecting as noise all those pixels that do not have at least 2 neighbors in a 3×3 neighborhood at Euclidean distance lower or equal to D (typically, $D \in [50, 60]$). In the worst case, it has to compute 8 distances per pixel which is $\frac{2}{9}$ of the distances needed by the VMF. Moreover, this method does not need to run over the whole image. Using only 25% of the image could be enough to have a fast and quite accurate estimation. So, including this estimation would involve, as much, an additional number of distance calculations equal to $\frac{1}{18}$ of the distances in the VMF. So, the computational load is only increased in a 5.5% approx.

Finally in this section, the proposed filter is assessed in comparison to some classical and well-known vector filters: VMF [4], *Extended Vector Median Filter* (EVMF) [4], BVDF [44], *Weighted Multichannel Median Filter* (WMMF) [18], *Vector Median-Rational Hybrid Filter* (VMRHF) [16] and *Bilateral Filter* (BF) [43]; some recent vector filters with good detail-preserving ability named *Adaptive Switching Vector Median Filter* (ASVMF) [26], *Adaptive Vector Median Filter* (AVMF) [27], *t-Test Vector Median Filter* (tTVMF) [6], *Fast Impulsive Vector Filter* (FIVF) [33], *Neighborhood Vector Filter* (NVF) [30] and *Peer Group Switching Arithmetic Mean Filter* (PGSAMF) [41]; and also with some impulsive noise filters for gray-scale images applied in a component-wise way: *Marginal Vector Median Filter* (MVMF) [34], *Truncation Filter* (TF) [15], *Modified Peak-Valley Filter* (MPVF) [1], *Median-Type Detection Filter* (MTDF) [7] and *Universal Filter* (UF) [10].

The proposed filter is easy to adjust by using the correlation function $f(p)$. In this way, instead of tuning a poor meaningful parameter, the tuning process is done with respect to an estimated percentage of noise which makes the process simpler.

In Tables 9.1-9.3, the performance comparison in terms of MAE, PSNR and NCD for different densities of noise using the test images (FIG. 9.3) is presented. The results of the CFM filter correspond to a fixed value of $t = 4$. The results denoted by CFM' correspond to $t = f(p')$ where p' is the impulsive noise percentage estimation. Note that the Lenna image was not

used in the process to determine the correlation function, so, these results validate its suitability.

Table 9.1. Comparison of the performance measured in terms of MAE, PSNR and NCD ($\times 10^2$) using the Lenna image contaminated with different types and percentages of impulsive noise

Filter	5% fixed-value			20% fixed-value			30% random-value		
	MAE	PSNR	NCD	MAE	PSNR	NCD	MAE	PSNR	NCD
None	2.519	22.198	3.458	9.830	16.320	13.507	23.018	13.894	20.756
VMF	2.747	32.060	1.778	3.082	31.300	1.997	5.019	26.672	3.330
EVMF	2.775	32.067	1.806	3.117	31.275	2.073	5.537	26.027	3.941
BVDF	2.954	31.492	1.701	3.765	29.544	2.181	5.970	24.665	3.479
WMMF	2.359	32.679	1.713	2.230	32.184	1.988	5.830	24.373	5.917
VMRHF	1.822	34.938	1.239	2.792	31.171	1.984	6.841	24.219	5.249
BF	5.722	28.364	4.366	9.921	24.694	8.948	18.029	20.420	15.310
ASVMF	0.474	36.219	0.366	1.393	32.147	1.288	2.836	27.986	1.959
AVMF	0.849	35.277	0.511	1.341	31.509	1.271	4.177	23.674	3.405
tTVMF	0.376	38.668	0.299	1.366	30.471	1.447	2.985	27.446	2.169
FIVF	0.427	36.318	0.353	1.476	31.748	1.078	2.485	28.897	1.548
NVF	0.302	39.431	0.239	1.315	31.228	1.199	2.619	28.352	1.709
PGSAMF	0.451	37.163	0.294	1.467	30.666	1.289	2.106	30.484	1.335
MVMF	2.770	32.119	1.940	3.137	31.177	2.481	5.875	25.717	5.313
UF	2.167	33.278	1.426	2.543	30.825	2.005	4.255	27.247	3.526
TF	6.323	26.107	4.400	6.366	25.681	4.870	9.418	22.825	7.752
MPVF	1.220	30.499	1.238	3.726	21.771	5.151	8.299	20.099	8.805
MTDF	0.826	36.723	0.787	0.909	36.423	1.025	11.040	18.401	11.349
CFM	0.787	34.398	0.451	1.565	31.853	1.030	2.553	28.896	1.586
CFM'	0.368	37.916	0.300	1.424	32.010	1.068	2.558	28.924	1.585

The results in Tables 9.1-9.3 and Figs. 9.6-9.8 show that the proposed approach is able to suppress different densities of the two types of impulsive noise and can outperform the competition in terms of performance. By visually inspecting the results in Figs. 9.6-9.8 it can be observed that VMF and the proposed filters show similar noise suppression ability, except for small impulses. On the other hand, the sharpness of edges and the fine details are better preserved. The experimental results show that the CFM' filter gives better results than the CFM filter in most of the cases. So, we can conclude that, if the additional computation load can be assumed, the adaptive computation of $t = f(p')$ is recommended to the use of a fixed value.

Conclusions

In this paper, fuzzy metrics are used to measure the similarity between colour image pixels. A fuzzy metric which simultaneously takes into account the

Fig. 9.6. Performance comparison: (a) Detail of Lenna image with 30% random-value impulsive noise, (b) VMF output, (c) FIVF output, (d) ASVMF output, (e) CFM' output.

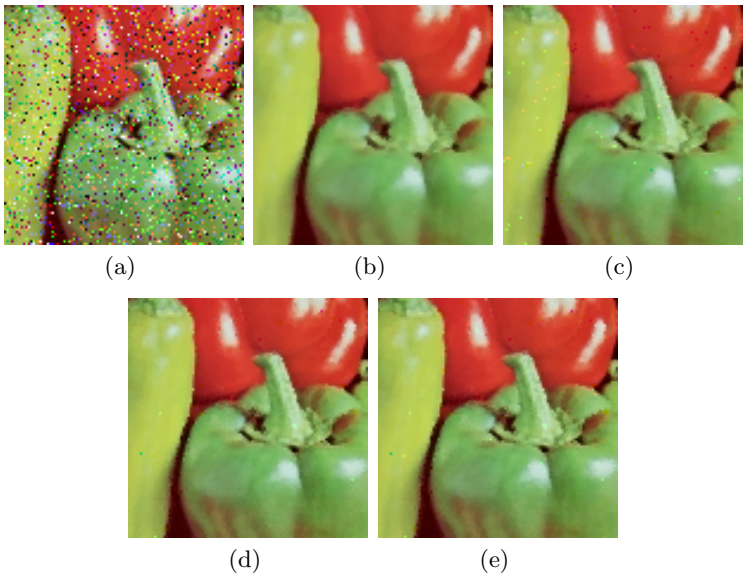

Fig. 9.7. Performance comparison: (a) Detail of Peppers image with 25% fixed-value impulsive noise, (b) VMF output, (c) tTVMF output, (d) CFM output, (e) CFM' output.

Table 9.2. Comparison of the performance measured in terms of MAE, PSNR and NCD ($\times 10^2$) using the Peppers image contaminated with different percentages of impulsive noise

Filter	5% random-value			25% fixed-value			60% fixed-value		
	MAE	PSNR	NCD	MAE	PSNR	NCD	MAE	PSNR	NCD
None	3.885	21.315	3.495	12.398	15.091	16.685	29.952	11.267	40.921
VMF	2.598	32.467	2.198	2.966	31.414	2.541	5.225	24.668	5.458
EVMF	2.646	32.540	2.234	3.004	31.399	2.615	5.176	25.112	5.357
BVDF	2.888	31.160	2.070	4.406	26.444	3.147	12.254	17.536	9.089
WMMF	1.261	35.153	1.329	1.951	31.097	2.395	4.383	24.058	5.983
VMRHF	1.839	34.285	1.643	2.904	30.077	2.740	8.541	21.442	10.326
BF	6.520	27.754	6.186	11.291	23.564	12.066	20.285	19.048	21.840
ASVMF	0.408	37.109	0.298	1.830	30.442	2.582	6.363	22.927	7.702
AVMF	0.559	37.090	0.385	1.808	28.555	2.499	13.648	15.870	21.099
tTVMF	0.480	36.231	0.397	1.630	32.069	1.775	4.565	25.187	5.949
FIVF	0.352	37.208	0.287	1.593	31.158	1.630	7.673	19.860	10.710
NVF	0.343	38.366	0.248	1.804	28.733	2.310	8.281	19.344	11.317
PGSAMF	0.407	38.080	0.279	2.032	28.294	2.755	11.666	18.062	16.541
MVMF	2.621	32.712	2.443	2.970	31.453	3.087	4.657	25.788	5.639
UF	2.108	33.198	2.043	2.588	29.351	2.934	5.100	23.414	6.801
TF	7.214	24.461	6.210	7.219	24.063	6.930	8.821	21.915	9.319
MPVF	1.012	32.370	1.187	5.066	19.598	7.312	20.253	13.154	29.109
MTDF	1.231	31.121	2.407	0.917	37.190	2.122	1.437	34.729	3.163
CFM	0.546	35.781	0.374	1.735	31.012	1.586	8.117	19.740	10.919
CFM'	0.373	37.666	0.291	1.721	30.915	1.632	7.944	20.037	9.990

value similarity between the colour vectors and the *spatial closeness* of the pixels in the image has been defined. Moreover, the fuzzy metric makes the spatial criterion flexible for the considered image processing operations.

The fuzzy metric is used to define an adaptive reduced ordering-based vector filter. The method allows to remove impulsive noise in multichannel images reaching a good trade-off between noise suppression and detail preservation. The proposed filter outperforms the considered classical vector filters and presents a competitive performance with respect to several recent filters.

A correlation study has been carried out to simplify the filter parameter adjusting process. In this way, a methodology that may be used to simplify analogous adjusting problems is proposed. Given the results of this approach, the authors feel that using fuzzy metrics to represent complex relations in other image processing tasks may also be suitable.

Acknowledgments

The authors thank the inestimable help of Dr. Etienne Kerre, Dr. Raymond Chan, Dr. Frank Ma, Dra. Teresa Magal, Dr. Pedro Latorre and Mr. Yuqiu Dong.

Table 9.3. Comparison of the performance measured in terms of MAE, PSNR and NCD ($\times 10^2$) using the Baboon image contaminated with different percentages of impulsive noise

Filter	10% fixed-value			20% random-value			30% fixed-value		
	MAE	PSNR	NCD	MAE	PSNR	NCD	MAE	PSNR	NCD
None	5.085	19.321	7.015	14.636	16.078	12.871	15.239	14.569	20.768
VMF	10.980	23.059	4.552	12.008	22.510	5.110	11.527	22.679	4.894
EVMF	11.044	23.070	4.687	12.201	22.454	5.602	11.627	22.669	5.244
BVDF	12.196	21.906	4.689	13.186	21.420	5.172	13.769	20.950	5.434
WMMF	7.158	25.389	3.660	9.217	23.417	5.852	8.059	24.028	5.248
VMRHF	4.076	25.894	2.685	11.260	22.919	5.162	10.633	23.004	5.236
BF	13.837	22.419	7.434	17.599	20.822	10.661	17.479	20.678	11.762
ASVMF	4.571	24.999	1.922	5.875	24.252	2.493	6.959	23.647	3.462
AVMF	5.244	24.923	2.103	5.888	24.086	2.717	6.418	22.803	4.641
tTVMF	2.809	27.318	1.471	5.430	24.214	2.792	7.207	24.034	3.455
FIVF	4.392	24.702	1.991	6.894	23.322	2.828	8.695	22.328	3.983
NVF	2.833	27.210	1.249	4.700	25.384	1.976	6.650	23.292	3.596
PGSAMF	3.179	26.463	1.390	5.368	24.633	2.142	8.241	22.167	4.212
MVMF	11.026	23.075	5.041	12.293	22.389	6.613	11.560	22.709	6.098
UF	8.444	24.101	3.778	9.846	23.223	4.926	9.455	23.043	5.102
TF	13.211	21.964	6.753	14.451	21.333	7.988	13.504	21.574	7.587
MPVF	5.941	23.342	4.318	8.577	21.635	6.745	10.777	17.813	12.539
MTDF	3.683	27.037	2.508	8.339	20.963	7.241	3.859	26.968	3.501
CFM	6.328	23.889	2.419	7.196	23.506	2.847	8.106	22.782	3.658
CFM'	3.623	25.822	1.562	6.173	23.988	2.523	8.171	22.764	3.667

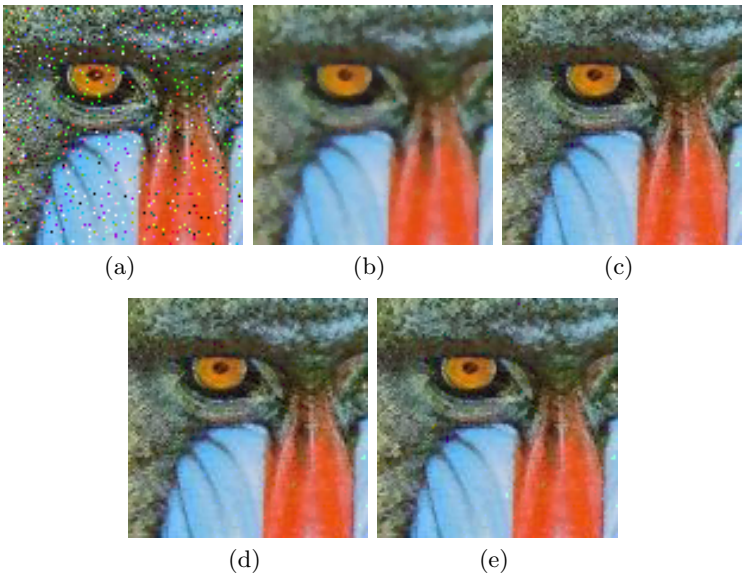

Fig. 9.8. Performance comparison: (a) Detail of Baboon image with 10% fixed-value impulsive noise, (b) VMF output, (c) NVF output, (d) PGSAMF output, (e) CFM' output.

References

1. N. Alajlan, M. Kamel, E. Jernigan, Detail preserving impulsive noise removal, *Signal Processing: Image Communication* 19 10 (2004) 993-1003.
2. H. Allende, J. Galbiati, A non-parametric filter for image restoration using cluster analysis, *Pattern Recognition Letters*, 25 8 (2004) 841-847.
3. K. Arakawa, Median filter based on fuzzy rules and its application to image restoration, *Fuzzy Sets and Systems*, 77 1 (1996) 3-13.
4. J. Astola, P. Haavisto, Y. Neuvo, Vector Median Filters, *Proc. IEEE.*, 78 4 (1990) 678-689.
5. K.E. Barner, T.C. Aysal, Polynomial weighted median filtering, *IEEE Transactions on Signal Processing*, 54 2 (2006) 636-650.
6. J. Camacho, S. Morillas, P. Latorre, Efficient impulsive noise suppression based on statistical confidence limits, *Journal of Imaging Science and Technology*, 50 5 (2006) 427-436.
7. R.H. Chan, H. Chung-Wa, M. Nikolova, Salt-and-pepper noise removal by median-type noise detectors and detail-preserving regularization, *IEEE Transactions on Image Processing* 14 10 (2005) 1479-1485.
8. V. Chatzis, I. Pitas, Fuzzy scalar and vector median filters based on fuzzy distances, *IEEE Transactions on Image Processing*, 8 5 (1999) 731-734.
9. H.A. David, *Order Statistics*. John Wiley and Sons, New York (1981).
10. R. Garnett, T. Huegerich, C. Chui, W. He, A universal noise removal algorithm with an impulse detector, *IEEE Transactions on Image Processing*, 14 11 (2005) 1747-1754.
11. A. George, P. Veeramani, On Some results in fuzzy metric spaces, *Fuzzy Sets and Systems*, 64 3 (1994) 395-399.
12. V. Gregori, S. Romaguera, Some properties of fuzzy metric spaces, *Fuzzy Sets and Systems*, 115 3 (2000) 477-483.
13. V. Gregori, S. Romaguera, Characterizing completable fuzzy metric spaces, *Fuzzy Sets and Systems*, 144 3 (2004) 411-420.
14. S. Hore, B. Qiu, and H.R. Wu, Improved vector filtering for color images using fuzzy noise detection, *Optical Engineering* , 42 6 (2003) 1656-1664.
15. X.D. Jiang, Image detail-preserving filter for impulsive noise attenuation, *IEE Proc. Vision, Image and Signal Proc.* 150 3 (2004) 179-185.
16. L. Khriji, M. Gabbouj, Vector median-rational hybrid filters for multichannel image processing, *IEEE Signal Processing Letters*, 6 7 (1999) 186-190.
17. L. Khriji, M. Gabbouj, Adaptive fuzzy order statistics-rational hybrid filters for color image processing, *Fuzzy Sets and Systems*, 128 1 (2002) 35-46.

18. Y. Li, J. Bacca-Rodríguez, G.R. Arce, Weighted median filters for multichannel signals, *in Proc. Int. Conf. Acoustics, Speech and Signal Processing* ICASSP'05 vol. IV, (2005) 157-160.
19. L. Lucchese, S.K. Mitra, A new class of chromatic filters for color image processing: Theory and applications, *IEEE Transactions on Image Processing* , 14 4 (2004) 534-548.
20. R. Lukac, B. Smolka, K. Martin, K.N. Plataniotis, A.N. Venetsanopoulos, Vector Filtering for Color Imaging, *IEEE Signal Processing Magazine, Special Issue on Color Image Processing*, 22 1 (2005) 74-86.
21. R. Lukac, K.N. Plataniotis, A taxonomy of color image filtering and enhancement solutions, in *Advances in Imaging and Electron Physics*, (eds.) P.W. Hawkes, Elsevier, 140 (2006) 187-264.
22. R. Lukac, K.N. Plataniotis, B. Smolka, A.N. Venetsanopoulos, Generalized Selection Weighted Vector Filters, *EURASIP Journal on applied signal processing: Special Issue on Nonlinear signal and image processing*, 2004 12 (2004) 1870-1885.
23. R. Lukac, B. Smolka, K.N. Plataniotis, A.N. Venetsanopoulos, Selection weighted vector directional filters, *Computer Vision and Image Understanding*, 94 1-3 (2004) 140-167.
24. R. Lukac, Adaptive Color Image Filtering Based on Center Weighted Vector Directional Filters, *Multidimensional Systems and Signal Processing*, 15 2 (2004) 169-196.
25. R. Lukac, K.N. Plataniotis, A.N. Venetsanopoulos, Color image image denoising using evolutionary computation, *International Journal of Imaging Systems and Technology* 15 5 (2005) 236-251.
26. R. Lukac, Adaptive vector median filtering, *Pattern Recognition Letters*, 24 12 (2003) 1889-1899.
27. R. Lukac, K.N. Plataniotis, A.N. Venetsanopoulos, B. Smolka, A Statistically-Switched Adaptive Vector Median Filter, *Journal of Intelligent and Robotic Systems*, 42 4 (2005) 361-391.
28. R. Lukac, B. Smolka, K.N. Plataniotis, A.N. Venetsanopoulos, Vector sigma filters for noise detection and removal in color images, *Journal of Visual Communication and Image Representation* 17 1 (2006) 1-26.
29. R. Lukac, K.N. Plataniotis, B. Smolka, A.N. Venetsanopoulos, cDNA Microarray Image Processing Using Fuzzy Vector Filtering Framework, *Fuzzy Sets and Systems: Special Issue on Fuzzy Sets and Systems in Bioinformatics*, 152 1 (2005) 17-35.
30. Z. Ma, D. Feng, H.R. Wu, A neighborhood evaluated adaptive vector filter for suppression of impulsive noise in color images, *Real-Time Imaging*, 11 5-6 (2005) 403-416.
31. Z. Ma, H.R. Wu, D. Feng, Partition-based vector filtering technique for suppression of noise in digital color images, *IEEE Transactions on Image Processing* , 15 8 (2006) 2324-2342.
32. Z. Ma, H.R. Wu, B. Qiu, A robust structure-adaptive vector filter for color image restoration, *IEEE Transactions on Image Processing* , 14 12 (2005) 1990-2001.
33. S. Morillas, V. Gregori, G. Peris-Fajarnés, P. Latorre, A fast impulsive noise color image filter using fuzzy metrics, *Real-Time Imaging*, 11 5-6 (2005) 417-428.

34. K.N. Plataniotis, A.N. Venetsanopoulos, *Color Image processing and applications*. Springer-Verlag, Berlin (2000).
35. A. Sapena, A contribution to the study of fuzzy metric spaces, *Appl. Gen. Topology*, 2 1 (2001) 63-76.
36. Y. Shen, K.E. Barner, Fuzzy Vector Median Based Surface Smoothing, *IEEE Transactions on Visualization and Computer Graphics*, 10 3 (2004) 252-265.
37. Y. Shen. K.E. Barner, Marginal fuzzy median and fuzzy vector median filtering of color images, *in Proc. 37th Annual Conf. Inf. Sciences & Systems* (2003).
38. Y. Shen, K.E. Barner, Optimization of fuzzy vector median filters, *in Proc. 38th Annual Conf. Inf. Sciences & Systems* (2004).
39. B. Smolka, R. Lukac, A. Chydzinski, K.N. Plataniotis, W. Wojciechowski, Fast adaptive similarity based impulsive noise reduction filter, *Real-Time Imaging, Special Issue on Spectral Imaging*, 9 4 (2003) 261-276.
40. B. Smolka, K.N. Plataniotis, A. Chydzinski, M. Szczepanski, A.N. Venetsanopoulos, K. Wojciechowski, Self-adaptive algorithm of impulsive noise reduction in color images, *Pattern Recognition*, 35 8 (2002) 1771-1784.
41. B. Smolka, A. Chydzinski, Fast detection and impulsive noise removal in color images, *Real-Time Imaging* 11 5-6 (2005) 389-402.
42. M. Szczepanski, B. Smolka, K.N. Plataniotis, A.N. Venetsanopoulos, On the distance function approach to color image enhancement, *Discrete Applied Mathematics*, 139 1-3 (2004) 283-305.
43. C. Tomasi, R. Manduchi, Bilateral filtering for gray and color images, *in Proc. 6th. IEEE Int. Conf. Computer Vision*, (1998) 839-846.
44. P.E. Trahanias, D. Karakos, A.N. Venetsanopoulos, Directional processing of color images: theory and experimental results, *IEEE Trans. Image Processing*, 5 6 (1996) 868-880 .
45. H.H. Tsai, P.T. Yu, Genetic-based fuzzy hybrid multichannel filters for color image restoration, *Fuzzy Sets and Systems*, 114 2 (2000) 203-224.
46. M.I. Vardavoulia, I. Andreadis, Ph. Tsalides, A new vector median filter for colour image processing, *Pattern Recognition Letters*, 22 6-7 (2001) 675-689.

10 Contribution (vii)

S. Morillas, Fuzzy metrics and peer groups for impulsive noise reduction in colour images, *in Proceedings of 14th European Signal Processing Conference EUSIPCO 2006*, 4-8 September 2006, Florence (Italy).

Abstract

A new method for removing impulsive noise pixels in colour images is presented. The proposed method applies the *peer group* concept defined by means of fuzzy metrics in a novel way to detect the noisy pixels. Then, a switching filter between the identity operation and the *Arithmetic Mean Filter* (AMF) is defined to perform a computationally efficient filtering operation over the noisy pixels. Comparisons in front of classical and recent vector filters are provided to show that the presented approach reaches a very good relation between noise suppression and detail preserving.

10.1 Introduction

Digital Colour Images are frequently disturbed by the presence of the so-called impulsive noise [19, 11]. In this context, the filtering process becomes an essential task to avoid possible drawbacks in the subsequent image processing steps.

When the images are contaminated with impulsive noise the switching approaches are widely used due to their sufficient performance and proven computational simplicity. On the basis of the classical vector filters as the *Arithmetic Mean Filter* (AMF) [19], the *Vector Median Filter* (VMF) [2] , the *Basic Vector Directional Filter* (BVDF) [24, 25], or the *Distance Directional Filter* (DDF) [9] the switching approaches aims at selecting a set of pixels of the image to be filtered leaving the rest of the pixels unchanged. A series of methods for selecting the noise-likely pixels have been proposed to date [1, 12, 13, 16, 21, 22, 15, 17, 23]. In [1] the authors propose to determine if the vector in consideration is likely to be noisy using cluster analysis. The standard deviation, the sample mean and various distance measures are used

in [12, 14] to form de adaptive noise detection rule. [13] proposes to use an statistical test and [3] uses statistical confidence limits. In [16, 21, 22] a neighborhood test is applied. Then, the filtering operation is performed only when it is necessary. In a similar way, in [26] a genetic algorithm is used to decide in each image position to perform the VMF operation, the BVDF operation or the identity operation. In [15, 17, 23], it is proposed to privilege the central pixel in each filtering window to reduce the number of unnecessary substitutions.

The *peer group* concept using classical metrics is employed in the approaches introduced in [21, 22] to detect impulsive noisy pixels by checking the size of the central pixel *peer group* . In this paper, the *peer group* concept is adapted to the use of a certain fuzzy metric. The use of this fuzzy metric is considered instead of the classical metrics since this fuzzy metric has provided better results than classical metrics in impulsive noise filtering [18, 17]. The proposed *peer group* concept is employed to define a switching filter between the AMF and the identity operation. Experimental results for performance comparison are provided to show that the proposed approach outperforms the classical vector filters and the recent approaches listed above.

The paper is organized as follows. In Section 10.2 the fuzzy metric is described. Section 10.3 presents the *peer group* concept. The method to detect the noisy pixels is defined in Section 10.4. Section 10.5 contains experimental results and discussion. Finally, conclusions are presented in Section 10.6.

10.2 An appropriate fuzzy metric

One of the most important problems in fuzzy topology is to obtain an appropriate concept of fuzzy metric. In [8] a particular class of fuzzy metrics in the George and Veeramani's sense, [5], called stationary fuzzy metrics, were defined; for simplicity they will be referred as fuzzy metrics. From now on, and according to [5, 8] a fuzzy metric space is an ordered triple $(X, M, *)$ such that X is a (nonempty) set, $*$ is a continuous t-norm and M is a fuzzy set of $X \times X$ satisfying the following conditions for all $x, y, z \in X$:

(FM1) $M(x, y) > 0$
(FM2) $M(x, y) = 1$ if and only if $x = y$
(FM3) $M(x, y) = M(y, x)$
(FM4) $M(x, z) \geq M(x, y) * M(y, z)$

$M(x, y)$ represents the degree of nearness of x and y and according to (FM2) $M(x, y)$ is close to 0 when x is far from y. If $(X, M, *)$ is a fuzzy metric space we will say that $(M, *)$ is a fuzzy metric on X.

The authors proved in [5] that every fuzzy metric $(M, *)$ on X generates a Hausdorff topology on X. Actually, this topology is metrizable as it was proved in [6, 7], and so the above definition can be considered an appropriate concept of fuzzy metric space.

The next proposition will be established to be applied in next sections when working with colour pixels $\mathbf{x}_i$ that are characterized by terns of values in the set $\{0, 1, \ldots, 255\}$. This proposition is a particular case of the one used in [17], inspired in [20], and its proof will be omitted.

Proposition. *Let X be the set $\{0, 1, \ldots, 255\}$ and let $K > 0$. Denote by $(x_i(1), x_i(2), x_i(3))$ the element $\mathbf{x}_i \in X^3$. The function M given by*

$$M(\mathbf{x}_i, \mathbf{x}_j) = \prod_{l=1}^{3} \frac{min\{x_i(l), x_j(l)\} + K}{max\{x_i(l), x_j(l)\} + K} \tag{10.1}$$

for all $\mathbf{x}_i, \mathbf{x}_j \in X^3$, is a fuzzy metric on X^3, where the t-norm $*$ is the usual product in $[0, 1]$.

In this way from now on,

$$M(\mathbf{x}_i, \mathbf{x}_j) \tag{10.2}$$

will be the fuzzy distance between the colour image vectors $\mathbf{x}_i$ and $\mathbf{x}_j$. According to [18, 17], an appropriate value for K when comparing RGB colour vectors is $K = 1024$.

10.3 Peer Groups in the fuzzy context

A colour RGB image is commonly represented as a multidimensional array $N_1 \times N_2 \times 3$, where every pixel $\mathbf{x}_i, i = 1, 2, \ldots, N_1 N_2$ is a three component vector in X^3, as mentioned above. The *peer group* concept introduced in [4, 10] have been used in various RGB colour image filter designs. In this work, the notion of *peer group* given in [21] will be adapted to the context of fuzzy metrics. So, attending to the concept of nearness (see axiom FM2 in the definition of fuzzy metric given in Section 10.2), for a central pixel $\mathbf{x}_i$ in a 3×3 filtering window W and fixed $d \in]0, 1]$, we denote by $\mathcal{P}(\mathbf{x}_i, d)$ the set

$$\{\mathbf{x}_j \in W : M(\mathbf{x}_i, \mathbf{x}_j) \geq d\}$$

that is, $\mathcal{P}(\mathbf{x}_i, d)$ is the set of pixels of the filtering window W whose fuzzy distance to $\mathbf{x}_i$ is not less than d. Obviously, $\mathcal{P}(\mathbf{x}_i, d)$ is not empty for each $\mathbf{x}_i$, since $\mathbf{x}_i \in \mathcal{P}(\mathbf{x}_i, d)$.

Now, employing the same terminology used in [21], given a natural number m, we denote by $\mathcal{P}(\mathbf{x}_i, m, d)$ a subset of $\mathcal{P}(\mathbf{x}_i, d)$ constituted by $\mathbf{x}_i$ and other m elements of $\mathcal{P}(\mathbf{x}_i, d)$, which will be called a *peer group* of m elements (associated to $\mathbf{x}_i$). Clearly, for each $\mathcal{P}(\mathbf{x}_i, d)$ we can find a *peer group* for $m = 0$, but it could not exist for $m \geq 1$.

10.4 Proposed filtering technique

As it was commented in Section 1, the filters in [21, 22] determine a *noise-free* pixel when its *peer group* reaches a minimum size m (see Section 3).

An appropriate value of m for any type and density of noise is difficult to find. In homogeneous regions, higher values of m would present a robust and proper performance. In edges or details, lower values of m are needed to properly preserve the uncorrupted data, however, the robustness is lower as m decreases.

In this work, an iterative algorithm aimed at solving the selection of m is proposed. First, a higher value of m is required to determine in a robust way *noise-free* pixels in homogeneous regions far from borders and details. Second, to reach an appropriate performance in edges and detailed regions, the value of m is iteratively decremented. Then the required *peer group* size is lower but the restriction of all the members of the *peer group* to be previous *noise-free* pixels is added. The intuitive underlying idea in this second step is that if a pixel is similar to some (m) *noise-free* pixels it should be *noise-free*, as well. Using the notation in Sections 10.2-10.3 the proposed algorithm for detection and removal of impulsive noise pixels which will be called *Iterative Peer Group Switching Arithmetic Mean Filter* (IPGSAMF) is defined as follows.

1. Every pixel $\mathbf{x}_i$ in the image for which it can be found a peer group $\mathcal{P}(\mathbf{x}_i, 4, d)$ is declared as *noise-free* . The rest of the pixels are declared as *non-assigned*.
2. For each *non-assigned* pixel $\mathbf{x}_i$ in the image, if a peer group $\mathcal{P}(\mathbf{x}_i, 3, d)$ where all the pixel members of the peer group excepting $\mathbf{x}_i$ are *noise-free* can be found, then $\mathbf{x}_i$ is declared as *noise-free* .
3. Repeat step 2 but searching peer groups $\mathcal{P}(\mathbf{x}_i, 2, d)$.
4. Repeat step 2 but searching peer groups $\mathcal{P}(\mathbf{x}_i, 1, d)$.
5. Each pixel declared as *non-assigned* is now declared as *noisy* .
6. The *noisy* pixels in the image are now substituted performing the filtering operation. Each *noisy* pixel is replaced by the output of the AMF (mimicking [21]) performing over the *noise-free* neighbors of the pixel in substitution in a 3×3 window. Notice that a *noisy* pixel may not have any *noise-free* neighbor in its 3×3 neighborhood. If it is the case, the window must be enlarged in size until at least one *noise-free* neighbor is included. The AMF is applied because of its computational simplicity, however other suitable filters as the VMF could be applied in the above conditions, as well.

   The proposed filter methods performs by detecting in step 1 a set of pixels which can be declared as *noise-free* with a high reliability since they are *similar* to, at least, the half of their neighbors. On the basis of these *noise-free* pixels, new *noise-free* pixels are detected in the steps 2,3 and 4 by relaxing the required condition respect to the number of pixels members of the peer group but requiring them to be previous *noise-free* pixels. Finally, the procedure leaves the impulsive noise pixels isolated (step 5). The *noisy* pixel substitution is finally performed in step 6.

   Figure 10.1 shows a noisy image along with the pixels declared as *noise-free* after each step and the final output of the filter. Notice that the

performance of the filter critically depends on the first selection of *noise-free* pixels performed in step 1 for which the value of d is quite important. The appropriate value of this parameter is studied in Section 10.5 and it is proposed a robust setting for it.

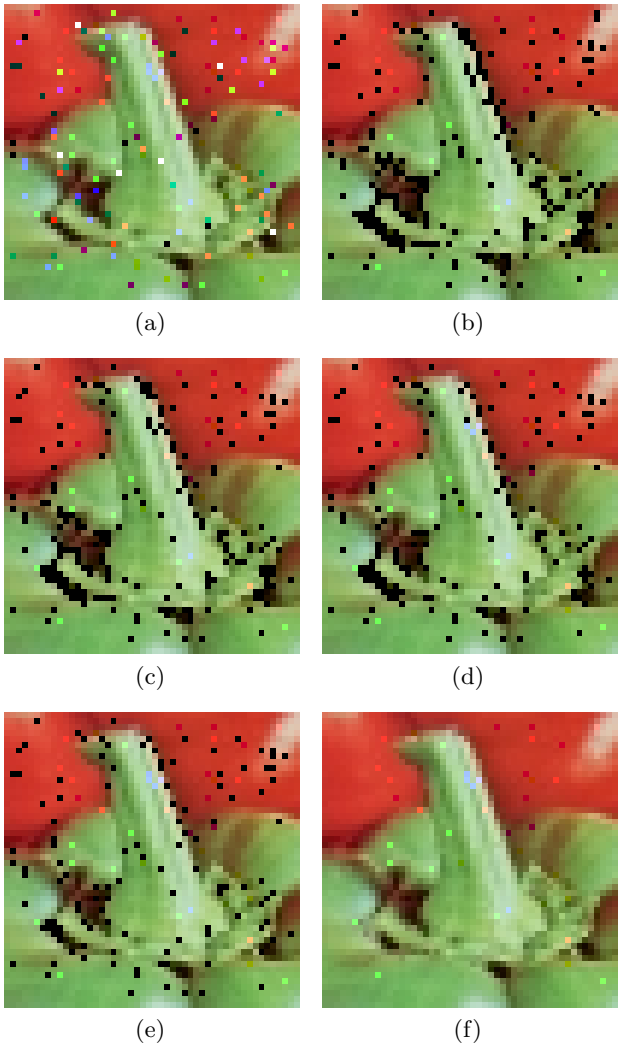

Fig. 10.1. Sample of performance of the proposed filter (*noisy* pixels in black, *noise-free* pixels coloured): (a) Detail of Peppers image with 5% impulsive noise, (b) *noise-free* pixels after step 1, (c) *noise-free* pixels after step 2, (d) *noise-free* pixels after step 3, (e) *noise-free* pixels after step 4, (f) IPGSAMF output,

Table 10.1. Filters taken for performance comparison and notation.

Notation	**Filter**
AMF	Arithmetic Mean Filter [19]
VMF	Vector Median Filter [2]
BVDF	Basic Vector Directional Filter [25]
DDF	Directional Distance Filter [9]
FIVF	Fast Impulsive Vector Filter [17]
PGSAMF	Peer Group Switching AMF [21, 22]
AVMF	Adaptive Vector Median Filter [13]
IPGSAMF	Iterative Peer Group Switching AMF

10.5 Experimental results

In this section, the impulsive noise model for the transmission noise, as defined in [19], has been used to add noise to some tests images in order to assess the performance of the proposed filter in front of the classical and recent filters in Table 10.1. For simplicity, it has been used the common objective quality measure PSNR defined as [19]

$$PSNR = 20 \log \left(\frac{255}{\sqrt{\frac{1}{NMQ} \sum_{i=1}^{N} \sum_{j=1}^{M} \sum_{q=1}^{Q} \left(F^q(i,j) - \hat{F}^q(i,j) \right)^2}} \right), \quad (10.3)$$

where M, N are the image dimensions, Q is the number of channels of the image ($Q = 3$ for colour image), and $F^q(i,j)$ and $\hat{F}^q(i,j)$ denote the q^{th} component of the original image vector and the filtered image, at pixel position (i,j), respectively.

The results of the assessment using some details of the images Peppers and Baboon are shown in Tables 10.2 and 10.3. Similar results can be obtained for other common objective quality measures as MAE or NCD. Some outputs of the filters in comparison are shown in Figures 10.2 and 10.3.

As it was commented in Section 10.4 the filter performance is influenced by the value of the d parameter. It has been found that appropriate values of d are in the range $[0.900, 0.940]$. The optimal value of d for a particular image is directly proportional to the density of the contaminating noise. However, a robust setting of d presenting a good performance for several images and noise densities is $d = 0.925$.

Table 10.2. Comparison of the performance in terms of PSNR using a detail of the Baboon image contaminated with different densities of impulsive noise.

Filter	5%	15%	25%
None	23.41	17.75	15.32
AMF	22.90	21.77	20.73
VMF	23.45	23.30	22.85
BVDF	21.33	20.99	20.31
DDF	23.37	23.07	22.58
FIVF	28.33	24.86	23.08
SAMF	27.08	25.34	22.84
AVMF	25.93	25.58	23.25
IPGSAMF	29.90	25.59	23.56

Table 10.3. Comparison of the performance in terms of PSNR using a detail of the Peppers image contaminated with different densities of impulsive noise.

Filter	5%	20%	30%
None	23.74	17.15	14.76
AMF	25.91	23.36	21.76
VMF	28.10	27.06	26.72
BVDF	27.32	25.75	24.00
DDF	28.08	26.46	25.56
FIVF	32.98	28.91	26.51
SAMF	32.93	27.67	24.95
AVMF	32.85	28.23	24.34
IPGSAMF	33.48	27.44	24.13

Conclusions

In this paper, the *peer group* concept has been adapted to the use of a certain fuzzy metric. Using this concept, a novel filter for impulsive noise removal has been introduced. The usefulness of the *peer groups* and fuzzy metrics for impulsive noise detection and removal is shown.
The proposed filtering method is able to properly isolate and remove impulsive noise pixels while preserving the uncorrupted image structures. The classical vector filters are significantly outperformed and the presented performance is competitive respect to recently introduced vector filters with good detail-preserving ability, outperforming them in many cases.

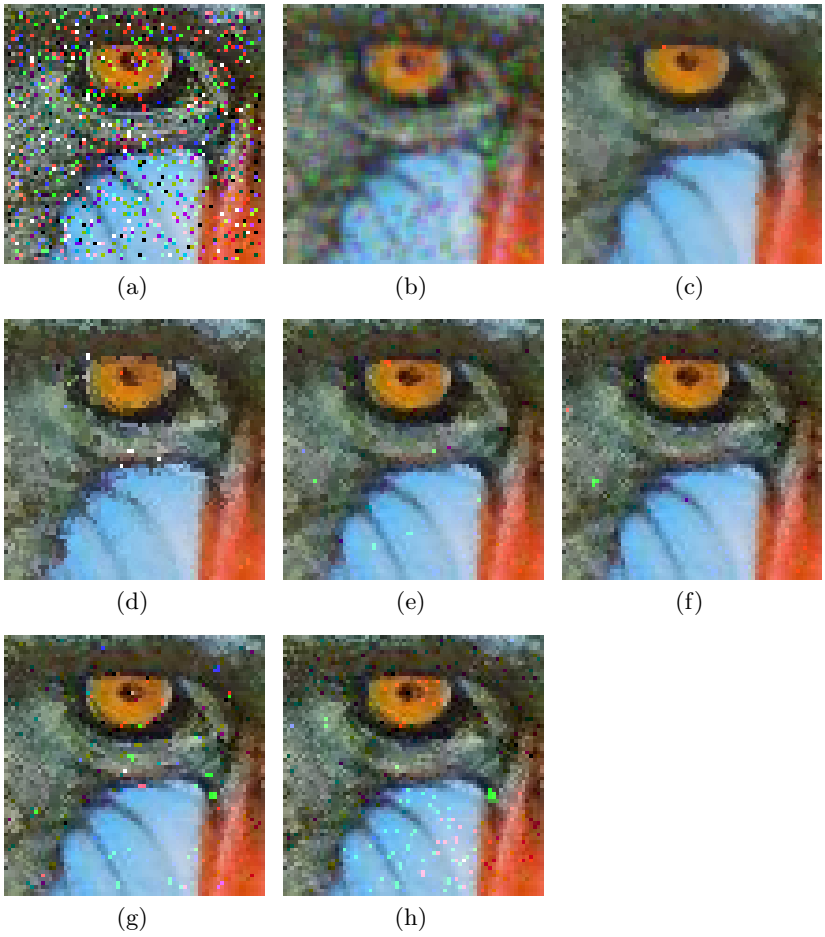

Fig. 10.2. Performance comparison: (a) Detail of Baboon image with 25% impulsive noise, (b) AMF output, (c) VMF output, (d) BVDF output, (e) FIVF output, (f) SAMF output, (g) AVMF output, (h) IPGSAMF output.

(a)

(b)

(c)

(d)

(e)

(f)

(g)

(h)

Fig. 10.3. Performance comparison: (a) Detail of Peppers image with 5% impulsive noise, (b) AMF output, (c) VMF output, (d) BVDF output, (e) FIVF output, (f) SAMF output, (g) AVMF output, (h) IPGSAMF output.

References

1. H. Allende, J. Galbiati, A non-parametric filter for image restoration using cluster analysis, *Pattern Recognition Letters*, 25 8 (2004) 841-847.
2. J. Astola, P. Haavisto, Y. Neuvo, Vector Median Filters, *Proc. IEEE.*, 78 4 (1990) 678-689.
3. J. Camacho, S. Morillas, P. Latorre, Efficient impulsive noise suppression based on statistical confidence limits, *Journal of Imaging Science and Technology*, 50 5 (2006) 427-436.
4. Y. Deng, C. Kenney, MS Moore, BS Manjunath, Peer group filtering and perceptutal color image quantization, *Proceedings of IEEE international symposium on circuits and systems* 4 (1999) 21-4.
5. A. George, P. Veeramani, On Some results in fuzzy metric spaces, *Fuzzy Sets and Systems*, 64 3 (1994) 395-399.
6. A. George, P. Veeramani, Some theorems in fuzzy metric spaces, *J. Fuzzy Math.* 3 (1995) 933-940.
7. V. Gregori, S. Romaguera, Some properties of fuzzy metric spaces, *Fuzzy Sets and Systems*, 115 3 (2000) 477-483.
8. V. Gregori, S. Romaguera, Characterizing completable fuzzy metric spaces, *Fuzzy Sets and Systems*, 144 3 (2004) 411-420.
9. D.G. Karakos, P.E. Trahanias, Generalized multichannel image-filtering structure, *IEEE Transactions on Image Processing* 6 7 (1997) 1038-1045.
10. C. Kenney, Y. Deng, BS Manjunath, G. Hewer, Peer group image enhancement, *IEEE Transactions on Image Processing* 10 2 (2001) 326-34.
11. R. Lukac, B. Smolka, K. Martin, K.N. Plataniotis, A.N. Venetsanopoulos, Vector Filtering for Color Imaging, *IEEE Signal Processing Magazine, Special Issue on Color Image Processing*, 22 1 (2005) 74-86.
12. R. Lukac, Adaptive vector median filtering, *Pattern Recognition Letters*, 24 12 (2003) 1889-1899.
13. R. Lukac, K.N. Plataniotis, A.N. Venetsanopoulos, B. Smolka, A Statistically-Switched Adaptive Vector Median Filter, *Journal of Intelligent and Robotic Systems*, 42 4 (2005) 361-391.
14. R. Lukac, B. Smolka, K.N. Plataniotis, A.N. Venetsanopoulos, Vector sigma filters for noise detection and removal in color images, *Journal of Visual Communication and Image Representation* 17 1 (2006) 1-26.
15. R. Lukac, Adaptive Color Image Filtering Based on Center Weighted Vector Directional Filters, *Multidimensional Systems and Signal Processing*, 15 2 (2004) 169-196.

16. Z. Ma, D. Feng, H.R. Wu, A neighborhood evaluated adaptive vector filter for suppression of impulsive noise in color images, *Real-Time Imaging*, 11 5-6 (2005) 403-416.
17. S. Morillas, V. Gregori, G. Peris-Fajarnés, P. Latorre, A fast impulsive noise color image filter using fuzzy metrics, *Real-Time Imaging*, 11 5-6 (2005) 417-428.
18. S. Morillas, V. Gregori, G. Peris-Fajarnés, P. Latorre, A new vector median filter based on fuzzy metrics, *ICIAR 2005, Lecture Notes in Computer Science* 3656 (2005) 81-90.
19. K.N. Plataniotis, A.N. Venetsanopoulos, *Color Image processing and applications*. Springer-Verlag, Berlin, 2000.
20. A. Sapena, A contribution to the study of fuzzy metric spaces, *Appl. Gen. Topology*, 2 1 (2001) 63-76.
21. B. Smolka, A. Chydzinski, Fast detection and impulsive noise removal in color images, *Real-Time Imaging* 11 5-6 (2005) 389-402.
22. B. Smolka, K.N. Plataniotis, Ultrafast technique of impulsive noise removal with application to microarray image denoising, *Lecture Notes in Computer Science* 3656 (2005) 990-997.
23. B. Smolka, K.N. Plataniotis, A. Chydzinski, M. Szczepanski, A.N. Venetsanopoulos, K. Wojciechowski, Self-adaptive algorithm of impulsive noise reduction in color images, *Pattern Recognition*, 35 8 (2002) 1771-1784.
24. P.E. Trahanias, A.N. Venetsanopoulos, Vector directional filters-a new class of multichannel image processing filters, *IEEE Trans. Image Process.* 2 4 (1993) 528-534.
25. P.E. Trahanias, D. Karakos, A.N. Venetsanopoulos, Directional processing of color images: theory and experimental results, *IEEE Trans. Image Processing*, 5 6 (1996) 868-880 .
26. H.H. Tsai, P.T. Yu, Genetic-based fuzzy hybrid multichannel filters for color image restoration, *Fuzzy Sets and Systems*, 114 2 (2000) 203-224.

11 Contribution (viii)

S. Morillas, V. Gregori, G. Peris-Fajarnés, Isolating impulsive noise pixels in colour images by peer group techniques, *accepted for publication in Computer Vision and Image Understanding*.

Abstract

A new method for removing impulsive noise in colour images is presented. The fuzzy metrics peer group concept is used to build novel switching vector filters. In the proposed filtering procedure, a set of noise-free pixels of high reliability is determined by applying a high demanding condition based on the peer group concept. Afterwards, an iterative detection process is used to refine the initial findings by detecting additional noise-free pixels. Finally, noisy pixels are filtered by maximizing the employed fuzzy distance criterion between the pixels inside the filter window. Comparisons are provided to show that our approach suppresses impulsive noise, while preserving image details. In addition, the method is analyzed in order to justify the necessity of the iterative process and demonstrate the computational efficiency of the proposed approach.

11.1 Introduction

Deficiencies in image acquisition, transmission, or storage often result in the introduction of noise into the digital images. In particular, errors that may arise during the transmission process have the character of impulsive noise. Since the presence of noise usually affects the accuracy of any image processing and analysis task, it is essential that images are filtered prior to subsequent processing and analysis.

In the processing of colour (or multichannel) images the vector approaches are preferred over componentwise solutions due to the correlation between the image channels that has to be taken into account to achieve the required performance [32]. The most well-known vector filters are the *Vector Median Filter* (VMF) [2] and the *Basic Vector Directional*

Filter (BVDF) [37]. These methods are widely used since they are robust and also hold other interesting properties. For instance: the VMF can be derived as a maximum likelihood estimate (MLE) when the underlying probability densities are double exponential and the filter output is restricted to be one of the input samples. The impulse response of VMF is zero, suggesting that VMF-like filters can remove impulsive noise. In the BVDF case, the filter output is the vector in the filter window whose direction is the MLE of directions of the input vectors. Since RGB vector direction is associated to chromaticity, BVDF may improve the VMF performance in terms of chromaticity preservation. For additional information, the reader is referred to the overviews of vector filters made in [17, 25].

The above mentioned classical vector filters have the drawback that the operations made in any image location are fixed, i.e. they are non-adaptive to local features. It has been widely observed that non-adaptive processing usually results in blurred edges and image details. To overcome this drawback, a number of vector processing solutions [25, 15, 18, 19, 20, 24, 33] have been proposed to adapt the filter to varying image characteristics and noise statistics, and to obtain good performance in real-life applications such as microarray image processing, television image enhancement, virtual restoration of artworks, and colour video processing.

A well-known approach to the problem of impulsive noise detection and removal is switching filtering which aims to affect only the noisy pixels while keeping the desired image structures (edges and fine details) unchanged. The method introduced in this paper follows the switching filtering paradigm and introduces an impulse detection procedure based on the peer group concept defined using the fuzzy metrics. Therefore, Section 11.2 presents an overview of switching vector filters whereas Section 11.3 proposes novel fuzzy metrics to obtain peer groups from the set of colour pixels. Section 11.4 defines and analyzes the novel method for impulsive noise detection and removal. Section 11.5 contains experimental results and discussion. Finally, conclusions are presented in Section 11.6.

11.2 Switching Vector Filters and Peer Groups

Existing switching vector filters use different approaches to identify impulses. For example, the solution in [1] performs a cluster analysis of the pixel neighbourhood and detects as *noisy* those pixels whose membership degree to the clusters is low. In [3] a multi-normal distribution of the colour vectors is assumed and the confidence limit of the colour vector under processing is checked. The work in [11] uses a fuzzy inference system which takes as inputs some statistical measures of the pixel

under processing and its neighbourhood. The method in [16] checks the difference between the input vector and the mean of several lowest ranked vectors. The method in [22] performs the detection by using the input vector, the vector median, the vector mean and their aggregated distances to other vectors inside the filter window. The work in [23] extends the former work in [22] by utilizing the variance approximation in the multivariate case. The solution presented in [21] uses center weighting coefficients and the methods in [26, 30, 34, 35] use a similarity based vector ordering to increase the importance of the pixel under consideration in the impulse detection process.

The *peer group* concept in [4, 5, 9, 13] has also been used to detect and filter out impulsive noise. The filters introduced in [5, 13] use the difference between the *peer group* of the pixel under consideration and other *peer groups* in its neighbourhood to form the detection rule. The work in [10] proposes to use windows of different size to determine the peer region of each pixel and then check the peer region size and shape. In the approach introduced in [36] for a pixel to be declared as *noise-free* it is required to have a *peer group* of a determined size around it. In [4], the *peer group* concept is defined in the fuzzy metrics context and the method in [36] is modified to perform filtering faster. The works in [27, 28] extend the filter defined in [13] to the directional domain and use it as a sub-filter in a hybrid structure.

The main motivation of this paper is the work in [36]. In the following subsection we describe the method in [36] in order to highlight the basic differences with respect to the proposed method.

11.2.1 Peer group switching filter

Let $||\cdot||$ be a norm on a non-empty set X and let $h > 0$. If $x \in X$, we denote by $\mathcal{P}(x,h)$ the set $\{y \in X : ||x-y|| \geq h\}$. Now, let W be a subset of X containing x and let m be a nonnegative integer. A subset of $\mathcal{P}(x,h) \cap W$ containing $m+1$ elements is called a *peer group* of cardinality m contained in W, and it is denoted by $\mathcal{P}(x,W,h,m)$ or $\mathcal{P}(x,h,m)$ if confusion is not possible.

Following the prior findings presented in [36], a pixel x is considered as *noise-free* only if there exists a *peer group* $\mathcal{P}(x,h,m)$ for some positive value of m. Otherwise, the pixel should be considered as *noisy*. The particular setting of the m parameter determines the filter performance. On the one hand, lower values of m provide a better signal-preserving ability to the filtering but sometimes also a lack of robustness. On the other hand, higher values of m provide a robust performance though a more smoothed output image is obtained. As a result, the work in [36] proposed the use of intermediate values of m in order to reach an appropriate trade-off between signal-preserving and noise smoothing.

On the basis of this work, the proposed method aims at achieving a filtering procedure which is robust in removing impulsive noise and preserving fine details. This performance is achieved by using two different values of the m parameter in the noise detection process. First, a set of *noise-free* pixels of high reliability is determined by applying a demanding condition on the *peer group* cardinality. Afterwards, an iterative detection process is used to refine the initial findings by detecting additional *noise-free* pixels. The remaining, undetected pixels represent impulses.

11.3 Fuzzy metrics peer groups and fuzzy distances

Let X be a non-empty set and $*$ a continuous t-norm. A (stationary) fuzzy metric [7, 8] on X is a function $M(x, y)$ defined on $X \times X$ with values in $(0, 1]$, symmetric with respect to x and y, which satisfies for all $x, y, z \in X$ the following:

(FM1) $M(x, y) = 1$ if and only if $x = y$

(FM2) $M(x, z) \geq M(x, y) * M(y, z)$

In the above expressions, $M(x, y)$ represents the degree of nearness of x and y and according to (FM1) $M(x, y)$ is close to 0 when x is far from y. In the following, the notion of *peer group* given in [36] is shown in the context of fuzzy metrics, as proposed in [4].

Take $d \in [0, 1]$. In the above context, if $x \in X$, we denote by $\mathcal{P}_M(x, d)$ the set $\{y \in X : M(x, y) \geq d\}$. Now, let W be a subset of X containing x and let m be a nonnegative integer. A subset of $\mathcal{P}_M(x, d) \cap W$ containing $m + 1$ elements is called a *peer group* of cardinality m contained in W, and it is denoted by $\mathcal{P}_M(x, W, d, m)$ or $\mathcal{P}(x, d, m)$, as in [36], if confusion is not possible. According to (FM1) it is always possible to find a *peer group* for $m = 0$, but it may not exist for $m \geq 1$.

Proposition 4. *Consider Z as the real interval $[0, 255]$, let $X = Z^3$ and $K > 0$. Denote the RGB colour vector at position i in the $\mathbf{F}$ image by $\mathbf{F}_i = (F_i(1), F_i(2), F_i(3)) \in X$. The function M_K given by*

$$M_K(\mathbf{F}_i, \mathbf{F}_j) = \prod_{l=1}^{3} \frac{min\{F_i(l), F_j(l)\} + K}{max\{F_i(l), F_j(l)\} + K} \tag{11.1}$$

for all $\mathbf{F}_i, \mathbf{F}_j \in X$, is a fuzzy metric on X when $*$ is the product t-norm in $[0, 1]$.

The fuzzy metric M_K, which was introduced in [29], presents the particular behaviour that the given value for two distinct pairs of consecutive numbers (or vectors) may not be the same. This effect can be smoothed by increasing the value of the K parameter in Eq. (11.1). So, the value of K should be set high enough to reduce this effect. However, if $K \to \infty$

then $M_K(\mathbf{F}_i, \mathbf{F}_j) \to 1$, so very high values of K should also be avoided. Several experiences have shown that for a range of values in $[0, C]$ appropriate values of K are in the range $[2C, 2^3C]$. This is shown in Figure 11.1 (a) for the case of RGB values where $K = 1024$ has been proved to be an appropriate value [30, 29]. Indeed, Figures 11.1(a) and 11.1(b) show that the behaviour of M_K for the suggested values of K is very similar, except range and scaling, to the behaviour of classical L_1 and L_2 (Euclidean) metrics. This suggests that these classical metrics could replace M_K in the filter design and similar performance should be expected. However, because the fuzzy metric in Eq. (11.1) allows for the design of hybrid (magnitude and directional processing-based) filters, we have preferred the usage of fuzzy metrics instead of classical metrics.

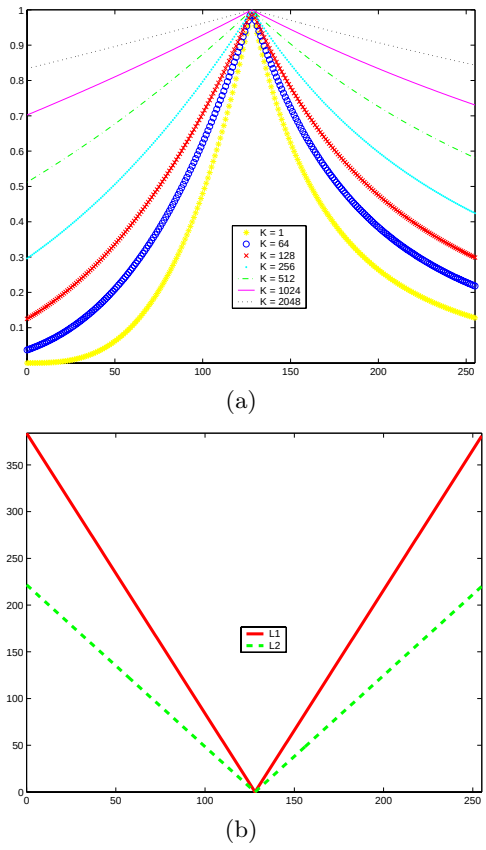

Fig. 11.1. Values given by (a) M_K for different values of K and (b) L_1 and L_2 metrics, when comparing a colour vector $[128, 128, 128]$ with the colour vectors $[V, V, V]$ where $V = 0, 1, \ldots, 255$.

11.3.1 Fuzzy magnitude distance

In the following, each pixel colour at position i in the image $\mathbf{F}$ is represented as a vector $\mathbf{F}_i = (F_i(1), F_i(2), F_i(3))$ comprised its R, G and B components. The term $M_K(\mathbf{F}_i, \mathbf{F}_j)$, for $K_1 = 1024$, is the *fuzzy magnitude distance* between the colour image vectors $\mathbf{F}_i$ and $\mathbf{F}_j$.

11.3.2 Fuzzy angular-like distance

To address directional vector processing [32, 37, 17] using the fuzzy metric M_K we use the approach introduced in [31]. First, each colour image vector $\mathbf{F}_i$ will be associated with an unitary vector $\mathbf{F}_i^{'}$ given by $\mathbf{F}_i^{'} = \frac{\mathbf{F}_i}{||\mathbf{F}_i||_2}$ where $||\cdot||_2$ denotes the Euclidean norm. Note that achromatic RGB pixels correspond to the vectors $\mathbf{V}_a = (a, a, a)$ where $a \in [0, 255]$ and that for any $a > 0$, $||\mathbf{V}_a||_2 = a\sqrt{3}$ and $\mathbf{V'}_a = \frac{\mathbf{V}_a}{||\mathbf{V}_a||_2} = (\frac{1}{\sqrt{3}}, \frac{1}{\sqrt{3}}, \frac{1}{\sqrt{3}})$. Therefore, achromatic (gray-scale) vectors imply $\mathbf{F}_i^{'} = (\frac{1}{\sqrt{3}}, \frac{1}{\sqrt{3}}, \frac{1}{\sqrt{3}})$. This unitary vector $\mathbf{F}_i^{'}$ characterizes the direction of the vector $\mathbf{F}_i$ in the Euclidean space. Then we can use the fuzzy metric M_K over these unitary vectors to measure *fuzzy angular-like distances*.
Operating on the unitary equivalents of the input vectors, the fuzzy metric in Eq. (11.1) can be used to evaluate the angular-like distances between $\mathbf{F}_i$ and $\mathbf{F}_j$. We found that $K_2 = 4$ constitutes an appropriate value for such a configuration.

11.3.3 Fuzzy magnitude-angular-like distance

An intuitive and straightforward approach from the fuzzy point of view consists of combining the magnitude and angular-like criteria by using an appropriate t-norm [31]. According to Proposition 1, the product t-norm should be used, so that the product function $M_{K_1K_2}(\mathbf{F}_i, \mathbf{F}_j) = M_{K_1}(\mathbf{F}_i, \mathbf{F}_j) \cdot M_{K_2}(\mathbf{F}_i', \mathbf{F}_j')$ will be the *fuzzy magnitude-angular-like distance* between $\mathbf{F}_i$ and $\mathbf{F}_j$, where $K_1 = 1024$ and $K_2 = 4$ as commented above. It can be verified that $M_{K_1K_2}$ is a fuzzy metric on X.
Unlike the above approach, directional-magnitude vector processing solutions presented in [20, 23, 12] join the Euclidean and the angular distances between the vectors. Since these metrics measure in quite different ranges, joining them is not as straightforward as in the fuzzy metrics context [31].

11.4 Proposed detection and filtering of corrupted pixels

Consider the use of a generic $n \times n$ window W where $n = 2c + 1$, $c = 1, 2, \ldots$. Consider also that $m = n + 1$, that the window is centered

at $\mathbf{F}_i$ and that the pixels in the filter window follow the classical 1-D indexing shown in Figure 11.2. The proposed *Iterative Peer Group Switching Vector Filter* (IPGSVF) operates as follows (Figure 11.3):

(i) For each image pixel $\mathbf{F}_i$, if there can be found a peer group $\mathcal{P}_M(\mathbf{F}_i, W, d, m)$, then the pixel $\mathbf{F}_i$ is declared as *noise-free*. In other case, the pixel $\mathbf{F}_i$ is declared as *non-assigned*.

(ii) For each *non-assigned* pixel $\mathbf{F}_i$ let W' be the set of *noise-free* pixels in W. If there can be found a peer group $\mathcal{P}_M(\mathbf{F}_i, W', d, 1)$, then the pixel $\mathbf{F}_i$ is declared as *noise-free*. Note that this condition is fulfilled if there exists some pixel $\mathbf{F}_j \in W'$ such that $M(\mathbf{F}_i, \mathbf{F}_j) \geq d$.

(iii) If new *noise-free* pixels were determined in the previous step, then repeat (ii).

(iv) Each *non-assigned* pixel is finally declared as *noisy* .

In step (i), the proposed method detects a set of pixels which can be declared as *noise-free* with a high reliability since they are *similar* to a considerable number m of their neighbors. In steps (ii) and (iii), initial findings are refined. The underlying idea is that if a pixel, which was initially marked as *non-assigned*, is *similar* to some *noise-free* neighbor then it should be considered as *noise-free*, as well. After the iterative procedure is completed, the remaining (undetected) pixels represent the noise. The *noisy* pixels are corrected using the filter in [29] which uses M_{K_1} as the distance criterion. The output of this filter is the vector $\mathbf{F}_{k^*} \in W$ that maximizes the fuzzy distance to the other samples. That is, the output is that $\mathbf{F}_{k^*}$ for which $k^* = arg\ max_k \sum_{j=1, j\neq k}^{n^2} M_{K_1}(\mathbf{F}_k, \mathbf{F}_j),\ k = 1, \ldots, n^2$.

Note that the employed smoothing filter operates solely in the magnitude domain. However, depending on the employed distance criterion, new variants of the proposed method, varying in performance and computational complexity, can be obtained.

i-4	i-3	i-2
i-1	i	i+1
i+2	i+3	i+4

Fig. 11.2. Indexing followed by vectors inside the filter window for the 3×3 case.

Figure 11.4(a) shows a noisy image. Figure 11.4(b) shows that after step (i) *noise-free* pixels in homogeneous regions are correctly detected. However, the performance near edges and details is far from accurate. To solve this, the different iterations of step (ii) (see Figure 11.4 (c),(d) and (e)) identify new *noise-free* pixels to achieve an accurate detection. From the

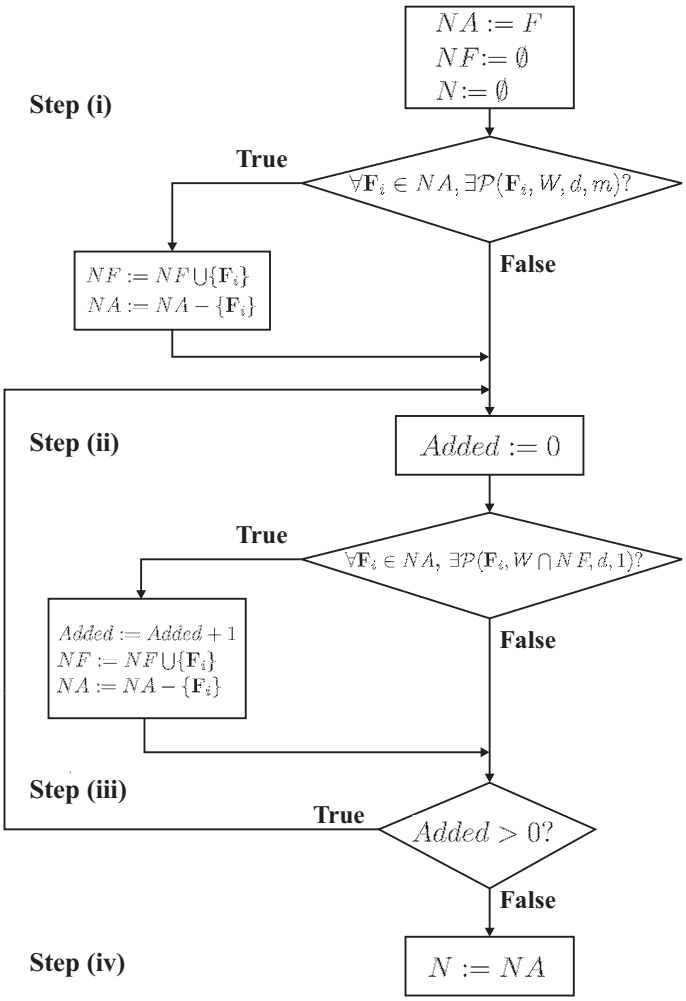

Fig. 11.3. Scheme of the proposed detection procedure, where **F** denotes the image to filter and W the set of pixels in the filter window. The procedure classifies all image pixels in two sets: *noise-free* (NF) and *noisy* pixels (N). Additionally, an auxiliary set of *non-assigned* pixels denotes the pixels to be explored in each iteration of step (ii).

output image in Figure 11.4 (f), it can be concluded that the *noise-free* image areas, edges and details are properly preserved and that except some small impulses the procedure removed most of the noisy pixels.

It should be noted that in the proposed filtering procedure, M_{K_1} can be replaced with M_{K_2} or $M_{K_1K_2}$, thus obtaining the filters with different design characteristics and performance. For example, since $M_{K_1K_2}$ combines both the magnitude and directional information, IPGSVF with $M_{K_1K_2}$ should outperform its variants based on M_{K_1} or M_{K_2}. This fact follows similar findings presented in [20, 23, 12].

Another advantage of the proposed filter is its computational efficiency. In order to compare the complexity of IPGSVF and VMF, we have to take into account that the most computationally demanding operation in vector filtering methods is the computation of distances between colour vectors. Therefore, the computational complexity can be simply compared using the average number of distance calculations per pixel needed by each method. In the following we estimate the average number of distance computations per pixel needed by the proposed method. A detailed computational complexity analysis of the proposed method is developed in Appendix A.

Let $\mathbf{F}_i$ be the central pixel of a $n \times n$ filter window W where $n = 2c+1, c = 1, 2, \ldots$. Let us denote by $\eta = n^2 - 1$ the number of neighbors of $\mathbf{F}_i$ in W, by p the probability of noise appearance, and by $t(p)$ the probability of a pixel to be declared as *noisy* in step (iv) of the proposed method. Then, the average number $c_d(p)$ of distance computations per pixel, including the VMF computation over the *noisy* pixels, is

$$c_d(p) = s(p) + t(p)\binom{\eta}{2}$$

where $s(p)$ is the average number of distances computed by the proposed method to determine whether a pixel is *noisy* or not.

In the case of the filter proposed in [36] this value is $s_1(p)+t_1(p)\binom{\eta}{2}$, where $s_1(p)$ denotes the average number of distances needed to diagnose a pixel in step (i) and $t_1(p)$ is the probability of a pixel to be *non-assigned* in step (i). The value of $t(p)$ can be approximated by the probability $t_N(p)$ of a pixel to be *non-assigned* in the Nth iteration of step (ii) if $t_N(p) - t_{N+1}(p)$ is very close to 0 (note that from now on, if confusion is not possible, we will omit to mention p).

In the following we aim at verifying our theoretical study. We have taken a detail of the Pills image (Fig. 11.5 (b)) and it has been contaminated with 10% of impulsive noise type I [32] (see Section 11.5). Then we run the IPGSVF with $M_{K_1}, n = 3, d = 0.95$. The comparison between theoretical values and obtained experimental values is shown in Table 11.1. In the table, $s_N^*(p)$ denotes the average number of distances needed to diagnose a pixel in the Nth iteration ($N \geq 2$) and λ_N denotes the average number of

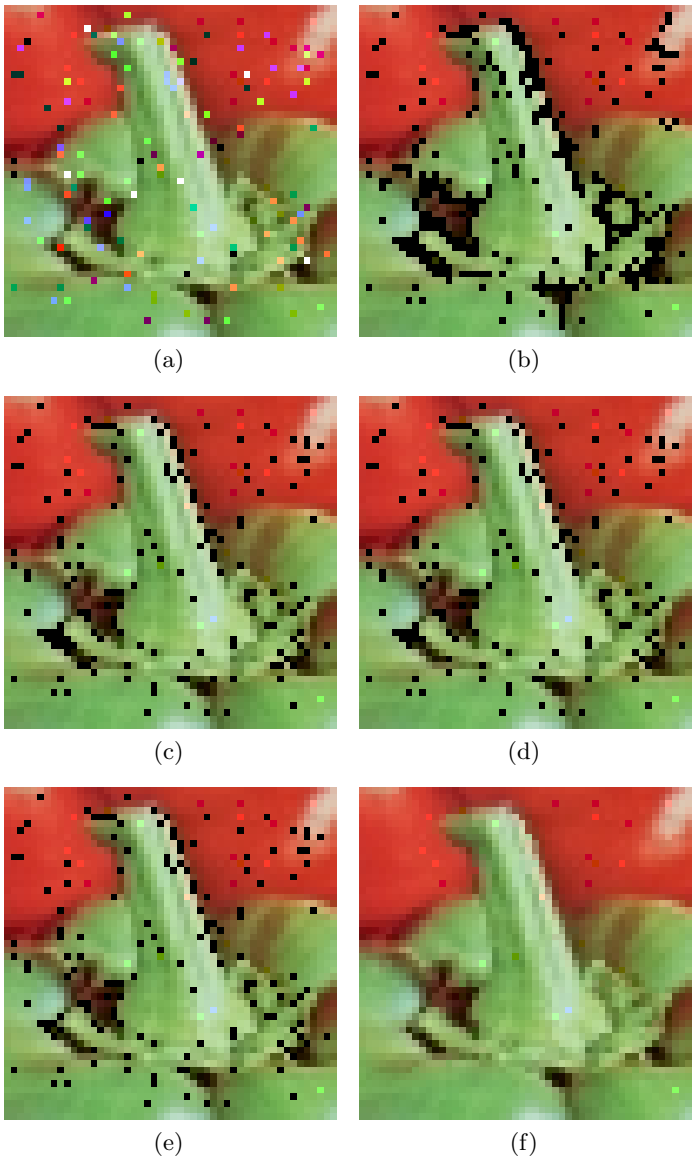

Fig. 11.4. Demonstration of the impulse noise detection and filtering process using IPGSVF with $M_{K_1}, 3 \times 3$ window and $d = 0.93$ (*noisy* pixels in black, *noise-free* pixels coloured): (a) Detail of Peppers image with 5% impulsive noise. *Noise-free* pixels after: (b) step (i), (c) step (ii), first iteration, (d) step (ii), third iteration, (e) step (ii), fifth iteration (last), and (f) filter output.

Table 11.1.

step 1	1st iteration	2nd iteration	3rd iteration	4th iteration	5th iteration	6th iteration
$s_1 = 6.4510$	$s_2^* = 3.8996$	$s_3^* = 0.9647$	$s_4^* = 0.0628$	$s_5^* = 0.0033$	$s_6^* = 0.0002$	$s_7^* = 8.86 \cdot 10^{-6}$
$\lambda_1 = 5.9499$	$\lambda_2 = 0.9647$	$\lambda_3 = 0.0628$	$\lambda_4 = 0.0033$	$\lambda_5 = 0.0002$	$\lambda_6 = 8.8 \cdot 10^{-6}$	$\lambda_7 = 4.5 \cdot 10^{-7}$
$t_1 = 0.2562$	$t_2 = 0.1356$	$t_3 = 0.1278$	$t_4 = 0.1274$	$t_5 = 0.1273$	$t_6 = 0.1273$	$t_7 = 0.1273$
$t'_1 = 0.2712$	$t'_2 = 0.1337$	$t'_3 = 0.1254$	$t'4 = 0.1223$	$t'_5 = 0.1215$	$t'_6 = 0.1210$	$t'_7 = 0.1210$

pixels in W already declared as *non-assigned* in the Nth iteration of step (ii). These values have been estimated by supposing that the probabilities of a pixel in W to be *similar* to $\mathbf{F}_i$ when $\mathbf{F}_i$ is non-corrupted or corrupted are $r = 0.6$ and $q = 0.05$, respectively. In addition, we have estimated that the probabilities of a pixel in W which was declared as *non-assigned* in step (i) to be *similar* to $\mathbf{F}_i$ are $R = 0.2$ and $Q = 0.01$ when $\mathbf{F}_i$ is non-corrupted or corrupted, respectively. Finally, we have assumed that a pixel $\mathbf{F}_j \in W$ is similar to $\mathbf{F}_i$ if $M_k(\mathbf{F}_i, \mathbf{F}_j) \geq 0.95$, i.e. $d = 0.95$. Moreover, Table 11.1 also shows a comparison between the t_N expected theoretical values and the t'_N values computed in the experience. Note that after the third iteration the differences $t_J - t_{J+1}$ are close to 0 and the algorithm stopped in the fifth iteration. It can be seen that there is a very close matching between theoretical and experimental values and therefore, this experimental results validate the developed analysis.
Now, if we approximate $t(p)$ by $t_5 = 0.1273$ then (by (11.19)-(11.20) in Appendix 11.5.2),

$$s(p) \approx s_1 + t_1 \cdot s_2^* + t_2 \cdot s_3^* + t_3 \cdot s_4^* + t_4 \cdot s_5^* = 7.5896$$

and hence, $c_d(p) \approx 7.5896 + 0.1273 \cdot \binom{8}{2} = 11.1568$
Computational analysis of the filter proposed in [36] demonstrated that this value is 13.6274 when $m = 4$, and 9.2496 when $m = 3$. In the case of the VMF, the needed average number of distances per pixel is constant and equal to $\binom{\eta+1}{2}$. In the case of a 3×3 filter window this value is 36. Therefore, it is easy to notice that the proposed algorithm is competitive in terms of computational complexity.

11.5 Experimental results

Impulsive noise corruption process affects only some pixels in the image while leaving other pixels unchanged. Typically, the noise process changes one or more colour components of the affected pixel by replacing its original values with the values which usually significantly deviates from the originals. The most common impulsive noise models consider that the impulse is either an extreme value in the signal range or a random uniformly distributed value within the signal range. For RGB images, these

possibilities are represented with the following two well-known models that have been used to add impulsive noise to the test images in Fig. 11.5.
In the so-called impulsive noise type I model, the corruption is modeled as follows:

$$\mathbf{F}^* = \begin{cases} \{d_1, F_G, F_B\} & \text{with probability } p \cdot p_1 \,, \\ \{F_R, d_2, F_B\} & \text{with probability } p \cdot p_2 \,, \\ \{F_R, F_G, d_3\} & \text{with probability } p \cdot p_3 \,, \\ \{d_1, d_2, d_3\} & \text{with probability } p \cdot \left(1 - \sum_{i=1}^{3} p_i\right) \,. \end{cases} \tag{11.2}$$

where $\mathbf{F} = \{F_R, F_G, F_B\}$ denotes the original pixel, $\mathbf{F}^*$ denotes the pixel corrupted by the noise process and d_1, d_2, d_3 are independent values equal to 0 or 255 with equal probability. The symbol p is the probability of the noise appearance and $p_i, i = 1, 2, 3$ determine the probability of appearance of the noise in the image channels.
In the so-called impulsive noise type II model, $\mathbf{F}* = \{d_1, d_2, d_3\}$ is obtained using d_1, d_2, d_3 which are random uniformly distributed independent integer values in the interval $[0, 255]$ with probability p.

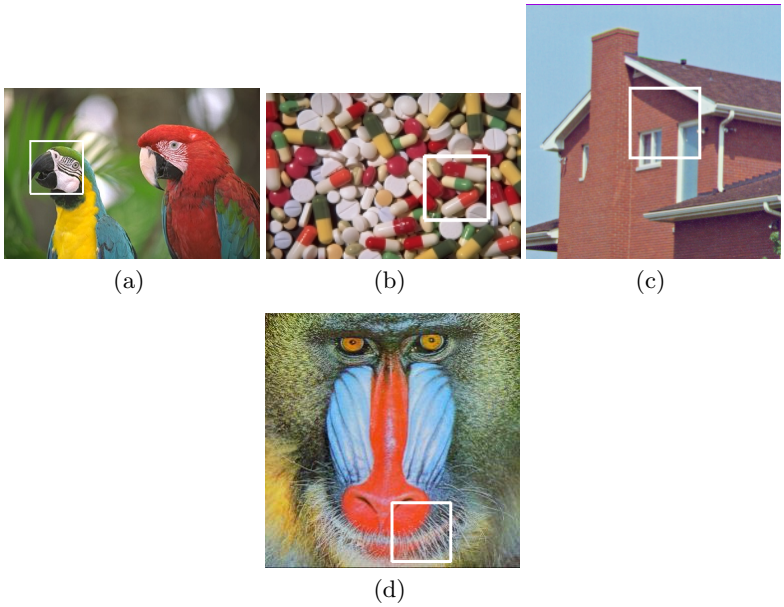

(a) (b) (c) (d)

Fig. 11.5. Test Images with 8 bits per colour channel: (a) Parrots, 256×384 (detail 80×80), (b) Pills, 130×200 (detail 50×50) , (c) House, 256×256 (detail 70×70) and (d) Baboon, 256×256 (detail 60×60).

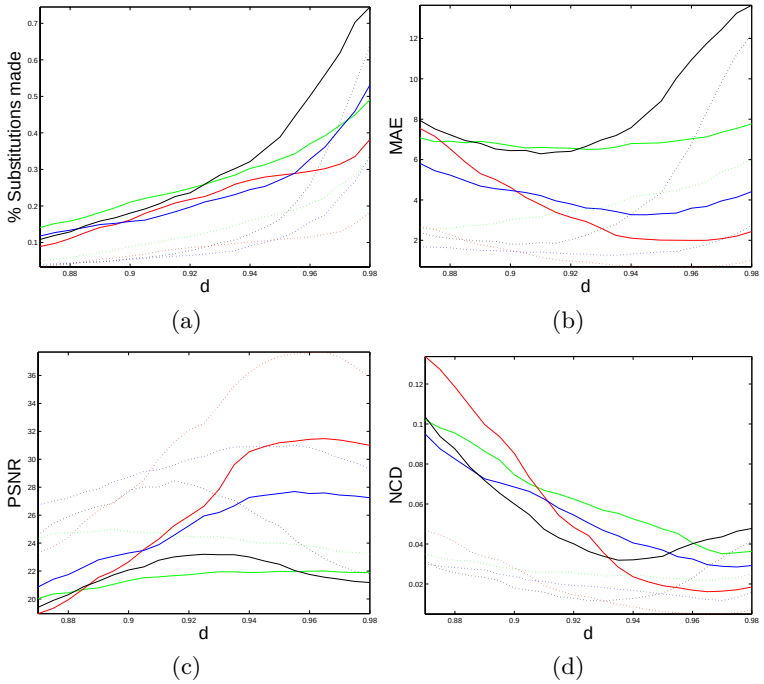

Fig. 11.6. Sample of performance of the IPGSVF with M_{K_1} filter as a function of the d adjusting parameter. Green colours correspond with the Parrots image, blue with Pills, red with House and black with Baboon. Continuous and dotted lines correspond with 30% and 10% of impulsive noise type I, respectively.

In order to assess the quality of the proposed filters both the noise suppression and the detail preserving abilities have to be evaluated. We have used the *Mean Absolute Error* (MAE) that approaches the detail-preserving assessment and the *Peak Signal to Noise Ratio* (PSNR) that expresses the noise suppression ability. In addition, the *Normalized Colour Difference* (NCD) measure has been used since it approaches the human perception [36, 6, 14]. These objective quality measures are defined as follows [32]:

$$MAE = \frac{\sum_{i=1}^{N \cdot M} \sum_{q=1}^{Q} \left| F_i^q - \hat{F}_i^q \right|}{N \cdot M \cdot Q} \tag{11.3}$$

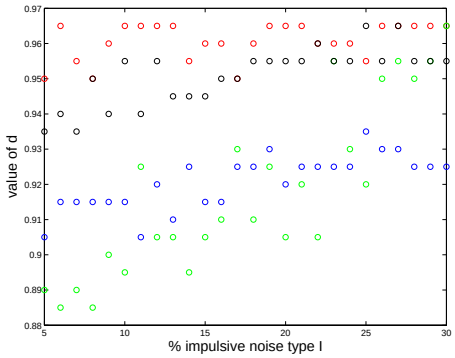

(a)

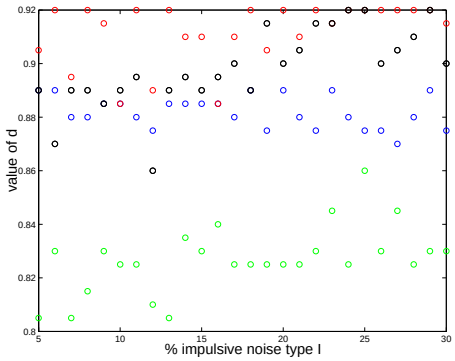

(b)

Fig. 11.7. Optimal PSNR values of the d parameter in the (a) IPGSVF using M_{K_1}, (b) IPGSVF using $M_{K_1K_2}$ for different percentages of impulsive noise type I. Blue points correspond to Baboon, red points to House, green points to Parrots and black points to Pills. Similar results are obtained for the IPGSVF using M_{K_2}.

$$PSNR = 20 \log \left(\frac{255}{\sqrt{\frac{1}{NMQ} \sum_{i=1}^{N \cdot M} \sum_{q=1}^{Q} \left(F_i^q - \hat{F}_i^q \right)^2}} \right) \tag{11.4}$$

where M, N are the image dimensions, Q is the number of channels of the image ($Q = 3$ for colour images), and F_i^q and $\hat{F}_i^q$ denote the q^{th} component of the original image vector and the filtered image, at pixel position i, respectively, and

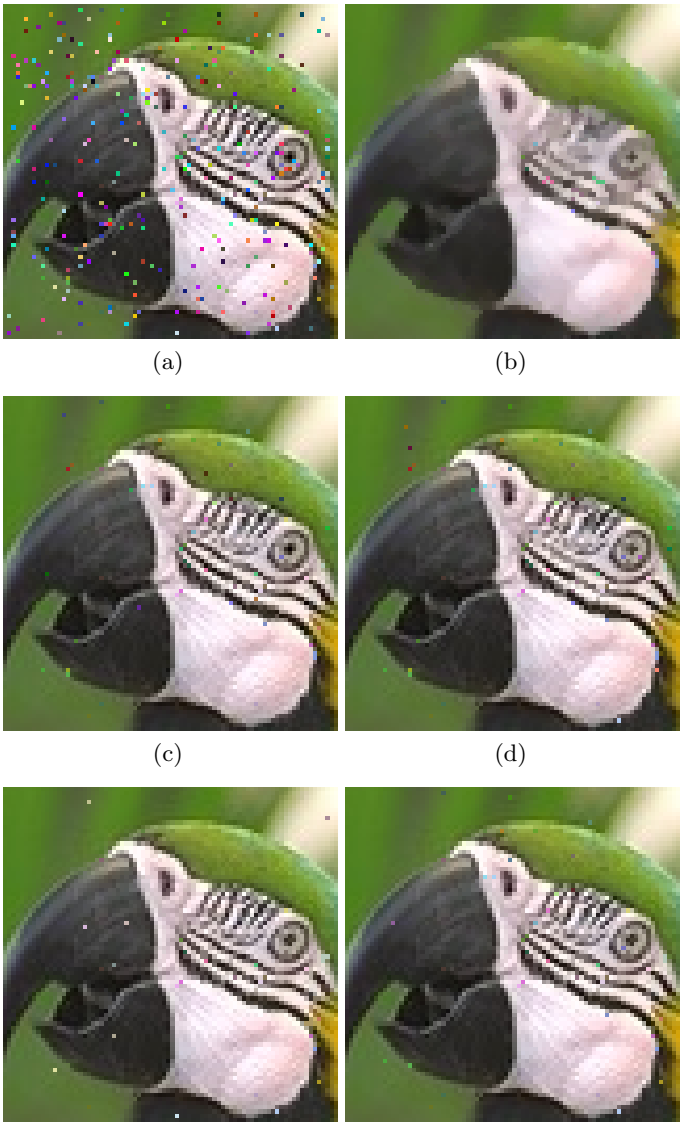

Fig. 11.8. Performance comparison: (a) Detail of Parrots image with 5% impulsive noise type II, (b) VMF output, (c) PGSVMF output, (d) IPGSVF output using M_{K_1}, (e) IPGSVF output using M_{K_2}, (f) IPGSVF output using $M_{K_1 K_2}$.

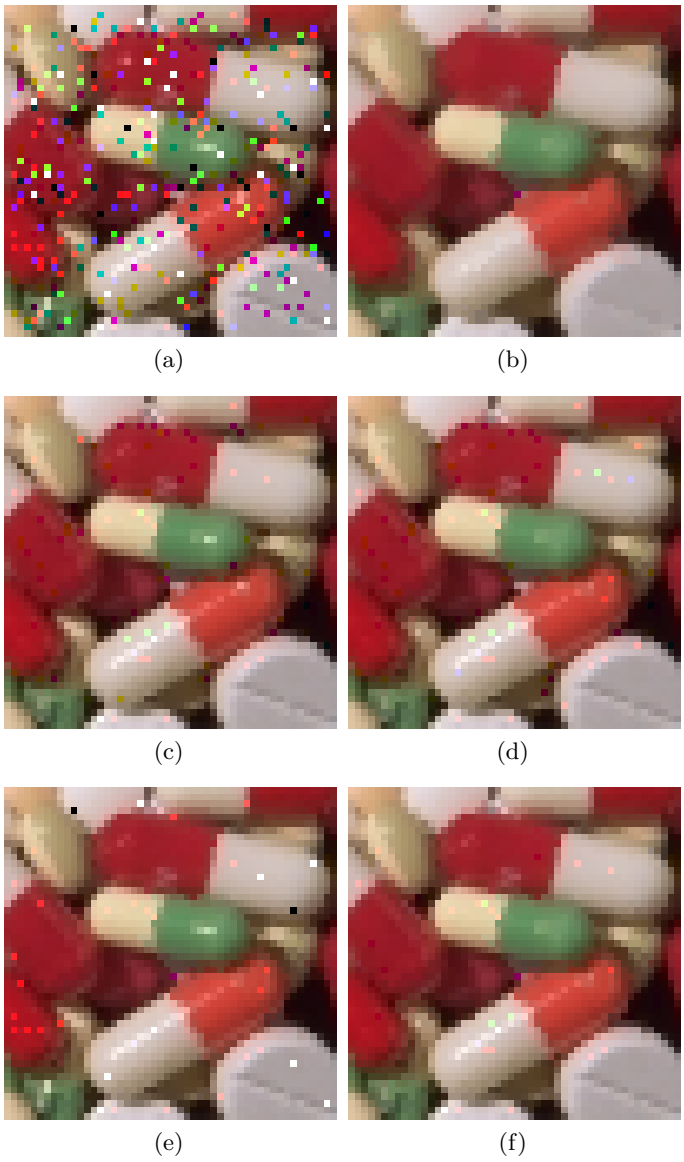

Fig. 11.9. Performance comparison: (a) Detail of Pills image with 15% impulsive noise type I, (b) VMF output, (c) PGSVMF output, (d) IPGSVF output using M_{K_1}, (e) IPGSVF output using M_{K_2}, (f) IPGSVF output using $M_{K_1K_2}$.

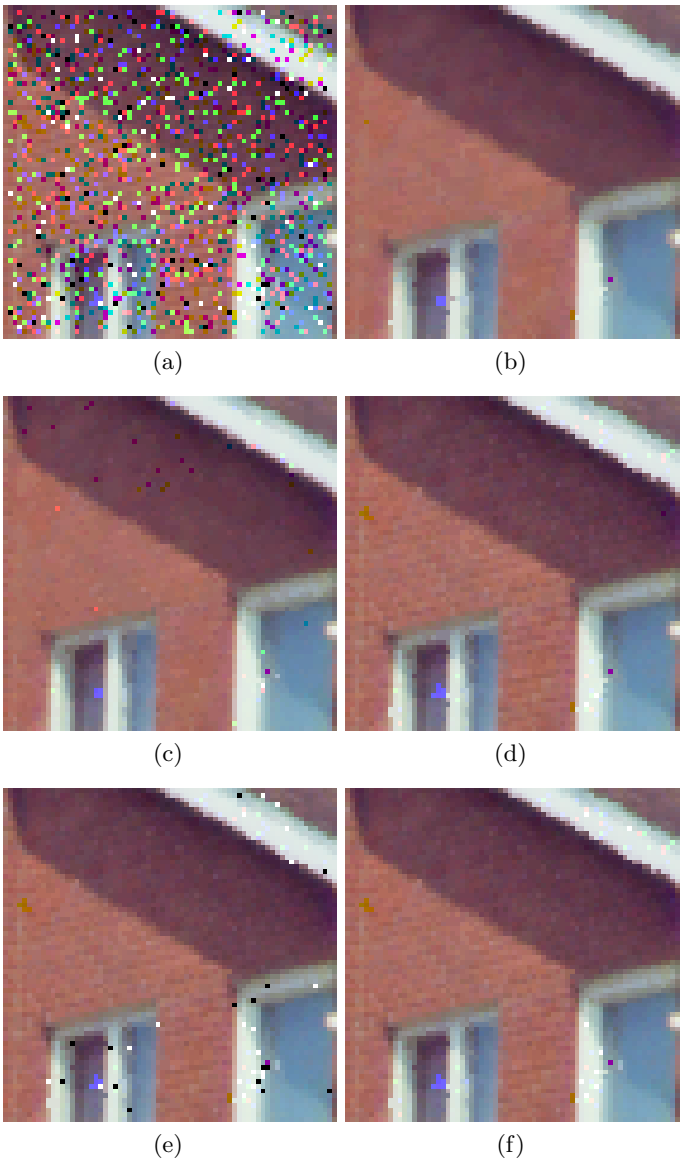

Fig. 11.10. Performance comparison: (a) Detail of House image with 30% impulsive noise type I, (b) VMF output, (c) tTVMF output, (d) IPGSVF output using M_{K_1}, (e) IPGSVF output using M_{K_2}, (f) IPGSVF output using $M_{K_1K_2}$.

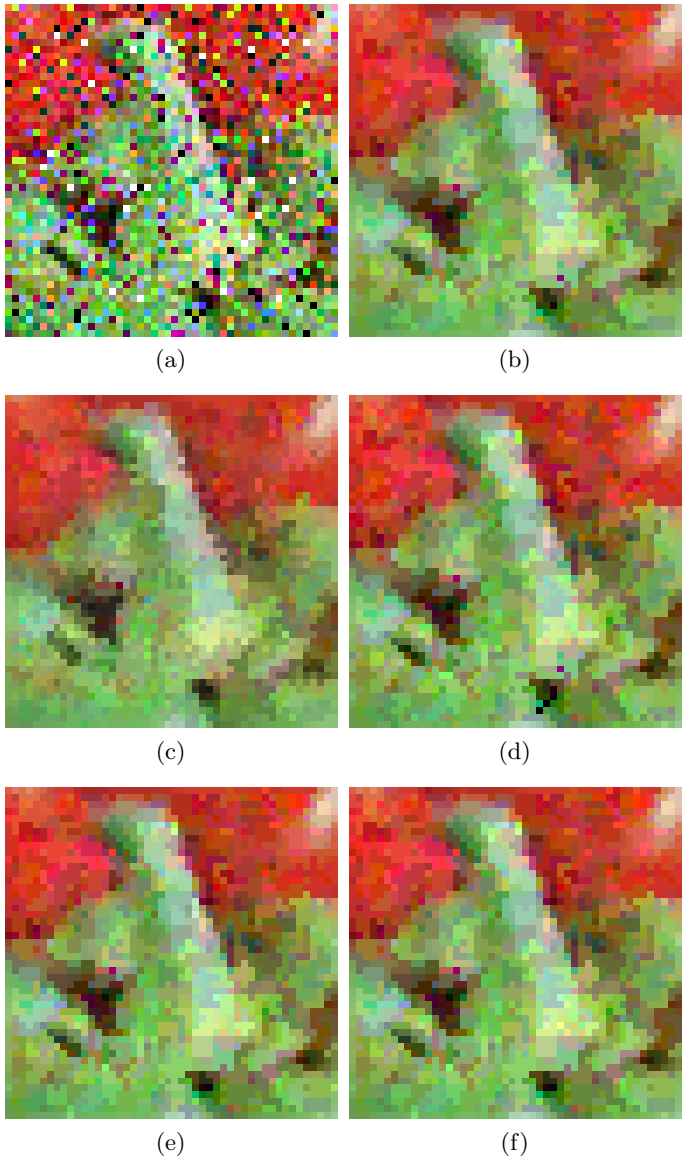

Fig. 11.11. Performance comparison: (a) Detail of Peppers image with mixed 30% impulsive noise type I and $\sigma = 30$ Gaussian noise, (b) VMF output, (c) FISF output, (d) PGSVMF output, (e) IPGSVF output using M_{K_2}, (f) IPGSVF output using $M_{K_1K_2}$.

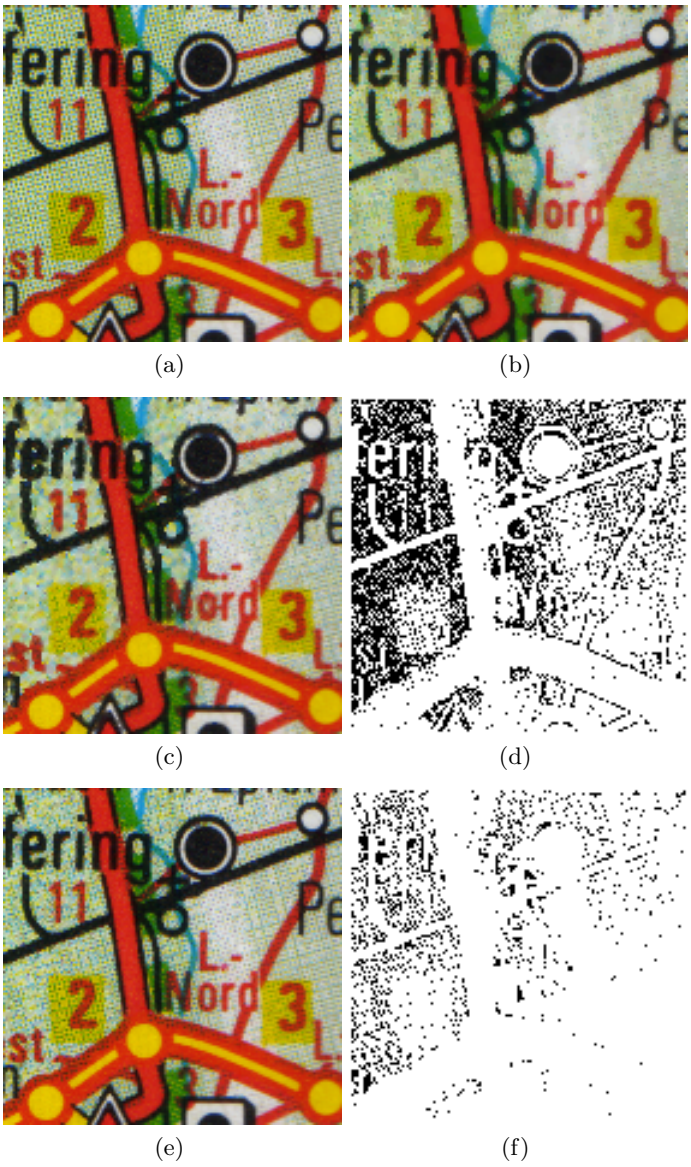

Fig. 11.12. Performance assessment using real noisy images: (a) Detail of a road map image, (b) VMF output, (c) PGSAMF output with $n = 3, m = 2, d = 50$, (d) *Noisy* pixels detected by PGSAMF (27.85%), (e) IPGSVF output with $M_{K_1 K_2}$, $n = 3, m = 4, d = 0.84$, (f) *Noisy* pixels detected by IPGSVF (8.09%).

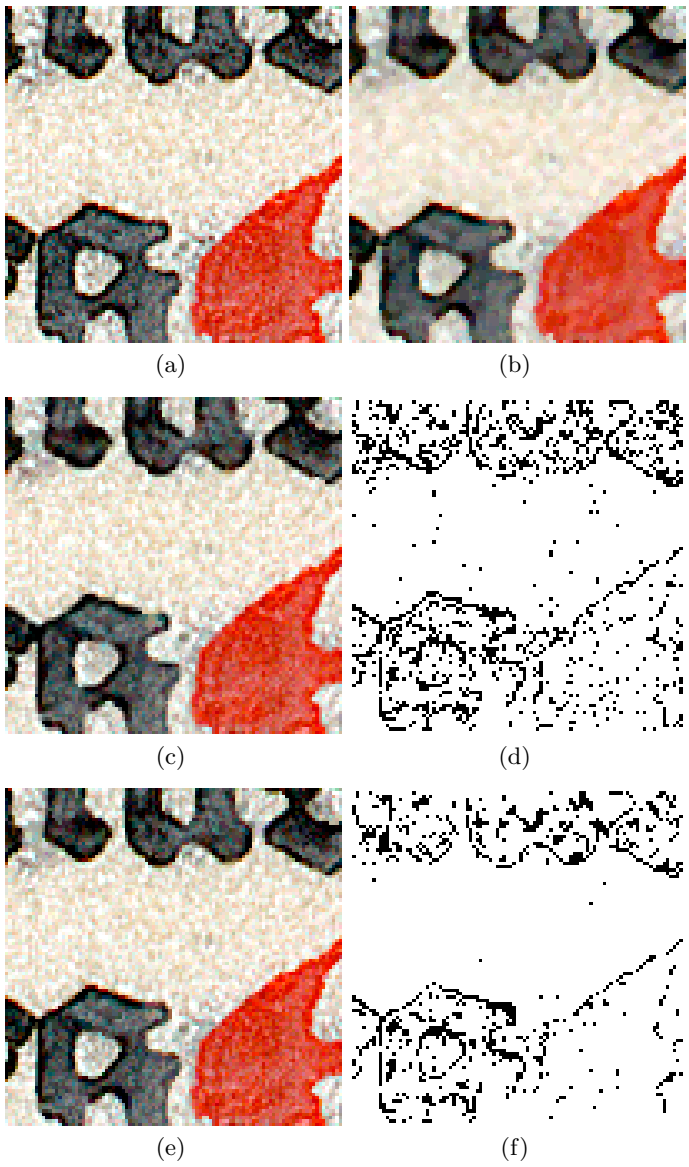

Fig. 11.13. Performance assessment using real noisy images: (a) Detail of an old manuscript image, (b) VMF output, (c) PGSAMF output with $n = 3, m = 2, d = 50$, (d) *Noisy* pixels detected by PGSAMF (14.00%), (e) IPGSVF output with M_{K_1}, $n = 3, m = 4, d = 0.93$, (f) *Noisy* pixels detected by IPGSVF (10.22%).

Table 11.2. Comparison of the performance in terms of MAE, PSNR and NCD using a detail of the Parrots image contaminated with different densities of impulsive noise of types I and II.

Filter	5% impulsive type II			15% impulsive type I			25% impulsive type II		
	MAE	PSNR	NCD (10^{-2})	MAE	PSNR	NCD (10^{-2})	MAE	PSNR	NCD (10^{-2})
None	3.85	21.30	3.26	7.66	17.06	11.34	20.04	14.10	17.08
VMF	8.50	22.57	3.97	8.34	22.65	3.92	11.48	20.56	5.73
FIVF	1.96	25.38	1.10	3.87	23.37	3.05	6.54	21.14	3.29
FISF	4.51	23.96	2.04	5.23	23.36	2.49	8.96	20.06	4.05
AVMF	2.59	25.71	1.20	3.07	24.80	2.31	6.66	20.72	4.38
tTVMF	1.34	27.84	0.79	2.54	25.33	2.23	6.37	21.76	3.61
PGSVMF	1.25	28.74	0.70	2.97	25.47	2.82	6.05	22.17	3.16
PRF	3.68	24.18	1.52	4.60	23.06	2.52	7.72	20.66	4.12
PGSAMF	3.44	23.74	1.23	4.35	23.21	3.06	6.31	21.62	2.71
FMPGSAMF	3.50	23.46	1.27	6.01	21.05	2.98	8.94	19.45	3.75
IPGSVF-M_{K_1}	1.66	27.29	0.85	4.15	24.03	3.16	6.60	21.73	3.46
IPGSVF-M_{K_2}	1.14	28.70	0.59	3.09	23.07	1.82	4.99	23.00	2.62
IPGSVF-$M_{K_1K_2}$	0.95	29.92	0.53	2.66	25.73	1.84	4.99	22.95	2.71

Table 11.3. Comparison of the performance in terms of MAE, PSNR and NCD using a detail of the Pills image contaminated with different densities of impulsive noise of types I and II.

Filter	5% impulsive type II			15% impulsive type I			25% impulsive type I		
	MAE	PSNR	NCD (10^{-2})	MAE	PSNR	NCD (10^{-2})	MAE	PSNR	NCD (10^{-2})
None	3.27	22.22	2.91	6.98	17.71	10.28	11.02	15.68	16.16
VMF	4.40	28.17	2.87	4.57	27.94	3.03	5.27	26.85	3.60
FIVF	0.72	32.56	0.47	1.87	29.42	1.92	3.09	27.01	3.01
FISF	2.25	28.27	1.32	3.04	27.81	1.89	4.52	26.76	2.15
AVMF	0.99	32.13	0.54	1.65	29.80	1.91	2.91	26.16	4.22
tTVMF	0.69	32.45	0.45	1.54	30.02	1.72	2.80	27.85	2.64
PGSVMF	0.58	34.54	0.36	1.56	30.61	2.14	2.77	27.69	2.74
PRF	1.07	30.41	0.63	2.15	26.77	2.16	3.56	24.25	3.46
PGSAMF	0.78	33.10	0.39	1.83	29.91	2.38	3.24	27.33	3.34
FMPGSAMF	0.83	33.02	0.39	2.34	28.75	2.18	3.96	26.30	4.10
IPGSVF-M_{K_1}	0.68	33.31	0.42	1.99	29.64	2.07	3.11	28.21	2.81
IPGSVF-M_{K_2}	0.65	33.49	0.45	1.87	28.34	1.34	3.31	25.48	2.39
IPGSVF-$M_{K_1K_2}$	0.53	34.41	0.33	1.90	30.15	1.28	2.66	28.82	2.00

$$NCD_{Lab} = \frac{\sum_{i=1}^{N \cdot M} \Delta E_{Lab}}{\sum_{i=1}^{N \cdot M} E^*_{Lab}} \tag{11.5}$$

where $\Delta E_{Lab} = [(\Delta L^*)^2 + (\Delta a^*)^2 + (\Delta b^*)^2]^{\frac{1}{2}}$ denotes the perceptual colour error and $E^*_{Lab} = [(L^*)^2 + (a^*)^2 + (b^*)^2]^{\frac{1}{2}}$ is the *norm* or *magnitude* of the original image colour vector in the $L^*a^*b^*$ colour space.

11.5.1 Parameter adjustment

In Figure 11.6 the performance of the IPGSVF using M_{K_1} is presented as a function of the d parameter. It can be observed that the percentage of substitutions made is an increasing function of d and that the value of d

Table 11.4. Comparison of the performance in terms of MAE, PSNR and NCD using a detail of the House image contaminated with different densities of impulsive noise of types I and II.

Filter	5% impulsive type II			20% impulsive type II			30% impulsive type I		
	MAE	PSNR	NCD (10^{-2})	MAE	PSNR	NCD (10^{-2})	MAE	PSNR	NCD (10^{-2})
None	3.22	22.92	3.01	13.10	16.77	12.26	14.12	15.09	20.97
VMF	3.68	32.63	2.95	4.79	29.78	3.53	4.33	30.21	3.41
FIVF	0.32	39.83	0.30	1.41	32.96	1.72	2.17	29.95	1.95
FISF	1.75	34.41	1.29	3.07	30.01	2.06	4.02	30.31	2.91
AVMF	0.85	37.58	0.57	1.89	30.09	1.48	2.71	26.46	3.37
tTVMF	0.87	36.89	0.66	2.24	29.35	1.88	2.65	31.48	2.38
PGSVMF	0.29	41.61	0.23	1.58	32.63	1.58	2.30	27.79	2.34
PRF	0.49	33.60	0.39	2.18	27.30	1.64	2.74	26.22	2.61
PGSAMF	0.36	41.36	0.26	1.39	34.48	0.99	2.74	27.32	2.81
FMPGSAMF	0.36	40.13	0.28	1.37	34.50	0.96	3.61	25.13	3.74
IPGSVF-M_{K_1}	0.29	41.55	0.23	1.59	32.69	1.07	2.00	31.48	1.61
IPGSVF-M_{K_2}	0.31	40.55	0.24	1.57	32.08	1.07	2.63	25.90	1.99
IPGSVF-$M_{K_1K_2}$	0.28	42.02	0.22	1.50	32.96	1.03	1.97	31.44	1.59

Table 11.5. Comparison of the performance in terms of MAE, PSNR and NCD using a detail of the Baboon image contaminated with different densities of impulsive noise of types I and II.

Filter	5% impulsive type I			20% impulsive type II			30% impulsive type I		
	MAE	PSNR	NCD (10^{-2})	MAE	PSNR	NCD (10^{-2})	MAE	PSNR	NCD (10^{-2})
None	2.28	23.02	3.40	13.40	16.56	11.61	13.63	15.10	18.73
VMF	13.75	21.58	4.81	15.11	20.79	5.49	14.47	21.12	5.15
FIVF	1.77	25.02	2.47	7.41	22.23	3.02	10.18	21.27	4.01
FISF	6.75	24.41	2.26	9.50	22.05	3.36	9.64	22.38	3.61
AVMF	5.72	24.15	1.88	6.99	22.78	2.84	7.61	21.74	4.71
tTVMF	2.29	27.99	0.96	8.51	22.46	3.06	8.48	22.75	3.36
PGSVMF	0.89	32.21	0.58	5.18	24.12	2.15	6.19	22.92	3.87
PRF	5.06	24.07	1.93	7.83	22.11	3.03	8.51	21.57	3.99
PGSAMF	3.19	26.00	1.08	7.06	22.81	2.42	9.77	21.30	4.10
FMPGSAMF	2.50	26.94	0.93	7.93	22.35	2.66	10.21	20.77	4.52
IPGSVF-M_{K_1}	1.14	30.14	0.80	5.33	24.01	2.24	6.65	23.20	3.63
IPGSVF-M_{K_2}	1.07	30.12	0.51	4.04	25.90	1.45	6.62	21.62	2.81
IPGSVF-$M_{K_1K_2}$	0.85	33.23	0.36	4.35	25.40	1.61	5.45	24.57	2.45

is needed to be higher when the density of contaminating noise is higher. Regarding the nature of the image, lower values of the d parameter are rather preferred for highly detailed or textured images and higher values for images with many homogeneous regions. It has been experimentally found that in the case of IPGSVF with M_{K_1} appropriate values of d are in the range $[0.900, 0.950]$. A similar behaviour is observed when using M_{K_2} and $M_{K_1K_2}$ for which the sub-optimal range of d is around $[0.940, 0.980]$ and $[0.830, 0.900]$, respectively. This is also shown in Fig. 11.7 where the optimal PSNR values of the d parameter for different images and percentages of impulsive noise type I are given.

Table 11.6. Comparison of the performance in terms of MAE, PSNR and NCD using a detail of the Peppers image contaminated with different densities of mixed impulsive noise type I and Gaussian noise.

Filter	10% impulsive type I and $\sigma = 10$ Gaussian noise			20% impulsive type I and $\sigma = 20$ Gaussian noise			30% impulsive type I and $\sigma = 30$ Gaussian noise		
	MAE	PSNR	NCD (10^{-2})	MAE	PSNR	NCD (10^{-2})	MAE	PSNR	NCD (10^{-2})
None	12.09	18.87	13.89	22.35	15.80	24.86	33.54	13.51	36.46
VMF	8.19	26.14	6.36	11.61	23.76	10.39	16.58	20.83	16.03
FIVF	8.44	25.93	8.56	13.62	22.66	13.47	18.47	19.73	18.46
FISF	7.90	26.03	6.83	11.82	23.49	10.64	15.08	21.60	12.60
AVMF	7.93	26.59	8.04	14.42	22.04	15.25	22.16	18.15	23.82
tTVMF	7.77	26.11	7.86	12.85	22.82	12.95	17.22	20.39	17.35
PGSVMF	8.17	26.36	9.01	14.77	21.94	15.57	17.40	20.50	17.02
PRF	8.54	25.44	8.44	14.63	21.27	14.51	20.29	18.93	20.51
PGSAMF	8.36	27.28	8.25	14.45	22.07	14.14	19.74	19.26	19.29
FMPGSAMF	8.33	26.23	8.48	14.36	21.55	13.41	20.38	18.60	20.10
IPGSVF-M_{K_1}	8.49	26.26	8.37	12.65	23.28	11.75	16.51	20.89	15.92
IPGSVF-M_{K_2}	8.43	25.80	7.74	12.23	23.40	10.87	16.52	20.89	15.90
IPGSVF-$M_{K_1K_2}$	8.40	26.32	8.26	13.73	22.66	12.92	16.80	20.80	16.11

Table 11.7. Average rank of performance in terms of PSNR achieved by the considered filters in the performed experiences.

Filter	Average Rank
IPGSVF-$M_{K_1K_2}$	1.72
PGSVMF	3.00
IPGSVF-M_{K_1}	3.83
tTVMF	5.17
IPGSVF-M_{K_2}	5.91
PGSAMF	6.08
FIVF	7.00
AVMF	7.42
FMPGSAMF	8.50
FISF	8.75
PRF	10.25
VMF	10.42

11.5.2 Proposed method assessment

The proposed method is assessed in front of the classical VMF [2] and the recent vector filters: *Fast Impulsive Vector Filter* (FIVF) [30], *Fuzzy Inference System Filter* (FISF) [11], *Adaptive Vector Median Filter* (AVMF) [22], *t-Student Test Vector Median Filter* (tTVMF) [3], *Peer Group Switching Vector Median Filter* (PGSVMF) [13], *Peer Region Filter* (PRF) [10], *Peer Group Switching Arithmetic Mean Filter* (PGSAMF) [36], and *Fuzzy Modified Peer Group Switching Arithmetic Mean Filter* (FMPGSAMF) [4]. These filters have been selected because of the following reasons: VMF is the most well-known vector filter and it is of common reference for all vector filters; FIVF, FISF, AVMF, tTVMF are some recent switching filters that present a good performance. In particular, FIVF and FISF are also based on fuzzy techniques; and, PGSVMF, PRF, PGSAMF and FMPGSAMF are recent switching vector filters based on

the peer group concept. The parameter setting advised by the authors in the respective works have been used in all considered filters.
For the assessment, test images in Figure 11.5 have been contaminated with different percentages of the considered impulsive noise types. This test database has been selected because it includes images presenting many homogeneous regions and sharp edges (House and Pills) and also images containing a lot of texture and fine details (Parrots and Baboon). The results for performance comparison in terms of MAE, PSNR and NCD are shown in Tables 11.2-11.6. Some outputs of the filters in comparison are shown in Figures 11.8-11.11. To summarize these results, for each considered case in Tables 11.2-11.5, we have sorted the filters in the comparison in decreasing order of PSNR performance. Then we have computed the average of the ranks achieved by each filter in the performed experiences. The result including the filters sorted in increasing order of average rank is shown in Table 11.7. After analyzing Table 11.7, the numerical results in Tables 11.2-11.5 and the visual results in Figures 11.8-11.11, the following conclusions can be drawn: Obviously, VMF provides the most smoothed images. The filters PRF, FISF, AVMF, FMPGSAMF and FIVF present some clear improvements over the VMF in terms of signal-preservation while efficiently reducing noise. However, the superior performance is achieved by the filters PGSAMF, tTVMF, PGSVMF and the proposed IPGSVF. The major differences, in terms of performance, between these techniques are listed below:

- PGSAMF: This solution is very effective when the images are contaminated with low-medium percentage of impulsive noise and specially for impulsive noise type II (see Table 11.4 central column). However, it may present some lack of robustness when similar *noisy* pixels appear very close to each other. This may happen for high percentages of noise and specially for impulsive noise type I (see Table 11.4 right column).
- tTVMF: This method performs a very accurate detection of *noise-free* pixels. However, it may eventually fail to detect *noisy* pixels if they appear close to an edge or surrounded by several impulses. This happens because in these cases the normal distribution extracted from the neighbors has a very large standard deviation and so, any pixel can easily belong to such a distribution with a quite high confidence level (for instance, see the green noise in the window in Figure 11.10 (c)).
- PGSVMF: This method accurately detects large impulses, though, it often omits small impulses (see small impulses close to the right-down corner in Figure 11.9 (c)). However, pixels in sharp borders may sometimes be regarded as noise. This happens because a sharp border makes the peer groups in each side of the border be at a

large distance which may be over the distance threshold (see blurred black-white area in Figure 11.8 (c)).

– IPGSVF: The proposed technique presents the best overall results in terms of the computed average rank when the $M_{K_1K_2}$ fuzzy metric is used. The method can accurately detect and remove impulsive noise and simultaneously preserve edges and fine details. This performance is achieved because of its two-stage based procedure. A deficiency of the proposed method is that small impulses are sometimes not correctly detected (see small impulses in white area close to the roof in Figure 11.10 (d),(e) and (f)). This drawback may not be very important if the proposed method is used in conjunction with some Gaussian noise smoothing filter since the smoothing filter will probably also smooth remaining small impulses.

We have also made some experiments using images corrupted with mixed (Gaussian-impulsive) noise in order to check whether the proposed method is able to correctly detect impulses in this case. From the results in Figure 11.11 it can be seen that the method is able to reduce impulsive noise even in the presence of Gaussian noise. However, the performance of the proposed method in the mixed noise case (see Table 11.6) is sometimes even inferior to the VMF. This is because the switching structure of the proposed filter is not appropriate to remove mixed noise and it is only able to reduce the impulses. In the case that the Gaussian noise should also be smoothed, then some Gaussian noise smoothing filter should be applied after the impulsive noise reduction.

In addition, the proposed method has been tested using real noisy images (see Figures 11.12-11.13). In the case of the image in Figure 11.12 we have used IPGSVF with $M_{K_1K_2}$ and for the image in Figure 11.13 we have used IPGSVF with M_{K_1}. We have changed the fuzzy metric to show that the method can perform well with different fuzzy metrics. The *noisy*-pixel selection made by the proposed method is compared with the selection made by the PGSAMF [36]. In the case of Figure 11.12 it can be seen that the proposed method makes a more accurate selection and that it generates a less smoothed output image. In the case of Figure 11.13 both methods perform in a similar way (and also similar if we use IPGSVF with $M_{K_1K_2}$ or M_{K_2}), but the PGSAMF still generates a little more smoothed output. However, in both cases it can be observed that the IPGSVF sometimes detect a group of several pixels as noise (for instance the up-right corner of black letter near the center of Figure 11.13 (f)). This happens because in this group of pixels there is a lot of fluctuations and no pixel can be regarded as *noise-free* with high reliability in step (i) of the method and so, no pixel is finally regarded as *noise-free*.

Conclusions

In this paper, a novel switching vector filter for impulsive noise removal using the peer group concept in the context of fuzzy metrics was introduced. The proposed filtering method is designed as such that instead of trying to find a condition able to separate impulses from noise-free data, it applies an iterative procedure to select the noise-free samples keeping the impulses isolated. Analysis of the method is provided to demonstrate the appropriateness of the iterative procedure and to show that the computational complexity of the proposed switching filter is lower than the complexity of the well-known vector median filter.
Experimental results show that the method is able to suppress noise while preserving desired image structures. The proposed method significantly outperforms classical VMF. In addition, the method has been compared with recently introduced vector filters including some based on similar peer group concepts. With respect to these filters, the filter performance has been demonstrated to be competitive and even superior in many cases.

Appendix: Computational complexity analysis

In this appendix a detailed analysis of the computational complexity of the proposed method is performed.
Let us consider a fixed value of $d \in [0,1]$ and let $\mathbf{F}_i$ be the central pixel of a $n \times n$ filter window W where $n = 2c+1, c = 1,2,\ldots$. We will say that the pixel $\mathbf{F}_j \in W$ is *close* to $\mathbf{F}_i$ if $M_K(\mathbf{F}_i, \mathbf{F}_j) \geq d$. Let us denote the probabilities of a pixel $\mathbf{F}_j$ in W to be *close* to $\mathbf{F}_i$, when $\mathbf{F}_i$ is non-corrupted (*noise-free*) or corrupted (*noisy*) by r and q, respectively. Let $\eta = n^2 - 1$ be the number of $\mathbf{F}_i$ neighbors in W.
From [36] Eq. (8), the probability that k distances ($k = m, \ldots, \eta$) are needed to diagnose $\mathbf{F}_i$ in step (i) of the proposed algorithm under the condition that it is non-corrupted is

$$f_1^1(k) = \begin{cases} \binom{k-1}{m-1} r^{m-1}(1-r)^{k-m} r & k = m, \ldots, \eta - 1 \\ \binom{\eta-1}{m-1} r^{m-1}(1-r)^{\eta-m} r + \sum_{l=0}^{m-1} \binom{\eta}{l} r^l (1-r)^{\eta-l} & k = \eta \end{cases} \tag{11.6}$$

The same probability under the condition that it is corrupted is denoted by $f_2^1(k)$ and its expression is similar to (11.6), but replacing r by q. Hence, the mean number of distances needed to diagnose the central pixel in step (i) is

$$s_1(p) = (1-p)\sum_{k=m}^{\eta} f_1^1(k)\cdot k + p\cdot\sum_{k=m}^{\eta} f_2^1(k)\cdot k \tag{11.7}$$

where p is the probability of the noise appearance. The probability of a pixel to be *non-assigned* in step (i) is

$$t_1(p) = (1-p)\sum_{l=0}^{m-1}\binom{\eta}{l} r^l(1-r)^{\eta-l} + p\sum_{l=0}^{m-1}\binom{\eta}{l} q^l(1-q)^{\eta-l} \tag{11.8}$$

Now, in order to analyze step (ii), let us also consider each *non-assigned* pixel $\mathbf{F}_i$ centered in a $n\times n$ filter window W. The average number of *noise-free* pixels in W which were diagnosed in step (i) is

$$\lambda_1(p) = (1-t_1(p))(n^2-1) \tag{11.9}$$

From now on, if confusion is not possible, we will omit to mention p.
Let us denote the probabilities of a *non-assigned* pixel of step (i) in W to be *close* to $\mathbf{F}_i$ when $\mathbf{F}_i$ is non-corrupted or corrupted by R and Q, respectively. In the following, we will find the probability of a pixel to be declared as *non-assigned* in the first iteration of step (ii) assuming that $t_1 > p$ (which agrees with the filter's design). Next, since the argument is the same and R and Q are assumed to be constant for all the iterations, we will prove our assertion but in the case of the $(N+1)$th iteration of step (ii) on the basis of the Nth iteration.
So, let us denote the probability of a pixel to be *non-assigned* in the Nth iteration by $t_N,\ N = 2,3,\ldots$ and assume $t_N > p$ (which also agrees with the filter's design). The average number of pixels in W which have been already declared as *non-assigned* in the Nth iteration is

$$\lambda_N = (t_{N-1} - t_N)(n^2-1),\ N = 2,3,\ldots \tag{11.10}$$

Now, let us denote the probabilities of a *non-assigned* pixel of the Nth iteration to be declared as *non-assigned* in the $(N+1)$th iteration, under the condition that it is not corrupted or corrupted, by $\tau_1(\lambda_N)$ and $\tau_2(\lambda_N)$, respectively. If λ_N is a positive integer then we have that $\tau_1(\lambda_N) = (1-R)^{\lambda_N}$ and that $\tau_2(\lambda_N) = (1-Q)^{\lambda_N}$.
Let us now suppose that λ_N is not integer and in this case denote $[\lambda_N]$ the integer value such that $[\lambda_N] < \lambda_N < [\lambda_N]+1$. Then, by linear interpolation we obtain

$$\tau_1(\lambda_N) = ([\lambda_N]+1-\lambda_N)(1-R)^{[\lambda_N]} + (\lambda_N - [\lambda_N])(1-R)^{[\lambda_N]+1} \tag{11.11}$$

and a similar expression is obtained for $\tau_2(\lambda_N)$ replacing R by Q.

The probability of a pixel in the image to be *non-assigned* in the $(N+1)$th iteration is

$$t_{N+1} = t_N \left(\frac{t_N - p}{t_N} \tau_1(\lambda_N) + \frac{p}{t_N} \tau_2(\lambda_N) \right) = (t_N - p) \cdot \tau_1(\lambda_N) + p \cdot \tau_2(\lambda_N) \tag{11.12}$$

Clearly, $t_{N+1} \leq t_N$. Further, $t_{N+1} = t_N$ if and only if $\tau_i(\lambda_N) = 1$, i.e. if and only if $\lambda_N = 0$.
The following expression denotes the probability $f_1^{N+1}(k)$ that k distances $k = 1, 2, \ldots, \lambda_N$ are needed to diagnose a not-corrupted pixel $\mathbf{F}_i$ in the Nth iteration if λ_N is a positive integer and $\lambda_N > 1$,

$$f_1^{N+1}(k) = \begin{cases} (1-R)^{k-1} \cdot R & k = 1, \ldots, \lambda_N - 1 \\ (1-R)^{\lambda_N - 1} \cdot R + (1-R)^{\lambda_N} & k = \lambda_N \end{cases} \tag{11.13}$$

Otherwise, when $\lambda_N = 1$ then $f_1^{N+1}(k) = f_1^{N+1}(1) = 1$.
Now we study the probability f_1^{N+1} when λ_N is not integer, and distinguish 3 cases.

a) $\lambda_N > 2$, then $f_1^{N+1}(k) =$

$$\begin{cases} (1-R)^{k-1} \cdot R & k = 1, \ldots, [\lambda_N] - 1 \\ ([\lambda_N] + 1 - \lambda_N + (\lambda_N - [\lambda_N]) \cdot R)\,(1-R)^{[\lambda_N]-1} & k = [\lambda_N] \\ (\lambda_N - [\lambda_N])(1-R)^{[\lambda_N]} & k = [\lambda_N] + 1 \end{cases} \tag{11.14}$$

b) $\lambda_N \in (1, 2)$, then

$$f_1^{N+1}(k) = \begin{cases} 2 - \lambda_N + (\lambda_N - 1) \cdot R & k = 1 \\ (\lambda_N - 1) \cdot (1-R) & k = 2 \end{cases} \tag{11.15}$$

c) $\lambda_N \in (0, 1)$, then

$$f_1^{N+1}(k) = \begin{cases} 1 - \lambda_N & k = 0 \\ \lambda_N & k = 1 \end{cases} \tag{11.16}$$

Finally when $\lambda_N = 0$, obviously

$$f_1^{N+1}(0) = 1 \tag{11.17}$$

The same probability under the condition that the central pixel is corrupted is obtained replacing R by Q in (11.13)-(11.17) and is denoted by $f_2^{N+1}(k)$.
In the following we compute the average number of distances needed to diagnose the central pixel in the $(N+1)$th iteration. If we suppose that λ_N is a positive integer and that $t_N > p$ then the average number of distances is

$$s^*_{N+1}(p) = \frac{t_N - p}{t_N} \cdot \sum_{k=1}^{\lambda_N} f_1^{N+1}(k) \cdot k + \frac{p}{t_N} \cdot \sum_{k=1}^{\lambda_N} f_2^{N+1}(k) \cdot k,\ N = 1, 2, \ldots \tag{11.18}$$

When λ_N is not integer, by (11.14)-(11.16) the above sum is extended from $k = 1$ to $k = [\lambda_N] + 1$ when $\lambda_N > 1$, and from $k = 0$ to $k = 1$ when $\lambda_N \in (0, 1)$. If $\lambda_N = 0$ then $s^*_{N+1}(p) = 0$.
So the mean number of distances needed to diagnose any pixel in the image is

$$s(p) = \sum_{J \geq 1} s_J(p) \tag{11.19}$$

where

$$s_J(p) = t_{J-1} \cdot s^*_J(p),\ J = 2, 3, \ldots \tag{11.20}$$

In our conditions we only can assert that the decreasing sequence $\{t_N\}$ converges in $[p, 1]$ since it is lower bounded. Therefore from a certain (N_0)th iteration all differences $t_J - t_{J+1},\ J \geq N_0$, are close to 0 and then by (11.10) λ_J is close to 0, hence by (11.16) $s_J(p)$ is negligible, for $J \geq N_0$.
According to the above, the algorithm can be necessarily executed in a finite number of iterations. Thus, it exists some Nth iteration such that $\lambda_N = 0$. Hence, by (11.17) $s^*_{N+1}(p) = 0$ and so $s_{N+1}(p) = 0$. Now, since $\lambda_N = 0$ implies $\tau_i(\lambda_N) = 1,\ (i = 1, 2)$(and conversely) then, by (11.12) $t_{N+1} = t_N$ and by (11.10) $\lambda_{N+1} = 0$. In this case, $s_{N+2}(p) = 0$, and employing a similar argument we can state that $s_{N+i}(p) = 0$, for all $i \geq 1$. Therefore, (11.19) contains a finite number of terms. Mostly, when using a 3×3 filter window the algorithm finalizes in 8 iterations, and only the first five values of $s_J(p)$ are really significative to approach the computational complexity.
Note that the algorithm does not include the condition that $t_J > p$ for $J = 1, 2, \ldots$, so some t_J could satisfy $t_J \leq p$. However, before this may occur the differences $t_J - t_{J-1}$ will be very close to 0 and, taking into account (11.10), (11.16), (11.18) and (11.19), the corresponding values of $s_J(p)$ can be ignored for the computational complexity calculation.
Finally, if we denote by $t(p)$ the probability of a pixel in the image to be declared as *noisy* in step (iv) (this value can be approximated by $t_N(p)$ when $t_N(p) - t_{N+1}(p)$ is close to 0), then the average number of distances per pixel needed for the filtering including those computed by the VMF operation over the *noisy* pixels is

$$c_d(p) = s(p) + t(p)\binom{\eta}{2}.$$

References

1. H. Allende, J. Galbiati, A non-parametric filter for image restoration using cluster analysis, *Pattern Recognition Letters* 25 8 (2004) 841-847.
2. J. Astola, P. Haavisto, Y. Neuvo, Vector Median Filters, *Proc. IEEE.* 78 4 (1990) 678-689.
3. J. Camacho, S. Morillas, P. Latorre, Efficient impulsive noise suppression based on statistical confidence limits, *Journal of Imaging Science and Technology*, to appear.
4. J.G. Camarena, V. Gregori, S. Morillas, A. Sapena, Fast detection and removal of impulsive noise using peer groups and fuzzy metrics, *revised version submitted to Journal of Visual Communication and Image Representation in May 2006*.
5. Y. Deng, C. Kenney, MS Moore, BS Manjunath, Peer group filtering and perceptutal color image quantization, *Proceedings of IEEE international symposium on circuits and systems* 4 (1999) 21-4.
6. F.J. Gallegos-Funes, V. Ponomaryov, Real-time image filtering scheme based on robust estimators in presence of impulse noise, *Real-Time Imaging* 10 2 (2004) 69-80.
7. A. George, P. Veeramani, On Some results in fuzzy metric spaces, *Fuzzy Sets and Systems* 64 3 (1994) 395-399.
8. V. Gregori, S. Romaguera, Characterizing completable fuzzy metric spaces, *Fuzzy Sets and Systems* 144 3 (2004) 411-420.
9. G. Hewer, C. Kenney, L. Peterson, A. Van Nevel, Applied partial differential variational techniques, *Proceedings of International Conference on Image Processing ICIP'97*, 3 (1997) 372-375.
10. J. Y. F. Ho, Peer region determination based impulsive noise detection, *Proceedings of International Conference on Acoustics, Speech and Signal Processing ICASSP'03* 3 (2003) 713-716.
11. S. Hore, B. Qiu, and H.R. Wu, Improved vector filtering for color images using fuzzy noise detection, *Optical Engineering* , 42 6 (2003) 1656-1664.
12. D.G. Karakos, P.E. Trahanias, Generalized multichannel image-filtering structure, *IEEE Transactions on Image Processing* 6 7 (1997) 1038-1045.
13. C. Kenney, Y. Deng, BS Manjunath, G. Hewer, Peer group image enhancement, *IEEE Transactions on Image Processing* 10 2 (2001) 326-334.
14. J. Kim, L.M. Wills, D.S. Wills, Effective detection and elimination of impulse noise for reliable 4:2:0 YCBCR signals prior to compression encoding, *Proceedings of the 30th IEEE conference on Acoustics, Speech and Signal Procesing ICASSP'05* 2 (2005) 1005-1008.

15. L. Lucat, P. Siohan, and D. Barba, Adaptive and Global Optimization Methods for Weighted Vector Median Filters, *Signal Processing: Image Communication* 17 7 (2002) 509-524.
16. R. Lukac, Adaptive vector median filtering, *Pattern Recognition Letters* 24 12 (2003) 1889-1899.
17. R. Lukac, B. Smolka, K. Martin, K.N. Plataniotis, A.N. Venetsanopoulos, Vector Filtering for Color Imaging, *IEEE Signal Processing Magazine, Special Issue on Color Image Processing* 22 1 (2005) 74-86.
18. R. Lukac, K.N. Plataniotis, B. Smolka, A.N. Venetsanopoulos, cDNA Microarray Image Processing Using Fuzzy Vector Filtering Framework, *Fuzzy Sets and Systems: Special Issue on Fuzzy Sets and Systems in Bioinformatics* 152 1 (2005) 17-35.
19. R. Lukac, K.N. Plataniotis, B. Smolka, A.N. Venetsanopoulos, A Multichannel Order-Statistic technique for cDNA Microarray Image Processing, *IEEE Transactions on Nanobioscience* 3 4 (2004) 272-285.
20. R. Lukac, K.N. Plataniotis, B. Smolka, A.N. Venetsanopoulos, Generalized Selection Weighted Vector Filters, *EURASIP Journal on Applied Signal Processing: Special Issue on Nonlinear Signal and Image Processing* 2004 12 (2004) 1870-1885.
21. R. Lukac, Adaptive Color Image Filtering Based on Center Weighted Vector Directional Filters, *Multidimensional Systems and Signal Processing* 15 2 (2004) 169-196.
22. R. Lukac, K.N. Plataniotis, A.N. Venetsanopoulos, B. Smolka, A Statistically-Switched Adaptive Vector Median Filter, *Journal of Intelligent and Robotic Systems* 42 4 (2005) 361-391.
23. R. Lukac, B. Smolka, K.N. Plataniotis, A.N. Venetsanopoulos, Vector sigma filters for noise detection and removal in color images, *Journal of Visual Communication and Image Representation* 17 1 (2006) 1-26.
24. R. Lukac, K.N. Plataniotis, A.N. Venetsanopoulos, Color image image denoising using evolutionary computation, *International Journal of Imaging Systems and Technology* 15 5 (2005) 236-251.
25. R. Lukac, K.N. Plataniotis, A taxonomy of color image filtering and enhancement solutions, in *Advances in Imaging and Electron Physics*, (eds.) P.W. Hawkes, Elsevier, 140, 187-264, 2006.
26. Z. Ma, D. Feng, H.R. Wu, A neighborhood evaluated adaptive vector filter for suppression of impulsive noise in color images, *Real-Time Imaging* 11 5-6 (2005) 403-416.
27. Z. Ma, H. R. Wu, B. Qiu, A window adaptive hybrid vector filter for color image restoration, *Proceedings of International Conference on Acoustics, Speech and Signal Processing ICASSP'04* 3 (2004) 205-208.
28. Z. Ma, H. R. Wu, B. Qiu, A robust structure-adaptive hybrid vector filter for color image restoration, *IEEE Trans. Image Processing* 14 12 (2005) 1990-2001.
29. S. Morillas, V. Gregori, G. Peris-Fajarnés, P. Latorre, A new vector median filter based on fuzzy metrics, *ICIAR 2005, Lecture Notes in Computer Science* 3656 (2005) 81-90.

30. S. Morillas, V. Gregori, G. Peris-Fajarnés, P. Latorre, A fast impulsive noise color image filter using fuzzy metrics, *Real-Time Imaging* 11 5-6 (2005) 417-428.
31. S. Morillas, V. Gregori, A. Sapena, Vector filtering approaches based on a fuzzy metric, *submitted to Fuzzy Sets and Systems in June 2006.*
32. K.N. Plataniotis, A.N. Venetsanopoulos, *Color Image processing and applications* (Springer-Verlag, Berlin, 2000).
33. V.I. Ponomaryov, F.J. Gallegos-Funes, A. Rosales-Silva, Real-Time color imaging based on RM-filters for impulsive noise reduction, *Journal of Imaging Science and Technology* 49 3 (2005) 205-219.
34. B. Smolka, R. Lukac, A. Chydzinski, K.N. Plataniotis, W. Wojciechowski, Fast adaptive similarity based impulsive noise reduction filter, *Real-Time Imaging, Special Issue on Spectral Imaging* 9 4 (2003) 261-276.
35. B. Smolka, K.N. Plataniotis, A. Chydzinski, M. Szczepanski, A.N. Venetsanopoulos, K. Wojciechowski, Self-adaptive algorithm of impulsive noise reduction in color images, *Pattern Recognition* 35 8 (2002) 1771-1784.
36. B. Smolka, A. Chydzinski, Fast detection and impulsive noise removal in color images, *Real-Time Imaging* 11 5-6 (2005) 389-402.
37. P.E. Trahanias, D. Karakos, A.N. Venetsanopoulos, Directional processing of color images: theory and experimental results, *IEEE Trans. Image Process.* 5 6 (1996) 868-880.

12 Contribution (ix)

S. Morillas, S. Schulte, E.E. Kerre, G. Peris-Fajarnés, A new fuzzy impulse noise detection method for colour images, *SCIA07, Lecture Notes in Computer Science, 4522 (2007) 492-501*.

Abstract

This paper focuses on fuzzy image denoising techniques. In particular, we develop a new fuzzy impulse noise detection method. The main difference between the proposed method and other state-of-the-art methods is the usage of the colour components for the impulse noise detection method that are used in a more appropriate manner. The idea is to detect all noisy colour components by observing the similarity between (i) the neighbours in the same colour band and (ii) the colour components of the two other colour bands. Numerical and visual results illustrate that the proposed detection method can be used for an effective noise reduction method.

12.1 Introduction

Reduction of noise in digital images is one of the most basic image processing operations.
Recently a lot of fuzzy based methods have shown to provide efficient image filtering [5, 9, 18, 19, 20, 21, 22, 23].
These fuzzy filters are mainly developed for images corrupted with fat-tailed noise like impulse noise. Although these filters are especially developed for greyscale images, they can be used to filter colour images by applying them on each colour component separately. This approach generally introduces many colour artefacts mainly on edge and texture elements. To overcome these problems several nonlinear vector-based approaches were successfully introduced [1, 2, 3, 4, 7, 8, 12, 13, 14, 15, 16, 17].
Nevertheless all these vector-based methods have the same major drawbacks, i.e. (i) the higher the noise level is the lower the noise reduction

capability is in comparison to the component-wise approaches and (ii) they tend to cluster the noise into a larger array which makes it even more difficult to reduce. The reason for these disadvantages is that the vector-based approaches consider each pixel as a whole unit, while the noise can appear in only one of the three components.
In this paper another colour filtering method is proposed. As in most other applications we use the RGB colour space. The main difference between the proposed method and other state-of-the-art methods is the usage of the colour components for the impulse noise detection. The idea behind this detection phase is to detect all colour components which are dissimilar (i) to the neighbours in the same colour band and (ii) to the colour components of the two other colour bands. The proposed method illustrates the advantage of using the colour information in a more appropriate way to improve the noise reduction method. This work should also stimulate more research in the field of colour processing for image denoising.
The paper is organized as follows: in section 12.2 the new colour based impulse noise detection method is explained. A noise reduction method that uses the performed detection is described in section 12.3. Section 12.4 illustrates the performance of the proposed method in comparison to other state-of-the-art methods and the conclusions are finally drawn in section 12.5.

12.2 Fuzzy impulse noise detection

In this section a novel fuzzy impulse noise detection method for colour images is presented. In comparison to the vector-based approaches the proposed fuzzy noise detection method is performed in each colour component separately. This implies that a fuzzy membership degree (within $[0, 1]$) in the fuzzy set *noise-free* will be assigned to each colour component of each pixel. When processing a colour, the proposed detection method examines two different relations between the central colour and its neighbouring colours to perform the detection: it is checked both (i) whether each colour component value is similar to the neighbours in the same colour band and (ii) whether the value differences in each colour band corresponds to the value differences in the other bands. In the following, the method is described in more detail.
Since we are using the RGB colour-space, the colour of the image pixel at position i is denoted as the vector $\mathbf{F}_i$ which comprises its red (R), green (G), and blue (B) component, so $\mathbf{F}_i = (F_i^R, F_i^G, F_i^B)$. Let us consider the use of a sliding filter window of size $n \times n$, with $n = 2c+1$ and $c \in \mathbb{N}$, which should be centered at the pixel under processing. The colours within the filter window are indexed according to the scheme shown in Figure 12.1 for the 3×3 case. For larger window sizes the indexing will be performed in

1	2	3
4	0	5
6	7	8

Fig. 12.1. Vector index in the filter window.

an analogous way. The colour pixel under processing is always represented by $\mathbf{F}_0 = (F_0^R, F_0^G, F_0^B)$.
First, we compute the absolute value differences between the central pixel $\mathbf{F}_0$ and each colour neighbour as follows:

$$\Delta F_k^R = |F_0^R - F_k^R|,\ \Delta F_k^G = |F_0^G - F_k^G|,\ \Delta F_k^B = |F_0^B - F_k^B| \tag{12.1}$$

where $k = 1, \ldots, n^2 - 1$ and $\Delta F_k^R, \Delta F_k^G, \Delta F_k^B$ denote the value difference with the colour at position k in the R, G and B component, respectively. Now, we want to check if these differences can be considered as small. Since small is a linguistic term, it can be represented as a fuzzy set [10]. Fuzzy sets in turn can be represented by a membership function. We compute the membership degree in the fuzzy set $small_1$ using the $1 - S$-membership function [10] over the computed differences. This function is defined as follows

$$1 - S(x) = \begin{cases} 1 & \text{if } x < \alpha_1 \\ 1 - 2\left(\frac{x-\gamma_1}{\gamma_1-\alpha_1}\right)^2 & \text{if } \alpha_1 < x < \frac{\alpha_1+\gamma_1}{2} \\ 2\left(\frac{x-\alpha_1}{\gamma_1-\alpha_1}\right)^2 & \text{if } \frac{\alpha_1+\gamma_1}{2} < x < \gamma_1 \\ 0 & \text{if } x > \gamma_1 \end{cases} \tag{12.2}$$

where we have experimentally found that $\alpha_1 = 10$ and $\gamma_1 = 50$ receive satisfying results in terms of noise detection. In this case we denote $1 - S$ by S_1, so that $S_1(\Delta F_k^R)$, $S_1(\Delta F_k^G)$, $S_1(\Delta F_k^B)$ denote the membership degrees in the fuzzy set $small_1$ of the computed differences with respect to the colour at position k. Now, we use the values $S_1(\Delta F_k^R)$, $S_1(\Delta F_k^G)$, $S_1(\Delta F_k^B)$ for $k = 1, \ldots, n^2 - 1$ to decide whether the values F_0^R, F_0^G and F_0^B are similar to its component neighbours. The calculation of the membership degree in the fuzzy set *noise-free* is illustrated for the R component only but is performed in an analogous way for the G and B component. Because of the noise some of the neighbours could be corrupted with noise and therefore the values of $S_1(\Delta F_k^R)$ for $k = 1, ..., n^2 - 1$ are sorted in descending order so that only the most relevant differences are considered. The value occupying the j-th position in the ordering is denoted by $S_1(\Delta F_{(j)}^R)$. Next, the similarity to the neighbour values is determined by checking that the value difference should be *small* with respect to, at least, a certain number K of neighbours. The number K of

considered neighbours will be a parameter of the filter and its importance is discussed in section 12.4. So, we apply a fuzzy conjunction operator (fuzzy AND operation represented here by the triangular product t-norm [11, 6]) among the first K ordered membership degrees in the fuzzy set $small_1$. The conjunction is calculated as follows:

$$\mu^R = \prod_{j=1}^{K} S_1(\Delta F^R_{(j)}), \tag{12.3}$$

where μ^R denotes the degree of similarity of F^R_0 with respect to K of its neighbours in the most favourable case. Notice that in the case that F^R_0 is noisy a low similarity degree μ^R should be expected.
The next step of the detection process is to determine whether the observed differences in the R component of the processed colour corresponds to the same observations in the G and B component. We want to check if these differences agree at least for a certain number K of neighbours. Then, for each neighbour we compute the absolute value of the difference between the membership degrees in the fuzzy set $small_1$ for the red and the green and for the red and the blue components, i.e. $|S_1(\Delta F^R_k) - S_1(\Delta F^G_k)|$ and $|S_1(\Delta F^R_k) - S_1(\Delta F^B_k)|$, where $k = 1, \ldots, n^2 - 1$, respectively. Now, in order to see if the computed differences are *small* we compute their fuzzy membership degrees in the fuzzy set $small_2$. A $1 - S$-membership function is also used but now we used $\alpha_2 = 0.10$ and $\gamma_2 = 0.25$, which also have been determined experimentally. In this case we denote the membership function as S_2. So we calculate

$$\begin{aligned} \mu^{RG}_k &= S_2(|S_1(\Delta F^R_k) - S_1(\Delta F^G_k)|), \\ \mu^{RB}_k &= S_2(|S_1(\Delta F^R_k) - S_1(\Delta F^B_k)|), \end{aligned} \tag{12.4}$$

where μ^{RG}_k and μ^{RB}_k denote the degree in which the observed difference in the red component is similar to the observed difference in the green and blue components with respect to the colour located at position k, respectively. Now, since we want to require that the differences are similar with respect to at least K neighbours, the values of μ^{RG}_k and μ^{RB}_k are also sorted in descending order, where $\mu^{RG}_{(j)}$ and $\mu^{RB}_{(j)}$ denote the values ranked at the j-th position. Consequently, the joint similarity with respect to K neighbours is computed as

$$\mu^{RG} = \prod_{j=1}^{K} \mu^{RG}_{(j)}, \quad \mu^{RB} = \prod_{j=1}^{K} \mu^{RB}_{(j)}, \tag{12.5}$$

where μ^{RG} and μ^{GB} denote the degree in which the observed differences for the red component are similar to the observed differences in the green and blue components, respectively. Notice that if F^R_0 is noisy and F^G_0

and F_0^B are not, then the observed differences can hardly be similar and therefore, low values of μ^{RG} and μ^{RB} are expected.
Finally, the membership degree in the fuzzy set *noise-free* for F_0^R is computed using the following fuzzy rule 3

Fuzzy Rule 3 *Defining the membership degree $NF_{F_0^R}$ for the red component F_0^R in the fuzzy set* noise-free*:*

IF μ^R *is* large *AND* μ^{RG} *is* large *AND* μ^G *is* large OR
μ^R *is* large *AND* μ^{RB} *is* large *AND* μ^B *is* large
THEN *the noise-free degree of* F_0^R *is* large

A colour component is considered as noise-free if (i) it is similar to some of its neighbour values (μ^R) and (ii) the observed differences with respect to some of its neighbours are similar to the observed differences in some of the other colour components (μ^{RG} and μ^{GB}). In addition, the degrees of similarity of the other components values with respect to their neighbour values, i.e. μ^G and μ^B, are included so that a probably noisy component (with a low μ^G or μ^B value) can not be taken as a reference for the similarity between the observed differences. The fuzzy rule 3 contains four conjunctions and one disjunction. In fuzzy logic triangular norms and co-norms are used to represent conjunctions and disjunctions [11, 6], respectively. Since we use the product triangular norm to represent the fuzzy AND (conjunction) operator and the probabilistic sum co-norm to represent the fuzzy OR (disjunction) operator the noise-free degree of F_0^R which we denote as $NF_{F_0^R}$ is computed as follows:

$$NF_{F_0^R} = \mu^R \mu^{RG} \mu^G + \mu^R \mu^{RB} \mu^B - \mu^R \mu^{RG} \mu^G \mu^R \mu^{RB} \mu^B. \tag{12.6}$$

Notice that all the variables in the antecedent of the fuzzy rule 3 are already appropriate fuzzy values, so that no *fuzzyfication* is needed. Moreover, since we aim at computing a fuzzy noise-free degree, any *defuzzyfication* is neither needed.
Analogously to the calculation of the noise-free degree for the red component described above, we obtain the noise-free degrees of F_0^G and F_0^B denoted as $NF_{F_0^G}$ and $NF_{F_0^B}$ as follows

$$\begin{aligned} NF_{F_0^G} &= \mu^G \mu^{RG} \mu^R + \mu^G \mu^{GB} \mu^B - \mu^G \mu^{RG} \mu^R \mu^G \mu^{GB} \mu^B, \\ NF_{F_0^B} &= \mu^B \mu^{RB} \mu^R + \mu^B \mu^{GB} \mu^G - \mu^B \mu^{RB} \mu^R \mu^B \mu^{GB} \mu^G. \end{aligned} \tag{12.7}$$

In fuzzy logic, involutive negators are commonly used to represent negations. We use the standard negator $N_s(x) = 1 - x$, with $x \in [0, 1]$ [11]. By using this negation we can also derive the membership degree in the fuzzy set *noise* for each colour component, i.e. $N_{F_0^R} = 1 - NF_{F_0^R}$, where N denotes the membership degree in the fuzzy set *noise*. An example of the proposed detection method is shown in Figure 12.2.

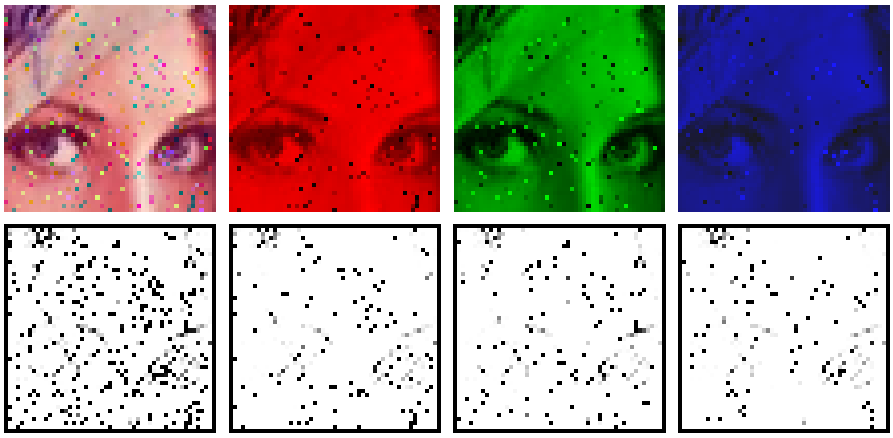

(a) (b) (c) (d)

Fig. 12.2. An example of the proposed noise detection performance, with (a)-(d) Detail of the "Lena" image contaminated with 10% random-value impulse noise in each colour channel, and the computed noise-free degrees. White/dark points indicate a high/low noise-degree, respectively.

12.3 Image denoising method

Now we briefly explain an image denoising method that uses the fuzzy detection in section 12.2. The image is denoised so that (i) each colour component is smoothed according to its noisy degree and (ii) the colour information is used to estimate the output values. We propose to compute a weight for each colour component in order to calculate a weighted averaging to obtain the output. Now we illustrate the case of the R component but it is done in an analogous way for the G and B components. The denoised R component is obtained as follows

$$\hat{F}_0^R = \frac{\sum_{k=0}^{n^2-1} W_{F_k^R} F_k^R}{\sum_{k=0}^{n^2-1} W_{F_k^R}} \tag{12.8}$$

where $\hat{F}_0^R$ denotes the estimated value for the R component, $F_k^R, k = 0, ..., n^2 - 1$ denote the R component values in the filter window and $W_{F_k^R}$ are their respective weights. The weight of the component being processed $W_{F_0^R}$ is set proportionally to its noise-free degree $NF_{F_0^R}$ so that it will be less weighted, and therefore more smoothed, if its noise-free degree is lower. The weight of the neighbour components is set inversely proportional to the noise-free degree of the component being denoised $NF_{F_0^R}$. Therefore, the neighbours are more weighted as $NF_{F_0^R}$ is lower.

In addition, in order to take into account the colour information, we will weigh more those components F_k^R for which it can be observed that F_k^G is similar to F_0^G or that F_k^B is similar to F_0^B. The underlying reasoning is that if two colours have similar G or B components then it is observed that the R component is also similar. Notice that in a extremely noisy situation it may happen that $W_{F_k^R} = 0, \forall k$ and then the weighted average cannot be performed. In such situations we perform a weighted vector median (WVM) operation, instead. In the WVM the weight of each vector should be set according to the vector noise-free degree which is computed as the conjunction of the noise-free degree of its RGB components.

12.4 Parameter setting and experimental results

In this section we evaluate the performance of the proposed method and compare it with the performance of other methods. We use the Peak Signal-to-Noise Ratio (PSNR) [16] as objective measure to evaluate the quality of the filtered images.

In order to set the K parameter of the filter we have taken different images and we have contaminated them with random-value impulse noise varying its percentage from 1% to 50% in each colour component. We have computed the performance (PSNR) achieved by the proposed filter using a 3×3 filter window for all possible values of $K \in \{1, \ldots, 8\}$. The obtained results seem to indicate that the most appropriate values of the K parameter are $K = 2, 3$. When the images are contaminated with low-medium percentages of noise, setting $K = 2, 3$ makes the filter able to properly detect and reduce impulse noise while preserving noise-free image areas, specially edges and textures. However, when the percentage of noise is high it is observed that some clusters of similar noisy pixels may occasionally appear in the noisy images. Using a value of $K = 2, 3$ may not be able to reduce clusters of noisy pixels larger than or equal to 3 or 4 pixels. This problem can be solved by using a larger value for K (maybe $K = 4, 5$), but in this case the performance for low densities of noise would be far from optimal because the detail-preserving ability is not so good as it is for lower values of K. Instead of this, we propose to perform a filtering based on a two-step approach. In the first step the noisy image is filtered using a 3×3 window and $K = 2$. In this step, isolated noisy pixels are reduced while uncorrupted edges and details are properly preserved. In the second step, the image is now filtered using a 5×5 window and $K = 5$. This step is intended to remove possible clusters of noisy pixels that may still remain in the image.

In the following the performance of the proposed filtering procedure, which we will entitle as *impulse noise reduction* method (INR), is compared to the performance of other state-of-the-art filters. The set of filters

Table 12.1. Some experimental results for comparison in terms of PSNR using the Baboon image corrupted with different densities of random-value impulse noise.

Filter	5%	10%	15%	20%	25%	30%	40%
	PSNR	PSNR	PSNR	PSNR	PSNR	PSNR	PSNR
None	21.98	18.95	17.18	15.95	15.01	14.18	12.97
VMF	22.95*	22.68*	22.35*	21.93*	21.70	21.46	20.77
PGSF	25.22*	24.00*	22.83*	22.04	21.51	20.95	19.66
FISF	25.29*	24.08*	23.33*	22.96*	22.39*	21.75*	20.74
FIDRMC	26.09*	25.48*	24.72*	24.02*	23.30*	22.86	21.85
UF	24.17*	23.94*	23.65*	23.37*	23.07*	22.72*	21.95
FRINRM	29.12*	26.85*	25.25	24.55	23.75	22.82	20.29
INR	**30.64***	**28.88***	**27.03**	**25.99**	**25.09**	**24.24**	**22.61**

Table 12.2. Some experimental results for comparison in terms of PSNR using the Boat image corrupted with different densities of random-value impulse noise.

Filter	5%	10%	15%	20%	25%	30%	40%
	PSNR	PSNR	PSNR	PSNR	PSNR	PSNR	PSNR
None	21.75	18.78	16.99	15.79	14.82	13.99	12.73
VMF	30.28*	29.42*	28.20*	26.70*	26.11	25.46	23.81
PGSF	33.42*	30.30*	28.45	27.24	26.08	24.64	22.08
FISF	31.63*	30.14*	29.01*	27.80*	26.73*	25.16*	23.87
FIDRMC	34.25*	32.41*	31.00	29.79	29.05	27.95	25.80
UF	33.08*	32.13*	31.32*	30.46*	29.65*	28.67*	**26.79**
FRINRM	36.80*	32.38	31.28	30.10	28.88	27.14	23.07
INR	**38.48***	**34.77***	**32.84**	**31.36**	**30.31**	**29.10**	26.37

chosen for the comparison includes some filters for grayscale images applied in a component wise way (UF [7] and FRINRM [19]) and some colour image filters (VMF [1], PGSF [17], FISF [8] and FIDRMC [20]). Notice that some of the mentioned filters are also based on fuzzy concepts (FRINRM, FISF and FIDRMC). We have used the three well-known images Baboon, Boats and Parrots for the tests. These images have been corrupted with different percentages of random-value impulse noise in each colour channel. We have used the following percentages: 5%, 10%, 15%, 20%, 25%, 30%, 40%.

Since the proposed method uses a two-step procedure we have also filtered the test-images with the proposed filters using an analogous two-step design. The first step uses a 3×3 filter window where we used the (optimal) parameter setting suggested in the corresponding works. After

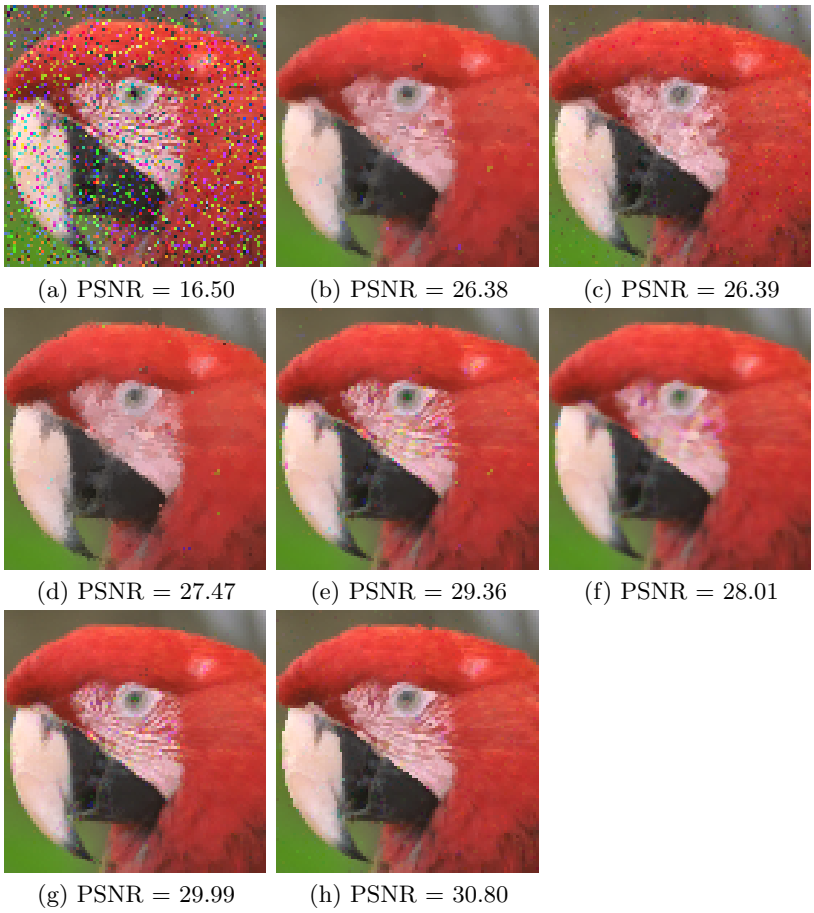

(a) PSNR = 16.50 (b) PSNR = 26.38 (c) PSNR = 26.39

(d) PSNR = 27.47 (e) PSNR = 29.36 (f) PSNR = 28.01

(g) PSNR = 29.99 (h) PSNR = 30.80

Fig. 12.3. Visual comparison of filters performance. (a) Detail of Parrots image with 15% of random-value impulse noise in each colour channel and outputs from (b) VMF, (c) PGSF, (d) FISF, (e) FIDRMC, (f) UF, (g) FRINRM and (h) INR.

the first step we have performed a second step where we use a 5×5 window size and where the corresponding (optimal) parameters are changed accordingly to the number of pixels in the window. In Tables 12.1-12.2 we have illustrated the PSNR performance achieved by all filters. The performance of the state-of-the-art methods included in the tables corresponds with the best performance achieved by the first or second step. Numbers followed by a $*$ indicate that the best performance is achieved in the first step. If no $*$ is used then the best performance is achieved by the second step. Some outputs of the filters for visual comparison are included in Figure 12.3 using a detail of the Parrots image corrupted by

15% of noise in each colour channel. From these results we can make the following conclusions:

- The proposed method generally receives the best PSNR values, which indicates that the proposed method receives the best filtering capability. Other filters such as the UF, may eventually receive slightly better PSNR values however, from the visual results we illustrate that the other methods have some important disadvantages in comparison to the proposed method.
- From the images we observe the main problem of the filtering algorithms that are applied component-wise, i.e. they even introduce (impulse like) colour artefacts in heterogeneous areas like edges or fine texture areas. By processing each component separately it often happens that colour component differences were destroyed.
- The vector based approaches do not introduce artefacts but tend to cluster the noise in larger areas, as in the case of PGSF. This makes it much more difficult to reduce the remaining noise. Additionally we observe that the results from the vector based approaches tend to make the images much blurrier (smoother) than the other methods so that important image structures are destroyed.
- The best visual results were obtained by the proposed method. We observe that the proposed method reduces the noise very well, while preserving the colour information and the important image features like edges and textures.

From both the numerical and visual results we can conclude that the proposed method can be advised for reducing random-value impulse noise in colour images since it generally outperforms other state-of-the-art methods.

Conclusion

In this paper a new fuzzy filter for impulse noise reduction in colour images is presented. The main difference between the proposed method (denoted as INR) and other classical noise reduction methods is that the colour information is taken into account in a more appropriate way (i) to develop a better impulse noise reduction method and (ii) to develop a noise reduction method which reduces the noise effectively. The advantages of the proposed method are (i) it reduces random-value impulse noise (for low and high noise levels) effectively, (ii) it preserves edge sharpness and (iii) it doesn't introduce blurring artefacts or new colours artefacts in comparison to other state-of-the art methods. This method also illustrates that colour images should be treated differently than grayscale images in order to increase the visual performance.

References

1. Astola, J., Haavisto, P., Neuvo, Y.: Vector Median Filters. IEEE Proceedings 78 4 (1990) 678-689
2. Barni, M., Cappellini, V., Mecocci, A.: Fast vector median filter based on Euclidean norm approximation. IEEE Signal Processing Letters 1 6 (1994) 92-94
3. Camacho, J., Morillas, S., Latorre, P.: Efficient Impulse Noise suppression based on Statistical Confidence Limits. Journal of Imaging Science and Technology 50 5 (2006) 427-436
4. David, H. A., Nagaraja, H. N.: Order Statistics (3rd Edition). Wiley, New York (2003)
5. Farbiz, F., Menhaj, M.B.: A fuzzy logic control based approch for image filtering. IN: Kerre, E.E., Nachtegael, M. (eds.): Fuzzy Techniques in Image Processing, Vol. 52, Springer Physica Verlag, Berlin Heidelberg New York (2000) 194-221
6. Fodor, J.: A new look at fuzzy-connectives. Fuzzy sets and Systems 57 2 (1993) 141-148
7. Garnett, R., Huegerich, T., Chui, C., He, W.: A universal noise removal algorithm with an impulse detector. IEEE Transactions on Image Processing 14 11 (2005) 1747-1754
8. Hore, S., Qiu, B., Wu, H.R.: Improved vector filtering for color images using fuzzy noise detection. Optical Engineering 42 6 (2003) 1656-1664
9. Kalaykov, I., Tolt, G.: Real-time image noise cancellation based on fuzzy similarity. IN: Nachtegael, M., Van der Weken, D., Van De Ville, D., Kerre, E.E. (eds.): Fuzzy Filters for Image Processing, Vol. 122 Springer Physica Verlag, Berlin Heidelberg New York (2003) 54-71
10. Kerre, E.E.: Fuzzy sets and approximate Reasoning. Xian Jiaotong University Press (1998).
11. Lee, C.C.: Fuzzy logic in control systems: fuzzy logic controller-parts 1 and 2. IEEE Transactions on Systems, Man, and Cybernetics 20 2 404-435
12. Lukac, R.: Adaptive vector median filtering. Pattern Recognition Letters 24 12 (2003) 1889-1899
13. Lukac, R., Plataniotis, K. N., Venetsanopoulos, A. N., Smolka, B.: A statistically-switched adaptive vector median filter. Journal of Intelligent and Robotic Systems 42 4 (2005) 361-391
14. Lukac, R., Smolka, B., Martin, K. , Plataniotis, K.N., Venetsanopoulos, A. N.: Vector filtering for color imaging. IEEE Signal Processing Magazine 22 1 (2005) 74-86

15. Morillas, S., Gregori, V., Peris-Fajarnés, G., Latorre, P.: A fast impulsive noise color image filter using fuzzy metrics. Real-Time Imaging 11 5-6 (2005) 417-428
16. Plataniotis, K. N., Venetsanopoulos, A. N.: Color Image Processing and Applications. Springer, Berlin (1998).
17. Smolka, B., Chydzinski, A.: Fast detection and impulsive noise removal in color images. Real-Time Imaging, 11 5-6 (2005) 389-402
18. Schulte, S., Nachtegael, M., De Witte, V., Van der Weken, D., Kerre, E. E.: A Fuzzy Impulse Noise Detection and Reduction Method. IEEE Transactions on Image Processing 15 5 (2006) 1153-1162
19. Schulte, S., De Witte, V., Nachtegael, M., Van der Weken, D., Kerre, E.E.: Fuzzy random impulse noise reduction method. Fuzzy Sets and Systems (in press. 2007)
20. Schulte, S., De Witte, V., Nachtegael, M., Van der Weken, D., Kerre, E. E.: Fuzzy two-step filter for impulse noise reduction from color images. IEEE Transactions on Image Processing 15 11 (2006) 3567-3578
21. Wang, J. H., Chiu, H. C.: An adaptive fuzzy filter for restoring highly corrupted images by histogram estimation. Proceedings of the National Science Council -Part A, 23 (1999) 630-643
22. Wang, J.H., Liu, W.J., Lin, L.D.: Histogram-Based Fuzzy Filter for Image Restoration. IEEE Transactions on Systems man and cybernetics part B-cybernetics 32 2 (2002) 230-238
23. Xu, H., Zhu, G., Peng, H., Wang, D.: Adaptive fuzzy switching filter for images corrupted by impulse noise. Pattern Recognition Letters 25 (2004) 1657-1663

Part III

Conclusions and Future Work

Conclusions and future work

In this dissertation, several filtering techniques based on the use of fuzzy metrics and fuzzy logic tools have been developed. The designed filtering techniques aim at taking advantage of fuzzy metrics and fuzzy logic for colour image filtering. Apart from the conclusions drawn in each contribution presented in this dissertation, the following overall conclusions may also be drawn.

- The fuzzy metric M_K introduced in Proposition 1 of Chapter 4 is suitable for RGB colour image processing and it has the advantage of being a little faster than other classical metrics. This fuzzy metric can be used to measure magnitude and directional differences between colour vectors and by employing it, variants of the vector median and vector directional filters can be designed. In fact, Contributions (i)-(v), (vii) and (viii) make use of M_K or some variant of it. Furthermore, this fuzzy metric has been proved to be specially useful within the similarity based vector filtering technique context studied in Contributions (iii) and (v).
- Fuzzy metrics provide a simple mechanism to handle multiple distance criteria simultaneously. Contributions (ii), (iv), (v), (vi) and (viii) propose filtering procedures where a fuzzy metric is successfully used to handle multiple distance criteria.
- As shown in Contributions (iii), (v)-(viii), it is possible to design adaptive filtering techniques using fuzzy metrics that are competitive with respect to recent state-of-the-art filters, outperforming them in many cases.
- As it is proposed in Contribution (ix), fuzzy logic techniques can be used to process colour images by taking into account the correlation among the image channels in a different way that the vector approach does. Indeed, the fuzzy-based technique studied in Contribution (ix) may outperform vector-based filtering techniques.

As a result of the above conclusions, the following future research issues could be of interest.

- To further study the applicability of fuzzy techniques to process multichannel images by taking into account the correlation among the image channels in a different way that the vector approach.

- To investigate on the usefulness of fuzzy metrics and fuzzy logic tools for the reduction of other defects in colour images. For instance, a recent and interesting sort of defects that appears in pictures from colour digital cameras are the so called hot and dead pixels (see, for instance, www.neatimage.com).
- To research on the applicability of fuzzy metrics in other image processing tasks such as, for instance, video deinterlacing, colour image demosaicking, image segmentation, and so on.